Quantification of Lymphocyte Dynamics

Liset Westera

Beach poles on Terschelling. Coastal dunes and beaches form an important line of defense against flooding by the sea, and their maintenance is critical to ensure safety of The Netherlands. The coastline is subject of continuous sedimentation and erosion as a result of tide, wind, and waves. Historically a reference line of wooden beach poles was used to quantify beach height and thus monitor the development of this dynamic coastline. After digitalization of beach height measurements, the poles lost this function but remained to serve as landmarks.

Quantification of Lymphocyte Dynamics

Author: Liset Westera
Cover and Layout: Liset Westera
Printing: Gildeprint, Enschede, The Netherlands

ISBN: 978-94-610-8634-1

Copyright © 2014 by Liset Westera

The research described in this thesis was performed at the Department of Immunology, Laboratory of Translational Immunology, Utrecht University Medical Center Utrecht, The Netherlands.

Quantification of Lymphocyte Dynamics

De dynamiek die schuilgaat achter lymfocytenpopulaties
(met een samenvatting in het Nederlands)

Proefschrift

ter verkrijging van de graad van doctor
aan de Universiteit Utrecht op gezag van de
rector magnificus, prof.dr. G.J. van der Zwaan,
ingevolge het besluit van het college voor promoties
in het openbaar te verdedigen op
donderdag 8 mei 2014 des middags te 2.30 uur

door

Liset Westera

geboren op 3 oktober 1985 te Vught

Promotoren: Prof.dr. F. Miedema
Prof.dr. R.J. de Boer

Copromotoren: Dr. J.A.M. Borghans
Dr. K. Tesselaar

This work was financially supported by a VIDI grant from the Netherlands Organisation for Scientific Research (NWO, grant 917.96.350)

Leescommissie: Prof.dr. L. Koenderman
Prof.dr. T. Schumacher
Prof.dr. P. Reiss
Prof.dr. R.J.M. ten Berge
Prof.dr. L. Willems

Paranimfen: Vera van Hoeven
Ida Hiemstra

Contents

	Glossary	9
Chapter 1	General introduction	11
Chapter 2	Quantitating lymphocyte homeostasis in vivo in humans using stable isotope tracers	27
Chapter 3	Maintenance of peripheral naive T cells is sustained by thymus output in mice but not humans	57
Chapter 4	Age-related decline of T-cell receptor excision circles in humans requires peripheral naive T-cell division.	85
Chapter 5	Closing the gap between T-cell life span estimates from stable isotope-labeling studies in mice and humans	103
Chapter 6	Similar estimates of cell turnover from stable isotope-labeling experiments using deuterated glucose or water	133
Chapter 7	Lymphocyte maintenance during healthy aging requires no substantial alterations in cell dynamics	155
Chapter 8	General discussion	181
Appendices	Nederlandse samenvatting voor niet-ingewijden	206
	Dankwoord	216
	Curriculum vitae	219
	List of publications	221

Glossary

Homeostasis: the ability or tendency to maintain a lymphocyte population of constant size, by altered cell production or loss rates when the steady state is threatened or disturbed.

Life span, longevity: the time between a cell's production (from a precursor compartment like the thymus or bone marrow, or by division of its mother cell) and a cell's disappearance (either by death or differentiation). The life span is obtained by inverting the loss rate (or turnover rate under steady state conditions), which can be derived from DNA labeling experiments.

Loss rate, disappearance rate: the rate at which cells are lost from a population, either by death or differentiation.

Peripheral cell division: division by a cell in the blood or peripheral lymphoid organs to produce two daughter cells.

De novo production: generation of cells by a series of differentiation and proliferation processes in a source, like the thymus or the bone marrow, which are subsequently exported to the blood or peripheral lymphoid organs.

Production rate: the rate at which cells are produced in a population, which in the case of naive T cells is a composite of thymic output and peripheral cell division.

Steady state: lymphocyte pools are typically in steady state, i.e., cell production equals cell loss.

Turnover rate: under steady state conditions, the rate at which old cells are replaced by newly generated cells.

1

General Introduction

The immune system

The immune system plays a key role in host defense by identifying and eliminating a variety of foreign species, like bacteria and viruses, which are encountered throughout life. Mammals are equipped with both an innate immune system and an adaptive, or acquired immune system, two arms that cooperate to provide a high degree of protection. Innate immune function relies on the recognition of evolutionary conserved structures on pathogens, so-called pathogen-associated molecular patterns, through germline-encoded pattern-recognition receptors. The various cell types of the innate immune system rapidly exert effector functions and thus provide a first line of defense. The action of the adaptive immune system, comprising T and B lymphocytes, relies on the specific recognition of antigens through unique antigen recognition receptors, and is hallmarked by the generation of immunological memory. T cells provide cell-mediated immunity, relying on direct cell-killing action by cytotoxic T cells, whereas B cells, with the help of T cells, mount a humoral or antibody response.

Lymphocyte development and differentiation in a nutshell

Lymphocytes develop from multipotent hematopoietic precursors in the specialized microenvironments of primary (or central) lymphoid organs, i.e., the bone marrow and the thymus. It is in the bone marrow and thymus, respectively, where the B-cell and T-cell receptor gene rearrangements and modifications take place that generate antigen receptors with novel specificities. These processes generate an enormous diversity in antigen receptors, allowing the adaptive immune system to recognize a wide range of unique foreign structures. Functionally rearranged lymphocytes undergo selection processes, also known as central tolerance mechanisms, aiming to select cells that are non-reactive to self but reactive to foreign antigens. Once matured, functional naive lymphocytes egress from the primary lymphoid organs to enter the peripheral lymphocyte pool (typically referring to the blood and peripheral lymphoid tissues). Cognate antigen encounter by circulating naive lymphocytes will lead to their activation and differentiation toward effector or memory cells, culminating in an immune response and, eventually, long-term immunity.

Maintenance of lymphocyte populations

The different lymphocyte populations of the immune system are maintained at fairly constant numbers throughout life. The importance of this lifelong maintenance is illustrated by clinical conditions of lymphopenia, such as human immunodeficiency virus infection, severe combined immune deficiency, or hematopoietic stem cell transplantation, when opportunistic infections can cause considerable morbidity and mortality. Maintenance of lymphocyte populations is a dynamic process in which cell

production and loss are balanced[1], and which is often referred to as a steady state[2]. In principle, the size of any lymphocyte population is the net effect of different processes: (1) an influx of cells from a precursor compartment, (2) peripheral cell division, and (3) loss of cells by death or differentiation to another cell type. Production of naive lymphocytes can occur de novo – from hematopoietic progenitor cells that mature in the bone marrow and thymus, or through division of naive cells already residing in the periphery[3-7].

It is generally thought that the thymus is primarily responsible for the maintenance of the naive T-cell pool, and that peripheral division of naive T cells plays a limited role. A second commonly held view is that homeostatic mechanisms become active in response to changes in lymphocyte production or loss, securing the steady state of the population. Such a homeostatic, or compensatory response could manifest either as an adaptation of lymphocyte production de novo, or as a change in peripheral lymphocyte division or loss rates. For example, if the supply of new naive T cells by the thymus declines, cells in the peripheral naive T-cell pool may numerically compensate for this either by increased peripheral naive T-cell division rates, or by reduced loss rates of naive T cells and hence by their increased survival.

Quantification of lymphocyte dynamics

Why quantify?

Over the past decades a large body of qualitative knowledge has been obtained in the field of immunology, unraveling the various cellular and molecular components of the immune system and their functions. By contrast, relatively little quantitative information is available on the dynamics of lymphocyte populations, involving fundamental questions like “How long do lymphocytes live?” and “How large is thymic output?”. Importantly, quantification of such biological processes is not merely about calculating *numbers*; quantitative insights typically also lead to a better *qualitative* understanding of the immune system in health and disease. One of the best examples is the groundbreaking discovery by David Ho and Alan Perelson in 1995, who, by quantifying human immunodeficiency virus-1 (HIV-1) viral load and $CD4^+$ T-cell numbers before and during antiretroviral treatment, demonstrated that what was then considered viral latency was in fact a balance between the rapid production and loss of virions[8]. The continuous, high-level replication of HIV-1 provided an explanation for its rapid evolution and underscored the risk of developing drug-resistant viral escape variants. These quantitative studies established the foundation for modern combination antiretroviral therapy, which has led to a dramatic reduction in AIDS-associated mortality in industrialized countries.

Quantitative insights into lymphocyte dynamics are crucial to understand

how for example a functional and diverse immune system is maintained into old age, what mechanisms preserve long-term immunological memory, whether and how the immune system adapts to changes that disturb the steady state of a lymphocyte population, and to unravel the pathology of a wide range of clinical conditions in which immune homeostasis is dysregulated. Such insights form the basis for developing and improving the treatment of clinical conditions with disturbed lymphocyte dynamics.

Controversy on lymphocyte dynamics

To date, the efforts that have been made to quantify lymphocyte dynamics have yielded valuable insights but also introduced discrepancies in the literature, which have been hampering our understanding of lymphocyte dynamics in health and disease. This seems to be due in part to the fact that many insights originate from mouse experiments. Because of the many parallels between the murine and human immune systems, in particular the age-related involution of the thymus[9, 10], mice have traditionally been the model of choice for basic research of T-cell immunity. Mice offer a great tool because of the possibilities to manipulate the system, e.g., by adoptive transfers or thymus transplantations, making it easier to test hypotheses in vivo. However, although many processes translate well between the two species and much of our knowledge of human immune function comes from mouse studies, such insights may be extrapolated to humans even when this is not justified[11, 12].

Investigating lymphocyte dynamics has also been hampered by the difficulty to experimentally address these questions in vivo, which is difficult in mice but even more so in humans, primarily because of technical and ethical limitations. Another challenge is the quantitative interpretation of experimental “dynamics” data, which has turned out to be notoriously difficult. Mathematical models have proven to be indispensable for proper interpretation and translation of such data into relevant parameters such as lymphocyte life spans or daily thymic output[2], and not seldom have they uncovered a tool’s pitfalls and possibilities. Over the years, they helped resolve many of the discrepancies in the field. The next sections highlight some of the most important steps that were undertaken to quantitatively address the two key topics of this thesis, lymphocyte longevity and thymic output, in humans. As the majority of research has been concentrated on T cells, these will be the main focus in the next section.

How long do lymphocytes live?

Tracking cells with radiation-induced chromosome damage in vivo

Historical estimates of human lymphocyte life spans date back to the 1960s, when researchers exploited a unique situation provided by patients treated with radiotherapy,

in whom the loss rate of lymphocytes with radiation-induced chromosomal damage provided a direct measure of the intermitotic time, or life span of the cells[13, 14]. These early studies demonstrated that lymphocytes with chromosomal lesions could persist for up to several years after radiation treatment, and they were estimated to have a mean life span of 530[13] to 1600 days[14]. Later studies distinguished naive and memory T-cell subsets on the basis of CD45 isoforms, which revealed that, with an estimated life span of 5 to 9 months, $CD45RO^+$ memory T cells were much shorter-lived than $CD45RA^+$ "naive" T cells, which were estimated to live about 2.5 to 3.5 years[15, 16]. This was a surprising result because it suggested that long-term immunological memory resides in a population of cells with rapid turnover, contradicting the widely held view of a long-lived memory cell. Although these studies provided important insights into immunological memory, clearly the method was not widely applicable. Moreover, it is not inconceivable that non-physiologically low cell numbers and perhaps also chromosomal damage had influenced lymphocyte kinetics, questioning how well these results translated to a natural situation.

Assessment of telomere lengths

Weng et al. studied the division rates of naive and memory T cells based on the length of their telomeres[17], the long tandem repeats at the end of chromosomes that shorten with each round of cell division[18, 19]. Telomere lengths declined with age at a similar rate for naive and memory T cells, with telomeres of memory T cells being consistently 1.4kb shorter than those of naive T cells. They concluded that naive T cells divide at a rate of 0.3 divisions per year, and that priming to the memory pool occurs with substantial clonal expansion, the magnitude of which is constant with age[17]. However, telomere lengths reflect the replicative history of not only the cell type studied but also its precursors, typically a source of relatively long telomeres; hence, loss of telomere length through naive T-cell division is counterbalanced by an influx of new T cells from the thymus, and, likewise, loss of telomere length through memory T-cell division is counteracted by an influx of naive T cells priming into the memory pool[20]. With the aid of a mathematical model for telomere loss it was shown that the intuitive derivation of turnover rates from telomere data is tricky[20]. The analysis pointed out that, for example, the rate of telomere shortening of both naive and memory T cells could be dictated by the division rate of naive T cells only and hence could be totally independent of memory T-cell division, and that the difference in telomere length between naive and memory T cells does not directly reflect the magnitude of clonal expansion upon priming but rather the difference in turnover rates between naive and memory T cells. This work has stressed the merit of mathematical models for the – sometimes counterintuitive – interpretation of experimental data.

DNA labeling techniques

The most direct way to study cell production and loss is by measuring the rates of DNA synthesis and breakdown, and this method relies on the incorporation of labeled DNA precursors into newly synthesized genomic DNA of dividing cells, which can be quantified ex vivo[21-23]. Because of the complex kinetics of label incorporation and loss by cell populations, interpretation by mathematical models has become an important component of DNA labeling experiments. The traditional DNA labels, tritiated thymidine and 5'bromo-3'-deoxyuridine (BrdU), have been widely used in vitro and in animal studies[21-23], but their use in humans has been limited because of radioactivity and potential toxicities associated with long-term administration[24,25.] Only a few studies have used short-term BrdU labeling in humans to investigate T-cell dynamics in HIV infection[26-29], but in a recent study the enrollment of subjects was prematurely stopped because of the occurrence of malignancies, for which an association with BrdU administration could not be excluded[30].

A major breakthrough came with the introduction of stable isotope-labeling techniques for in vivo quantification of cellular turnover rates, which applied the non-radioactive, non-toxic compounds deuterium-labeled glucose ($^2H_2$-glucose)[31] or deuterium-labeled water (^2H_2O, heavy water)[32], and thereby finally permitted safe, direct measurement of lymphocyte turnover and longevity in humans under physiological circumstances. This advent has instigated investigations of lymphocyte turnover in different circumstances including healthy aging, HIV infection, leukemia, and diabetes[33-43]. Stable isotope-labeling techniques have provided a major step toward consensus regarding lymphocyte life spans, and have considerably reduced the discrepancies between human T-cell life span estimates[2,44]. Yet consensus is lacking even among stable-isotope labeling studies, and this residual controversy is a major theme addressed in this thesis.

How large is thymic output?

Although stable isotope-labeling techniques are considered the state of the art technique for quantification of lymphocyte turnover, they do not allow cells that divided in the periphery to be distinguished from those that were generated in the thymus and then entered the periphery, and can therefore not be used to estimate thymic function. To estimate this parameter, a number of different approaches have been developed over the years.

Biopsy studies

Steinmann et al. quantified the rate of thymic involution during aging by morphometric analyses of autopsy and biopsy material[9]. Contrary to the then widely held view

that thymic involution starts at puberty under the influence of sex hormones, they found that the thymus reaches its maximum size during the first year of life, and then gradually involutes, with the volume of functional thymic epithelium (cortex and medulla) progressively declining until the end of life, resulting in loss of thymopoiesis[9]. Although this study clearly demonstrated how the *capacity* of the thymus to produce new T cells declines with age, it did not actually quantify the decline in the *number of cells* generated by the thymus.

T-cell receptor excision circles (TRECs)

A large step forward was made by the introduction of an assay to measure T-cell receptor excision circles (TRECs)[45]. This assay exploits the principle that T-cell receptor rearrangements in the thymus yield small, extra-chromosomal byproducts that remain present in peripheral T cells. The frequency of TRECs in lymphocytes and T cell subsets is high in children and declines with increasing age[45], which is well in line with the progressive involution of the thymus[9]. Hence, TREC measurements seemed to permit the quantification of recent thymic emigrants (RTE) and hence of thymic output in a variety of clinical situations. Reduced TREC contents (i.e., the number of TRECs per cell) in the T cells of HIV-infected patients, and normalization of these levels upon antiretroviral treatment, suggested that HIV interferes with thymic function and that this function is restored upon treatment[45]. Supranormal TREC contents in cancer patients who received a stem cell transplantation were taken as evidence for the occurrence of thymic rebound, referring to the capacity of the organ to increase its production upon naive T-cell depletion[46].

However, it soon became clear that the intuitive interpretation of TREC data as ongoing thymic output could be dangerous for two main reasons[47]. First, because both T cells and TRECs are long-lived, the presence of $TREC^+$ cells not necessarily reflects actual thymic output. Because of this longevity, alterations in thymic output also cannot instantly affect TREC dynamics in the periphery. Second, because TRECs are not replicated during mitosis but passed on randomly to one of the daughter cells, TREC contents are strongly influenced by cell division (and in fact even by cell death). The reduced TREC contents in untreated HIV infection, initially thought to reflect virus-induced thymic dysfunction, are in fact more likely to be the result of increased T-cell proliferation rates[48]. The latter is also in line with stable-isotope labeling experiments showing increased T-cell turnover rates in HIV patients[40-42]. In addition, the elevated TREC contents after stem cell transplantation can be the mere effect of $TREC^+$ cells entering a depleted pool, rather than providing evidence for thymic rebound[47]. Nevertheless, when interpreted with the necessary caution, TREC analysis can provide valuable information about T-cell dynamics. Both the interpretation of TREC data and their added value for quantification of thymic output are extensively addressed in this thesis.

CD31 and PTK7, surrogate $CD4^+$ RTE markers

Ideally a marker that identifies RTE should be expressed on newly exported T cells only transiently (e.g., 24 hours), and be lost upon cell division. As post-thymic maturation of newly produced T cells is found to coincide with the loss of proteins such as CD31 and protein tyrosine kinase-7 (PTK7), expression of these proteins has been considered a measure for recent thymic progeny[49, 50].

CD31 expression on naive $CD4^+$ T cells has been proposed as a marker for $CD4^+$ RTE, because the fraction of $CD31^+$ naive $CD4^+$ T cells declines with age, in line with the age-related decline in thymic output[49]. Analysis of TREC contents, which are much higher in $CD31^+$ than in $CD31^-$ naive $CD4^+$ T cells, has suggested that $CD31^+$ cells are more proximal to the thymus than their $CD31^-$ counterparts[3]. However, the observation that even in the $CD31^+$ subset TREC contents display an age-related decline suggests that CD31 expression is not necessarily lost upon cell division, and disqualifies the use of CD31 as a strict RTE marker[51, 52].

PTK7 expression was proposed to identify $CD4^+$ T cells that were even more proximal to the thymus than $CD31^+$ naive $CD4^+$ T cells, first because $PTK7^+$ naive $CD4^+$ T cells, which are uniformly $CD31^+$, decline more rapidly after thymectomy than $PTK7^-$ $CD31^+$ naive $CD4^+$ T cells, and second because TREC contents in $PTK7^+$ naive $CD4^+$ T cells are higher than in $PTK7^-$ naive $CD4^+$ T cells[50]. However, despite a rapid drop in $PTK7^+$ naive $CD4^+$ T cells after thymectomy, a residual population of $PTK7^+$ cells was found to persist in these individuals for at least half a year post-thymectomy. Because these $PTK7^+$ cells could impossibly be *recently* produced by the thymus, the expression of PTK7 apparently did not only identify thymic emigrants that recently emigrated, but also older cells of thymic origin, as confirmed later in a mathematical analysis by Bains et al.[53].

To date, the perfect, unambiguous marker that quantifies the *actual* thymic output of new $CD4^+$ and $CD8^+$ T cells has not been identified. Nevertheless, particularly CD31 is widely used as thymic proximity marker, or surrogate RTE marker[54-57]. Moreover, researchers have become increasingly aware that combining different tools can have significant added value when studying T-cell dynamics, as will also be addressed in this thesis.

Scope of the thesis

Immunologists have adopted a variety of approaches to address questions related to lymphocyte dynamics. Yet distilling the desired information from experimental data has remained a challenge, even with the aid of mathematical models. This thesis integrates experimental approaches and mathematical modeling to gain insights into the biology of human lymphocyte populations. The key aims of this research were 1) to improve the interpretation of experimental data in order to provide the most reliable information about lymphocyte dynamics, which should help explain discrepancies in the literature and reach consensus in the field; and 2) to gain insights into the lifelong maintenance of the peripheral lymphocyte pools in healthy humans.

Chapter 2 describes the use of in vivo stable isotope-labeling techniques, one using deuterated glucose and the other using deuterated water, for the quantification of lymphocyte homeostasis in humans. It describes their approach through all four phases of investigation: labeling, sampling, analysis, and interpretation.

Chapter 3 combines stable isotope-labeling experiments in mice and humans with thymectomy experiments, CD31 expression and TREC data, and mathematical modeling, to find out that mice and humans are incomparable with respect to naive T-cell maintenance – thereby disqualifying the mouse as an animal model for the investigation of human T-cell dynamics.

While in chapter 3, the age-related decline in naive T-cell TREC contents is interpreted as dilution through peripheral naive T-cell division, **chapter 4** investigates whether this decline could alternatively be due to intracellular decay of TRECs rather than to cell division.

Chapter 5 tackles discrepancies between life spans estimated from different stable isotope-labeling studies, by investigating the positive correlation between published life span estimates and the duration of label administration. It addresses the hypothesis that the typically used, single-exponential models yield life span estimates that are sensitive to the length of the labeling period, and introduces an alternative, multi-exponential modeling approach for reliable quantification of average life spans.

In an attempt to explain the last remaining discrepancies between life span estimates published in the literature, **chapter 6** investigates whether biochemical differences between deuterated glucose and deuterated water, or methodological differences between studies using either compound, could affect the estimated turnover rate.

Chapter 7 implements the newest insights regarding the interpretation of stable isotope-labeling data to study the effects of healthy aging on the dynamics of a variety of human T-cell and B-cell subsets. It also investigates whether in elderly individuals a homeostatic response is triggered to compensate for declining thymic T-cell production, by dissecting the contributions of thymic output and peripheral division to naive T-cell production.

Chapter 8 summarizes the findings presented in this thesis and puts them into a broader perspective.

References

1. Asquith, B., Debacq, C., Macallan, D.C., Willems, L., & Bangham, C.R. Lymphocyte kinetics: the interpretation of labelling data. Trends Immunol. 23, 596-601 (2002).
2. Borghans, J.A. & de Boer, R.J. Quantification of T-cell dynamics: from telomeres to DNA labeling. Immunol. Rev. 216, 35-47 (2007).
3. Kohler, S. et al. Post-thymic in vivo proliferation of naive CD4+ T cells constrains the TCR repertoire in healthy human adults. Eur. J. Immunol. 35, 1987-1994 (2005).
4. Pekalski, M.L. et al. Postthymic expansion in human CD4 naive T cells defined by expression of functional high-affinity IL-2 receptors. J. Immunol. 190, 2554-2566 (2013).
5. Hazenberg, M.D. et al. Establishment of the CD4+ T-cell pool in healthy children and untreated children infected with HIV-1. Blood 104, 3513-3519 (2004).
6. Bains, I., Antia, R., Callard, R., & Yates, A.J. Quantifying the development of the peripheral naive CD4+ T-cell pool in humans. Blood 113, 5480-5487 (2009).
7. van Zelm, M.C., Szczepanski, T., van der Burg, M., & van Dongen, J.J. Replication history of B lymphocytes reveals homeostatic proliferation and extensive antigen-induced B cell expansion. J. Exp. Med. 204, 645-655 (2007).
8. Ho, D.D. et al. Rapid turnover of plasma virions and CD4 lymphocytes in HIV-1 infection. Nature 373, 123-126 (1995).
9. Steinmann, G.G., Klaus, B., & Muller-Hermelink, H.K. The involution of the ageing human thymic epithelium is independent of puberty. A morphometric study. Scand. J. Immunol. 22, 563-575 (1985).
10. Hale, J.S., Boursalian, T.E., Turk, G.L., & Fink, P.J. Thymic output in aged mice. Proc. Natl. Acad Sci. U. S. A 103, 8447-8452 (2006).
11. Mestas, J. & Hughes, C.C. Of mice and not men: differences between mouse and human immunology. J. Immunol. 172, 2731-2738 (2004).
12. Seok, J. et al. Genomic responses in mouse models poorly mimic human inflammatory diseases. Proc. Natl. Acad. Sci. U. S. A 110, 3507-3512 (2013).
13. Norman, A., Sasaki, M.S., Ottoman, R.E., & Fingerhut, A.G. Lymphocyte lifetime in women. Science 147, 745 (1965).
14. Buckton, K.E., Brown, W.M., & Smith, P.G. Lymphocyte survival in men treated with x-rays for ankylosing spondylitis. Nature 214, 470-473 (1967).
15. Michie, C.A., McLean, A., Alcock, C., & Beverley, P.C. Lifespan of human lymphocyte subsets defined by CD45 isoforms. Nature 360, 264-265 (1992).
16. Mclean, A.R. & Michie, C.A. In vivo estimates of division and death rates of human T lymphocytes. Proc. Natl. Acad. Sci. U. S. A 92, 3707-3711 (1995).
17. Weng,N.P., Levine,B.L., June,C.H., & Hodes,R.J. Human naive and memory T lymphocytes differ in telomeric length and replicative potential. Proc. Natl. Acad. Sci. U. S. A 92, 11091-11094 (1995).
18. Harley, C.B., Futcher, A.B., & Greider, C.W. Telomeres shorten during ageing of human fibroblasts. Nature 345, 458-460 (1990).
19. Blackburn, E.H. Structure and function of telomeres. Nature 350, 569-573 (1991).
20. de Boer, R.J. & Noest, A.J. T cell renewal rates, telomerase, and telomere length shortening. J. Immunol. 160, 5832-5837 (1998).
21. Waldman, F.M. et al. A comparison between bromodeoxyuridine and 3H thymidine labeling in human breast tumors. Mod. Pathol. 4, 718-722 (1991).
22. Gratzner, H.G. Monoclonal antibody to 5-bromo- and 5-iododeoxyuridine: A new reagent for detection of DNA replication. Science 218, 474-475 (1982).
23. Hellerstein, M.K. Measurement of T-cell kinetics: recent methodologic advances. Immunol. Today 20, 438-441 (1999).
24. Asher, E., Payne, C.M., & Bernstein, C. Evaluation of cell death in EBV-transformed lymphocytes using agarose gel electrophoresis, light microscopy and electron microscopy. II. Induction of non-classic apoptosis ("para-apoptosis") by tritiated thymidine. Leuk. Lymphoma 19, 107-119 (1995).
25. Rocha, B. et al. Accumulation of bromodeoxyuridine-labeled cells in central and peripheral lymphoid organs: minimal estimates of production and turnover rates of mature lymphocytes. Eur. J. Immunol. 20, 1697-1708 (1990).
26. Lempicki, R.A. et al. Impact of HIV-1 infection and highly active antiretroviral therapy on the kinetics of CD4+ and CD8+ T cell turnover in HIV-infected patients. Proc. Natl. Acad. Sci. U. S. A 97, 13778-13783 (2000).
27. Kovacs, J.A. et al. Identification of dynamically distinct subpopulations of T lymphocytes that are differentially affected by HIV. J. Exp. Med. 194, 1731-1741 (2001).
28. Kovacs, J.A. et al. Induction of prolonged survival of CD4+ T lymphocytes by intermittent IL-2 therapy in HIV-infected patients. J. Clin. Invest 115, 2139-2148 (2005).
29. Di, M.M. et al. Naive T-cell dynamics in human immunodeficiency virus type 1 infection: effects of highly active antiretroviral therapy provide insights into the mechanisms of naive T-cell depletion. J. Virol. 80, 2665-2674 (2006).
30. Srinivasula, S. et al. Differential effects of HIV viral load and CD4 count on proliferation of naive and memory CD4 and CD8 T lymphocytes. Blood 118, 262-270 (2011).
31. Hellerstein, M.K. & Neese,R.A. Mass isotopomer distribution analysis: a technique for measuring biosynthesis and turnover of polymers. Am. J. Physiol. 263, E988-1001 (1992).
32. Neese, R.A. et al. Measurement in vivo of proliferation rates of slow turnover cells by 2H2O labeling of the deoxyribose moiety of DNA. Proc. Natl. Acad. Sci. U. S. A 99, 15345-15350 (2002).
33. Vrisekoop, N. et al. Sparse production but preferential incorporation of recently produced naive T cells in the human peripheral pool. Proc. Natl. Acad. Sci. U. S. A 105, 6115-6120 (2008).
34. Macallan, D.C. et al. Rapid turnover of effector-memory CD4(+) T cells in healthy humans. J. Exp. Med. 200, 255-260 (2004).
35. Zhang, Y. et al. In vivo kinetics of human natural killer cells: the effects of ageing and acute and chronic viral infection. Immunology 121, 258-265 (2007).
36. Wallace, D.L. et al. Direct measurement of T cell subset kinetics in vivo in elderly men and women. J. Immunol. 173, 1787-1794 (2004).
37. Macallan, D.C. et al. B-cell kinetics in humans: rapid turnover of peripheral blood memory cells. Blood 105, 3633-3640 (2005).
38. Bollyky, J.B. et al. Evaluation of in vivo T cell kinetics: use of heavy isotope labelling in type 1 diabetes. Clin. Exp. Immunol. 172, 363-374 (2013).
39. Zhang, Y. et al. Accelerated in vivo proliferation of memory phenotype CD4+ T-cells in human HIV-1 infection irrespective of viral chemokine co-receptor tropism. PLoS. Pathog. 9, e1003310 (2013).
40. Mohri, H. et al. Increased turnover of T lymphocytes in HIV-1 infection and its reduction by antiretroviral therapy. J. Exp. Med. 194, 1277-1287 (2001).

41. Hellerstein, M. et al. Directly measured kinetics of circulating T lymphocytes in normal and HIV-1-infected humans. Nat. Med. 5, 83-89 (1999).

42. Hellerstein, M.K. et al. Subpopulations of long-lived and short-lived T cells in advanced HIV-1 infection. J. Clin. Invest. 112, 956-966 (2003).

43. van Gent, R. et al. In vivo dynamics of stable chronic lymphocytic leukemia inversely correlate with somatic hypermutation levels and suggest no major leukemic turnover in bone marrow. Cancer Res. 68, 10137-10144 (2008).

44. Asquith, B. & Borghans, J.A. Modeling lymphocyte dynamics in vivo in Mathematical models and immune cell biology (eds. Molina-París,C. & Lythe,G.) 141-169 (Springer, 2011).

45. Douek, D.C. et al. Changes in thymic function with age and during the treatment of HIV infection. Nature 396, 690-695 (1998).

46. Douek, D.C. et al. Assessment of thymic output in adults after haematopoietic stem-cell transplantation and prediction of T-cell reconstitution. Lancet 355, 1875-1881 (2000).

47. Hazenberg, M.D., Borghans,J.A., de Boer,R.J., & Miedema,F. Thymic output: a bad TREC record. Nat. Immunol. 4, 97-99 (2003).

48. Hazenberg, M.D. et al. Increased cell division but not thymic dysfunction rapidly affects the T-cell receptor excision circle content of the naive T cell population in HIV-1 infection. Nat. Med. 6, 1036-1042 (2000).

49. Kimmig, S. et al. Two subsets of naive T helper cells with distinct T cell receptor excision circle content in human adult peripheral blood. J. Exp. Med. 195, 789-794 (2002).

50. Haines, C.J. et al. Human CD4+ T cell recent thymic emigrants are identified by protein tyrosine kinase 7 and have reduced immune function. J. Exp. Med. 206, 275-285 (2009).

51. Kilpatrick, R.D. et al. Homeostasis of the naive CD4+ T cell compartment during aging. J. Immunol. 180, 1499-1507 (2008).

52. den Braber, I. et al. Maintenance of peripheral naive T cells is sustained by thymus output in mice but not humans. Immunity 36, 288-297 (2012).

53. Bains, I., Yates, A.J., & Callard, R.E. Heterogeneity in thymic emigrants: implications for thymectomy and immunosenescence. PLoS. One 8, e49554 (2013).

54. Oraei, M. et al. Naive CD4+ T cells and recent thymic emigrants in common variable immunodeficiency. J. Investig. Allergol. Clin. Immunol. 22, 160-167 (2012).

55. Schurmann, M. et al. Impaired thymic function and CD4+ T lymphopenia, but not mannose-binding lectin deficiency, are risk factors for Pneumocystis jirovecii pneumonia in kidney transplant recipients. Transpl. Immunol. 28, 159-163 (2013).

56. Sandgaard, K.S., Lewis, J., Adams, S., Klein, N., & Callard, R. Antiretroviral therapy increases thymic output in children with HIV. AIDS (2013).

57. Lario, M. et al. Defective thymopoiesis and poor peripheral homeostatic replenishment of T-helper cells cause T-cell lymphopenia in cirrhosis. J. Hepatol. 59, 723-730 (2013).

2

Quantitating Lymphocyte Homeostasis In Vivo in Humans Using Stable Isotope Tracers

Liset Westera[1], Yan Zhang[2], Kiki Tesselaar[1], José AM Borghans[1], Derek C Macallan[2]

[1] Department of Immunology, University Medical Center Utrecht, Utrecht, The Netherlands; [2] Division of Clinical Sciences, Infection & Immunity Research Centre, St George's, University of London, London, UK

Methods Mol Biol. 2013;979:107-31

Humans have a remarkable ability to maintain relatively constant lymphocyte numbers across many decades, from puberty to old-age, despite a multitude of infectious and other challenges and a dramatic decline in thymic output. This phenomenon, lymphocyte homeostasis, is achieved by matching the production, death, and phenotype transition rates across a network of varied lymphocyte subpopulations. Understanding this process in humans depends on the ability to measure in vivo rates of lymphocyte production and loss. Such investigations have been greatly facilitated by the advent of stable isotope labeling approaches, which use the rate of incorporation of a tracer into cellular DNA as a marker of cell division. Two labeling approaches are commonly employed, one using deuterium-labeled glucose and the other using deuterium-labeled water, also known as heavy water (^2H_2O). Here we describe the application of these two labeling techniques for measurement of human in vivo lymphocyte kinetics through the four phases of investigation: labeling, sampling, analysis, and interpretation.

1. Introduction

1.1. Quantification of Lymphocyte Dynamics in Human Clinical Studies

Long-term maintenance of immune homeostasis is essential for proper functioning of the immune system, as illustrated by several diseases including HIV infection and leukemia, in which immune homeostasis is disturbed. Immune homeostasis is directly linked to the dynamics of the lymphocytes that comprise the cellular immune system. In order for populations to be maintained over time, cell production and loss must be balanced. To better understand normal lymphocyte homeostasis and the pathology of conditions that perturb lymphocyte numbers, quantification of production and loss rates of lymphocytes is crucial[1].

Several approaches have been used to quantify lymphocyte dynamics, including measurement of telomere length or Ki-67 expression, quantitation of T-cell receptor excision circles (TRECs), tracking cells with radiation-induced chromosomal damage, cell labeling with carboxyfluorescin diacetate succinimidylester (CFSE), and DNA labeling with the thymidine analog 5'-bromo-3'-deoxyuridine (BrdU). Although all of these approaches have contributed significantly to our understanding of lymphocyte dynamics, most are not applicable to in vivo human clinical studies. By contrast, recently introduced stable isotope labeling techniques have made the in vivo investigation of lymphocyte dynamics in humans feasible[2–7]. Stable isotopes have the great advantage of being suitable for human (clinical) investigation since they are nonradioactive and have no inherent toxicity in tracer doses.

1.2. Stable Isotope Labeling

The key to the use of stable isotopes to measure cell turnover is the link between cell division and DNA synthesis[2, 4]. Although DNA synthesis occurs in S-phase of the cell cycle, it can be used as a surrogate marker for proliferation at the population level[3]. Similarly, since non-replicative DNA turnover (including non-replicative DNA repair, nucleoside substitutions during RNA–DNA interactions during message transcription and DNA unfolding) is relatively slow, loss of labeled DNA can be used as a marker of death of labeled cells, or of disappearance of labeled cells from the compartment being sampled.

Stable isotope tracer studies are based on a generic principle; when a product arises from a labeled precursor, the rate of incorporation of label from precursor to product yields the synthesis rate of the product[8]. In this case the product is DNA and the immediate precursor is deoxynucleotide triphosphate (dNTP)[2, 4, 5]. The precursor pool can be labeled in in vivo studies using deuterium-labeled glucose or water. Both result in deuterium-labeled dNTP through the de novo nucleotide synthesis (DNNS) pathway[2]. Glucose carries two deuterium atoms into the pentose moieties, which form

the building blocks for nucleotide synthesis; the label is thus specifically incorporated into the sugar-phosphate backbone of DNA. Deuterated water-derived deuterium is incorporated at multiple sites (C–H bonds) within the newly synthesized purine dNTPs in DNA[2, 3, 6]. Hence, cells that replicate in the presence of deuterium-labeled precursors, either glucose or water, will incorporate deuterium into the DNA of their progeny, whilst non-dividing cells remain unlabeled. The label is retained within the progeny, even if the cell divides again, until the cell dies or leaves the pool of cells under investigation, either by localization elsewhere or by phenotype transition[3].

One advantage of the use of deuterated glucose or heavy water over thymidine nucleoside analogue labels such as BrdU is that deuterated glucose and heavy water predominantly label through the de novo nucleoside synthesis pathway, whereas thymidine nucleoside analogues enter cellular dNTP pools via the salvage pathways. Salvage pathway activity is highly variable, being modulated by cellular physiology and this variability may interfere with BrdU labeling in an unpredictable way[9, 10]. Quantitation is achieved by analyzing (by mass spectrometry) the fraction of deuterium-labeled moieties within the DNA of sampled cell populations during and/or after labeling. Analysis only allows conclusions to be drawn about populations of cells. By contrast, approaches such as BrdU labeling, ^{3}H-thymidine labeling, Ki-67 expression analysis or CFSE dilution enable cell-by-cell analysis, which should be seen as yielding complementary data. A population of cells with a high rate of turnover will incorporate large amounts of the isotope deuterium, whereas one with few mitoses will incorporate little.

In this paper we describe the use of deuterium-labeled compounds to quantify production and loss rates of different types of lymphocytes and demonstrate how mathematical modeling may be used to interpret the experimental data[11–14]. Although stable isotope labeling has many potential applications (virtually any cell type can be studied[1]), this protocol is limited to its application to the study of human lymphocyte homeostasis. Modification for animal studies is also possible.

The next section introduces the four different components that characterize a stable isotope labeling experiment from beginning to end: (1) labeling, (2) sampling, (3) analysis, and (4) interpretation (Fig. 1.).

1.3. The Four Components of a Labeling Experiment

1.3.1. Labeling

Glucose or Water?

The expected turnover rate of a cell population is a key determinant in the choice between labeling with deuterated water or glucose. Because of its rapid “on” and “off” kinetics, glucose is appropriate for cells with rapid turnover. Conversely, deuterated water is the method of choice when analyzing slow turnover populations since it can

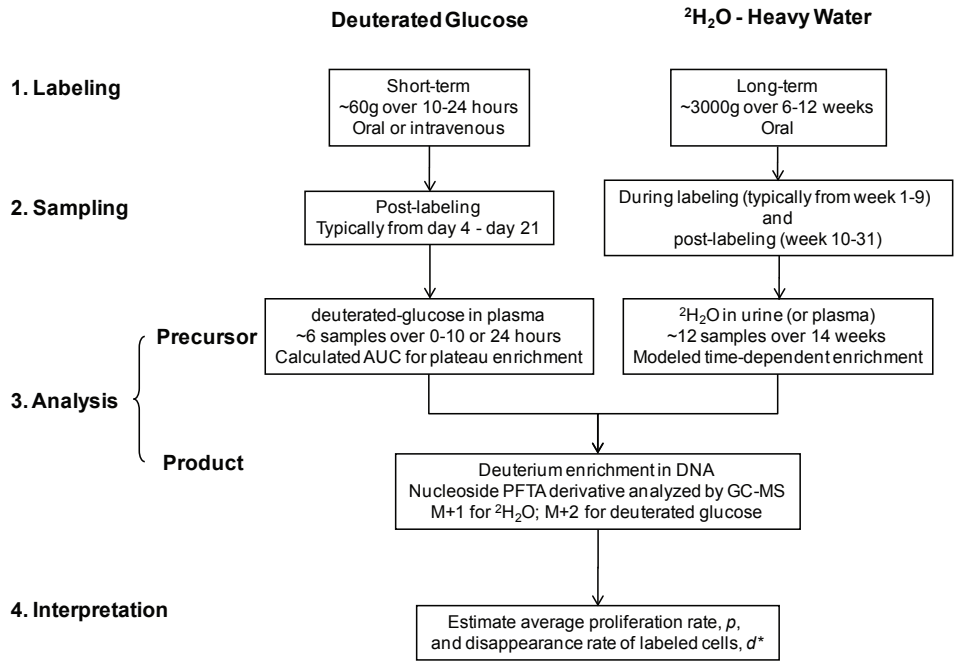

Figure 1. Overview of stable isotope labeling strategies. Comparison of deuterated glucose and heavy water labeling approaches.

be administered over long periods of time (even months if necessary). The resulting long-lasting enrichment in body water permits a reliable labeling of cell populations that rarely divide, such as human naive T cells. Importantly, it is impossible to use heavy water labeling for the study of cell types that turn over much more rapidly than water itself. For such cell types, glucose labeling is the appropriate method.

Deuterated Glucose Labeling

Glucose may be given either orally or by intravenous infusion. Oral labeling is less invasive but requires at least half-hourly administration and for this reason overnight administration is difficult. Oral labeling for 10h gave sufficient signal to measure the kinetics of $CD4^{+}CD45RO^{+}CD25^{hi}$ T cells, but not slowly-dividing $CD4^{+}CD45RA^{+}$ T cells, in which enrichment was not quantifiable[15]. Intravenous infusion allows a longer labeling phase but is more invasive and requires more intensive attention to safety issues such as the sterility/pyrogenicity of the infusate. Labeling for 24 h is adequate to capture the kinetics of $CD45RO^{+}$ and $CD45RA^{+}$ T cells[12, 16–18], B cells[19], central and effector memory T cells[17], regulatory T cells[7, 15], and leukemic cells in chronic lymphocytic leukemia[20]. Longer infusions have been used, such as 48 h[21–23] or 5 days[24–26]. The sustained levels

of enrichment achieved by longer infusions allow analysis of less rapidly dividing cell populations[5], but for very slowly dividing populations, the heavy water approach should be preferred.

Heavy Water Labeling

Heavy water labeling experiments in humans typically start with an oral bolus (or ramp-up) to achieve near-plateau body water enrichment, after which smaller daily doses are given (orally) to maintain body water enrichment at approximately the same level over a timescale of several weeks. During intake of the initial bolus subjects may experience transient vertigo or nausea due to an effect on the inner ear vestibular apparatus (see Note 8)[27]. Both the level of body water enrichment that is achieved and the duration of exposure to enriched body water influence the extent of label incorporation by a given cell population; depending on the cell population of interest, both the intended body water enrichment and the duration of labeling can be varied. Labeling protocols to study lymphocyte dynamics typically reach long-term body water enrichments of 1–3%[6, 13, 22, 28, 29]. Heavy water administration can in principle be continued as long as necessary for the cell populations under investigation; for lymphocyte studies the labeling period has typically been in the order of a few months[6, 13, 22, 28, 29]. Continuous administration for 9 weeks has been successfully applied to measure lymphocyte turnover in healthy individuals[13], in B-cell chronic lymphocytic leukemia (B-CLL) patients[28], and in HIV-1 patients (Vrisekoop, unpublished), and resulted in readily measurable label incorporation even by very slowly dividing human naive ($CD27^+CD45RO^-$) T cells[13].

1.3.2. Sampling

There are two elements to sampling: timing and cell selection. (A further consideration is the "compartment" in which the cells reside, but peripheral blood is the only compartment considered herein.) In both labeling approaches, both the precursor and product are sampled.

Deuterated Glucose Labeling

For glucose labeling, glucose enrichment in plasma (precursor) must be measured at sufficient time-points during the labeling phase to derive an area-under-curve estimate of enrichment × time (see Note 13)[5]. The number of samples is a compromise between reducing errors of estimation and reducing subject discomfort. Typically we use 6 time-points for 10-h oral labeling. Pinprick samples yield more than sufficient sample, although an indwelling intravenous catheter is an alternative (Fig. 2). For DNA analysis (product), all samples are typically taken during the post-labeling phase, although longer infusion studies have also collected up-labeling data[24–26]. We assume

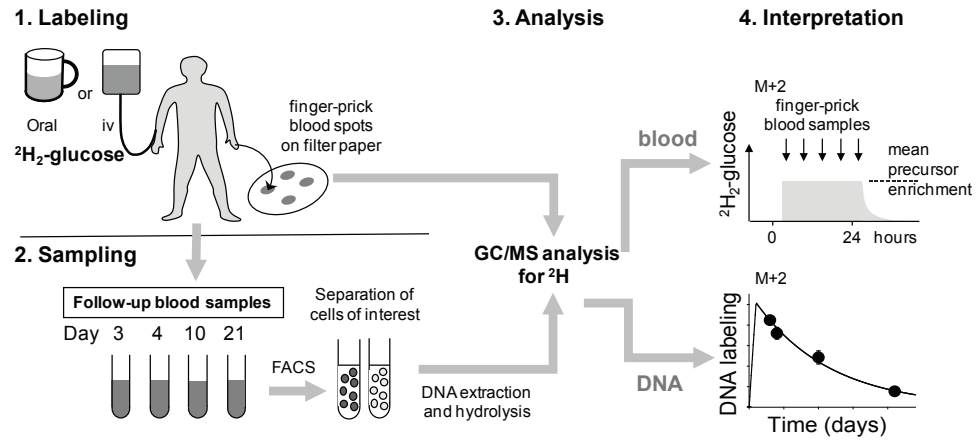

Figure 2. General schematic of protocol for analysis of lymphocyte kinetics using deuterium-labeled glucose. The example shown illustrates how either oral or intravenous administration of (6,6-$^2H_2$)-glucose may be used to label dividing lymphocytes in vivo. The deuterium content of DNA, analyzed by gas chromatography-mass spectrometry (GC/MS) is compared to the average glucose enrichment in plasma, E_{Glu} (both M+2) to derive fractional labeling curves over time. FACS, fluorescence activated cell sorting. Modified from Macallan et al.[5].

that maximal intracellular labeling occurs at or very shortly after the end of the glucose administration phase on the basis that blood glucose and intracellular dNTP pools are likely to be small and short-lived; *t½* for blood glucose is <2 h and in vitro DNA labeling occurs within an hour of introduction of labeled glucose to the culture media (Macallan, unpublished observations). However, maximal labeling of circulating cells in blood does not occur until considerably later; the length of this "lag" phase has not been well-defined but we find what appears to be a delay of about 2–3 days between division, presumably in lymphoid compartments or tissues, and release into the bloodstream[5]. We therefore suggest delaying initial sampling until ≥day 3. After this peak of labeling, multiple follow-up samples are collected from which the progressive loss of label can be monitored.

Heavy Water Labeling

For heavy water labeling, body water ^2H_2O enrichment (precursor) must be well monitored both during the labeling and post-labeling phases. Because it takes several days to reach plateau levels of heavy water in the body fluids (plasma, urine), it is essential to sample frequently in the period from start of labeling until steady-state levels of heavy water have been reached. Similarly, heavy water has a slow wash-out after labeling has been terminated, hence monitoring how body water enrichment decreases post-labeling is important. Plasma or urine can be used, but urine is the

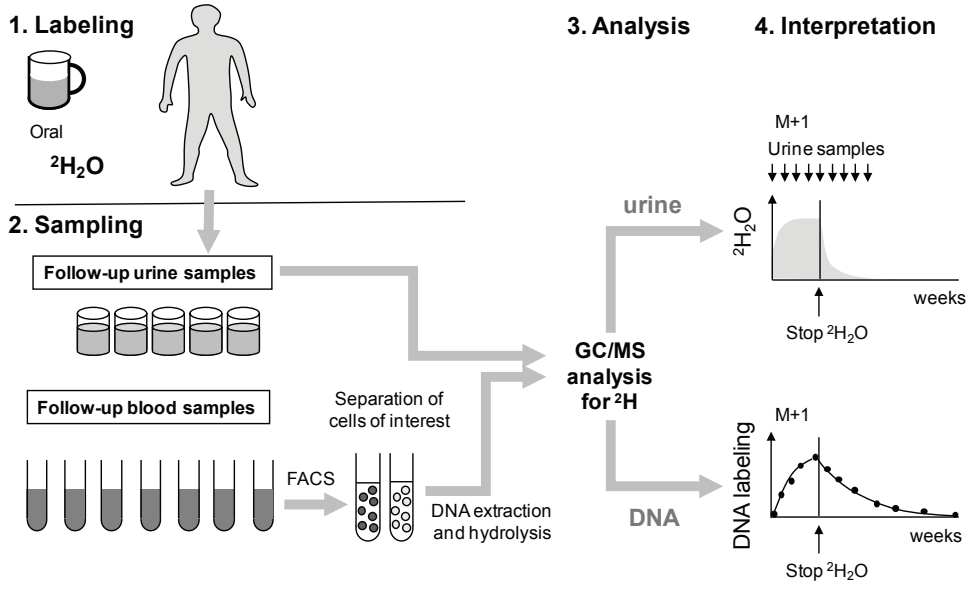

Figure 3. General schematic (as Figure 2.) of protocol for analysis of lymphocyte kinetics using deuterium-labeled water. The example shown illustrates how oral intake of ^2H_2O may be used to label dividing lymphocytes in vivo. In addition to measuring the deuterium content in DNA, urine samples are taken to allow monitoring of the deuterium enrichment in body water over time. Both DNA and urine deuterium enrichment are analyzed for M+1 enrichment by gas chromatography-mass spectrometry (GC/MS).

most practical because urine samples are easy for subjects to collect at home. Enough samples can thus readily be collected for reliable curve-fitting (Fig. 3).

For DNA analysis (product), samples are taken during the labeling and post-labeling phases. Cell analysis can be less frequent than urine sampling and is a compromise between reducing errors of estimation and reducing subject discomfort. Since a great deal of information can be obtained from the start of the early labeling phase and the start of the post-labeling phase, it is important to collect sufficient early sampling points. Typically, 6 samples (in addition to the baseline sample) are taken during the labeling phase, and 7 samples post-labeling, but this can be varied according to the cell type investigated and the subjects that are included.

The maximum level of label incorporation that cells can possibly obtain should be determined by including granulocytes (or another cell type with rapid turnover, such as monocytes), in the analysis. Label incorporation by cell populations of interest can be scaled between 0% and 100% by normalizing to this granulocyte maximum.

Details of how to sort the cells of interest are beyond the scope of this article. However, cell population purity needs to be considered carefully. Interpretation artefacts are likely if a high turnover population contaminates a low turnover one;

hence for example, excluding monocytes (high turnover) from lymphocyte preparations is critical.

1.3.3. Analysis

Isotopic Measurement

Isotopic enrichments are measured by mass spectrometry. Several approaches are possible. We use gas chromatography/mass spectrometry (GC/MS), which is sensitive, reproducible, and requires a relatively modest hardware investment. Alternatively, LC/MS approaches[30] require less sample processing whilst gas chromatography/ pyrolysis/ isotope ratio–mass spectrometry is able to measure very low enrichments but requires larger cell numbers (>10^7) [31]. For GC/MS, derivatization is required and most analyses of DNA enrichment have either used a pentose tetraacetate (PTA) derivative, analyzed by positive chemical ionization (PCI)[32] or a pentafluoro triacetate (PFTA) derivative which ionizes well under negative chemical ionization (NCI). The latter approach was described by Busch et al.[2] and is reproduced here with minor modifications. The same analysis is used for glucose and water labeling except that glucose labeling is monitored by measuring the ion with two additional mass units (M+2) and water labeling is monitored by measuring the ion with one additional mass unit (M+1)[2]. For analysis of (precursor) deuterium enrichment in glucose and urine, several alternative approaches have been described. We describe the procedures used in our laboratories.

1.3.4. Interpretation

The use of appropriate mathematical models to translate the enrichment data into biologically meaningful parameters is a critical step in this type of investigation. This is not straightforward and several approaches have been described. One important consideration is the discrepancy between information collected during labeling (typically for heavy water studies) and information collected post-labeling (both for deuterated glucose and heavy water studies). The rate of label acquisition during labeling is determined by the average turnover rate of the population: all cells, i.e., cells that divided and incorporated label and non-divided unlabeled cells, together determine the fraction of label in the total cell population. This part of the labeling curve therefore reflects what is happening in the population as a whole. In contrast, the rate of loss of label during the post-labeling phase reflects the loss of only those cells that became labeled because of recent cell division. If cell populations are kinetically heterogeneous, i.e., if they consist of 2 or more sub-populations with different turnover characteristics, the loss rate of labeled cells tends to be higher than the average turnover rate of the population as a whole, because the labeled fraction is biased towards cells with rapid turnover[1, 11]. Only if populations are kinetically homogeneous, i.e., if all cells have the same rate of turnover, will the loss rate of labeled cells truly

reflect the average turnover rate. Because of this complication, mathematical models are needed to extract the average turnover rate of a population of cells from deuterium labeling data.

Deuterated Glucose Labeling

Because deuterium enrichment cannot be detected in lymphocytes during the first days of deuterated glucose labeling and labeling periods are generally very short, it is difficult to estimate the average turnover rate during the labeling phase in deuterated glucose labeling experiments. Instead, data collected during the post- labeling phase are typically used to estimate the average turnover rate. Because the loss of label

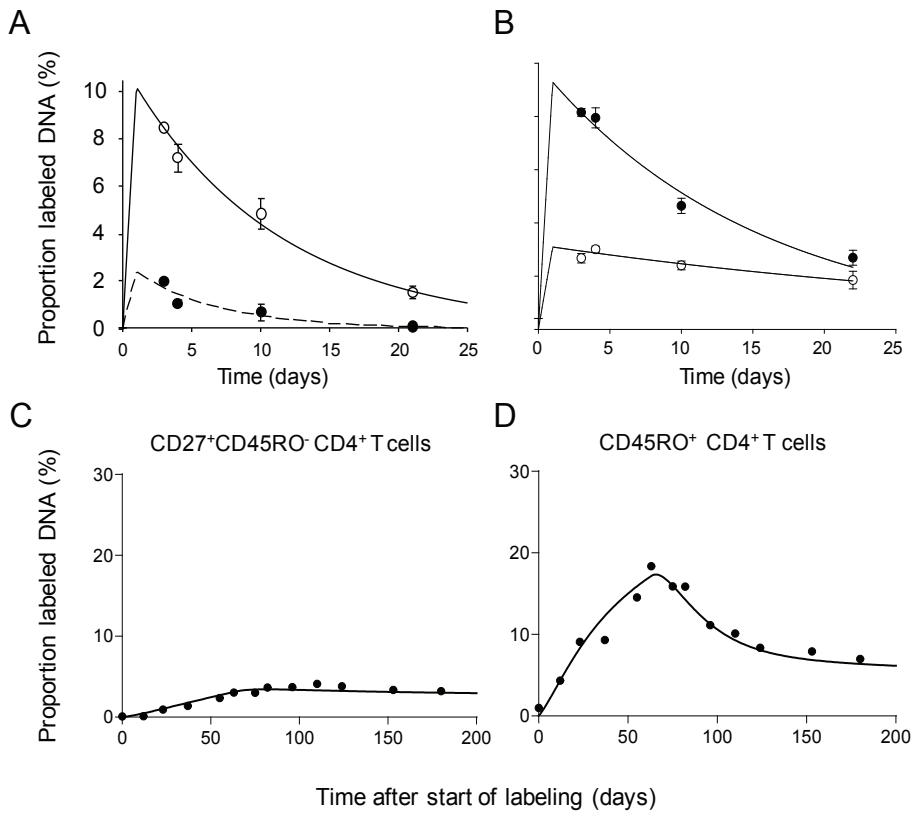

Figure 4. Typical lymphocyte subpopulation enrichment curves. (A) and (B) Fraction of labeled DNA, taken as fraction of labeled cells (*F*, %) from DNA labeling of T-lymphocyte subpopulations for 1 day: (A) $CD4^+$ $CD25^{bright}$ regulatory T cells (open circles) with high turnover versus $CD4^+$ $CD25^-$ cells (filled circles, dashed line), and (B) $CCR5^+$ (filled circles) and $CCR5^-$ (open circles) $CD45RO^+CD4^+$ T cells, from healthy young subjects following labeling with $^2H_2$-glucose. (Adapted from [15] and [37].) (C) Slowly dividing naive ($CD27^+$ $CD45RO^-$) $CD4^+$ T cells, and (D) rapidly dividing memory ($CD45RO^+$) $CD4^+$ T cells from a healthy individual after labeling with heavy water for 9 weeks (vertical bar) (Adapted from [13]).

post-labeling does not reflect the cell population as a whole, the average turnover rate is estimated via back-extrapolation of the post-labeling data to the moment of label cessation. Using this approach, information about the labeling phase can be obtained even though no data points were collected during this phase (Fig. 4A, B).

Heavy Water Labeling

In heavy water labeling experiments, the duration of heavy water administration permits frequent sampling both during the labeling and the post-labeling phase. The entire labeling curve (composed of both labeling and post-labeling data) can therefore yield reliable average production estimates (Fig. 4C, D).

Because body water enrichment is changing during the labeling period (it takes several days before body fluids reach a stable level of ^2H_2O enrichment) and after cessation of labeling (it takes several days before ^2H_2O is completely washed out), the fraction of labeled nucleotides in the dNTP pool progressively changes over time. Hence, cells that divide shortly after the start of labeling will not have the same probability of incorporation of labeled dNTPs as cells that divide when body water enrichment has reached a plateau. Conversely, during the post-labeling phase newly synthesized dNTPs will still become labeled as long as ^2H_2O has not been fully washed out. Therefore the loss of label does not simply reflect the disappearance rate of (labeled) cells, as dividing cells continue to incorporate label during the post-labeling phase. Mathematical modeling is essential to correct for the changing levels in body water enrichment during the entire sampling period (Fig. 1)[13].

2. Materials

For human studies, prior institutional and ethical approval should be obtained in accordance with local and national guidelines and regulations; informed consent must be obtained from all subjects before any interventions.

2.1 Labeling

2.1.1. Deuterium-labeled glucose

1. (6,6-$^2H_2$)-glucose (Cambridge Isotopes Inc or Isotec, Sigma-Aldrich); should be sterile and, if given intravenously (Option B), certified pyrogen-free (see Note 1).
2. Infusion fluids: water for injections or 0.45% saline for injection (Baxter Healthcare UK).

Option A—Oral Administration

1. Weigh out 0.6–1.0 g/kg body weight deuterated glucose.

2. Make up to 240 ml final volume with water. Once dissolved use fresh or store at 4°C (see Note 2).

Option B—Intravenous Administration

1. Prepare (6,6-$^2H_2$)-glucose infusate by taking 0.5–1 g/kg body weight (6,6-$^2H_2$)-glucose and reconstituting into 1,000 ml of 0.45% saline or water for injection (see Note 3). Withdraw approximately 200 ml, dissolve the glucose powder, and reinject into the infusate bag(s) through a 0.2 µm filter (because of volume expansion, the final volume will be increased). Prepare shortly before use and store at 4°C (see Note 3). Observe sterility precautions throughout to avoid contamination.

2.1.2. Deuterated water

1. Deuterium oxide (D, 99.8%, Cambridge Isotope Laboratories). Follow local and national guidelines and regulations for testing: usual requirements would be for confirmation that the product meets requirements for purified water.
2. For the oral bolus, weigh out 10 ml deuterated water per kg body water (see Note 4). Body water is assumed to be 60% and 50% of body weight for males and females, respectively.
3. Maintenance dose = 1.25 ml deuterated water/kg body water per day. Subjects can take their deuterated water doses at home. Aliquot into amounts depending on the volume of their personal maintenance dose, the frequency of visits, and shelf-life.
4. Use fresh water; the shelf-life is determined locally and relates primarily to possible microbial contamination.

2.2. Sampling

2.2.1. Blood withdrawal and urine sampling

1. Equipment for venepuncture and collection of samples: heparin-containing tubes, urine containers (for ^2H_2O labeling only), etc., and standard reagents for PBMC isolation by Ficoll density gradient centrifugation will be required.

2.2.2. Cell separation reagents

1. Reagents for magnetic or flow-cytometric separation will be required but are beyond the scope of this protocol.

2.3. Analysis

2.3.1. DNA extraction reagents

1. Use a proprietery DNA extraction kit, e.g., Qiagen QiaAmp Micro DNA extraction kit for small cell number samples; alternatively, use Macherey Nagel NUCLEOSPIN Blood Quick Pure or Qiagen DNeasy kit if cellular material/DNA is abundant, or Qiagen Flexigene kit for whole blood (baseline).

2.3.2. DNA hydrolysis reagents (following published protocols[2])

1. Water, molecular biology grade.
2. 1 M NaOH, molecular biology grade.
3. Sodium acetate.
4. Acetic acid.
5. Zinc sulphate.
6. Acid phosphatase (potato, 1 kU; Calbiochem).
7. S1 nuclease (Sigma).

2.3.3. GC/MS derivatization reagents for DNA analysis

Reagents marked * have significant toxicities — use protective equipment and follow local and national guidelines.

1. Pentafluorobenzyl hydroxylamine* (PFBHA, 1 mg/ml aqueous solution). Prepare solution fresh; store at 4°C for <1 week.
2. Acetic Anhydride* (Sigma-Aldrich).
3. N-methylimidazole* (Sigma-Aldrich). Store dry at 4°C.
4. Sodium sulphate, granular, anhydrous.
5. Dichloromethane* (Sigma-Aldrich).
6. Ethyl acetate (VWR International).

2.3.4. GC/MS derivatization reagents

Plasma Glucose Enrichment

1. Hydroxylamine hydrochloride* (Sigma-Aldrich).
2. Pyridine* (Sigma-Aldrich).

Body water enrichment

1. Calcium carbide (Sigma-Aldrich).

2.3.5. Standard solutions

1. Unlabeled DNA (molecular biology grade, e.g., calf thymus, Sigma-Aldrich).

Deuterated Glucose Labeling

1. DNA enrichment analysis: Combine (5,5-$^{2}H_{2}$)-2-deoxyribose (Cambridge Isotopes Inc.), which generates an (M+2) ion, with unlabeled deoxyribose (Sigma) to produce solutions of known proportions of labeled/unlabeled material covering the expected analytic range (0–1% atom percent express, APE = (M+2)/((M+0) + (M+2))).
2. Analysis of precursor (glucose) enrichment: Glucose (Sigma). Combine with (6,6-$^{2}H_{2}$)-glucose from Subheading 2.1.1 to prepare a standard curve of 0–50% enriched glucose.

Heavy Water Labeling

1. DNA enrichment analysis: Combine 1-^{13}C-deoxyadenosine (Cambridge Isotopes Inc.), which generates an (M+1) ion, with unlabeled deoxyadenosine (Sigma) in known proportions to cover the expected analytic range (0–10% APE for water labeling).
2. Analysis of precursor (body water) enrichment: Combine $^{2}H_{2}O$ (see Subheading 2.1.2) with $H_{2}O$ to prepare standards with enrichment 0.25%, 0.5%, 1%, 2% (volume to volume ratio), and higher if the experimental range is larger. As controls, use urine to which $^{2}H_{2}O$ is added in multiple concentrations.

2.3.6. Equipment

1. Heat block to dry under nitrogen gas, “speedvac” or equivalent sample concentrator.
2. Cell sorting equipment.
3. Gas Chromatograph Mass Spectrometer (GC/MS; Agilent 5973/6890 with HP-225 or DB-17 column, Agilent Technologies, or equivalent).

Deuterated Glucose Labeling

1. Lancets.
2. Filter paper.

Option B—Intravenous administration

1. 0.2 µm filters (Sartorius Stedim Biotech GmbH).
2. Infusion pump (IVAC 590 volumetric pump, or equivalent), calibrated gravimetrically (see Note 5).
3. Canula and intravenous administration sets (Venflon, BD Medical or equivalent).

Heavy Water Labeling

1. GC/MS equipment with column: Porabond Q, 25 m × 0.32 mm × 15 µm (Chrompack).

3. Methods

3.1. Labeling

Remember to take baseline samples (Subheading 3.2.1) before labeling.

3.1.1. Deuterated glucose

Option A—Oral Administration

1. Take oral glucose solution (Subheading 2.1 —option A); concentration should be about 200 g/l and volume 240 ml. Administer 36 ml oral glucose solution at time zero (T0). Aliquot the glucose solution into a disposable cup from which the subject drinks. Follow with >2 rinses of the cup with water, each of which the subject should drink. Repeat for all doses.
2. Administer further 10 ml doses every half-hour thereafter until 10 h later (T10). Meals should be restricted to ≤200 kcal (low glycaemic index foods are preferred) to avoid large changes in glucose enrichment. Commercially available “diet” meals that typically comprise about 200 kcal each (~15 g carbohydrate, ~8 g fat) are suitable. Meals may be given every 2–3 h. Discourage physical activity.
3. Monitor glucose enrichment with finger-prick blood samples, as below, Subheading 3.2.2 .

Option B—Intravenous Administration

1. Insert intravenous canula — can also be used for baseline blood sample (Subheading 3.2.1); flush canula with 0.9% saline.
2. Take intravenous glucose solution (Subheading 2.1 — Option B); concentration should be about 60 g/l and volume about 1,100 ml (see Note 2).
3. Set up infusion equipment. Start infusion at 300 ml/h and record the exact start time.
4. Run at 300 ml/h for 15 min (75 ml), as priming dose, then at ~43 ml/h thereafter (see Note 6).
5. Administer small regularly-spaced meals. We typically give four meals (each ≤200 kcal) at ~3, 6, 9, and 12 h with a snack at 15h and a smaller meal at 23 h. Discourage excessive physical activity.
6. Monitor subject body temperature, pulse and blood pressure at least every 4 h (see Note 7).

7. Monitor glucose enrichment with finger-prick blood samples (see Subheading 3.2.2).
8. At the end of infusion, record the exact time. This is needed to calculate the area under curve of glucose enrichment versus time, against which DNA labeling is compared (Subheading 3.3.1 , step 17).

3.1.2. Heavy water

Remember to take baseline samples (Subheading 3.2.1) before labeling.

1. Calculate the volume of the start bolus (typically between 200 and 400 ml based on the weight of the participant (as in Subheading 2.1.2). Divide into aliquots, for half-hourly administration, distributed evenly over the day. Phased intake is important to reduce the occurrence/severity of dizziness due to transient side effects on the vestibular apparatus (see Note 8). Every half hour, aliquot one portion into a disposable cup from which the subject drinks. Do this until the last dose is taken (see Note 8). Subjects are encouraged to have breakfast and eat and drink normally during the day.
2. Monitor the increase in body water enrichment resulting from the start bolus by taking a urine sample after administration of the last portion of the start bolus (see Subheading 3.2.2, body water enrichment).
3. After administration of the bolus, subjects are given heavy water to drink their daily maintenance dose at home for the indicated period of time.

3.2. Sampling

3.2.1. Baseline samples

1. Take baseline blood sample by venepuncture (*before labeling*); aliquot for tests as follows:
   (a) Baseline DNA enrichment—heparinized whole blood or sorted cells (the baseline DNA sample may be processed straightaway or frozen at −20°C and processed later as described in Subheading 3.3.2).
   (b) Complete blood count/differential lymphocyte count to aid interpretation of results.
   (c) Other clinical samples, e.g., biochemistry, serology (~5 ml) as required for clinical interpretation.
   (d) For glucose labeling: Baseline glucose enrichment — 3–4 blood spots on filter paper; air-dry then store at 4°C until analysis.

3.2.2. Monitoring precursor enrichment

Glucose Enrichment

1. Pinprick carefully cleaned finger/thumb and blot 3–4 spots onto filter paper at time-points: 1, 4, 7, and 10 h for Option A (oral administration), or 1, 4, 8, 12, 20 and 23 h for Option B (intravenous administration), in addition to baseline (T0), already taken (see Subheading 3.2.1) (see Note 9).
2. Leave to air-dry (≥10 min).
3. Store dried blood spots on filter paper at 4°C until glucose extraction.

Body water enrichment

1. Take the first urine sample directly after the last aliquot of the oral bolus (see Subheading 3.1.2). After this, it is recommended and sufficient to sample once or twice a week from start of labeling until a steady-state level is reached (usually within the first 3 weeks of labeling), and from the end of labeling until heavy water is completely washed out (usually within the first 3 weeks post-labeling). Depending on the length of the plateau phase during labeling, urine can be collected during this phase once a week or less, to ensure that steady state levels are maintained. For example, in a 9 week labeling experiment, urine can be collected once or twice in week 1 and 2 and once in week 3, 4, 5, 6, 7, and 9 during labeling, and post-labeling once or twice in week 10 and 11, and once in week 12, 13 and 14 of the study. Urine samples can easily be collected at home, reducing the number of visits and can be frozen at −20°C until further analysis (see Subheading 3.3.1).

3.2.3. Blood sampling and cell sorting to monitor DNA deuterium enrichment

1. Take follow-up blood samples (~50 ml; volume will depend upon the frequency of the cell of interest and analytic sensitivity) into preservative-free heparin (≥20 U/ml blood) collection tubes (alternative tubes may be suitable for some cell-sorting procedures).
   (a) For glucose labeling, e.g., at 3, 4, 10, and 21 days postlabeling.
   (b) For $^{2}H_{2}O$ labeling, at frequent intervals over the following weeks, both during and after labeling. For example, after 1, 2, 3, 4, 6, and 9 weeks (during labeling) and after 10, 11, 12, 14, 16, 21, and 30 weeks of the start of the study (post-labeling).
2. Isolate PBMC by density centrifugation on Ficoll-Paque (Amersham Biosciences) and sort cell populations of interest (see Note 10).
3. Proceed to DNA extraction (Subheading 3.3.2) or store separated cells frozen at −70°C until DNA extraction (see Note 10).

3.3 Analysis

3.3.1. Precursor enrichment analysis

Blood Glucose Enrichment

1. This is achieved by first extracting glucose from filter paper blood spots, then derivatizing to the aldonitrile triacetate (ATA) derivative and finally GC/MS analysis (see Note 11).
2. Cut at least two blood drops on filter paper from Subheading 3.2.2 into a 1.5 ml centrifuge tube and add 1 ml 50% ethanol. To avoid contamination, wear gloves and use designated scissors, cleaning blades between samples (see Note 9).
3. Leave at ambient temperature (approximately 20°C) for at least 30 min.
4. Vortex and transfer supernatant to another microcentrifuge tube.
5. Centrifuge (>15,000 × *g*, 10 min, ambient temperature, in a 1.5 ml centrifuge tube) to remove any precipitate; transfer to a clean tube and dry under nitrogen gas at 50°C. Ethanol extract can be stored at –20°C until derivatization.
6. Make a fresh solution of 1% w/v hydroxylamine·HCl in pyridine (1 mg/100 µl).
7. To the dried samples from step 5, and to standards of glucose of known enrichment (from Subheading 2.3.5), add 25 µl of hydroxylamine/pyridine reagent, seal and mix gently.
8. Heat the samples at 100°C for 60 min in a dry heat block.
9. Cool and quick spin the samples in a microfuge.
10. At ambient temperature, add 25 µl of acetic anhydride and seal the tube. Mix gently.
11. Incubate at room temperature for 30 min. To ensure completion of the derivatization reaction, heat for the last 10 min at 70°C in a heat block.
12. Quick spin the samples in a microfuge, to ensure all the solution is at the bottom of the tube, then dry at 50°C under nitrogen.
13. Resuspend the derivatized samples and standards in 400 µl of ethylacetate.
14. Vortex briefly, then pulse-microfuge to remove any particulate matter or precipitate, transferring the supernatant to vials ready for analysis by GC/MS.
15. Analyze by GC/MS, monitoring in SIM mode for ions *m/z* 328 (M+0) and 330 (M+2). We use an Agilent 5973/6890 with HP-225 column (Agilent Technologies) (see Note 12).
16. Determine enrichment from the ratio of ions (M+2)/((M+0)+(M+2)), calibrating against standard glucose samples of known enrichment from Subheading 2.3.5 .
17. Calculate the area under curve (AUC) for glucose enrichment versus time by the trapezoid method[5, 7] (see Note 13). The corrected value gives the mean glucose × time enrichment value.

Body Water Enrichment

This section of the protocol follows the method described by Van Kreel et al.[33] by converting calcium carbide (CaC_2) and urine or plasma-derived water to acetylene (C_2H_2), with minor modifications. During this reaction, deuterium atoms from water are transferred to acetylene. Measured enrichment in acetylene is equal to the enrichment in urine or plasma (hence body water).

1. Weigh 30 mg powdered calcium carbide (CaC_2) in each GC vial.
2. Cap each vial and evacuate using a needle connected to vacuum.
3. Pipette 2 µl of urine (or plasma) through the cap on the calcium carbide using a microliter syringe (see Note 14).
4. Include a blank (distilled water), standards and controls.
5. Incubate for 5 min.
6. The gas inside the vials can now be injected into the GC/MS.
7. Analyze by GC/MS using selective ion monitoring (SIM) quantifying ions *m/z* 26 (M+0) and *m/z* 27 (M+1) for H_2O and ^2H_2O, respectively.

3.3.2. DNA enrichment analysis

This section of the protocol follows the method described by Busch et al.[2] digesting DNA to release nucleosides, then derivatizing to the pentafluoro triacetate (PFTA) derivative before GC/MS.

1. Take sorted cells from Subheading 3.2.3 (including baseline) and extract DNA using a commercial kit (see Note 15). If using the Qiagen QiaAmp Micro DNA extraction kit, follow the protocol modifications described by Busch et al.[2]; specifically, at the end of extraction, DNA should be suspended in 200 µl water, not buffer. Store DNA at −20°C or proceed directly to hydrolysis, (see next step). The minimum number of cells will depend upon local analytic sensitivity and should be derived prior to defining blood volumes required for the subpopulation of interest. Alternatively, sorted cell pellets can be boiled at 100°C in 200 ul of water for one hour and put on ice immediately for 10 minutes.
2. To digest the extracted DNA samples, or boiled samples, as described by Busch et al.[2], add 50 µl of hydrolysis cocktail and incubate at 37°C overnight with shaking.
3. Derivatize the digested DNA samples to nucleoside pentafluoro triacetate (PFTA) derivatives as follows, alongside (5,5-$^2H_2$)-ribose (for M+2) or 1-^{13}C-deoxyadenosine (for M+1) standard solutions of known enrichment from Subheading 2.3.5 to calibrate isotope ratios.
4. Transfer the digested samples into 16 mm × 100 mm screwcapped glass tubes. To each sample/standard add:

(a) 100 µl of freshly made aqueous pentafluorobenzyl hydroxylamine solution (1 mg/ml).
(b) 75 µl of glacial acetic acid.

5. Cap the tubes and incubate on heating block for 30 min at 100°C.
6. Remove samples and allow to cool to room temperature.
7. Add 1 ml of acetic anhydride, then 100 µl of N-methylimidazole, mixing immediately. Perform this step in a fume hood, wearing protective goggles and pointing the opening of the tube away from you. Samples may splash as the exothermic acetylation reaction proceeds due to sudden overheating. Allow the reaction to proceed at ambient temperature for 15–20 min during which the samples will cool down.
8. Add 2 ml of water to the reactions, vortex for 10 s.
9. Add 750 µl of dichloromethane to the tubes and vortex for 5 s. Allow phases to separate (~1 min).
10. Transfer 500 µl of the bottom (organic) layer (from step 9) into 2 ml microcentrifuge tubes. Avoid transferring any of the aqueous phase, which may introduce contaminants. Wet the pipette tip with dichloromethane before transfer to help reduce inadvertent mixing.
11. Add a further 750 µl of dichloromethane to the reaction tubes and repeat the dichloromethane extraction (vortex for 5 s, then allow phases to separate, ~1 min), adding the organic layer to that already extracted.
12. Dry the microcentrifuge tubes — we use content using a SpeedVac at ambient temperature for at least 4 h, or ideally overnight. Leave the heat setting "off" as heating may cause evaporative loss of some derivative. Verify complete drying visually; avoid residual moisture or acid as this may damage the GC column. Drying in a stream of nitrogen is not sufficient to remove residual acetic acid.
13. Resuspend each sample in 250 µl of ethyl acetate, vortex and pulse centrifuge to remove any precipitate or solid material. Transfer the supernatant to a GC glass insert. Avoid transfering any precipitate or solid material.
14. Evaporate ethyl acetate (SpeedVac, ambient temperature, ~1 h).
15. Resuspend each sample in a volume of ethyl acetate suitable for the GC/MS autosampler (typically 50 µl). Place the glass insert into a labeled GC vial and cap immediately.
16. Analyze by GC/MS using selective ion monitoring (SIM) quantifying ions *m/z* 435 (M+0), and *m/z* 437 (M+2) for deuterated glucose or *m/z* 436 (M+1) for heavy water labeling (see Note 16). Use the isotope ratio of abundance-matched samples to calculate the enrichment of deuterated deoxyadenosine, calibrating against standard curves of known enrichment from Subheading 2.3.5 (see Note 17).

3.4. Interpretation

Data Analysis: deduction of cellular production and disappearance rates

Different models have been proposed to analyze enrichment data from stable isotope labeling experiments. The most appropriate model depends on the exact biology of the cells under investigation (see Note 18). Here we present a basic model that is applicable to many circumstances, and which captures the general principles of a stable isotope labeling experiment. Models like these need to be fitted to the labeling data to obtain biological parameters such as the average turnover rate of a lymphocyte population.

1. Express the enrichment data as the ratio of labeled to total PFTA-nucleoside derivative (predominantly arising from deoxyadenosine, although all purine nucleosides should be similarly labeled). This gives the fraction of labeled DNA fragments $L(t)$. Plot the enrichment data as a function of time t. Enrichment should start at zero at baseline, rise to a peak (at or after label cessation), then fall thereafter.
2. Independent of the source of stable isotope that is used (i.e., deuterated glucose or heavy water), the change in the fraction of labeled DNA fragments in a population of cells over time can be described by the following differential equation:

$$dL(t) / dt = pc\,P(t) - d^* L \quad (1)$$

where p is the average production rate of the cells, d^* the loss rate of labeled cells, and $c\,P(t)$ is the chance that an incorporated deoxyadenosine is labeled (see Note 18). The latter term is a composite between the availability of deuterium (the precursor) $P(t)$ which changes over time, and an amplification factor c accounting for the fact that there are multiple hydrogen atoms in a single DNA fragment that can be replaced by deuterium[13].

3. The curve described by Eq. 1. is fitted to the enrichment data using nonlinear least squares regression. This can be done with a number of software packages that allow user-defined equations, such as *R* or *Sigmaplot* (Systat Software Inc). Typical data plots and curve-fitting are shown in Fig. 4 .
4. The half-life, $t½$, of the lymphocytes under investigation can be calculated as $\ln 2/ p$. Note that p will include proliferation at all sites, e.g., for naive T cells it will include not only peripheral T-cell proliferation but also production of new lymphocytes by the thymus.

Deuterated Glucose Labeling

1. Because of the fast turnover of glucose, during the labeling phase, $P(t)$ can

be assumed to be continuously at its maximal level, while after label cessation $P(t) = 0$. Precursor enrichment during labeling is typically measured as the label enrichment in plasma glucose multiplied by a factor 0.73 to account for intracellular label dilution[4] (see Note 13).

2. In most deuterated glucose labeling experiments, label is given so briefly that enrichment data during the labeling phase are lacking. In that case, the average turnover rate of the cell population, p , is estimated by fitting the loss of label after label cessation to the solution of Eq. 1 with $P(t) = 0$ [11, 12]. The loss curve is subsequently back-extrapolated to the moment of label cessation in order to estimate p. If deuterated glucose is given for longer periods, proceed as under *Heavy water labeling*, step 2.

Heavy Water Labeling

1. Because the turnover rate of water is relatively slow, changes in the availability of deuterium need to be explicitly taken into account. This can be done by fitting a simple exponential accrual and loss function to the enrichment data from urine:

$$P(t) = f\,(1 - e^{-\varepsilon t}) + \beta e^{-\varepsilon t} \text{ during label administration} \quad (2a)$$

and

$$P(t) = (f\,(1 - e^{-\varepsilon T}) + \beta e^{-\varepsilon T}) e^{-(\varepsilon t - T)} \text{ after label cessation} \quad (2b)$$

where f represents the fraction of deuterated water in the drinking water, ε the turnover rate of body water per day, and β the body water enrichment that is attained after the boost of label by the end of day 0.

2. The best fit of the function $P(t)$ is substituted into Eq. 1 , after which the latter function is fitted to (a) the level of label incorporation in a population of cells that turn over very rapidly, such as granulocytes, so as to estimate the value of c, and subsequently to (b) the enrichment data of the cell population of interest during and after the labeling phase, so as to estimate its turnover parameters p and d^*.

4. Notes

Parentheses demonstrate whether the note refers to glucose or heavy water labeling.

1. (gluc) (6,6-$^2H_2$)-glucose should be tested for sterility and pyrogenicity and certified by the manufacturer. Microbial contamination of the infusate must be avoided. Reconstitution as an infusate must be performed under sterile conditions. Passage of reconstituted glucose through a 0.2 µm filter is advisable to ensure sterility.
2. (gluc) Once reconstituted, use fresh or store at 4°C. Glucose is chemically stable; the shelf-life is determined by local pharmacy guidelines and relates primarily to possible microbial contamination.
3. (gluc) Hyperosmolar solutions may cause phlebitis. The final osmolarity of the solution will be about 450 mOsmol/L; this should not cause phlebitis. Avoid using infusion volumes of less than 1,000 ml.
4. (water) Because the administration of the bolus of deuterated water during the first day can lead to vertigo and/or nausea, one can lower the dose to, for example, 7.5 ml deuterated water per kg body water to minimize side effects. A draw-back is that the maximal level of label enrichment in the body water is attained later, but more frequent sampling of urine during the labeling phase will help to obtain the necessary information of how much label was available at any time-point. See also Note 8.
5. (gluc) Infusion pumps may not always run at the stated rate and should be calibrated gravimetrically prior to research use.
6. (gluc) A priming dose of about 1.8 times the hourly dose was found empirically to reach plateau levels in most subjects; under-priming or over-priming results in rising or falling glucose enrichments in plasma (respectively) and should be avoided. Glucose enrichment tends to rise overnight as feeding is not continued during this time. Such curves can be converted to a “square wave” by calculating AUC (see Note 13) and expressing this as the mean enrichment achieved throughout the duration of label administration However, results may be slightly biased either towards the earlier or later part of the day; this is not considered a significant bias.

   The infusion rate may need to be modified empirically as it will depend upon the infusion pump characteristics (which should be calibrated) and because the volume of the infusate is difficult to predict; bags often contain slightly more than the nominal volume to allow for line priming, and because adding glucose expands the volume, depending upon the amount added. Aim to give the whole dose over 24 h.
7. (gluc) In order to monitor for the possibility of a pyrogen or infusion reaction, subjects should be closely monitored by a clinically trained staff member and pulse, temperature, and blood pressure recorded at least every 4 h.
8. (water) Transient nausea or vertigo during intake of the initial bolus of ^2H_2O has been attributed to the density of heavy water being higher than the density of the endolymph fluid, which creates a transient density gradient to which the hair cells of the inner ear are sensitive[27]. Phased administration of the bolus in small portions spread over the day is usually effective in preventing or strongly reducing side effects on the inner ear. However, if individuals experience more severe and/or longer lasting side effects, it is possible to postpone the next

dose of $^{2}H_{2}O$ and have longer intervals between doses, or divide the bolus into even smaller doses. If side effects persist, the rampup protocol can be discontinued. In this case, body water enrichment will plateau later (see also Note 4). Intake of the daily maintenance dose has never been associated with any side effects.

9. (gluc) Aberrant or unexpectedly high glucose enrichment levels in blood spots may indicate contamination. Always plot the glucose time-profile. Avoid any possible contamination from the infusate or oral solution onto filter paper blood spots. This is a particular risk with the oral solution, which is easy to transfer from mouth or cup via hand to filter paper and is highly concentrated such that even trivial contamination will give aberrant results. Use disposable cups; take care that both the subject and operator wear gloves when handling oral glucose solution even though it is nonhazardous. Clean the subject's finger carefully prior to pinprick blood testing.
10. (both) We recommend sorting cells fresh. It may be possible to freeze the cells at –70°C prior to sorting. If cells are frozen, it needs to be established that freezing does not preferentially affect the recovery of the labeled cells of interest. We also recommend commencing DNA extraction from fresh cells by adding lysis buffer straight after sorting rather than storing as cell pellets. Note also that the use of intracellular staining protocols for cell sorting may reduce DNA yield.
11. (gluc) There are many published alternative derivatization and GC/MS protocols for analysis of isotopic enrichment of glucose.
12. (both) Detailed GC/MS protocols are beyond the scope of this article, but note that optimization of chromatography is crucial for reliable quantitation.
13. (gluc) Calculation of the area under curve (AUC) for glucose enrichment versus time by the trapezoid method applies the equation:

$$AUC = [E_0 + E_1] \times t_1 / 2 + [E_1 + E_2] \times (t_2 - t_1) / 2 + [E_2 + E_3] \times (t_3 - t_2) / 2 + \ldots t_n + AUC_{add}$$

where E is the glucose enrichment at times, 0, 1, 2, 3 … n , and AUC_{add} is an estimated additional post-infusion area (AUC_{add}) in order to allow for additional labeling that occurs during the die-away of labeled glucose. For a full discussion see Macallan et al.[5] and Vukmanovic-Stejic et al.[7].

Dividing this sum by the infusion/administration time gives the mean glucose enrichment, E_{Glu}. Multiply this by the correction factor derived for this cell type to obtain the mean precursor enrichment. (We have used 0.65 previously[5], but more recent studies suggest a value of 0.73 is appropriate for dividing lymphocytes; Kovacs et al. have used a slightly lower value of 0.60 in their studies[24, 25, 34].)

14. (water) Carbide and water form an explosive mixture. Do not weigh too much carbide in to the GC vials and do not pipette more than 2 µl of water onto the carbide.
15. (both) Alternative DNA extraction protocols and kits are available and may be used.
16. (both) Detailed gas chromatography and mass spectrometry (GC/MS) analysis protocols for DNA from deuterium labeling studies have been described in Busch et al.[2]. An alternative microcapillary liquid chromatography-electrospray ionization (LC-ESI)/MS has been described[30], an advantage of which is that it does not require a derivatization step. However, it may require larger sample amounts for quantitation.
17. (both) Isotope ratios are susceptible to abundance artifacts. Run samples as single injections first, to check abundance; then dilute or adjust injection volume to ensure equal abundances are achieved for all samples and standards; then repeat analysis of ratios in duplicate or triplicate.
18. (both) Most models assume that the size of the cell population under investigation is constant during the labeling protocol. Nevertheless, the average turnover rate p of the cell population does not necessarily equal the loss rate of labeled cells d^*. Equations can be adapted to model cell population sizes that are not constant over time.

The production rate p includes both production of the cells of interest within the specific cell population as well as any immediate precursors which divided in the presence of label and subsequently matured or trafficked to the pool of interest. The disappearance rate d^* includes cell death, net trafficking of cells out of the peripheral blood and disappearance due to phenotype switching.

This model has been widely applied[13, 17, 35], but it should be noted that this is not the only model available. For a review of alternative models see Borghans et al.[14]. For example, specific models have been developed to describe populations of cells that are kinetically heterogeneous, i.e., that consist of sub populations of cells with different rates of turnover[36].

Acknowledgments

We acknowledge financial support from the Medical Research Council (UK), the Wellcome Trust, the Charitable Trustees of St George's Hospital, London, and the Netherlands Organization for Scientific Research (NWO, grants 917.96.350 and 836.07.002) during the execution of studies included in this report.

References

1. Asquith B., Borghans J.A., Ganusov V.V., Macallan D.C. Lymphocyte kinetics in health and disease. Trends Immunol. 30:182–189 (2009).
2. Busch R., Neese R.A., Awada M., Hayes G.M., Hellerstein M.K. Measurement of cell proliferation by heavy water labeling. Nat. Protoc. 2:3045–3057 (2007).
3. Hellerstein M.K. Measurement of T-cell kinetics: recent methodologic advances. Immunol. Today 20:438–441 (1999).
4. Macallan D.C., Fullerton C.A., Neese R.A., Haddock K., Park S., Hellerstein M.K. Measurement of cell proliferation by labeling of DNA with stable isotope-labeled glucose: studies in vitro, in animals and in humans. Proc. Natl. Acad. Sci. U. S. A 95:708–713 (1998).
5. Macallan D.C., Asquith B., Zhang Y., de Lara C.M., Ghattas H., Defoiche J., Beverley P.C. Measurement of proliferation and disappearance of rapid turnover cell populations in human studies using deuterium-labelled glucose. Nat. Protoc. 4:1313–1327 (2009).
6. Neese R.A., Misell L.M., Turner S., Chu A., Kim J., Cesar D., Hoh R., Antelo F., Strawford A., McCune J.M., Christiansen M., Hellerstein M.K. Measurement in vivo of proliferation rates of slow turnover cells by 2H2O labeling of the deoxyribose moiety of DNA. Proc. Natl. Acad. Sci. U. S. A 99:15345–15350 (2002).
7. Vukmanovic-Stejic M., Zhang Y., Akbar A.N., Macallan D.C. Measurement of proliferation and disappearance of regulatory T cells in human studies using deuterium-labeled glucose. Methods Mol. Biol. 707:243–261 (2011).
8. Hellerstein M. Methods for measuring polymerisation biosynthesis: three general solutions to the problem of the “true precursor”. Diabetes Nutr. Metab. 13:46–60 (2000).
9. Cohen A., Barankiewicz J., Lederman H.M., Gelfand E.W. Purine and pyrimidine metabolism in human T lymphocytes. Regulation of deoxyribonucleotide metabolism. J. Biol. Chem. 258:12334–12340 (1983).
10. Reichard P. Interactions between deoxyribonucleotide and DNA synthesis. Annu. Rev. Biochem. 57:349–374 (1988).
11. Asquith B., Debacq C., Macallan D.C., Willems L., Bangham C. Lymphocyte kinetics: the interpretation of labelling data. Trends Immunol. 23:596–601 (2002).
12. Macallan D.C., Asquith B., Irvine A., Wallace D., Worth A., Ghattas H., Zhang Y., Griffin G.E., Tough D., Beverley P.C. Measurement and modeling of human T cell kinetics. Eur. J. Immunol. 33:2316–2326 (2003).
13. Vrisekoop N., den Braber I., de Boer A.B., Ruiter A.F., Ackermans M.T., van der Crabben S.N., Schrijver E.H., Spierenburg G., Sauerwein H.P., Hazenberg M.D., De Boer R.J., Miedema F., Borghans J.A., Tesselaar K. Sparse production but preferential incorporation of recently produced naive T cells in the human peripheral pool. Proc. Natl. Acad. Sci. U. S. A 105:6115–6120 (2008).
14. Borghans J.A., De Boer R.J. Quantification of T-cell dynamics: from telomeres to DNA labeling. Immunol. Rev. 216:35–47 (2007).
15. Vukmanovic-Stejic M., Zhang Y., Cook J.E., Fletcher J.M., McQuaid A., Masters J.E., Rustin M.H., Taams L.S., Beverley P.C., Macallan D.C., Akbar A.N. Human CD4+ CD25hi Foxp3+ regulatory T cells are derived by rapid turnover of memory populations in vivo. J. Clin. Invest. 116:2423–2433 (2006).
16. Macallan D.C., Wallace D.L., Irvine A., Asquith B., Worth A., Ghattas H., Zhang Y., Griffin G.E., Tough D.F., Beverley P.C. Rapid turnover of T cells in acute infectious mononucleosis. Eur. J. Immunol. 33:2655–2665 (2003).
17. Macallan D.C., Wallace D., Zhang Y., De Lara C., Worth A.T., Ghattas H., Griffin G.E., Beverley P.C., Tough D.F. Rapid turnover of effector-memory CD4(+) T cells in healthy humans. J Exp Med. 200:255–260 (2004).
18. Wallace D.L., Zhang Y., Ghattas H., Worth A., Irvine A., Bennett A.R., Griffin G.E., Beverley P.C., Tough D.F., Macallan D.C. Direct measurement of T cell subset kinetics in vivo in elderly men and women. J. Immunol. 173:1787–1794 (2004).
19. Macallan D.C., Wallace D.L., Zhang Y., Ghattas H., Asquith B., De Lara C., Worth A., Panayiotakopoulos G., Griffin G.E., Tough D.F., Beverley P.C. B cell kinetics in humans: rapid turnover of peripheral blood memory cells. Blood 105:3633–3640 (2005).
20. Defoiche J., Debacq C., Asquith B., Zhang Y., Burny A., Bron D., Lagneaux L., Macallan D.C., Willems L. Reduction of B cell turnover in chronic lymphocytic leukaemia. Br. J. Haematol. 143:240–247 (2008).
21. Hellerstein M., Hanley M.B., Cesar D., Siler S., Papageorgopoulos C., Wieder E., Schmidt D., Hoh R., Neese R., Macallan D., Deeks S., McCune J.M. Directly measured kinetics of circulating T lymphocytes in normal and HIV-1-infected humans. Nat. Med. 5:83–89 (1999).
22. Hellerstein M.K., Hoh R.A., Hanley M.B., Cesar D., Lee D., Neese R.A., McCune J.M. Subpopulations of long-lived and short-lived T cells in advanced HIV-1 infection. J. Clin. Invest. 112:956–966 (2003).
23. McCune J.M., Hanley M.B., Cesar D., Halvorsen R., Hoh R., Schmidt D., Wieder E., Deeks S., Siler S., Neese R., Hellerstein M. Factors influencing T-cell turnover in HIV-1-seropositive patients. J. Clin. Invest. 105:R1–R8 (2000).
24. Kovacs J.A., Lempicki R.A., Sidorov I.A., Adelsberger J.W., Sereti I., Sachau W., Kelly G., Metcalf J.A., Davey R.T. Jr, Falloon J., Polis M.A., Tavel J., Stevens R., Lambert L., Hosack D.A., Bosche M., Issaq H.J., Fox S.D., Leitman S., Baseler M.W., Masur H., Di M.M., Dimitrov D.S., Lane H.C. Induction of prolonged survival of CD4+ T lymphocytes by intermittent IL-2 therapy in HIV-infected patients. J. Clin. Invest. 115:2139–2148 (2005).
25. Read S.W., Lempicki R.A., Di M.M., Srinivasula S.,Burke R., Sachau W., Bosche M., Adelsberger J.W., Sereti I., Davey R.T. Jr, Tavel J.A., Huang C.Y., Issaq H.J., Fox S.D., Lane H.C., Kovacs J.A. CD4 T cell survival after intermittent interleukin-2 therapy is predictive of an increase in the CD4 T cell count of HIV-infected patients. J. Infect. Dis. 198:843–850 (2008).
26. Mohri H., Perelson A.S., Tung K., Ribeiro R.M., Ramratnam B., Markowitz M., Kost R., Hurley A., Weinberger L., Cesar D., Hellerstein M.K., Ho D.D. Increased turnover of T lymphocytes in HIV-1 infection and its reduction by antiretroviral therapy. J. Exp. Med. 194:1277–1287 (2001).
27. Brandt T. Positional and positioning vertigo and nystagmus. J. Neurol. Sci. 95:3–28 (1990).
28. Van Gent R., Kater A.P., Otto S.A., Jaspers A., Borghans J.A., Vrisekoop N., Ackermans M.A., Ruiter A.F., Wittebol S., Eldering E., van Oers M.H., Tesselaar K., Kersten M.J., Miedema F. In vivo dynamics of stable chronic lymphocytic leukemia inversely correlate with somatic hypermutation levels and suggest no major leukemic turnover in bone marrow. Cancer Res. 68:10137–10144 (2008).
29. Messmer B.T., Messmer D., Allen S.L., Kolitz J.E., Kudalkar P., Cesar D., Murphy E.J., Koduru P., Ferrarini M., Zupo S., Cutrona G., Damle R.N., Wasil T., Rai K.R., Hellerstein M.K., Chiorazzi N. In vivo measurements document the dynamic cellular kinetics of chronic lymphocytic leukemia B cells. J. Clin. Invest. 115:755–764 (2005).
30. Fox S.D., Lempicki R.A., Hosack D.A., Baseler M.W., Kovacs J.A., Lane H.C., Veenstra T.D., Issaq H.J. A comparison of microLC/electrospray ionization-MS and GC/MS for the measurement of stable isotope enrichment from a (2H2)-glucose metabolic probe in T-cell genomic DNA. Anal. Chem. 75:6517–6522 (2003).

31. Voogt J.N., Awada M., Murphy E.J., Hayes G.M., Busch R., Hellerstein M.K. Measurement of very low rates of cell proliferation by heavy water labeling of DNA and gas chromatography/ pyrolysis/isotope ratio-mass spectrometric analysis. Nat. Protoc. 2:3058–3062 (2007).

32. Neese R.A., Siler S.Q., Cesar D., Antelo F., Lee D., Misell L., Patel K., Tehrani S., Shah P., Hellerstein M.K. Advances in the stable isotopemass spectrometric measurement of DNA synthesis and cell proliferation. Anal. Biochem. 298:189–195 (2001).

33. Van Kreel B.K., van der Vegt F., Meers M., Wagenmakers T., Westerterp K., Coward A. Determination of total body water by a simple and rapid mass spectrometric method. J. Mass Spectrom. 31:108–111 (1996).

34. Stevens R.A., Lempicki R.A., Natarajan V., Higgins J., Adelsberger J.W., Metcalf J.A. General immunologic evaluation of patients with human immunodeficiency virus infection. In: Detrick B, Hamilton RG, Folds JD (eds). Manual of molecular and clinical laboratory immunology. ASM Press, Washington, DC, pp 848–861 (2006).

35. Asquith B., Zhang Y., Mosley A.J., de Lara C.M., Wallace D.L., Worth A., Kaftantzi L., Meekings K., Griffin G.E., Tanaka Y., Tough D.F., Beverley P.C., Taylor G.P., Macallan D.C., Bangham C.R. In vivo T lymphocyte dynamics in humans and the impact of human T-lymphotropic virus 1 infection. Proc. Natl. Acad. Sci. U. S. A 104:8035–8040 (2007).

36. Ganusov V.V., Borghans J.A., De Boer R.J. Explicit kinetic heterogeneity: mathematical models for interpretation of deuterium labeling of heterogeneous cell populations. PLoS Comput. Biol. 6:e1000666 (2010).

37. Macallan D.C., Zhang Y., De Lara C., Worth A., Beverley P.C. CD4+ T cell turnover is related to chemokine receptor expression and HIV viral co-receptor tropism. Proceedings of 17th conference on retroviruses and opportunistic infections abstract #270 (2011).

3

Maintenance of Peripheral Naive T cells is Sustained by Thymus Output in Mice but Not Humans

Ineke den Braber[1]*, Tendai Mugwagwa[2]*, Nienke Vrisekoop[1]*, Liset Westera[1], Ramona Mögling[1], Anne Bregje de Boer[1], Neeltje Willems[1], Elise H R Schrijver[1], Gerrit Spierenburg[1], Koos Gaiser[1], Erik Mul[3], Sigrid A Otto[1], An FC Ruiter[4], Mariëtte T Ackermans[4], Frank Miedema[1], José AM Borghans[1,2#], Rob J de Boer[2#], Kiki Tesselaar[1#]

[1] Department of Immunology, University Medical Center Utrecht, Utrecht, The Netherlands; [2] Theoretical Biology and Bioinformatics, Utrecht University, Utrecht, The Netherlands; [3] Sanquin Research, Landsteiner Laboratory and Academic Medical Center, University of Amsterdam, Amsterdam, The Netherlands; [4] Laboratory of Endocrinology and Radiochemistry, Academic Medical Center, University of Amsterdam, Amsterdam, The Netherlands

*, # These authors contributed equally.

Immunity, 2012 Feb 24;36(2):288-97

Parallels between T cell kinetics in mice and men have fueled the idea that a young mouse is a good model system for a young human, and an old mouse, for an elderly human. By combining in vivo kinetic labeling using deuterated water, thymectomy experiments, analysis of T cell receptor excision circles and CD31 expression, and mathematical modeling, we have quantified the contribution of thymus output and peripheral naive T cell division to the maintenance of T cells in mice and men. Aging affected naive T cell maintenance fundamentally differently in mice and men. Whereas the naive T cell pool in mice was almost exclusively sustained by thymus output throughout their lifetime, the maintenance of the adult human naive T cell pool occurred almost exclusively through peripheral T cell division. These findings put constraints on the extrapolation of insights into T cell dynamics from mouse to man and vice versa.

Introduction

Insights into human T cell dynamics, whether in healthy aging or during lymphopenia, have been largely based on experiments in mice. For example, slow naive T cell recovery in lymphopenic humans is thought to be caused by age related thymic atrophy[1], and long-term failure of immune reconstitution after stem cell transplantation (SCT) has been related to exhaustion of thymic output[2, 3]. Both interpretations were influenced by the important role of thymic output in naive T cell generation in mice. Likewise, thymic failure has been suggested to be important in $CD4^+$ T cell loss during HIV infection[4], and rapid thymic rebound is proposed to be responsible for T cell reconstitution in HIV infected patients during antiviral treatment[5]. The reason why insights into T cell dynamics are so widely extrapolated from mice to men and vice versa is that there are clear parallels between these species. In both species, thymus output declines with age[6, 7], which is probably responsible for the gradual decline in naive $CD4^+$ and $CD8^+$ T cell numbers, although naive T cell numbers decline less dramatically than thymocyte numbers[8, 9]. At old age the peripheral T cell pool becomes dominated by memory T cells[8, 10], coinciding with severe perturbations of the naive T cell repertoire and impaired immunity[11-13]. Together, such parallels have fuelled the idea that a young adult mouse is a good model system for a young adult human, and an old mouse, for an elderly human. In fact, there is no formal proof that such extrapolations are justified[14].

Using a unique combination of state of the art techniques in mice and men, we have directly quantified the contribution of de novo T cell production by the thymus and peripheral T cell division in mice and men. Based on T cell receptor excision circle (TREC) data, the by-products of V(D)J recombination in the thymus[15], we estimated that in healthy human adults ~90% of the naive $CD4^+$ T cell pool has been generated by peripheral T cell proliferation. By labeling mice with deuterated water (^2H_2O)[16], we estimated that the average life span of murine naive $CD4^+$ and $CD8^+$ T cells throughout life is ~7 and 11 weeks, respectively, which is ~40-fold shorter than in humans[17]. Analyses of the change in naive T cell numbers following thymectomy revealed that in mice, naive T cells are almost exclusively derived from thymus output, even at very old age.

Summarizing, our data show that mice and men are incomparable with respect to naive T cell maintenance because the major source by which naive T cell numbers are maintained is fundamentally different in mice and men. These results have obvious limitations for mouse experiments that aim to understand e.g., T cell reconstitution in lymphopenic patients or the effects of aging in healthy humans.

Results

Contribution of thymic output to the human naive T cell pool

To quantify the relative contribution of thymic output in humans, we measured the TREC content of naive CD4⁺ T cells in healthy individuals of different ages (Fig. 1A). We have previously argued that TREC contents cannot be used as a measure for daily thymic output, because the TREC content of a T cell population increases with thymic output and with cell loss and declines with cell division[18-20]. Given that TRECs are not copied during peripheral proliferation, each TREC remains a true marker of thymic origin, and the number of TREC-positive cells in a population reflects the number of cells that were produced by the thymus at any point in time and that are still present in the periphery. Conversely, the number of TREC-negative naive T cells reflects the number of cells in the population that have been produced by peripheral proliferation. The average TREC content of a naive T cell population can therefore be used to estimate the fraction of cells that were originally produced by the thymus.

One complication is that only a fraction of the cells leaving the thymus is actually carrying a TREC. To estimate the fraction of cells that originated from the thymus, one therefore has to normalize the observed TREC content by the average TREC content of a recent thymic emigrant (RTE). Thanks to the fact that the average TREC content of thymocytes does not decrease with age[21], we could estimate the TREC content of RTEs by measuring TRECs in single positive (SP) thymocytes from children who underwent cardiac surgery. Along with these samples, we measured TRECs in naive CD4⁺ T cells from healthy volunteers of different ages. When these peripheral TREC contents were normalized to the average TREC contents of CD4⁺ SP thymocytes, we found that the median fraction of naive CD4⁺ T cells that were originally produced by the thymus in adults was 11% (see Fig. 1B). Thus, ~90% of the naive T cell pool in these adults had been formed by peripheral naive T cell proliferation.

Contribution of peripheral proliferation to the human CD31⁺ naive CD4⁺ T cell pool

Naive CD4⁺ T cells expressing CD31 (PECAM-1) are thought to be enriched in cells that were produced by the thymus[22, 23]. In agreement with previous studies[22-24], we found that the fraction of CD31⁺ T cells within the naive CD4⁺ T cell pool of healthy individuals decreased substantially – and almost linearly – with age (Fig. 1C), and that the CD31⁺ naive CD4⁺ T cell population always had a higher TREC content than the CD31⁻ population. The average TREC contents of CD31⁺ and CD31⁻ naive CD4⁺ T cells declined substantially and at similar rates with age (Fig. 1D), confirming that even CD31⁺ naive CD4⁺ T cells are in part produced by peripheral T cell division[24].

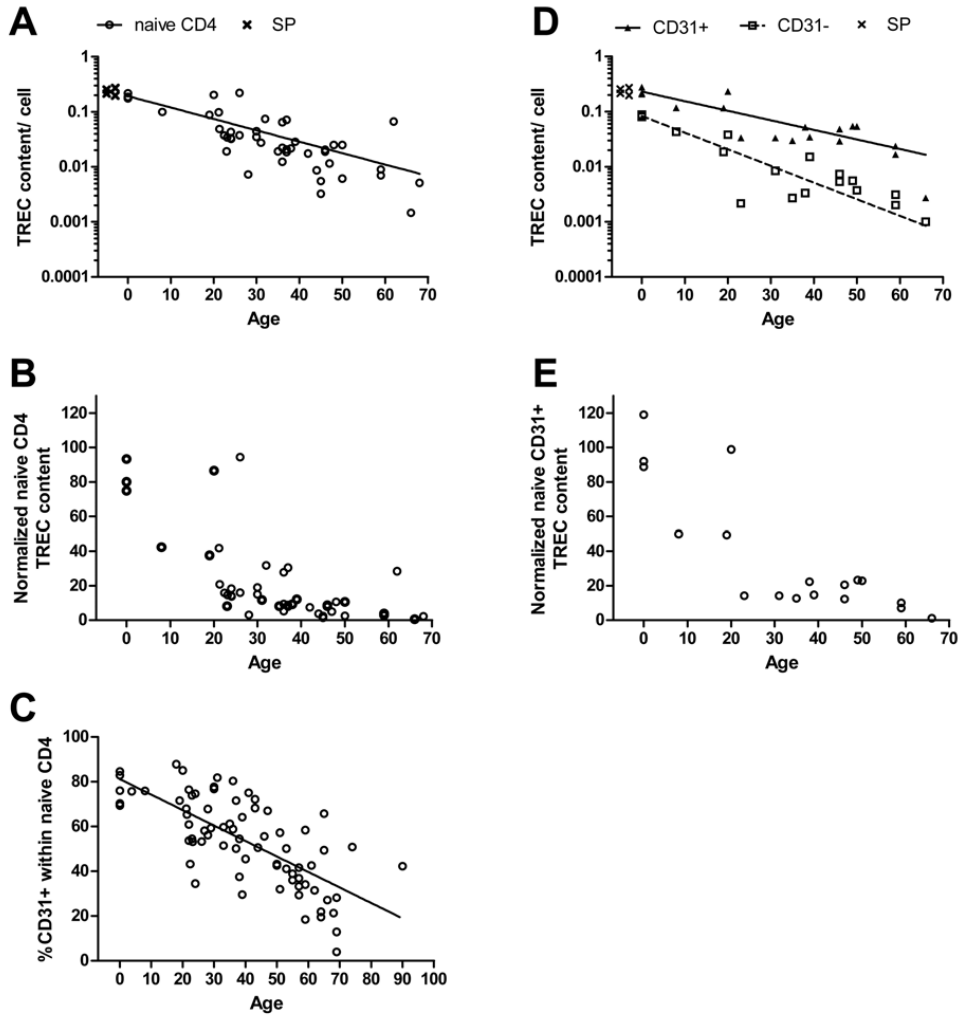

Figure 1. Quantification of the contribution of thymic output in humans. (A) TREC content of naive CD4⁺ T cells as a function of age (n = 45). (B) Percentage of naive CD4⁺ T cells that were originally produced in the thymus, calculated by normalizing the TREC content of peripheral naive CD4⁺ T cells by the TREC content of SP CD4⁺ thymocytes (n = 45). (C) The percentage of CD31⁺ T cells within the naive CD4⁺ T cell pool of healthy individuals (n = 76) decreased significantly (R_p = -0.72, p<0.001) with age. (D) TREC contents of CD31⁺ (▲) and CD31⁻ (□) naive CD4⁺ T cells in healthy donors (n = 18) of different ages. The TREC content of both CD31⁺ naive CD4⁺ T cells (R_s = -0.78, p<0.001) and CD31⁻ naive CD4⁺ T cells (R_s = -0.80, p<0.001) declined significantly with age; their slopes were not significantly different (p=0.25). TREC contents of CD31⁺ cord blood CD4⁺ T cells (n = 3) were similar to TREC contents of single positive CD4⁺CD8⁻ thymocytes (n = 4, p=0.86). (E) The percentage of CD31⁺ naive CD4⁺ T cells that were originally produced in the thymus, calculated by normalizing the TREC content of CD31⁺ naive CD4⁺ T cells in the blood by the TREC content of SP CD4⁺ thymocytes (n = 18).

To quantify which fraction of CD31⁺ naive CD4⁺ T cells originated from peripheral renewal, and which from thymic output, we normalized the TREC content of CD31⁺ naive CD4⁺ T cells to the average TREC content of SP CD4⁺CD8⁻ thymocytes. The TREC content of CD31⁺ naive CD4⁺ T cells in cord blood turned out to be very similar to the TREC content of SP CD4⁺CD8⁻ thymocytes, suggesting that cord blood CD31⁺ naive CD4⁺ T cells had not markedly proliferated since they emerged from the thymus, and that the average TREC content of SP thymocytes was indeed representative for the TREC content of RTE. We found that the percentage of naive CD31⁺ CD4⁺ T cells that had originally been produced in the thymus decreased with age, from a median of >99% in neonates to 23% in adults (see Fig. 1E). Thus, even the vast majority of CD31⁺ naive CD4⁺ T cells in human adults are formed by peripheral proliferation.

Daily thymic output in humans

From the basic model for TREC and naive T cell dynamics[20] one can deduce that, in equilibrium, the normalized TREC content (A/c) of naive T cells is given by:

$$\frac{A}{c} = \frac{\sigma(t)}{\sigma(t) + pN(t)} \qquad [1]$$

where A is the TREC content of naive T cells, c is the TREC content of SP thymocytes, $\sigma(t)$ represents thymic output at time t, p is the rate of naive T cell proliferation, and $N(t)$ is the number of naive T cells at time t. This equation confirms that the TREC content of two individuals with the same thymic output may be totally different if they differ in their peripheral renewal $pN(t)$ [20]. If the current total daily production of naive T cells $\sigma(t)+pN(t)$ is known, Equation 1 can be used to obtain an upper estimate of the number of cells $\sigma(t)$ exported by the thymus. In five healthy volunteers we previously quantified the total daily production of naive T cells using deuterium labelling[17], (see Table 1). Combining these estimates with the normalized TREC contents of naive CD4⁺ T cells in these individuals revealed a median daily thymic output of 1.7×10^7 CD4⁺ T cells per day (see Table 1).

Turnover of naive T cells in mice

To compare the above insights obtained in humans to T cell dynamics in mice, we determined the normal turnover rates of naive CD4⁺ and CD8⁺ T cells in young adult mice. To this end, we administered a bolus of 99.8% deuterated water (^2H_2O) to 12-week-old C57Bl/6 mice and then performed long-term maintenance labeling with 4% deuterated water in the drinking water. Deuterium enrichment in the DNA of thymocytes (Sup. Fig. 1) and naive T cells from the spleen (Fig. 2) was determined during four weeks of label administration and a subsequent 18 weeks downlabeling period. It took approximately a week for the first labeled naive T cells to appear in the

Table 1: Total and thymic daily naive T cell production in young human adults

Individual	Age (years)	Normalized naive CD4⁺ TREC content[a]	Total daily naive CD4⁺ T cell production ($\times 10^7$) (cells/day)[b]	Maximal daily CD4⁺ thymic output ($\times 10^7$) (cells/day)[c]
A	24	14%	12	1.6
B	22	16%	5.4	0.85
C	25	ND	2.2	ND
D	20	21%	8.2	1.7
E	22	15%	13	1.9

[a] Normalized naive CD4⁺ TREC content, calculated by dividing the TREC content of peripheral naive CD4⁺ T cells by the TREC content of SP CD4⁺ thymocytes.

[b] Total production of naive CD4⁺ T cells per day, calculated as p × [the naive T cell count per liter blood] × [5 liter blood] × 50, assuming that 2% of lymphocytes reside in the blood[51], where p is the average turnover rate estimated by ^2H_2O labeling[17].

[c] Daily CD4⁺ thymic output, calculated by multiplying the normalized naive CD4⁺ TREC content with the total daily naive CD4⁺ T cell production.

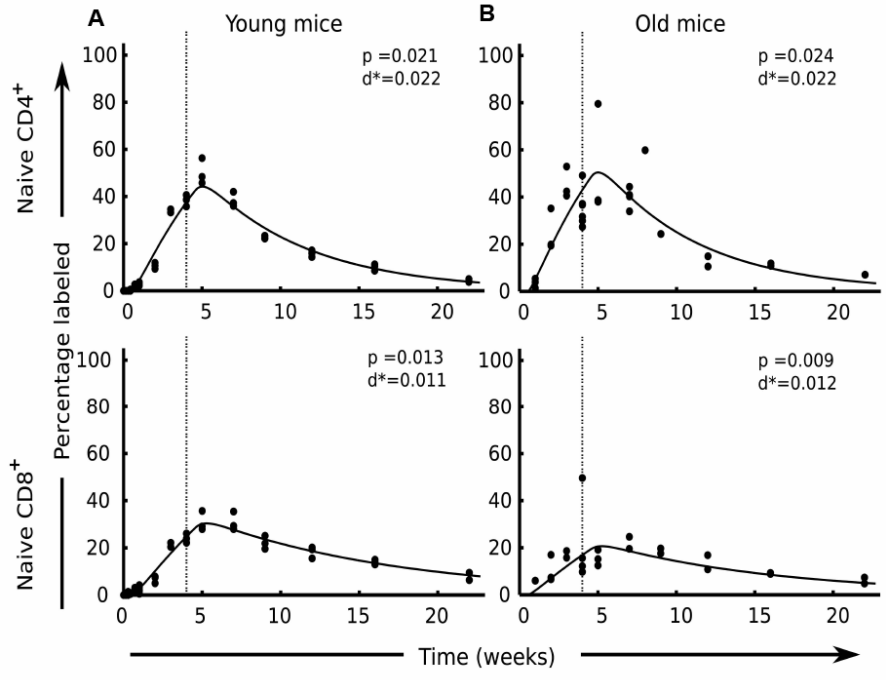

Figure 2. Estimating mouse naive T cell turnover using deuterium labeling. Twelve-week-old (n = 28, A) and 85-week-old mice (n = 28, B) were given 4% ^2H_2O for 4 weeks. Each dot represents the normalized deuterium enrichment in the DNA of naive CD4⁺ (upper graphs) or naive CD8⁺ T cells (lower graphs) in the spleen of one C57Bl/6 mouse. Vertical lines mark the end of ^2H_2O administration at 4 weeks. The estimated average turnover rates (p) and death rates of the labeled cells (d^*) resulting from the best fits of the mathematical model to the data are given in each graph.

spleen, where they kept on accumulating up to a week after the end of labeling (Fig 2A), suggesting that these cells were labeled by cell division in another compartment.

The cellular turnover rates were estimated by fitting the labeling data to a mathematical model[17, 25], which distinguishes between an average turnover or production rate, *p*, and a death rate of labeled cells, *d** (see Materials and Methods and Sup. Table 1). The average turnover rates of naive CD4⁺ and CD8⁺ T cells in young adult mice were found to be 0.021 and 0.013 per day (Fig. 2A), corresponding to average life spans (1/*p*) of 47 and 80 days, respectively. In contrast to what is commonly observed in deuterium-labeling studies in man[25], the death rates of labeled cells, *d**, did not significantly differ from the average turnover rates, *p* (Fig. 2A), suggesting that naive T cells form a dynamically homogeneous population in the mouse.

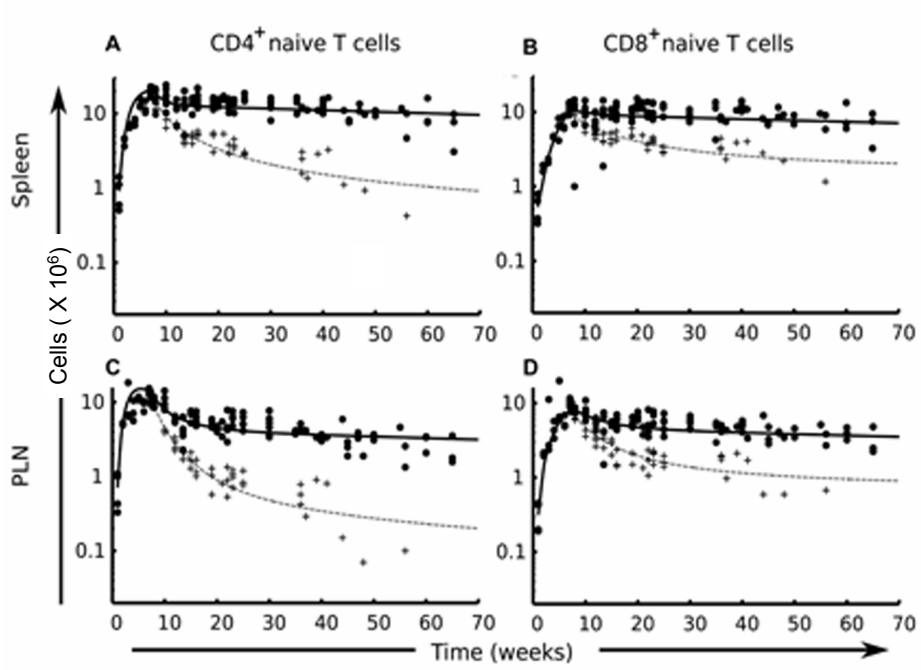

Figure 3. Effect of thymectomy on the size of the naive T cell population in mice. Numbers (×10⁶) of naive CD4⁺ (A,C) and naive CD8⁺ T cells (B,D) were determined in spleen (A,B) and PLNs (C,D) of euthymic mice (●, n = 130) and mice that had been thymectomized at week 7 (+, n = 43). Population densities in control and thymectomized mice were fitted with a mathematical model in which the cellular death rate increased linearly with the population density (model (1), see Materials and Methods). The best fits of the model to the combined data sets of spleen and lymph nodes of normal and thymectomized mice are depicted by the continuous and dotted lines, respectively. Best fitting parameters are given in Table 2, and corresponding average life spans are given in Table 3.

Table 2: Parameters values of the two mathematical models describing naive T cell numbers.

	Parameter	Value (confidence limits)[a]
Model (1): homeostatic survival[b]		
CD4⁺	d_n (×10⁻⁹ day⁻¹)	2.5 (2.3- 2.7)
	r_n (day⁻¹)	0
CD8⁺	d_n (×10⁻⁹ day⁻¹)	1.5 (1.4- 1.6)
	r_n (day⁻¹)	0
Shared[c]	ε (day⁻¹)	0.034 (0.032- 0.036)
Model (2): homeostatic proliferation		
CD4⁺	d_n (day⁻¹)[d]	0.021
	r_n (day⁻¹)[e]	1
	h (×10⁴ cells)	2.4 (1.8- 2.4)
CD8⁺	d_n (day⁻¹)[d]	0.013
	r_n (day⁻¹)[e]	1
	h (×10⁴ cells)	3.0 (2.6- 3.5)
Shared[c]	ε (day⁻¹)	0.022 (0.021- 0.023)

[a] 95% confidence intervals.

[b] Values are estimates of the best fit depicted in Fig. 3.

[c] These parameters were forced to be equal when fitting CD4⁺ and CD8⁺ data.

[d] Parameter fixed to deuterium enrichment estimate.

[e] The best fit of the model gives a maximal renewal rate r_n=1 for both CD4⁺ and CD8⁺ naive T cells.

Thymus output in mice

Although deuterium-labeling experiments provide the most reliable tool to estimate cellular turnover rates, they fail to distinguish between production of naive T cells in the thymus and their peripheral renewal[26]. In a separate set of experiments we therefore enumerated SP CD4⁺ and CD8⁺ thymocytes and naive CD4⁺ and CD8⁺ T cells in the spleen and PLNs of normal euthymic or sham thymectomized mice and mice that had been thymectomized at 7 weeks of age (Fig. 3). There were no significant differences in thymocyte or naive T cell numbers between normal mice and sham thymectomized mice at any age (data not shown), allowing us to combine the data from both types of mice in one euthymic control group. In euthymic mice, the numbers of SP CD4⁺ and CD8⁺ thymocytes were found to increase exponentially after birth, after which they peaked at week 6-7, and decreased by almost 40% during week 7 (data not shown). Thereafter, thymocyte numbers declined exponentially at a rate of 50% per year (see Materials and Methods). Naive T cell numbers in spleen and PLNs peaked at week 7-8 (see Fig. 3), and subsequently declined more slowly than thymocyte numbers, suggesting that a homeostatic mechanism compensated for loss of thymus output.

Table 3: Estimated average life spans of naive CD4⁺ and CD8⁺ T cells in euthymic and thymectomized mice.

Method	Age	Average life spans (days)[a]	
		Naive CD4⁺	Naive CD8⁺
^2H_2O	12 weeks	47 (41 – 54)[b]	80 (67 – 92)
	85 weeks	41 (36 – 47)	116 (94 –139)
Cell counts	7 weeks	23 (22 – 25)	70 (63 – 78)
	12 weeks	31 (29 – 33)	72 (65 – 75)
	85 weeks	46 (43 – 49)	101 (94 – 105)
	12 weeks (Tx)	62 (61 – 64)	113 (105 – 117)

[a] The average life spans of young adult and old mice were based on the estimated turnover rate (life span = 1/*p*) from the deuterium-labeling experiments (^2H_2O, see Fig. 2), and on the combination of estimated parameters from the homeostatic survival model (see Fig. 3) and the T cell counts at the indicated ages (cell counts; where the average life span is defined as $1/(r+d_nN)$, where N is the average number of naive T cells at the indicated age).

[b] 95% confidence limits are given in parentheses.

Homeostatic compensation through decreased peripheral cell death

A likely homeostatic mechanism by which cell numbers are regulated is a cellular survival rate that depends on the population density[27]. When T cell numbers are low, T lymphocytes will experience less competition for survival signals, such as contact with MHC–peptide ligands or cytokines, and may thus have a longer life expectancy. To study the relative contribution of thymus output and peripheral T cell proliferation to the maintenance of the naive T cell pool in mice, we fitted a mathematical model to the naive T cell counts of euthymic and thymectomized mice of different ages that were measured experimentally. The model describes thymus output, peripheral T cell renewal, and naive T cell loss, which represents both cell death and priming of naive T cells into the memory T cell pool and depends on the number of T cells present (see Materials and Methods and Sup. Table 2). The naive CD4⁺ and CD8⁺ T cell counts of euthymic and thymectomized mice turned out to be described very well with a simple model that totally lacks peripheral renewal of naive T cells and only allows for an increase in the average life span when T cell numbers decline (Fig. 3; Table 2).

According to this "homeostatic survival" model, the average life spans of naive CD4⁺ and CD8⁺ T cells in 12 week old mice are 31 and 72 days, respectively, which is in reasonable agreement with the 47 and 80 day expected life spans estimated from the deuterium-labeling experiments (Table 3). Because the export of naive T cells from the thymus is proportional to the number of SP thymocytes[28], we estimated that every day 3.4% (3.2% – 3.6%) of the SP thymocyte pool emigrates from the thymus to the spleen (Table 2). In 12-week-old mice this corresponds to a daily emigration of 3.6×10^5 (confidence interval: $1.3 \times 10^5 – 6.2 \times 10^5$) newly produced naive CD4⁺ and 1.5×10^5 (confidence interval: $0.7 \times 10^5 – 2.3 \times 10^5$) naive CD8⁺ T cells from the thymus to the spleen. These estimates were solely derived from naive T cell numbers in euthymic and thymectomized mice. From the ^2H_2O labeling experiments in euthymic mice described above, we independently calculated the total daily production of naive T cells by multiplying the average turnover rates (*p)* with the actual number of splenic naive T cells (*N*), yielding a total daily production of 2.7×10^5 (confidence interval: $0.9 \times 10^5 – 4.9 \times 10^5$) naive CD4⁺ and 1.2×10^5 (confidence interval: $0.2 \times 10^5 – 2.2 \times 10^5$) naive CD8⁺ T cells in the spleen (Sup. Fig. 2A). Because total daily production and daily thymic output are so similar, we conclude that naive CD4⁺ and CD8⁺ T cells in young adult C57Bl/6 mice are almost entirely thymus derived and are hardly formed by peripheral T cell proliferation.

Homeostatic compensation through increased peripheral cell division

Because some studies have suggested that T cell proliferation rates may increase when T cell numbers decrease[29], we also analyzed the data with an alternative model, in which the rate of T cell proliferation increases when cell numbers are low. The fit of this alternative model to the data of euthymic and thymectomized mice was almost as good as the fit with the model in which T cell death rates are dependent on T cell densities. T cell proliferation rates resulting from these analyses were used to calculate average interdivision times. In normal 12 week old mice, the average time between T cell divisions was estimated to be 218 and 655 days for naive CD8⁺ and CD4⁺ T cells, respectively. Comparison of the estimated average life spans from the deuterium-labeling experiments with these average interdivision times shows that the average time it takes for naive CD8⁺ and CD4⁺ T cells in euthymic mice to divide is 3- to 14-fold longer than the expected lifespan of these cells, implying that during their stay in the naive T cell pool most naive T cells never divide.

T cell dynamics in old mice

Knowing that naive T cell production in young adult mice is almost exclusively due to T cell production by the thymus, we studied naive T cell life spans in old mice which have much lower thymus output. To this end, we performed deuterium labeling experiments in 85-week-old mice (Fig. 2B). Naive CD4⁺ T cells in aged mice were found to have an average life span of 41 days, which did not significantly differ from that in 12-week-old mice (47 days). The expected life span of naive CD8⁺ T cells was found to be 116 days, which is nearly 50% longer than that in young adult mice (80 days, Table 3). Total daily splenic naive CD4⁺ T cell production ($p \times N$) of old mice was on average 1.4×10^5 (confidence interval: $0.4 \times 10^5 – 2.9 \times 10^5$) cells, of which 0.9×10^5 (confidence interval: $0.4 \times 10^5 – 1.4 \times 10^5$) were produced by the thymus (Sup. Fig. 2B). Similarly, 0.3×10^5 (confidence interval: $0.1 \times 10^5 – 0.5 \times 10^5$) of the 0.6×10^5 (confidence interval: 0.1 ×

10^5 – 1.5 × 10^5) naive CD8⁺ T cells produced per day in old mice were produced by the thymus (Sup. Fig. 2B). Thus, even in old mice, in which thymus output has dropped significantly, naive CD4⁺ and CD8⁺ T cell proliferation hardly contributes to naive T cell maintenance.

TREC dynamics in aging mice

The result that peripheral T cell proliferation hardly contributes to the maintenance of the naive T cell pool throughout the life of a mouse is in sharp contrast with observations on naive TREC dynamics in humans (See Fig. 1A and B)[24, 30-32]. An experimental prediction that naturally follows from our results is that – in contrast to what is observed in humans – the fraction of TREC positive naive CD4⁺ and CD8⁺ T cells in healthy mice should not decrease with age. We tested this prediction by comparing the average TREC contents of naive and memory CD4⁺ and CD8⁺ T cells from normal euthymic mice between 12 and 126 weeks of age. We found no evidence for TREC dilution in mouse naive T cells with age, even though the average TREC contents of memory CD4⁺ and CD8⁺ T cells clearly declined with age (Fig. 4A). The average TREC contents of naive CD4⁺ and CD8⁺ T cells throughout life were very similar to the average TREC contents of CD4⁺ and CD8⁺ SP thymocytes, confirming that naive T cells in mice hardly divide. Taken together, this is independent experimental confirmation of our main finding that – irrespective of their age – naive CD4⁺ and CD8⁺ T cells in euthymic mice are almost exclusively formed by thymus output. Interestingly, in thymectomized mice the fractions of TREC positive naive T cells were moderately decreased (Fig. 4B), suggesting that in the absence of the thymus, naive T cells in mice may ultimately proliferate.

Discussion

We here show that the source by which naive T cell numbers are maintained during aging differs fundamentally between mouse and man. Not only in young adult but even in very old mice, the vast majority of the naive T cell pool is sustained by thymic output, while in human adults, the majority of naive cells are produced by peripheral T cell proliferation. Our results are in line with studies in lymphopenic humans and mice receiving bone marrow transplantation, which collectively suggested that T cell reconstitution in adult humans is more comparable to that in thymectomized mice than that in euthymic mice[14]. It is important to realize that these quantitative differences between mouse and man will also have qualitative effects on the naive T cell pool because the thymus is capable of producing new T cell specificities, whereas peripheral T cell proliferation can only lead to the expansion of already existing T cell clones.

The contribution of the thymus to the maintenance of the naive T cell pool in healthy adults, and its potential to reconstitute the T cell pool in lymphopenic individuals has been much debated. While some have ascribed a crucial role to the thymus in human adults[15], others have argued that during adulthood the thymus is producing too few T cells to have a significant effect on the size of the naive T cell pool[20]. Our

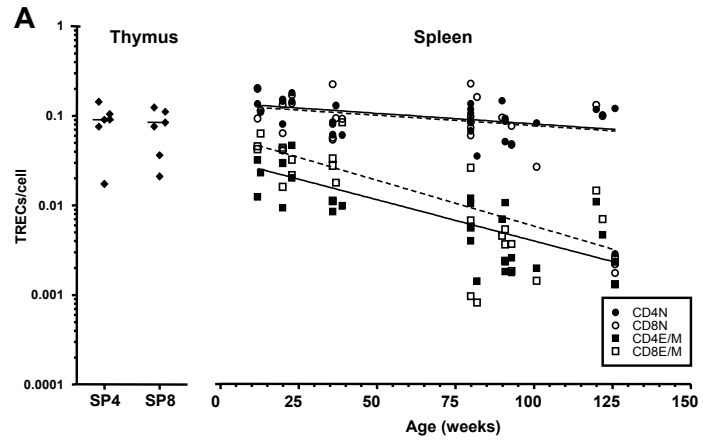

Figure 4. TREC analysis in mouse thymocytes and peripheral T cell subsets. (A) The average number of TRECs per T cell (on a logarithmic scale) from the spleens of mice ranging from 12 to 126 weeks of age (n = 29). Lines show the regression analyses through the data in each T cell subset. TREC contents of SP CD4⁺ (p = 0.13) and SP CD8⁺ (p = 0.60) thymocytes did not change with age (not shown) and are plotted separately. TREC contents of naive CD4⁺ (●, p = 0.11) and naive CD8⁺ (○, p = 0.46) T cells did not decrease significantly with age, whereas TREC contents of memory CD4⁺ (■, p = 0.0002, R^2 = 0.56) and memory CD8⁺ (□, p = 0.0001, R^2 = 0.56) T cells did. Analyses in LN from the same mice revealed similar data (not shown). (B) TREC contents of naive CD4⁺ and CD8⁺ T cells in age matched healthy control (▼, n = 13) and thymectomized mice (ATx at week 7, ▽, n = 8). Horizontal bars depict median values. TREC contents of naive CD4⁺ T cells in the spleen (p = 0.023) and naive CD4⁺ (p = 0.024) and naive CD8⁺ (p = 0.011) T cells in the LNs were significantly lower in ATx mice compared to healthy controls.

data point out that the vast majority of naive T cells in human adults are maintained through peripheral T cell proliferation. Several recent studies have suggested that even in young, healthy children, a substantial proportion of naive T cells are derived from peripheral T cell renewal[33, 34].

Our current estimates of the contribution of thymic output to the total daily production of naive CD4⁺ T cells were much lower than previous estimates based on CD31 expression alone[24]. While the fraction of CD31⁺ T cells within the naive CD4⁺ T cell pool of healthy individuals decreased from approximately 80% in neonates to 60% around the age of 30, and 40% at the age of 60, our TREC analyses pointed out that, throughout adulthood, maximally 30% – and on average only 11% – of the naive T cell pool was originally formed by the thymus. In line with this, we found that in adults, as many as 77% of CD31⁺ naive CD4⁺ T cells were in fact formed by peripheral T cell proliferation. Although these data show that in terms of naive T cell numbers created per day, peripheral T cell proliferation by far exceeds thymic output in human adults, the thymus may still have an essential role – if only because new T cell specificities can only be created by the thymus.

In contrast to the large contribution of peripheral T cell proliferation to the maintenance of naive T cells in humans, we here show that naive T cells in euthymic mice are almost exclusively formed by thymic output. Such a limited role for peripheral naive T cell division in mice is fully compatible with in vivo BrdU labeling results in several classical studies[35, 36], which showed that BrdU accrual in naive T cells of young adult mice strongly depended on the presence of a thymus. Here we extend this by showing that naive T cell division in mice hardly occurs not only in young-adult mice but even in mice in old age. Apparently, if present at all, most naive peripheral T cell proliferation in mice induces loss of the naive phenotype. This agrees well with the view that most naive T cells triggered to divide in lymphopenic mice obtain effector or memory (like) T cell characteristics[29]. The conclusion that peripheral T cell proliferation hardly contributes to the maintenance of the naive T cell pool in euthymic mice was independently confirmed by the lack of TREC dilution in the naive T cell compartment of aging mice. In contrast, the average naive T cell TREC content in humans has been shown to decline by 90% to 99%[21, 24, 30]. Although one could argue that mice do not live long enough for changes in naive T cell TREC contents to occur during their life, our quantification of T cell turnover in mice (this paper) and men[17] has demonstrated that naive T cell turnover rates in mice are ~40-fold higher than in humans. If naive T cell production in mice were to be due to peripheral T cell proliferation, as it is in humans, the decline of naive T cell TREC contents over two years in mice would thus be expected to be similar to the decline observed in ageing humans.

The interpretation of TREC data remains difficult because the average TREC content of the naive T cell pool reflects a complex balance between thymic output, T cell proliferation, and cell death[18, 20, 32]. We have shown that the normalized TREC content (defined by Equation 1) nevertheless quantifies which fraction of all naive T cells that are produced per day is generated by the thymus. In this equation we have assumed that TRECs themselves do not decay, unless their host cell dies. It is indeed widely assumed that TRECs are extremely stable, in part because TRECs have been shown to persist for decades in fully thymectomized individuals[15, 31, 37, 38]. Because a role for TREC decay cannot formally be ruled out, however, we sought for further – TREC independent – arguments that support our claim that naive T cell maintenance is different in mice and men.

The first argument comes from estimates of thymic T cell production in mice and men. Studies in different species have shown that the thymus exports ~1% of thymocytes per day[39-41]. A human thymus has been shown to contain on average ~10^7 thymocytes per gram of thymic tissue at the age of 20 years, which further declines with age[42], and the total weight of the human thymus in adults between 20 and 84 years of age has been shown to be on average 23 g, and to be remarkably constant with age[7]. With a daily export rate of 1%, naive T cell export from the thymus would thus be estimated to be maximally 2.3×10^6 cells per day. Our heavy-water studies show that total daily naive T cell production in humans is much higher, in the order of 10^8 naive T cells per day (calculated as $p \times$ [the naive cell count per liter blood] × 5 liter blood × 50, assuming that 2% of lymphocytes reside in the blood[17]). If all these new naive T cells in humans were to be produced by the thymus, it would mean that – in contrast to all other species investigated – in humans as much as 44% of thymocytes would have to be exported into the periphery on a daily basis. A much more likely explanation is that the vast majority of the 10^8 naive T cells that are produced per day in a healthy human, are produced by peripheral T cell proliferation. In mice, in contrast, the total production of 4×10^5 naive T cells per day in the spleen that we measured using heavy water labeling, is perfectly in line with a ~1% output of thymocytes per day. Since the number of naive T lymphocytes in the spleen represents ~30 to 40% of the total number of naive T lymphocytes in the mouse, and our deuterium labeling studies showed that T cells in lymph nodes and spleen behave kinetically similarly (data not shown), the total daily production in a young adult mouse is ~1.0 to 1.3×10^6 naive T cells. All these cells can be produced by the thymus since the thymus of a young adult male mouse contains approximately 1.2×10^8 thymocytes (data not shown).

The second argument is based on the quantification of total daily T cell production versus daily T cell proliferation. Our deuterium labeling results in mice and men point out that the fraction of the naive T cell pool that is being renewed per day differs dramatically between mice and men: In mice, 2.1% and 1.3% of the naive CD4⁺ and CD8⁺ T cell pool is being replaced per day, whereas in humans, as little as 0.05% and 0.03% of the naive CD4⁺ and CD8⁺ T cell pool is replaced per day, i.e., in mice naive

T cells are renewed ~40 times more quickly than in men. If the relative contribution of thymus output and peripheral T cell proliferation were to be similar in mice and men, one would predict that T cell proliferation rates in men should be about 40 times lower than in mice. When we measured the expression of the intracellular proliferation marker Ki67 of naive T cells in both mice and men – based on the very same markers that were used to distinguish naive T cells in our deuterium labeling studies – we found however, that the fraction of the naive T cell pool that is proliferating at any moment in time is very similar between mice and men (data not shown). Together these data show that the relative contribution of peripheral proliferation to the maintenance of the naive T cell pool must be completely different in mice and men.

The finding that naive T cells in mice have a relatively short life span, and are almost completely thymus derived, contrasts strongly with the long life span of naive T cells and the predominant role of peripheral T cell proliferation in the maintenance of the naive T cell pool in humans. We defined the human naive T cell population by the expression of CD27 and lack of CD4RO expression[43, 44]. It is important to stress that the human naive T cells that we thus analyzed were naive according to all commonly accepted phenotypical markers for naive T cells (including CD62L, CCR7, CD127 and CD28, data not shown). Conversely, the expression of CD95 and CD57, which is known to be very low on naive T cells, was indeed very low within our $CD45RO^{-}CD27^{+}$ (naive) T cell populations (data not shown). We thus conclude, that by all current standards we have studied what is conventionally defined as naive T cells in humans. Our TREC data of $CD31^{+}$ naive T cells provide further support for the fundamental difference in naive T cell maintenance between mice and men. CD31 is generally thought to be a marker for naive T cells that are most proximal to the thymus[22-24]. The observation that even the majority of $CD31^{+}$ human naive T cells have been produced by peripheral T cell proliferation demonstrates that our results are not due to the specific markers that we used.

These results not only have bearing on our ideas about T cell renewal in healthy individuals with a full T cell compartment, but are also critical to our understanding of human T cell reconstitution in clinical conditions characterized by severe T cell depletion. The quantification of naive T cell production by the thymus and by peripheral proliferation demonstrates that the contribution of the thymus in young healthy adults is much smaller than widely assumed on the basis of the mouse model. Indeed, the major implication of this work is that one cannot freely extrapolate insights about naive T cell kinetics in young adult (or old) mice to young adult (or old) humans, or vice versa, for the source by which naive T cells are produced differ qualitatively between mice and men.

Acknowledgments

The authors would like to thank Vitaly Ganusov, Mette Hazenberg, Loes Rijswijk, Henk Starrevelt, Sjaak Greeven, and Linda Nijdam for technical assistance and theoretical input, and Linde Meyaard and Grada van Bleek for critical comments on an earlier version of the manuscript. Thymic tissue for TREC analyses in thymocytes was kindly provided by Koos Jansen. This research has been funded by the Landsteiner Foundation for Blood Transfusion Research (LSBR grant 0210) and the Netherlands Organization for Scientific Research (NWO, grants 016.048.603, 917.96.350 and 836.07.002). The authors have no conflicting financial interests.

Materials and Methods

Blood and tissue samples. Buffy coats or whole heparine anticoagulated blood samples were obtained by venapuncture from human blood bank donors and children visiting the UMCU. Cord blood samples were obtained from healthy full-term neonates directly after delivery. Thymocytes were obtained from children who were thymectomized because of complicated heart surgery at very young age. Written informed consent was obtained from all participants or their legal guardians in agreement with the Helsinki Declaration of 1975, revised in 1983.

Mice. C57Bl/6 mice were maintained by in house breeding at the Netherlands Cancer Institute in Amsterdam or the Central Animal Facility at Utrecht University under specific pathogen-free conditions in accordance with institutional and national guidelines. Thymectomy was performed at 7 weeks of age as described before[17]. Completeness of thymectomy was confirmed by visual inspection, both directly after removal of the organ and at the end of the experiment. Only fully thymectomized animals were included in this study.

Cell preparation and flow cytometry. Blood mononuclear cells were obtained by Ficoll Paque density gradient centrifugation and cryopreserved until further use. Single cell suspensions were obtained by mechanically disrupting spleen, thymus, or (axillary, brachial, inguinal and superficial cervical) peripheral lymph nodes (PLNs). Red blood cells in blood samples were lysed with ammonium chloride solution (155 mM NH_4Cl, 10 mM $KHCO_3$ and 0.1 mM EDTA, pH 7.4). For measuring the fraction of $CD31^{+}$ T cells within the human naive $CD4^{+}$ T cell population and for purifying $CD4^{+}CD45RO^{-}CD27^{+}CD31^{+}$ and $CD4^{+}CD45RO^{-}CD27^{+}CD31^{-}$ cells, cryopreserved PBMC were thawed and incubated with monoclonal antibodies (mAb) to CD45RO(Caltag), CD31, CD4 (BD) and CD27 (Sanquin Reagents), after which they were analysed (using Cellquest or FACS Diva software) or sorted on a flow cytometer (FACS Calibur, LSRII, FacsAria (BD) or MoFlow (Dako)). In 13 of 18 sorts we omitted the mAb to CD27 but confirmed the percentage contaminating effector $CD4^{+}CD45RO^{-}CD27^{-}$ T cells was on average only 0.75%. Sort purity was on average 93%. To determine the fraction of the different mouse T cell populations, fresh cells were washed, resuspended in IMDM/7% FCS and counted.

For isolating naive ($CD62L^+$, $CD44^{-/low}$) and memory/effector ($CD62L^+$, $CD44^{high}$ and $CD62L^-CD44^{high}$) $CD4^+$ and $CD8^+$ T cells, splenocytes and LN suspensions were stained with CD4 (clone RM4-5) or CD8 (clone 53-6.7), in combination with CD44 (clone IM7) and CD62L (clone MEL-14) (BD) in the presence of blocking 2.4G2 mAb in PBS/1% BSA. Sort purity was 98.4 ± 1.0% (naive $CD4^+$), 97.2 ± 1.6% (effector/memory $CD4^+$), 98.4 ± 1.1% (naive $CD8^+$), 96.0 ± 2.1% (effector/memory $CD8^+$). To isolate single positive $CD4^+CD8^-$ thymocytes, thymocyte suspensions were stained with anti CD4 and CD8 (BD) and sorted by flow cytometry. Mouse thymocytes were also stained for CD44 (BD) to exclude peripheral T cells that reentered the thymus ($CD44^{high}$). Sort purities were 93.5 ± 3.3% (human $CD4^+$ SP), 97.1 ± 1.9% (mouse $CD4^+$ SP) and 90.5 ± 3.4% (mouse $CD8^+$ SP). Isolated mouse cells were frozen until further processed.

TREC analyses. Genomic DNA was isolated using the QIAamp Blood Kit according to manufacturer's instructions (Qiagen, Hilden, Germany). Mouse genomic DNA was isolated by cell lysis (10,000 cells/µl) in 0.05% Tween-20, 0.05% NP-40, and 100 µg/ml Proteinase K for 30 min at 56˚C, followed by 15 min at 99˚C. Lysates were spun down for 15 min. Signal joint (Sj) TREC numbers and DNA input were quantified using an ABI Prism 7900HT Real Time PCR System (Applied Biosystems, Foster City, CA) . The number of Human Sj TREC copies in a cell population and the input DNA were determined and calculated as described previously[20]. For the TREC content within naive $CD4^+$ T cells we combined previously measured healthy controls (TREC content within $CD4^+CD45RA^+$)[20] with data from 11 healthy volunteers (TREC content within $CD4^+CD45RO^-CD27^+$, average sort purity of 98%), including 4 volunteers from a ^2H_2O labelling study[17]. For 17 individuals the TREC content of naive $CD4^+$ T cells was calculated with the formula: (fraction $CD31^+$ within naive $CD4^+$ T cells) × (TREC content $CD31^+$ naive $CD4^+$ T cells) + (1 – fraction $CD31^+$ within naive $CD4^+$ T cells) × (TREC content $CD31^-$ naive $CD4^+$ T cells). Mouse TREC analysis was performed as described[45]. To correct for input genomic DNA, the CD45 reference gene was separately amplified by forward primer 5'-TCAGAGGCCAGGCTCACTCAAG-3' and reverse primer 5'-CTAGGCCAACCACTCCCACTGT-3' (MWG Operon, Ebersberg, Germany), and detected by fluorescent probe FAM-5'-CAATGTTCAAGTTGCCCAGCGATGCCAGC-3'-TAMRA (Applied Biosystems, Foster City, CA).

^2H_2O labeling. ^2H_2O labeling was achieved by giving mice one boost injection (i.p.) of 15 ml/kg with 99.8% ^2H_2O (Cambridge Isotopes, Cambridge, MA), followed by feeding with 4% ^2H_2O in the drinking water for four weeks.

Measurement of ^2H_2O enrichment in plasma and DNA. Deuterium enrichment in plasma was measured as reported by Previs et al.[46]. The isotopic enrichment of DNA was determined as previously described[17].

Mathematical modeling of ^2H_2O data. Enrichment data were fitted using a previously developed mathematical model[17], which was extended to take into account a delay with which labeled cells reach the spleen[47]. Best fits were determined by minimizing the sum of squared residuals after arcsin (sqrt) transformation. Availability of deuterium was measured in plasma, and all cellular enrichment data were normalized by the maximal enrichment level observed in thymocytes[17].

Mathematical modeling of thymectomy data. We devised a mathematical model to quantify naive T cell dynamics in control and thymectomized mice, assuming that under normal conditions naive T cells are produced by thymic output and peripheral T cell proliferation, and lost via differentiation into effector/memory T cells and cell death. Thymic output was described by a phenomenological function $f_1(t)$, which was fitted to the number of SP thymocytes (data not shown), and multiplied by ε, the fraction of SP thymocytes exported to the spleen per day. The function is a modification of the thymus involution function described by Steinmann et al.[7] and is explained below.

In the model, both cell death rates (d_nN) and proliferation rates ($r/(1+N/h)$ could be density-dependent; i.e., cells live longer and/or proliferate more frequently under lymphopenic conditions, when survival or stimulatory signals are abundant. The differential equation for the number of naive T cells (N) is:

$$\frac{\mathrm{d}N}{\mathrm{d}t} = \varepsilon f_1(t) + \frac{r}{1+N/h}N - d_nN^2$$

We considered two extreme cases of this model by allowing for:

1) density-independent proliferation and density-dependent death rates, i.e.:

$$\frac{\mathrm{d}N}{\mathrm{d}t} = \varepsilon f_1(t) + rN - d_nN^2 \ ,$$

or for:

2) density-independent death and density-dependent proliferation rates, i.e.:

$$\frac{\mathrm{d}N}{\mathrm{d}t} = \varepsilon f_1(t) + \frac{r}{1+N/h}N - d_nN \ .$$

Because naive T cells have an intrinsic (limited) lifespan[48], a density-independent death term should always be present. In model (1), proliferation, differentiation and density-independent cell death rates were all combined in a single net proliferation rate r. In model (2) the net death rate d_n includes both cell death and differentiation.

Because T cells continuously recirculate through the body, we assumed that naive T cell dynamic parameters are equal in different organs. We therefore simultaneously fitted the dynamics in the spleen and PLN, and related the two with a proportionality function, $f_2(t)$, described below. The parameters of the function $f_2(t)$ were first determined by fitting the function to all cell numbers available from the two organs of euthymic and thymectomized mice (data not shown), i.e., $N_{PLN} = f_2(t)\ N_{Spleen}$, where N_{PLN} and N_{Spleen} are the numbers of naive $CD4^+$ and $CD8^+$ T cells in peripheral lymph nodes and spleen, respectively. Parameter estimates of the differential equations were obtained by fitting the total cell number, N, to the data (taking the natural logarithm) based on the Levenberg Marquardt algorithm[49] for solving nonlinear least-squares problems.

Mathematical modeling of the thymic output and proportionality functions. We described both the thymic output function and the proportionality function between cell numbers in lymph nodes and spleen by a phenomenological function $f_i(t)$ (where i = 1 for the function describing thymic output and i = 2 for the proportionality function):

$$f_i(t) = \begin{cases} \sigma(1-e^{-s_1 t}); & t \le T_{off} \\ f_i(T_{off})\left[\alpha e^{-s_2(t-T_{off})} + (1-\alpha)e^{-s_3(t-T_{off})}\right]; & t > T_{off} \end{cases}$$

The function is composed of a sum of exponents with constants s_1, s_2 and s_3; the two exponental decays for $t > T_{off}$ are weighted by a constant $0 \le \alpha \le 1$.

Statistical analysis. Normality of the human data was tested using the Shapiro Wilk *W* test for normality. Based on the outcome of this test, correlations were calculated using Pearson's (R_p) or Spearman's rank correlation coefficients (R_s). The Mann Whitney U test was used to determine differences between group characteristics. Differences between the TREC content within $CD31^+$ and $CD31^-$ naive $CD4^+$ T cells were analysed using the Wilcoxon signed rank test. We tested if there was a significant difference between the rate of TREC loss in $CD31^+$ and $CD31^-$ naive T cells using a linear model including an interaction term between age and group ($CD31^+$ versus $CD31^-$). Statistical analyses were performed using SPSS 15.0 (SPSS Inc, Chicago, Illinois). Differences with $p < 0.05$ were considered significant. Mathematical models for mouse cell densities (model 1 and model 2) were compared based on sums of squared residuals. The 95% confidence intervals (CIs) for the inferred parameters were determined using a bootstrap method[50], where the residuals to the optimal fit were resampled 500 times.

References

1. Crooks,G.M., Weinberg,K., & Mackall,C. Immune reconstitution: from stem cells to lymphocytes. Biol. Blood Marrow Transplant. 12, 42-46 (2006).
2. Patel,D.D. et al. Thymic function after hematopoietic stem-cell transplantation for the treatment of severe combined immunodeficiency. N Engl J Med 342, 1325-1332 (2000).
3. Sarzotti,M. et al. T cell repertoire development in humans with SCID after nonablative allogeneic marrow transplantation. J Immunol 170, 2711-2718 (2003).
4. Douek,D.C. et al. Evidence for increased T cell turnover and decreased thymic output in HIV infection. J Immunol 167, 6663-6668 (2001).
5. Dion,M.L. et al. HIV infection rapidly induces and maintains a substantial suppression of thymocyte proliferation. Immunity. 21, 757-768 (2004).
6. Hale,J.S., Boursalian,T.E., Turk,G.L., & Fink,P.J. Thymic output in aged mice. Proc. Natl. Acad. Sci. U. S. A 103, 8447-8452 (2006).
7. Steinmann,G.G., Klaus,B., & Muller-Hermelink,H.K. The involution of the ageing human thymic epithelium is independent of puberty. A morphometric study. Scand. J. Immunol. 22, 563-575 (1985).
8. Fagnoni,F.F. et al. Shortage of circulating naive CD8(+) T cells provides new insights on immunodeficiency in aging. Blood 95, 2860-2868 (2000).
9. Sempowski,G.D., Gooding,M.E., Liao,H.X., Le,P.T., & Haynes,B.F. T cell receptor excision circle assessment of thymopoiesis in aging mice. Mol. Immunol 38, 841-848 (2002).
10. Lerner,A., Yamada,T., & Miller,R.A. Pgp-1hi T lymphocytes accumulate with age in mice and respond poorly to concanavalin A. Eur. J Immunol 19, 977-982 (1989).
11. Ahmed,M. et al. Clonal expansions and loss of receptor diversity in the naive CD8 T cell repertoire of aged mice. J. Immunol. 182, 784-792 (2009).
12. Naylor,K. et al. The influence of age on T cell generation and TCR diversity. J. Immunol. 174, 7446-7452 (2005).
13. Yager,E.J. et al. Age-associated decline in T cell repertoire diversity leads to holes in the repertoire and impaired immunity to influenza virus. J. Exp. Med. 205, 711-723 (2008).
14. Mackall,C.L. & Gress,R.E. Pathways of T-cell regeneration in mice and humans: implications for bone marrow transplantation and immunotherapy. Immunol Rev 157, 61-72 (1997).
15. Douek,D.C. et al. Changes in thymic function with age and during the treatment of HIV infection. Nature 396, 690-695 (1998).
16. Neese,R.A. et al. Measurement in vivo of proliferation rates of slow turnover cells by 2H2O labeling of the deoxyribose moiety of DNA. Proc. Natl. Acad. Sci. U. S. A 99, 15345-15350 (2002).
17. Vrisekoop,N. et al. Sparse production but preferential incorporation of recently produced naive T cells in the human peripheral pool. Proc. Natl. Acad. Sci. U. S. A 105, 6115-6120 (2008).
18. de Boer,R.J. Estimating the role of thymic output in HIV infection. Curr. Opin. HIV. AIDS 1, 16-21 (2006).
19. Dutilh,B.E. & de Boer,R.J. Decline in excision circles requires homeostatic renewal or homeostatic death of naive T cells. J Theor. Biol. 224, 351-358 (2003).
20. Hazenberg,M.D. et al. Increased cell division but not thymic dysfunction rapidly affects the T-cell receptor excision circle content of the naive T cell population in HIV-1 infection. Nat. Med. 6, 1036-1042 (2000).

21. Jamieson,B.D. et al. Generation of functional thymocytes in the human adult. Immunity. 10, 569-575 (1999).
22. Kimmig,S. et al. Two subsets of naive T helper cells with distinct T cell receptor excision circle content in human adult peripheral blood. J. Exp. Med. 195, 789-794 (2002).
23. Kohler,S. et al. Post-thymic in vivo proliferation of naive CD4+ T cells constrains the TCR repertoire in healthy human adults. Eur. J. Immunol. 35, 1987-1994 (2005).
24. Kilpatrick,R.D. et al. Homeostasis of the naive CD4+ T cell compartment during aging. J. Immunol. 180, 1499-1507 (2008).
25. Asquith,B., Debacq,C., Macallan,D.C., Willems,L., & Bangham,C.R. Lymphocyte kinetics: the interpretation of labelling data. Trends Immunol. 23, 596-601 (2002).
26. Borghans,J.A. & de Boer,R.J. Quantification of T-cell dynamics: from telomeres to DNA labeling. Immunol. Rev. 216, 35-47 (2007).
27. Freitas,A.A. & Rocha,B. Population biology of lymphocytes: the flight for survival. Annu. Rev. Immunol. 18, 83-111 (2000).
28. Berzins,S.P., Boyd,R.L., & Miller,J.F. The role of the thymus and recent thymic migrants in the maintenance of the adult peripheral lymphocyte pool. J Exp. Med 187, 1839-1848 (1998).
29. Surh,C.D. & Sprent,J. Homeostasis of naive and memory T cells. Immunity. 29, 848-862 (2008).
30. Harris,J.M. et al. Multiparameter evaluation of human thymic function: interpretations and caveats. Clin. Immunol. 115, 138-146 (2005).
31. Prelog,M. et al. Thymectomy in early childhood: significant alterations of the CD4(+) CD45RA(+)CD62L(+) T cell compartment in later life. Clin. Immunol. 130, 123-132 (2009).
32. Ribeiro,R.M. & de Boer,R.J. The contribution of the thymus to the recovery of peripheral naive T-cell numbers during antiretroviral treatment for HIV infection. J Acquir. Immune. Defic. Syndr. 49, 1-8 (2008).
33. Bains,I., Antia,R., Callard,R., & Yates,A.J. Quantifying the development of the peripheral naive CD4+ T-cell pool in humans. Blood 113, 5480-5487 (2009).
34. Hazenberg,M.D. et al. Establishment of the CD4+ T-cell pool in healthy children and untreated children infected with HIV-1. Blood 104, 3513-3519 (2004).
35. Tough,D.F. & Sprent,J. Turnover of naive- and memory-phenotype T cells. J. Exp. Med. 179, 1127-1135 (1994).
36. von Boehmer,H. & Hafen,K. The life span of naive alpha/beta T cells in secondary lymphoid organs. J. Exp. Med. 177, 891-896 (1993).
37. Halnon,N.J. et al. Thymic function and impaired maintenance of peripheral T cell populations in children with congenital heart disease and surgical thymectomy. Pediatr. Res. 57, 42-48 (2005).
38. Sempowski,G. et al. Effect of thymectomy on human peripheral blood T cell pools in myasthenia gravis. J. Immunol. 166, 2808-2817 (2001).
39. Binns,R.M., Pabst,R., & Licence,S.T. Subpopulations of T lymphocytes emigrating in venous blood draining pig thymus labelled in vivo with fluorochrome. Immunology 63, 261-267 (1988).
40. Holder,J.E., Washington,E.A., Cunningham,C.P., Cahill,R.N., & Kimpton,W.G. Cell death and thymic export during fetal life. Eur. J Immunol 36, 2624-2631 (2006).
41. Scollay,R., Smith,J., & Stauffer,V. Dynamics of early T cells: prothymocyte migration and proliferation in the adult mouse thymus. Immunol Rev 91, 129-157 (1986).
42. Baars,P.A., Maurice,M.M., Rep,M., Hooibrink,B., & van Lier,R.A. Heterogeneity of the circulating human CD4+ T cell population. Further evidence that the CD4+CD45RA-. J Immunol 154, 17-25 (1995).
43. Hamann,D. et al. Phenotypic and functional separation of memory and effector human CD8+ T cells. J Exp. Med 186, 1407-1418 (1997).
44. Broers,A.E. et al. Quantification of newly developed T cells in mice by real-time quantitative PCR of T-cell receptor rearrangement excision circles. Exp. Hematol. 30, 745-750 (2002).
45. Previs,S.F. et al. Assay of the deuterium enrichment of water via acetylene. J Mass Spectrom. 31, 639-642 (1996).
46. Pillay,J. et al. In vivo labeling with 2H2O reveals a human neutrophil lifespan of 5.4 days. Blood 116, 625-627 (2010).
47. Di,R.F., Ramaswamy,S., Ridge,J.P., & Matzinger,P. On the lifespan of virgin T lymphocytes. J Immunol 163, 1253-1257 (1999).
48. Marquardt,D.W. An algorithm for least-squares estimation of nonlinear parameters. J. Soc. Indust. Appl. Math. 11, 431-441 (1963).
49. Efron,B. & Tibshirani,R. Bootstrap Methods for Standard Errors, Confidence Intervals, and Other Measures of Statistical Accuracy. Statist. Sci. 1, 54-75 (1986).
50. Westermann,J. & Pabst,R. Lymphocyte subsets in the blood: a diagnostic window on the lymphoid system? Immunol. Today 11, 406-410 (1990).

Supplementary Information

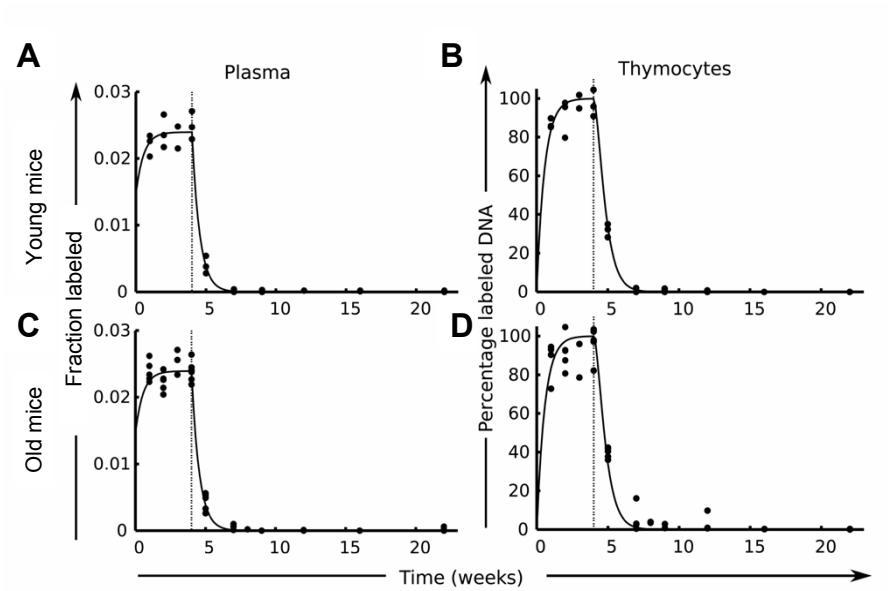

Supplementary Figure 1. Deuterium enrichment in plasma and thymocytes (related to Figure 2). Best fits of plasma ^2H_2O (A) and thymocyte (B) deuterium enrichment in young adult and old mice. Parameter values are given in Supplemental Table 1.

Supplementary Table 1: Parameter values of deuterium enrichment in plasma and in thymocytes (related to Figure 2).

	Parameter	Value[a] (confidence limits)[b]
Plasma[c]	S_0[d]	0.015 (0.012- 0.018)
	d_s (day^{-1})[e]	0.26 (0.23- 0.27)
	α (day^{-1})[f]	0.006 (0.006- 0.007)
Thymocytes[g]	$p_{\text{young mice}}$ (day^{-1})	0.42 (0.38- 0.47)
	$p_{\text{old mice}}$ (day^{-1})	0.31 (0.25- 0.47)

[a] Values are estimates of the best fit depicted in Supplementary Fig. 1.

[b] 95% confidence intervals.

[c] Deuterium enrichment in plasma was measured to estimate the enrichment in body water.

[d] S_0 represents the baseline plasma enrichment attained after the boost at the end of day 0.

[e] d_s is the turnover rate of body water.

[f] α is the fraction of deuterated water consumed daily.

[g] Thymocytes were used to normalize the data as described in Vrisekoop et al., 2008[1]

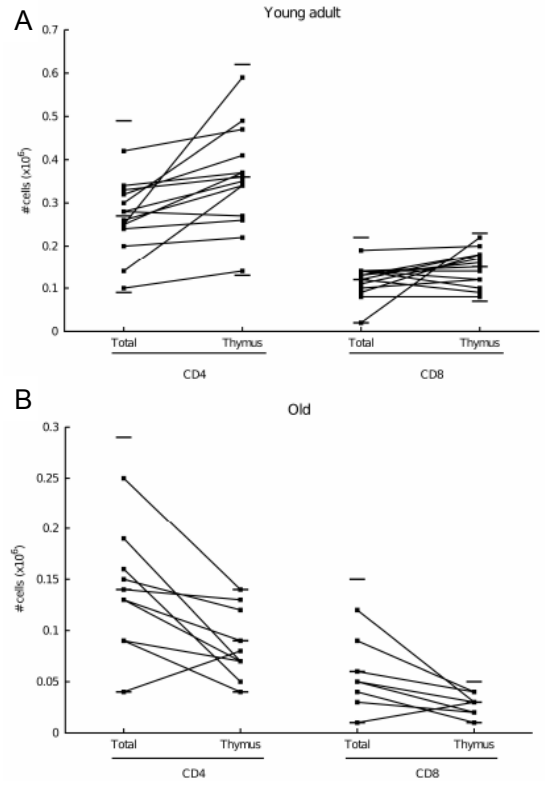

Supplementary Figure 2. Comparison of total daily naive T-cell production and thymic output (related to Figure 3). Total daily naive T-cell production in spleens from young adult mice (A) and old mice (B) were estimated by multiplying the average production rates from the ^2H_2O-labeling experiment in young adult (Fig. 2A) and old (Fig. 2B) mice with the naive T-cell numbers in the spleen of each mouse (Fig. 3A,B). Thymic output of the same mice was calculated by multiplying the estimated thymic output rate (ε = 0.034) from the survival model (= model (1)) with the absolute number of single positive thymocytes of the mice. The medians of the data in each group are indicated by a horizontal line. The upper and lower horizontal bars represent the maximum and minimum values that could be attained (based on the confidence limits of p and ε).

Supplementary Table 2: Parameters values of the best fit of the phenomenological functions $f_1(t)$ describing thymic output (A) and $f_2(t)$ describing the ratio of naive T-cell numbers in LN and spleen (B) (related to Figure 3).

A	Parameter	Value[a] (confidence limits)[b]
CD4⁺ SP[c]	σ ($\times 10^7$ cells)[d]	3.5 (3.2- 3.8)
	s_1 (day^{-1})[d]	0.084 (0.065- 0.11)
CD8⁺ SP[c]	σ ($\times 10^7$ cells)[d]	1.7 (1.1- 9.8)
	s_1 (day^{-1})[d]	0.023 (0.003- 0.056)
CD4⁺ SP, CD8⁺ SP[c]	s_2 (day^{-1})[e]	0.5 (0.2 – 3.0)
	s_3 (day^{-1})[e]	0.001 (0.001- 0.002)
	T_{off} (days)	47 (42- 49)
	α	0.35 (0.31- 0.38)

[a] Values represent the best fit of the model to the CD4⁺ and CD8⁺ SP thymocyte data.

[b] 95% confidence intervals.

[c] While the generation of CD4⁺ and CD8⁺ SP thymocytes differs, the mechanism and driving force of thymus involution is the same. Therefore, we allowed CD4⁺ and CD8⁺ SP thymocytes to have different dynamics during the establishment of the immune system (σ, s_1) but to have the same thymus involution dynamics (s_2, s_3, T_{off} and α).

[d] $\sigma \times s_1$ is the initial rate at which the thymus becomes populated by thymocytes.

[e] s_2 and s_3 describe the involution of the thymus. The initial involution rate (s_2) was so fast that the number of SP thymocytes halved within a week.

B	Parameter	Value (confidence limits)[f]	
		CD4⁺	**CD8⁺**
	Control[g]		
	σ	1.6 (1.2- 2.4)	5.4 (1.4- 19)
	s_1	0.098 (0.049- 0.17)	0.017 (0.004- 0.096)
	s_2	0.024 (0.020- 0.030)	0.022 (0.015- 0.030)
	s_3	0	0
	α	0.72 (0.69- 0.75)	0.58 (0.52- 0.62)
	T_{off}	14 (12- 18)	15(12- 20)
	After thymectomy[h]		
	s_2	0.025 (0.016- 0.041)	0.024 (0.011- 0.054)
	s_3	0	0
	α	0.68 (0.60- 0.78)	0.46 (0.36- 0.59)

[f] 95% confidence intervals.

[g] The upper part of the table shows parameter values of the best fit to control mice data.

[h] The lower part shows parameters values of the best fit to data from thymectomized mice (from the time of thymectomy onward, $t > 49$ days).

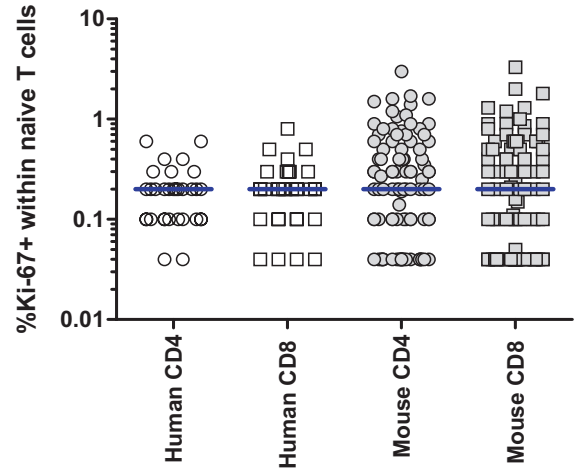

Supplementary Figure 3.

References Supplementary Information

1. Vrisekoop, N., den Braber, I., de Boer, A.B., Ruiter, A.F., Ackermans, M.T., van der Crabben, S.N., Schrijver, E.H., Spierenburg, G., Sauerwein, H.P., Hazenberg, M.D., et al. Sparse production but preferential incorporation of recently produced naive T cells in the human peripheral pool. Proc. Natl. Acad. Sci. U. S. A 105, 6115-6120 (2008).

4

Age-related Decline of T-cell Receptor Excision Circles in Humans Requires Peripheral Naive T-cell Division

Liset Westera[1], Julia Drylewicz[1,2], Sara van den Berg[1], Anouk BC Schuren[1], Simone Havenith[3,4], Ineke JM Ten Berge[3], Arjan van Zuilen[5], José AM Borghans[1], Kiki Tesselaar[1]

[1] Laboratory of Translational Immunology, University Medical Center Utrecht, Utrecht, The Netherlands; [2] Theoretical Biology and Bioinformatics, Utrecht University, Utrecht, The Netherlands; [3] Renal Transplant Unit, Department of Internal Medicine, Academic Medical Center, University of Amsterdam, Amsterdam, The Netherlands; [4] Department of Experimental Immunology, Academic Medical Center, University of Amsterdam, Amsterdam, The Netherlands; [5] Department of Nephrology, University Medical Center Utrecht, Utrecht, The Netherlands

The presence of an age-related decline of T-cell receptor excision circle (TREC) contents of naive T cells in healthy humans but not in mice has been interpreted to reflect a fundamental difference in naive T-cell maintenance between the species: not thymic output but peripheral cell division is the major source of new T cells in human adults. This interpretation is based on the assumption that TRECs are very stable and that dilution of TRECs is due to peripheral naive T-cell division and not to intracellular TREC decay. To find evidence for this key assumption we investigated the effects of blocking peripheral T-cell division on naive T-cell TREC contents in silico and in vivo. We measured naive T-cell TREC contents in renal transplant patients who had received immunosuppressive drugs that block cell division for several years to decades. On average, patients treated with mycophenolate mofetil (MMF) had higher naive T-cell TREC contents than age-matched controls. Comparing the TREC contents of these patients after years of immunosuppression to their projected TREC content at the age of transplantation suggested that on average naive T-cell TREC contents had declined less than normal. Our in silico experiments show that a block of cell division would not affect TREC contents if the TREC decline in healthy individuals were only due to intracellular TREC decay. Our combined data thus suggest that the age-related decline in naive T-cell TREC contents is not merely due to intracellular TREC decay, but indeed depends on human naive T-cell division.

Introduction

A commonly held view is that in mice the thymus plays an important role in maintenance of the peripheral naive T-cell pool whereas the role of peripheral naive T-cell division is limited. This understanding originates mainly from classical mouse experiments which showed that, e.g., incorporation of 5'-bromo-3'deoxyuridine by naive T cells strongly relies on the presence of a thymus[1, 2], and that division by naive T cells in lymphopenic mice induces loss of the naive phenotype[3-11].

A few studies have suggested that in this respect the mouse is not a good model system for what is occurring in humans[12-14]. Using a combination of stable-isotope labeling and analysis of T-cell receptor excision circles (TRECs), we recently demonstrated that the mechanism for naive T-cell maintenance in humans differs essentially from that in mice[14]. While in mice – even at very old age – the vast majority of the naive T-cell pool is sustained by thymic output, the human naive T-cell pool is maintained predominantly by peripheral T-cell division[14]. Importantly, the latter conclusion relies on the assumption that TRECs themselves are very stable and that a TREC content decline is due to cell division, when a TREC is passed on to either one of the daughter cells.

The observation that TREC$^+$ cells can still be found, albeit at lower levels, in individuals thymectomized many decades ago supports the notion that TRECs are very stable[15-19]. The interpretation of this "experiment of nature" is however complicated by the fact that there is evidence for regrowth of functional thymic tissue after thymectomy[20], providing a potential source of new TREC$^+$ T cells in the peripheral pool and challenging the long-term persistence of TRECs. To date, there is no unambiguous evidence that the age-related decline in naive T-cell TREC contents observed in humans[14, 21-23] is due to peripheral naive T-cell division.

We sought for additional evidence that peripheral division, and not intracellular TREC decay, engenders the age-related TREC decline in naive T cells, by investigating naive T-cell TREC contents in a situation in which T-cell division was suppressed for prolonged periods of time. This condition was present in renal transplant patients who had been treated with the immunosuppressive drugs mycophenolate mofetil (MMF, CellCept®) or azathioprine (AZA, Imuran®) for many years. Both MMF and AZA target the de novo purine synthesis, a pathway on which T and B cells depend more than any other cell type as they have little or no nucleotide salvage pathway[24-26]. We measured TRECs in longitudinal samples from patients up to ten years post transplantation and in cross-sectional samples from patients between 10 and 35 years post transplantation and related them to values of healthy controls. Our data showed that prolonged MMF treatment, but not AZA treatment, results in increased naive T-cell TREC contents in renal transplant patients.

Results

Approach and hypothesis

To investigate TREC dynamics in a situation without T-cell division, we collected longitudinal blood samples from renal transplant patients over a follow-up period of up to 11 years, and cross-sectional blood samples from patients that had been transplanted 10-35 years ago (see Table 1 for patient characteristics). From these samples naive $CD4^+$ and $CD8^+$ T-cell subsets were sorted for TREC analysis. All patients had been treated with the immunosuppressive drugs MMF and/or AZA since their transplantation; both drugs are known to inhibit lymphocyte division[24-26].

Figure 1 depicts the *expected* TREC dynamics during prolonged immunosuppression in either of two extreme scenarios: in scenario A (Fig. 1A), the age-related naive T-cell TREC decline in healthy individuals (solid line) is due to dilution by peripheral naive T-cell division, as assumed in Den Braber et al.[14]; in alternative scenario B (Fig. 1B), the age-related naive T-cell TREC decline in healthy individuals (solid line) is due to intracellular TREC decay. In scenario B TRECs decay at a rate of 0.08% per year, which is more than two times faster than the turnover rate of naive T cells ($CD4^+$: 0.04%; $CD8^+$: 0.03%) (Westera et al., Lymphocyte maintenance during healthy aging requires no substantial alterations in cell dynamics, submitted). If the TREC decline in healthy individuals were to be due to TREC degradation, blocking cell division by drugs in patients should not influence the TREC decline. Regardless of the duration of immunosuppression, transplantation patients will therefore have TREC contents similar to controls (Fig. 1B). By contrast, if the TREC decline in healthy individuals is due to cell division, blocking cell division by drugs can affect the patients' TREC content changes over time: because TREC dilution by cell division is not expected to occur and thymic output continues to contribute to the peripheral TREC content, over time naive T-cell TREC contents of immune suppressed patients would decline less than in healthy aging and could even increase (Fig. 1A).

Table 1. Patient characteristics.

Drug	Number	Median age* (range)	Median years on immunosuppressive drug therapy (range)
Longitudinal			
MMF	9	52 (28-63)	8.1 (4.0-10.5)
AZA	1	48	9.7
Cross-sectional			
MMF	8**	58 (40-79)	15.6 (10.6-18.9)
AZA	9***	65 (42-70)	18.2 (10.5-34.6)

* For longitudinal patients: age of last measurement; for cross-sectional patients: age at study visit.
** 1 patient received AZA during the first 3 years
*** 1 patient received MMF during the first year

No effect of dialysis on TREC contents

A state of chronic immune activation has been observed in patients on dialysis[27], the stage that typically precedes renal transplantation. As this immune activation might decrease TREC contents, we first measured TRECs in naive $CD4^+$ and $CD8^+$ T cells isolated from dialysis patients and from healthy individuals of different ages (Sup, Fig. 1). In agreement with the literature[14, 15, 22], naive T-cell TREC contents in healthy individuals

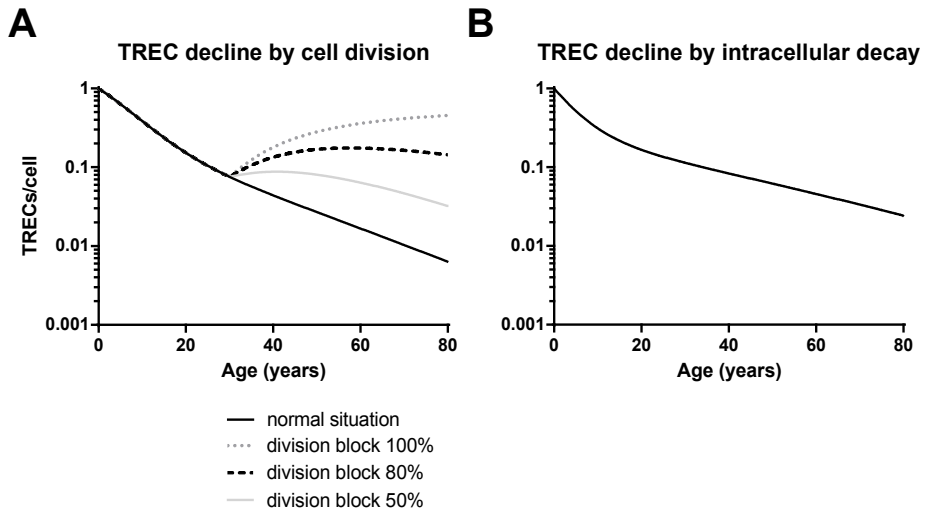

Figure 1. Expected naive T-cell TREC contents during long-term immunosuppression for the 2 extreme scenarios of a TREC content decline. Scenario A: the age-related TREC dilution in healthy individuals (solid line) is due to naive T-cell division. Scenario B: the age-related TREC decline in healthy individuals (solid line) is due to intracellular TREC decay. In silico experiments show that an age-related naive T-cell TREC content decline (solid black line) observed in healthy individuals can be explained both by peripheral naive T-cell division (A) and by intracellular TREC decay (B). However, the dynamics of TREC contents during immunosuppression (blocking cell division) are different for the two scenarios. In Scenario A, TREC dynamics during immunosuppression are different from the TREC content decline in healthy individuals. When peripheral naive T-cell division is blocked by long-term immunosuppression, TRECs are no longer diluted by division and only thymic output contributes to the peripheral TREC content. Blocking division, either completely (dotted gray line), for 80% (dashed black line), or for 50% (solid gray line), can lead to enrichment of TRECs in the population or slow down the age-related TREC content decline. In scenario B, the normal TREC decline is due to intracellular TREC decay. In this scenario, TREC contents during immunosuppression will follow the same decline as in a normal situation, because intracellular TREC decay is not affected by block of cell division. Expected TREC contents in a normal situation and during long-term immunosuppression were derived from in silico experiments (see Materials and Methods).

declined about one order of magnitude between the 3rd and the 7th decade of life. TREC contents in dialysis patients were similar to those in healthy, age-matched individuals, following the same age-associated decline (slopes of the exponential growth equation were not significantly different, p-value=0.75 for naive $CD4^+$ and p-value=0.54 for naive $CD8^+$). Since dialysis had no substantial effect on naive T-cell TREC contents, we combined TREC data from healthy subjects and dialysis patients, to obtain a larger set of reference TREC values with age.

Naive T-cell TREC contents in immune suppressed patients

To study if and how TREC dynamics would be affected by drug-induced immunosuppression, we next measured naive T-cell TREC contents in longitudinal samples collected from renal transplant patients over a follow-up period of 4 to 11 years (Fig. 2A). Although most published TREC data are cross-sectional, a previous study by Kilpatrick et al. reported longitudinal naive T-cell TREC contents in healthy individuals over a time period of on average 16 years[23]. This reconfirmed a net age-related decline in TREC contents but also revealed a considerable intra-individual variation over time[23]. Likewise, our longitudinal TREC data in immune suppressed patients displayed considerable intra-individual variation (Fig. 2A). This, combined with the relatively short time frame of 4-11 years post transplantation, made it difficult to draw firm conclusions regarding the net change in TREC contents over time (Fig. 2C). The change in naive T-cell TREC contents per year in patients was not significantly different from the normal age-related decline ($CD4^+$: p-value=0.2; $CD8^+$: p-value=0.7), yet the results also did not exclude the possibility that TREC contents in immune suppressed patients had declined less than in healthy individuals (Fig. 2C), a scenario that might be more evident after a longer period of time. We therefore also measured TRECs in cross-sectional samples collected from patients that had a much longer history of immunosuppression. TREC contents of naive $CD4^+$ and $CD8^+$ T cells from patients transplanted 10 to 35 years ago showed a considerable interindividual variation (Fig. 2B, Sup. Fig. 1), which might be due to for example differences in duration of immunosuppression or to the drug type used. Classifying patients based on MMF or AZA use (the 2 patients who had used both drugs were classified according to the drug they had used for the longest period of time, see Table 1) revealed a dichotomy between the two treatments: MMF-treated patients tended to have higher naive T-cell TREC contents than AZA-treated patients. When we compared the difference of each patient's naive T-cell TREC content to the normal naive T-cell TREC content of that age, MMF-treated but not AZA-treated patients tended towards higher naive T-cell TREC

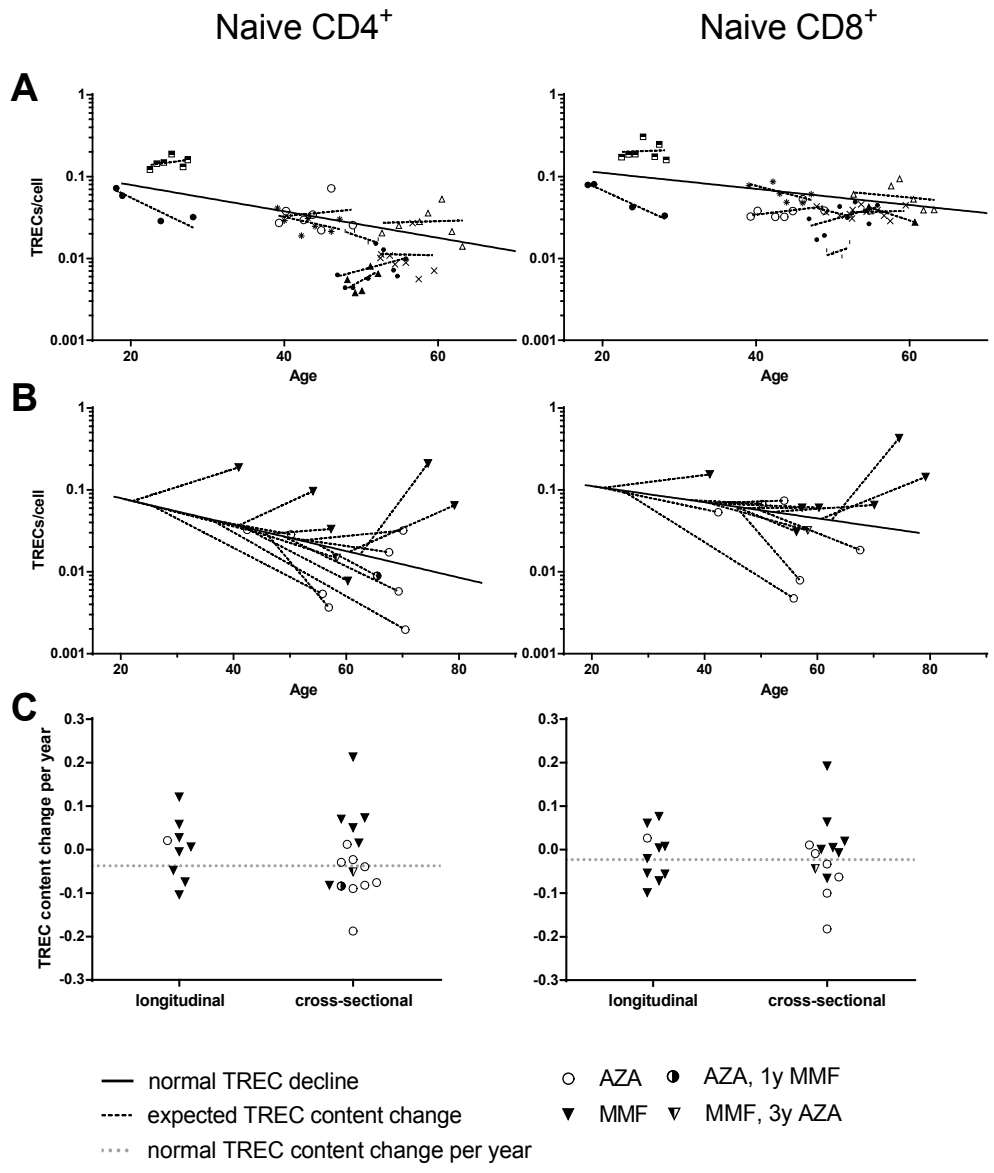

Figure 2. TREC contents during immunosuppression. (A) Longitudinal TREC contents of naive $CD4^+$ (left) and $CD8^+$ (right) T cells isolated from renal transplant patients over a follow-up period of 4 to 10 years. Different symbols reflect different individuals (open circles: AZA-treated; other symbols: MMF-treated), and exponential growth curves are plotted through individual data sets. The solid line shows the normal age-related TREC decline. (B) Cross-sectional TREC contents of naive $CD4^+$ (left) and $CD8^+$ (right) T cells isolated from renal transplant patients transplanted at least 10 years ago. 8 patients received MMF (closed inverted triangles; semi-closed triangle depicts a patient who had AZA for 3 years), and 9 patients received AZA (open circles; semi-closed circle depicts a patient who had MMF for 1 year). Dotted lines represent the expected TREC change, assuming that each patient had a "normal" TREC content at the age of transplantation. The solid line shows the normal age-related TREC decline. (C) The expected TREC content change per year in these patients for naive $CD4^+$ (left) and $CD8^+$ T cells (right). Symbols are used as in panel B. The normal age-related TREC content change per year is indicated by a dashed horizontal line.

contents than age-matched controls (MMF: $CD4^+$ p-value=0.08; $CD8^+$: p-value=0.11). Because patients differed in the number of years they had been on immunosuppressive drugs, we next estimated their TREC content change per year, by assuming that all patients had a normal TREC content before transplantation (Fig. 2B,C). This allowed for a fair comparison between the treatment groups, which showed that the change in naive T-cell TREC contents per year seemed different between MMF-treated patients and AZA-treated patients ($CD4^+$: p-value=0.02; not significant for $CD8^+$: p-value 0.08). TREC contents in AZA-treated patients declined at a similar rate as normal TREC contents ($CD4^+$: p-value=0.25; $CD8^+$: p-value=0.31, Fig. 2C). In contrast, TREC contents in MMF-treated patients tended to increase rather than to follow the normal decline ($CD4^+$: p-value=0.08; $CD8^+$: p-value=0.19, Fig. 2C).

The apparent dichotomy between MMF-treated and AZA-treated patients suggested a fundamental difference between the effects of the two drugs. The observation that TREC contents in AZA-treated patients seemed to follow the normal age-related TREC decline at first glance suggested that AZA was simply not effectively suppressing peripheral naive T-cell division. However, both MMF-treated and AZA-treated patients had lower absolute numbers of naive $CD4^+$ and $CD8^+$ T cells compared to healthy individuals (Sup. Fig. 2), indicating that both drugs were clearly effective. Because TREC contents are strongly influenced not only by peripheral cell division but also by thymic output, we investigated whether the normal TREC contents in AZA-treated patients could be related to additional suppressive effects of this drug on the thymus. In silico experiments confirmed that blocking thymic output can indeed influence TREC dynamics over time, the outcome of which depends on the relative inhibition of peripheral cell division and thymic output (Sup. Fig. 3).

Discussion

In this work we have studied whether the age-related naive T-cell TREC content decline in healthy individuals could be explained by intracellular TREC decay (Fig. 1B), instead of by TREC dilution through peripheral naive T-cell division (Fig. 1A). Given the large interindividual variation in cross-sectional data, longitudinal patient samples are in principle the best to study TREC dynamics over time, yet the window of 4-10 years post-transplantation was still relatively short to draw conclusions about TREC content changes over time. By contrast, cross-sectional samples from patients transplanted at least a decade ago revealed that in MMF-treated patients, but not in AZA-treated patients, naive T-cell TREC contents were higher than those in age-matched controls. The supranormal naive T-cell TREC contents in MMF-treated patients are consistent with the idea that the normal TREC decline observed with age is due to naive T-cell division (Fig. 1A).

To illustrate how cross-sectional TREC contents in patients had changed during prolonged immunosuppression, we estimated the expected TREC content change based on the assumption that all patients had a normal TREC content at the time of transplantation (Fig. 2B,C). It should be emphasized that the *actual* TREC content at the age of transplantation was unknown and could also be lower or higher than the expected TREC content, mainly because the interindividual variation around TREC contents is considerable (Sup. Fig. 1). Although our approach introduces an uncertainty in the interpretation of the expected TREC content change per individual, it does permit interpretation at the group level. Based on our results in MMF-treated patients, we can exclude a scenario in which the age-related TREC decline is entirely due to intracellular degradation of TRECs. However, even though all data, including this work, point into the direction that TRECs are very stable[15-19], we cannot exclude that TREC degradation to some extent contributes to declining TREC contents over time.

Our in silico experiments suggested that the apparent dichotomy between the two treatment groups might be related to possible inhibitory effects of AZA but not MMF on the thymus (Sup. Fig. 3). This is plausible given that MMF is a more selective inhibitor of lymphocyte proliferation than AZA, which has multiple active metabolites and is generally associated with broader effects[24-26]. A number of animal studies have reported thymic atrophy after AZA use, as evidenced by reduced thymic weight and cellularity[28-30], perhaps as a consequence of increased apoptosis. The interaction of AZA's metabolite 6-mercaptopurine with the guanosine triphosphate-binding protein Rac-1 was found to block Rac1 activity and thus inhibit the upregulation of dominant regulator of apoptosis Bcl-xL, a protein which normally promotes cell survival by inhibiting apoptosis[31]. Moreover, in mice Rac1 was shown to be essential for thymic epithelial cell homeostasis, as deletion of Rac1 in embryonic and in adult thymic epithelial cells resulted in failure of thymic ontogeny and thymic atrophy, respectively[32]. Although the effects of AZA on the thymus are not well studied in humans, such effects are not unlikely to occur. In addition, the main adverse effect of AZA, bone marrow depression[33], could contribute indirectly to a reduction of thymic output by a poor supply of early T-cell progenitors to the thymus.

In summary, although group sizes are still relatively small, our data show that long-term MMF-treated patients, but not AZA-treated patients, tend to have increased naive T-cell TREC contents compared to age-matched controls. Although these are not significant differences, it should be noted that this project is at an intermediate stage and that current group sizes are still relatively small. At present, our results exclude a scenario in which the age-related TREC decline in healthy individuals is due to intracellular TREC degradation (Fig. 1B) and are consistent with the idea that this decline is due to peripheral division of human naive T cells, reconfirming our previous work on human naive T-cell division[14]. Finally, our findings have prompted us to pursue the current work by including a larger number of MMF-treated patients in our cross-sectional study.

Acknowledgments

We thank Koos Gaiser, Gerrit Spierenburg, Jeroen van Velzen, and Pien van der Burght for technical support, and Anne Moazzeni, Sanne Bosman, Alies Rijksen-de Bruin, and Anka Snel-de Bell for their support around study visits. We also acknowledge the help of clinicians in asking patients for participation to our studies.

Materials and Methods

Subjects. Longitudinal cryopreserved PBMC samples were previously obtained from 10 renal transplant patients in the Academic Medical Center in Amsterdam over a follow-up period of at most 10 years post transplantation. 9 patients were treated with mycophenolate mofetil (MMF) and 1 patient was treated with azathioprine (AZA). Cryopreserved PBMC were stored in liquid nitrogen until further processing. From all patients written informed consent was obtained. Blood from anonymous healthy donors was obtained from the Mini Donor Service of the University Medical Center Utrecht and was tested negative for hepatitis B, hepatitis C and HIV. Isolated PBMC were processed fresh or frozen in liquid nitrogen. Cross-sectional blood samples were collected from 17 renal transplant patients in the University Medical Center Utrecht. Patients were transplanted at least 10 years ago and treated with either MMF, AZA, or both during this period. Additional blood samples were collected from 10 patients receiving hemodialysis for at least 1 year. In addition, medical data were collected from patient medical records. The study was approved by the medical ethics committee (METC) of the University Medical Center Utrecht and was conducted in agreement with the Helsinki declaration revised in 2008. From all patients written informed consent was obtained. Isolated PBMC were always processed fresh to maximize cell yields after sorting.

Determination of absolute numbers / Flow cytometric analyses. Absolute peripheral T-cell numbers were determined using TruCOUNT tubes (BD), in which whole blood was stained using CD45-PerCP, CD3-FITC, CD8-PE, and CD4-Pacific Blue (all from BioLegend) antibodies. After erythrocyte lysis with FACS Lysing Solution (BD) tubes were instantly analyzed on an LSR-II using FACSDiva software.

Cell sorting. For longitudinal samples from transplantation patients and cross-sectional samples from healthy controls, PBMCs were stained with CD3-FITC, CD8-PerCP (both BD), CD4-Pacific Blue CD45RO-PE (both BioLegend), and CD27-APC (eBioscience) antibodies, and sorted into $CD4^+$ and $CD8^+$ naive ($CD27^+$ $CD45RO^-$) and memory ($CD45RO^+$) T cells. For cross-sectional samples of transplantation and dialysis patients, PBMCs were stained with CD3-FITC (BD), CD4-Pacific Blue (BioLegend), CD8-PerCp-Cy5.5 (BioLegend), CD27-APC-eFluor780 (eBioScience), CD45RO-PE-Cy7 (BD), CD95-PE (BD), and CCR7-APC (BioLegend) antibodies. $CD4^+$ and $CD8^+$ naive ($CD27^+$ $CCR7^+$ $CD45RO^-$ $CD95^-$) and memory ($CD45RO^+$), and whenever possible $CD8^+$ effector ($CD27^-CD45RO^-$) $CD3^+$ T cells were sorted on a FACS Aria II or FACS Aria III cell sorter using FACSDiva software (all BD).

DNA isolation. Genomic DNA was isolated from sorted T-cell subsets using the Reliaprep Blood gDNA Miniprep System (Promega), and stored at -20°C until further analysis.

Measurement of TRECs by quantitative PCR. Signal joint T cell receptor excision circles (TRECs) were detected with a real-time quantitative PCR method [REF Hazenberg 2000], using a ViiA™ 7 Real-Time PCR System and ViiA™ 7 software (Applied Biosystems). TREC contents (the number of signal joint TRECs per cell) were calculated as described previously[34].

Mathematical modeling for in silico TREC dynamics. TREC dynamics were investigated using a previously developed mathematical model describing the dynamics of naive T cells and their TRECs[34]. In this model, N is the total number of naive $CD4^+$ T cells and T the total amount of TRECs in the naive T-cell population, $\sigma(t)$ is the time-dependent source of naive T cells from the thymus where t is the age of the individual in years, c is the average number of TRECs per recent thymic emigrant, $d(N)$ the rate of cell death and priming of naive into memory T cells which depends on cell density, δ_i the intra-cellular degradation of TRECs and p the rate of naive T-cell division. The model can be written as follows:

$$\frac{dT}{dt} = c\sigma(t) - d(N)T - \delta_i T$$

$$\frac{dN}{dt} = \sigma(t) + pN - d(N)N \quad ,$$

where $\sigma(t) = \sigma_0 \exp(-vt)$.

Since TRECs can only be produced in the thymus, the total number of TRECs is not affected by peripheral T-cell division. We define the TREC content of naive T cells as $A=T/N$. We allow the loss rate of cells to be density dependent rather than constant: cells tend to be lost more frequently when cell numbers are high. Therefore, the T-cell loss rate is set as follows:

$$d(N) = d_0(1 + \varepsilon N).$$

Parameters were set to describe a TREC content decline over age in agreement with current knowledge: thymus involution[35], thymic output contribution[14, 36] and loss rate of naive T cells[13]. Parameter values used in Fig. 1 and Sup. Fig. 3: for scenario A, c=1, σ_0=3.653 x 10^{10} cells, υ=0.05, p=0.1662 per year, d_0= 0.0073 per year, ε=5 10-11, δ_i= 0; for scenario B: c=1, σ_0=3.653 x 10^{10} cells, υ=0.05, p=0, d_0=0.0073 per year, ε=5 10-11, δ_i=0.29 per year.

Statistics. TREC contents with age were fitted with an exponential growth equation, given by Y=Y0*exp(*k**X), where Y0 is the Y value when X (time in years) is zero, and *k* is the rate constant, expressed in reciprocal of the X axis time units (per year) (Graphpad Prism). The fits of the exponential growth equation to the TREC contents in healthy subjects and in dialysis patients were compared with an extra sum-of-squares F-test (Graphpad Prism). Values for the slopes *k* were used as the TREC content change per year. Groups were compared to each other with a Mann-Whitney test, and compared to a theoretical value using a Wilcoxon Signed Rank test (Graphpad Prism). Differences with p-value<0.05 were considered significant. In silico TREC dynamics were performed using Berkeley Madonna software.

References

1. Tough, D.F. & Sprent, J. Turnover of naive- and memory-phenotype T cells. J. Exp. Med. 179, 1127-1135 (1994).
2. von Boehmer, H. & Hafen, K. The life span of naive alpha/beta T cells in secondary lymphoid organs. J. Exp. Med. 177, 891-896 (1993).
3. Surh, C.D. & Sprent, J. Homeostasis of naive and memory T cells. Immunity 29, 848-862 (2008).
4. Beutner, U. & MacDonald, H.R. TCR-MHC class II interaction is required for peripheral expansion of CD4 cells in a T cell-deficient host. Int. Immunol. 10, 305-310 (1998).
5. Ernst, B., Lee, D.S., Chang, J.M., Sprent, J., & Surh, C.D. The peptide ligands mediating positive selection in the thymus control T cell survival and homeostatic proliferation in the periphery. Immunity 11, 173-181 (1999).
6. Cho, B.K., Rao, V.P., Ge, Q., Eisen, H.N., & Chen, J. Homeostasis-stimulated proliferation drives naive T cells to differentiate directly into memory T cells. J. Exp. Med. 192, 549-556 (2000).
7. Goldrath, A.W., Bogatzki, L.Y., & Bevan, M.J. Naive T cells transiently acquire a memory-like phenotype during homeostasis-driven proliferation. J. Exp. Med. 192, 557-564 (2000).
8. Gudmundsdottir, H. & Turka, L.A. A closer look at homeostatic proliferation of CD4+ T cells: costimulatory requirements and role in memory formation. J. Immunol. 167, 3699-3707 (2001).
9. Kieper, W.C. & Jameson, S.C. Homeostatic expansion and phenotypic conversion of naive T cells in response to self peptide/MHC ligands. Proc. Natl. Acad. Sci. U. S. A 96, 13306-13311 (1999).
10. Murali-Krishna, K. & Ahmed, R. Cutting edge: naive T cells masquerading as memory cells. J. Immunol. 165, 1733-1737 (2000).
11. Oehen, S. & Brduscha-Riem, K. Naive cytotoxic T lymphocytes spontaneously acquire effector function in lymphocytopenic recipients: A pitfall for T cell memory studies? Eur. J. Immunol. 29, 608-614 (1999).
12. Mackall, C.L. & Gress, R.E. Thymic aging and T-cell regeneration. Immunol. Rev. 160, 91-102 (1997).
13. Vrisekoop, N. et al. Sparse production but preferential incorporation of recently produced naive T cells in the human peripheral pool. Proc. Natl. Acad. Sci. U. S. A 105, 6115-6120 (2008).
14. den Braber, I. et al. Maintenance of peripheral naive T cells is sustained by thymus output in mice but not humans. Immunity 36, 288-297 (2012).
15. Douek, D.C. et al. Changes in thymic function with age and during the treatment of HIV infection. Nature 396, 690-695 (1998).
16. Halnon, N.J. et al. Thymic function and impaired maintenance of peripheral T cell populations in children with congenital heart disease and surgical thymectomy. Pediatr. Res. 57, 42-48 (2005).
17. Sempowski, G. et al. Effect of thymectomy on human peripheral blood T cell pools in myasthenia gravis. J. Immunol. 166, 2808-2817 (2001).
18. Prelog, M. et al. Thymectomy in early childhood: significant alterations of the CD4(+) CD45RA(+)CD62L(+) T cell compartment in later life. Clin. Immunol. 130, 123-132 (2009).
19. Storek, J. et al. Low T cell receptor excision circle levels in patients thymectomized 25-54 years ago. Immunol. Lett. 89, 91-92 (2003).

20. van Gent, R. et al. Long-term restoration of the human T-cell compartment after thymectomy during infancy: a role for thymic regeneration? Blood 118, 627-634 (2011).

21. Harris, J.M. et al. Multiparameter evaluation of human thymic function: interpretations and caveats. Clin. Immunol. 115, 138-146 (2005).

22. Jamieson, B.D. et al. Generation of functional thymocytes in the human adult. Immunity 10, 569-575 (1999).

23. Kilpatrick, R.D. et al. Homeostasis of the naive CD4+ T cell compartment during aging. J. Immunol. 180, 1499-1507 (2008).

24. Allison, A.C. & Eugui,E.M. Mycophenolate mofetil and its mechanisms of action. Immunopharmacology 47, 85-118 (2000).

25. Maltzman, J.S. & Koretzky,G.A. Azathioprine: old drug, new actions. J. Clin. Invest 111, 1122-1124 (2003).

26. Khan, M.M. Immunosuppressive agents in Immunopharmacology (2008).

27. Meijers, R.W. et al. Uremia causes premature ageing of the T cell compartment in end-stage renal disease patients. Immun. Ageing 9, 19 (2012).

28. De Waal, E.J., Timmerman,H.H., Dortant,P.M., Kranjc,M.A., & Van,L.H. Investigation of a screening battery for immunotoxicity of pharmaceuticals within a 28-day oral toxicity study using azathioprine and cyclosporin A as model compounds. Regul. Toxicol. Pharmacol. 21, 327-338 (1995).

29. Smith, H.W., Winstead,C.J., Stank,K.K., Halstead,B.W., & Wierda,D. A predictive F344 rat immunotoxicology model: cellular parameters combined with humoral response to NP-CgammaG and KLH. Toxicology 194, 129-145 (2003).

30. Molyneux, G. et al. The haemotoxicity of azathioprine in repeat dose studies in the female CD-1 mouse. Int. J. Exp. Pathol. 89, 138-158 (2008).

31. Tiede, I. et al. CD28-dependent Rac1 activation is the molecular target of azathioprine in primary human CD4+ T lymphocytes. J. Clin. Invest 111, 1133-1145 (2003).

32. Hunziker, L. et al. Rac1 deletion causes thymic atrophy. PLoS. One. 6, e19292 (2011).

33. Lennard, L. The clinical pharmacology of 6-mercaptopurine. Eur. J. Clin. Pharmacol. 43, 329-339 (1992).

34. Hazenberg, M.D. et al. Increased cell division but not thymic dysfunction rapidly affects the T-cell receptor excision circle content of the naive T cell population in HIV-1 infection. Nat. Med. 6, 1036-1042 (2000).

35. Steinmann, G.G., Klaus,B., & Muller-Hermelink,H.K. The involution of the ageing human thymic epithelium is independent of puberty. A morphometric study. Scand. J. Immunol. 22, 563-575 (1985).

36. Murray, J.M. et al. Naive T cells are maintained by thymic output in early ages but by proliferation without phenotypic change after age twenty. Immunol. Cell Biol. 81, 487-495 (2003).

Supplementary Information

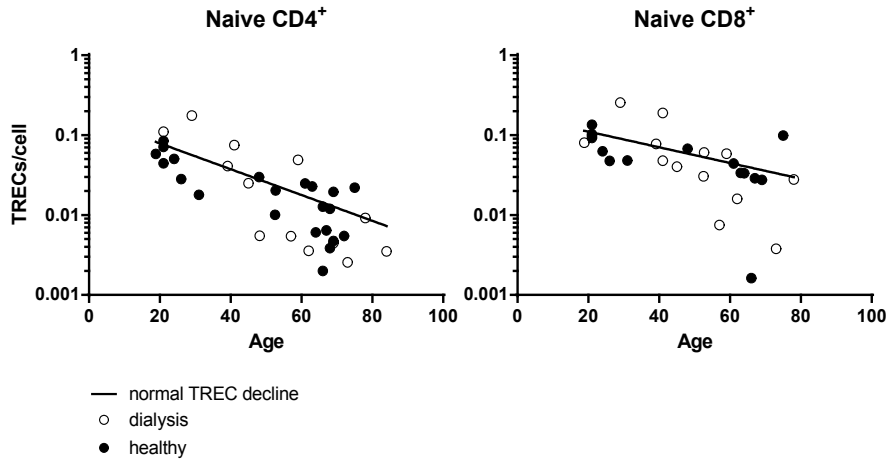

Supplementary Figure 1. Normal age-related TREC content decline in cross-sectional data from dialysis patients and healthy individuals. TREC contents were determined in naive $CD4^+$ and $CD8^+$ T cells from dialysis patients (open circles) and healthy individuals (closed circles). Because TREC contents showed a similar age-related decline in the two groups (slopes of the exponential growth equation were not significantly different), data of the groups were pooled to display one "normal TREC decline" (solid line). The graph illustrates the large interindividual variation in TREC contents.

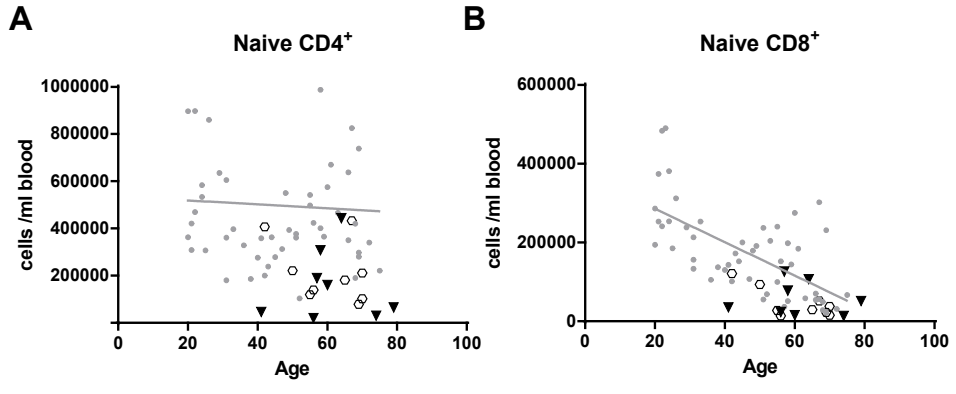

Supplementary Figure 2. Cross-sectional measurements of naive T-cell numbers in renal transplant patients after >10 years immunosuppression. The number of naive $CD4^+$ (A) and $CD8^+$ (B) T cells was determined in samples from renal transplant patients treated for >10 years with AZA (open circles) or MMF (closed inverted triangles). Gray, smaller dots represent naive T-cell numbers determined in 52 healthy individuals of different age; the solid line depicts the age-related change in naive T-cell numbers in healthy individuals.

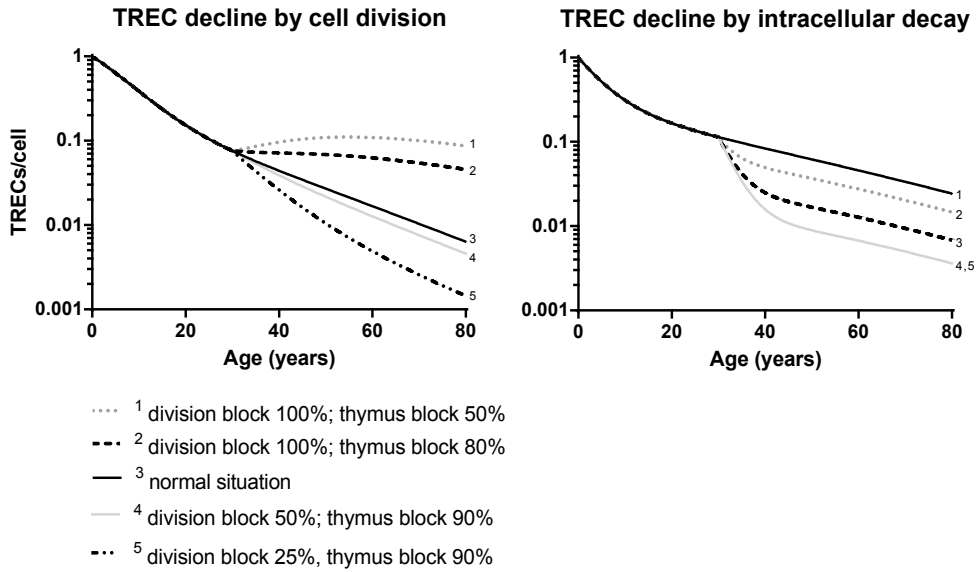

Supplementary Figure 3. Expected naive T-cell TREC contents during long-term immunosuppression when also thymic output is affected. Scenario A: the age-related TREC dilution in healthy individuals (solid line) is due to cell division. Scenario B: the age-related TREC decline in healthy individuals (solid line) is due to intracellular TREC decay. In silico experiments reveal how different degrees of blocking cell division and thymic output have different effects on TREC dynamics. In Scenario A, if immunosuppressive drugs completely block cell division but also affect thymic output (lines 1 and 2), TREC contents are expected to decline less than the normal age-related TREC decline or remain "normal" (solid black line 3). However, if division is only partially blocked, and thymic output is affected a lot (lines 4 and 5), TREC contents follow the normal age-related TREC decline or decline even faster over time. In scenario B, if immunosuppressive drugs also affect thymic output (lines 1-5), TREC contents will become lower than those in age-matched controls, because loss of TRECs by intracellular decay is compensated to a lesser extent by thymic production of new $TREC^+$ cells. Expected TREC contents were derived from in silico experiments (see Materials and Methods).

5

Closing the Gap between T-cell Life Span Estimates from Stable Isotope Labeling Studies in Mice and Humans

Liset Westera[1]*, Julia Drylewicz[1,2]*, Ineke den Braber[1]*, Tendai Mugwagwa[2], Iris van der Maas[1], Lydia Kwast[1], Thomas Volman[1], Elise HR Van de Weg-Schrijver[1], István Bartha[2-5], Gerrit Spierenburg[1], Koos Gaiser[1], Mariëtte T Ackermans[6], Becca Asquith[7], Rob J de Boer[2#], Kiki Tesselaar[1#], José AM Borghans[1#]

[1] Laboratory of Translational Immunology, University Medical Center Utrecht, Utrecht, The Netherlands; [2] Theoretical Biology and Bioinformatics, Utrecht University, Utrecht, The Netherlands; [3] Institute of Biology, Eötvös Loránd University, Budapest, Hungary; [4] School of Life Sciences, Ecole Polytechnique Fédérale de Lausanne, Lausanne, Switzerland; [5] Institute of Microbiology, University Hospital and University of Lausanne, Lausanne, Switzerland [6] Department of Clinical Chemistry, Laboratory of Endocrinology, Academic Medical Center, University of Amsterdam, Amsterdam, The Netherlands; [7] Department of Immunology, Imperial College, Londen, United Kingdom

*, [#] These authors contributed equally.

Blood. 2013 Sep 26;122(13):2205-12

Quantitative knowledge of the turnover of different leukocyte populations is key to our understanding of immune function in health and disease. Much progress has been made thanks to the introduction of stable isotope labeling, the state of the art technique for in vivo quantification of cellular life spans. Yet, even leukocyte life span estimates based on stable isotope labeling can vary up to ten-fold among laboratories. We investigated whether these differences could be the result of variances in the length of the labeling period among studies. To this end, we performed deuterated water-labeling experiments in mice, in which only the length of label administration was varied. The resulting life span estimates were indeed dependent on the length of the labeling period when the data were analyzed using a commonly used single-exponential model. We show that multi-exponential models provide the necessary tool to obtain life span estimates that are independent of the length of the labeling period. Use of a multi-exponential model enabled us to reduce the gap between human T-cell life span estimates from two previously published labeling studies. This provides an important step toward unambiguous understanding of leukocyte turnover in health and disease.

Introduction

Quantitative insights into leukocyte turnover are vital for a better understanding of immune function in health and disease[1,2]. These insights help understand the pathogenesis and treatment of clinical conditions of leukocyte depletion – such as HIV infection[3], bone marrow transplantation, or chemotherapy – and leukocyte excess – including leukemia[4]. In vivo stable isotope labeling with deuterated (heavy) water (^2H_2O) or deuterated glucose is one of the most reliable ways to measure leukocyte turnover, because deuterium labeling can be safely applied in humans and does not interfere with cell turnover at the doses used[2,5]. Nevertheless, T-cell life span estimates can differ up to 10-fold between stable isotope-labeling studies[2]. The cause of this discrepancy has yet to be elucidated.

A meta-analysis of different stable isotope-labeling studies revealed a positive correlation between the estimated T-cell life span and the duration of label administration[2]. Studies based on deuterated glucose, which is typically administered for shorter periods of time than ^2H_2O, consistently yielded shorter average life spans than studies based on heavy water[2]. Although it cannot be excluded that a difference between the ^2H-labeled compounds may have an influence[1], the correlation between the expected life span and the length of the labeling period remained when comparing life span estimates derived from glucose labeling or water labeling separately[2]. This suggests that at least some of the discrepancy between estimated T-cell life spans from stable isotope-labeling studies is attributable to the duration of label administration.

Mathematical modeling is essential for the interpretation of stable isotope labeling data. Typically these models are differential equations, which are based on the assumption that cellular events like division and death are distributed exponentially. Depending on the complexity of the population structure of the model, its solution involves one to several exponentials. We therefore refer to these models as exponential models. A major step forward was made by Asquith et al.[6], who argued that if a cell population is kinetically heterogeneous (i.e., a population comprising multiple sub-populations with different turnover rates, or a population in which recently divided cells and quiescent cells have different life expectancies), the rate of label uptake during the labeling period may not be equal to the rate at which label is lost after label cessation, because the kinetics of labeled cells may not be representative of the cell population as a whole. To account for this heterogeneity a model was proposed that distinguishes two parameters: the average turnover rate p, and the average loss rate of labeled cells d^*. This model is now commonly used[7,8,9,10,11,4] and has stressed the importance of deducing average life spans from p. The rate at which label is lost (d^*) has previously been shown to be dependent on the length of the labeling period: the shorter the labeling period, the stronger the bias towards rapidly proliferating cells in the labeled fraction, and hence the faster the loss of label d^*[6]. To date, the question why

also the average turnover rate *p* is higher (and hence the average life span shorter) in short-term compared to longer-term labeling studies[2] has not yet been experimentally addressed.

Unlike delabeling curves, which may vary according to the length of the labeling period, the shape of the uplabeling curve is independent of the length of the labeling period. It is determined by the weighted average of turnover rates of all sub-populations, and its initial slope should reflect the average turnover rate *p* (Fig. 1A). We here test the hypothesis that during long-term labeling, the label uptake of cells with fast turnover may start to saturate[7] (Fig. 1A). If label administration is continued beyond this point, subsequent label accrual is mainly due to cells with relatively slow kinetics. Because single exponential models cannot capture the saturation behavior and instead are forced to make a compromise, the average turnover rate *p* could become increasingly underestimated as the length of the labeling period increases (Fig. 1B). This might explain the positive correlation between the estimated T-cell life span and the length of the labeling period observed in the literature.

Here, we have investigated this hypothesis by performing ^2H_2O labeling experiments in mice in which only the duration of label administration was varied. We confirm that life spans estimated by fitting single-exponential models to stable isotope labeling data are sensitive to the length of the labeling period. When using a multi-exponential model (describing label accrual with more than one exponential), which explicitly captures kinetic heterogeneity within a cell population[12] (Fig. 1B), we found that life span estimates became independent of the duration of label administration. By labeling mice in utero to have all leukocytes of newborn mice equally labeled, we confirmed that the life span estimates that were obtained with the multi-exponential model were reliable. Application of the model to published human deuterium-labeling data reduced the difference between life span estimates based on glucose and ^2H_2O labeling studies[10,13]. Both our findings and approach present a major step toward consensus on how long different types of leukocytes live in health and disease.

Results

Life span estimates can be influenced by the duration of label administration

The observed correlation in literature between average life span estimates and the duration of label administration[2] prompted us to investigate whether we could reproduce this correlation within one experiment, in which only the duration of label administration was varied. Twelve-week old C57Bl/6 mice were given a bolus of ^2H_2O and subsequently 4% ^2H_2O in the drinking water for 1, 4, or 8 weeks. Splenic effector/memory ($CD44^+$), and naive ($CD62L^+CD44^-$) T cells were isolated at different time points during ^2H_2O administration (labeling phase), and after ^2H_2O administration (delabeling

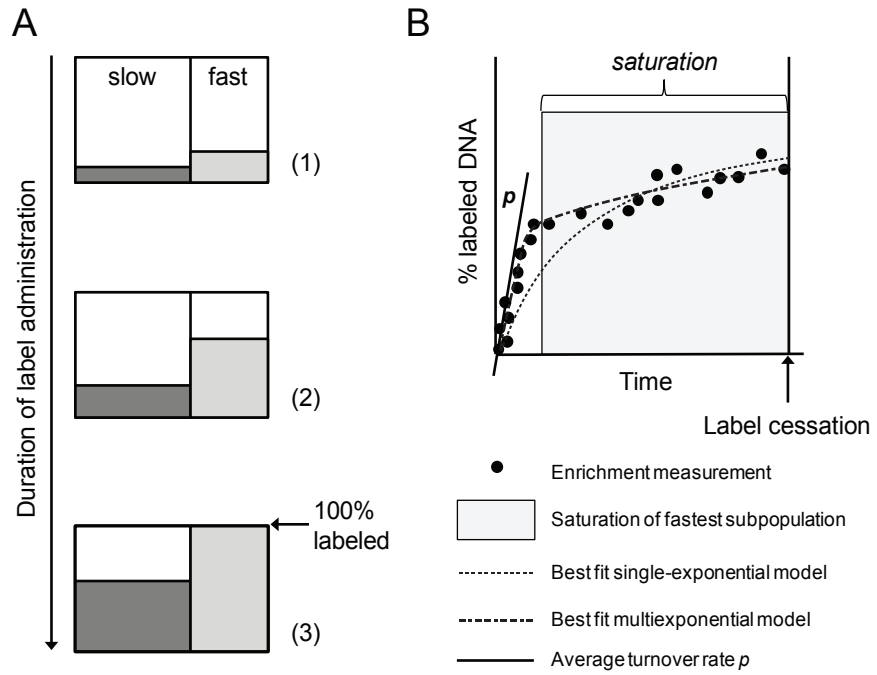

Figure 1. The influence of the length of the labeling period on the estimated turnover rate *p*. Consider an artificial long-term labeling experiment of a kinetically heterogeneous cell population, in which the labeled fractions of a slow (dark gray) and a fast sub-population (light gray) gradually increase with the duration of label administration (panel A). During labeling, samples are obtained and the percentage of labeled DNA is determined at several time points (panel B, black circles). During the labeling phase, the initial accrual of label (the slope nearby the origin, as indicated by the black tangent line) reflects the average turnover rate (*p*) of the kinetically heterogeneous population (panel A, situations 1 and 2; panel B, white area). If labeling is continued, the enrichment level of the fastest sub-population may start to saturate (panel A, situation 3). Although cells of the fastest sub-population continue to divide after this point, this is no longer reflected by a corresponding increase in their enrichment level. If sampling is continued (panel B, gray area), any further increase in labeled DNA is largely due to cell production in the slow sub-population, reflected by a second, flatter slope of the labeling curve (panel B). If the label enrichment data are fitted using a single-exponential model (dotted black curve), the model seeks a compromise between the initial, steep increase and the later, slower increase of label enrichment. As a result, the model fit is forced to bend downwards from the initial slope, and the average turnover rate will become increasingly underestimated with increasing duration of label administration. In contrast, the multi-exponential model corrects for this effect by allowing for multiple slopes during the labeling phase (panel B, dashed black curve), and thereby yields a reliable estimate of the average turnover rate, independent of the length of the labeling period.

phase), and deuterium enrichment in the DNA was measured. Labeling curves for naive (Fig. 2A) and effector/memory (Fig. 2B) $CD4^+$ and $CD8^+$ T-cell subsets of the 1-week, the 4-week, and the 8-week labeling experiments were fitted separately with the single-exponential model proposed for interpreting deuterated glucose experiments[6]

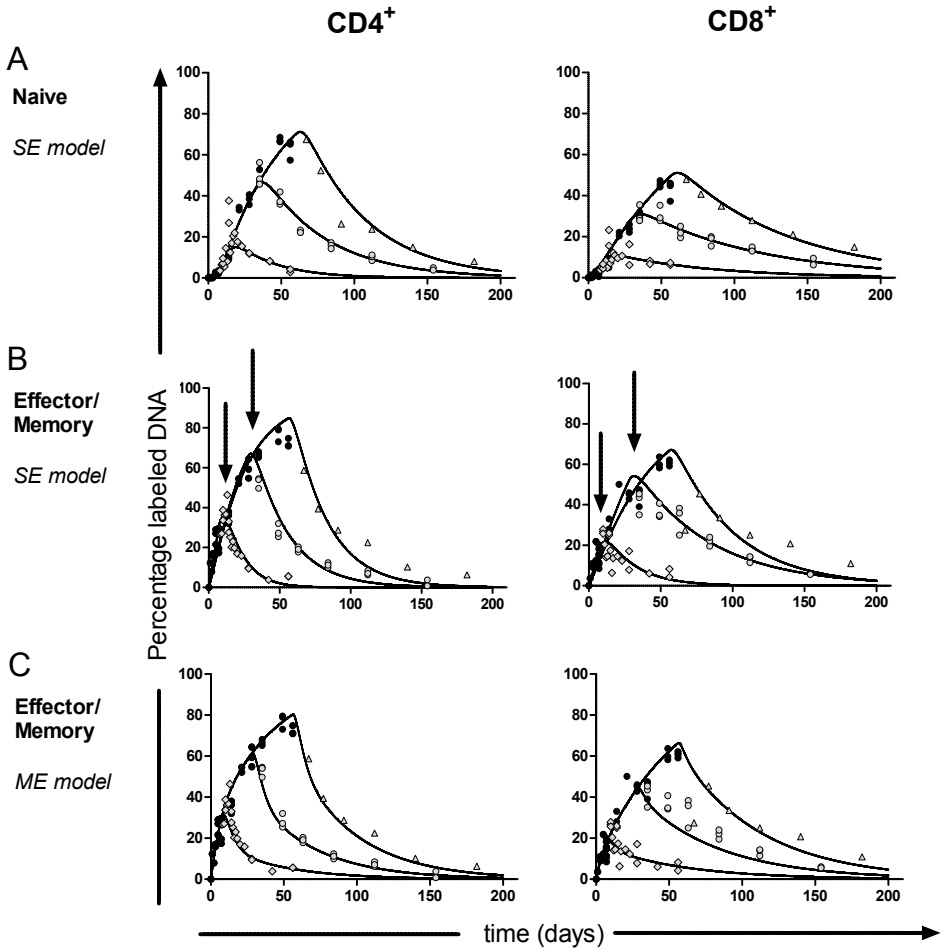

Figure 2. Best fits of the single-exponential model and the multi-exponential model to labeling experiments of different duration. At different time points during and after labeling, the percentage of labeled DNA of splenic (A) naive, and (B and C) effector/memory (E/M) CD4+and CD8+ T cells was determined. Dots represent measurements (i.e., individual mice) at different time points during labeling for 1, 4 and 8 weeks (● black circles), and during de-labeling after 1 week of labeling (⟐gray diamonds), 4 weeks of labeling (◍gray circles), or 8 weeks of labeling (▵ gray triangles). (A and B) Data were fitted separately for each labeling period using the single-exponential (SE) model to estimate the average turnover rate *p* of the cells and the disappearance rate *d** of the labeled cells for the corresponding labeling period. For naive T cells, a delay was added in the model as described in Supplemental Materials equation 9 and equation 10 and was estimated to be 4 (95% confidence interval = 2-6) days. For effector/memory T cells (B), the best-fitting curves during the labeling period were not identical for the different labeling periods (indicated by arrows). (C) When the data were fitted separately for each labeling period using the multi-exponential (ME) model (describing two kinetically different sub-populations; the addition of more sub-populations did not change the average turnover rate) the best-fitting curves during the labeling period were almost identical. Label enrichment was corrected for ^2H_2O enrichment in plasma (supplemental Fig. 1A) and scaled between 0 and 100% by normalizing for the maximum percentage of labeled DNA as measured in thymocytes (Sup. Fig. 1B).

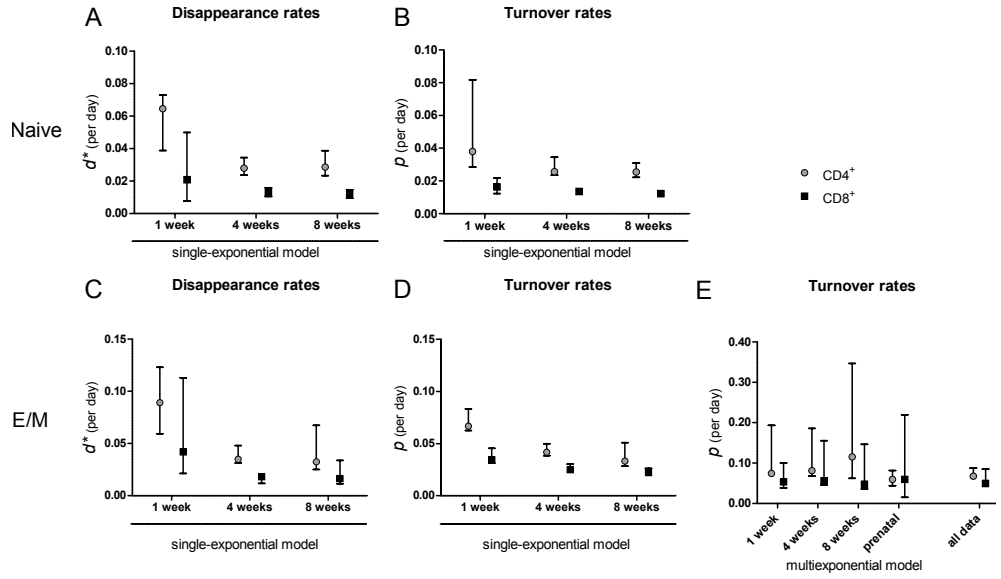

Figure 3. Summary of parameter estimates. Estimates of the disappearance rate of labeled cells d* (A and C) and the average turnover rate p (B and D) of naive (A and B) and effector/memory (C and D) CD4+ (◍ gray circles) and CD8+ (■ black squares) T cells, obtained by fitting the single-exponential model to the data collected during 1, 4 or 8 weeks of labeling. (E) Estimates of the average turnover rate of CD4+ (◍ gray circles) and CD8+ (■ black squares) effector/memory T cells obtained by fitting a multi-exponential model (describing two sub-populations) to the individual data sets (labeling for 1, 4, or 8 weeks, or prenatal labeling) and simultaneously to all data combined. Bars with whiskers represent the 95% confidence intervals of the estimates obtained by bootstrapping the residuals.

which we have previously adapted for use with ^2H_2O labeling[10] (see Supplementary Information).

For naive CD4+ and CD8+ T cells, the disappearance rate of labeled cells *d** (Fig. 3A) was somewhat higher than the estimated average turnover rate *p* (Fig. 3B), especially in the 1-week labeling experiment, and tended to decrease with the length of the labeling period, although not significantly (p-value CD4+=0.07, p-value CD8+=0.19; Fig. 3A). The estimated average turnover rate *p* (and hence the average life span) of naive T cells was similar for the three durations of label administration (p-value CD4+=0.30, p-value CD8+=0.41; Fig. 3B). For CD4+ and CD8+ effector/memory T cells the disappearance rate of labeled cells *d** decreased as the length of the labeling period increased (p-value $<10^{-4}$; Fig. 3C), and unlike what was observed for naive T cells, even the estimated average turnover rate *p* decreased significantly as the duration of label administration increased (p-value $<10^{-4}$; Fig. 3D). Hence, within one experiment, we reproduced the previously observed correlation in the literature between the duration of label administration and the estimated average life span[2].

Inspection of the best fits to the data shows that the discrepancy in the estimated average turnover rate of memory T cells is caused by the model that was fitted to the data. Although the curves of the three labeling experiments should be identical during labeling (as we observed for naive T cells, Fig. 2A), the separate fits to the 1-, 4-, and 8-week labeling data of effector/memory T cells differed during labeling (Fig. 2B, indicated by arrows). Apparently, the model could not capture saturation of the fastest cells in the effector/memory pool, and thereby underestimated the average turnover rate during long-term labeling (see Fig. 1).

Multi-exponential models correct for the influence of the length of the labeling period

Because the correlation between *p* and the duration of label administration was most evident for the $CD4^+$ and $CD8^+$ effector/memory T-cell pools, we used the labeling data from those cell populations to investigate how life spans can be determined reliably when cell populations are kinetically heterogeneous. We propose using a multi-exponential model that explicitly accounts for kinetic heterogeneity[12], by describing multiple subpopulations each with their own production and disappearance rate. Each subpopulation is assumed to be in equilibrium, i.e., its production equals loss (see Supplementary Materials). In contrast to the single-exponential models that are typically used, a multi-exponential model describes both the labeling and the de-labeling phase by a multiple-exponential function[12]. Because a very similar model is obtained in populations with temporal heterogeneity, e.g., consisting of quiescent and activated cells[17], we here use the multi-exponential model generally to account for heterogeneity in the population. Although the number of kinetically different subpopulations within a cell population may not be known, one can increase the number of subpopulations in the model until the estimated average turnover rate no longer markedly changes provided sufficient data are available (see Supplementary Information).

To test whether a multi-exponential model would correct for the influence of the length of label administration on the estimated average turnover rate, we fitted the individual labeling curves of T cells from the 1-, 4-, and 8-week labeling experiments separately using a multi-exponential model. As the multi-exponential model did not improve the fits of the naive T-cell data for any duration of label administration (not shown), but did influence the average life span estimates of effector/memory T cells, we further focus on the latter. The labeling data from the $CD4^+$ and $CD8^+$effector/memory T-cell pools were well described by a model describing two kinetically different subpopulations (the addition of more subpopulations did not change the average turnover rate). In contrast to the single-exponential model (Fig. 2B), the multi-exponential model described the 1-, 4-, and 8-week labeling data with largely overlapping curves during labeling (Fig. 2C) and thus yielded three similar turnover rates (p-value=0.08 for $CD4^+$ and p-value=0.60 for $CD8^+$) that were independent of the length of the labeling period (Fig. 3E). As expected, the estimates obtained by either the single- or multi-exponential model differed most for the longer labeling periods, and the multi-exponential model gave significantly better fits (8 weeks of labeling: p-value<0.0001 for $CD4^+$ and p-value=0.0028 for $CD8^+$; 4 weeks of labeling: p-value<0.0001 for $CD4^+$). For the 1-week data both models behaved similarly.

It should be noted that the 4-week data of CD8 effector/memory T cells are not fitted well during the delabeling phase, and that the multi-exponential model does not describe the 4-week data significantly better than the single-exponential model (p-value=0.08). Importantly, our estimates of the average turnover rate of CD8 effector/memory T cells do not depend on the 4-week data, as using only 1-week and 8-week data (separately or combined) yielded consistent estimates.

Hence, the correlation of published turnover rates with the length of the labeling period may be due to kinetic heterogeneity that was not fully accounted for by the models that were used to fit the data. Mathematical models that explicitly capture such kinetic heterogeneity yield average turnover rates that do not depend on the duration of label administration.

Prenatal labeling experiments yield similar life span estimates

We next sought to obtain independent confirmation of the turnover rates that we estimated when fitting the multi-exponential model to the 1-, 4-, and 8-week labeling data. Because the main difficulty in the interpretation of “finite-term” labeling experiments is caused by the difference between cells that are and are not labeled during the experiment, we designed a labeling experiment in which, at stop of label administration, all cells were labeled. Female mice received a bolus of ^2H_2O and were subsequently fed with 4% ^2H_2O in the drinking water before conception and throughout pregnancy. Female mice thus gave birth to pups that had been labeled in utero (referred to as “prenatal labeling”) and in which all cells were equally labeled. Pups received ^2H_2O until the age of 16 weeks, after which ^2H_2O was withdrawn from the drinking water. They were euthanized at different time points post-labeling to measure the loss of deuterium enrichment in the DNA of their T cells. The resulting delabeling curves were used to deduce the average disappearance rate *d*, which in this case reflects the cell population as a whole, and can directly be interpreted as the average turnover rate.

In line with the finite-term labeling experiments, fitting the multi-exponential model (describing two kinetically different subpopulations; the addition of more subpopulations did not change the average turnover rate, Fig. 4A) to the effector/memory delabeling data gave a significantly better description of the data (p-values<0.01) than

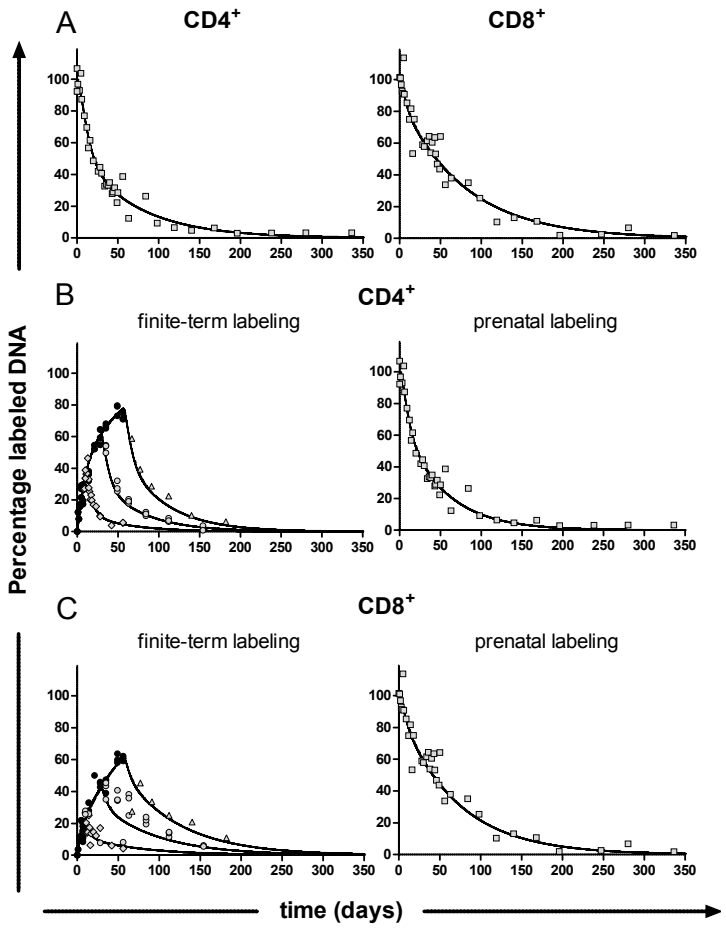

Figure 4. Best fits of the multi-exponential model to effector/memory T-cell data from prenatal and finite-term labeling experiments. (A) Mice were labeled prenatally and drank ^2H_2O until 16 weeks of age. At different time points after label cessation, the percentage of labeled DNA of splenic effector/memory CD4$^+$ (left) and CD8$^+$ T cells (right) was determined. Gray squares (▫) represent measurements (i.e., individual mice) at different time points post-labeling. Data were fitted with the multi-exponential model (describing two sub-populations) to estimate the average turnover rate of the total cell population. (B and C) Effector/memory CD4$^+$ (B) and CD8$^+$ (C) T-cell labeling data from the finite-term (left) and prenatal labeling (right) experiments were simultaneously fitted with the multi-exponential model to estimate the average turnover rate. Symbols represent measurements (i.e., individual mice) at different time points during labeling (● black circles), during de-labeling after 1 week of labeling (◇ gray diamonds), 4 weeks of labeling (○ gray circles), or 8 weeks of labeling (△ gray triangles), and during de-labeling of prenatally labeled mice (▫ gray squares).

the single-exponential model (not shown). Fitting the prenatal data yielded average turnover rates for effector/memory CD4$^+$ and CD8$^+$ T cells that were similar to the estimates obtained in the 1-, 4- and 8-week labeling experiments (p-value=0.68 for

Table 1. Life span estimates of CD4$^+$ and CD8$^+$ effector/memory T cells from different labeling experiments.

	Life span, days (95% confidence intervals)	
	CD4$^+$effector/memory T cells	CD8$^+$ effector/memory T cells
No. of weeks		
1	13.46 (5.17-15.02)	18.68 (10.00-26.30)
4	12.30 (5.38-14.75)	17.82 (6.43-22.06)
8	8.67 (2.88-16.05)	20.94 (6.82-27.56)
prenatal	16.85 (12.29-22.64)	16.82 (4.55-66.53)
all data	14.78 (11.39-15.39)	20.14 (11.73-22.04)

CD4$^+$ and p-value=0.54 for CD8$^+$; Fig. 3E). Indeed, we found that delabeling of a fully labeled population behaved similarly to labeling of an unlabeled population. For all cell subsets analyzed, both the average turnover rate and the number of exponentials required to describe the data were similar for the finite-term labeling data and the corresponding prenatal labeling data. This independent experiment confirmed the turnover estimates obtained by fitting the multi-exponential model to the finite-term labeling data above.

Simultaneously fitting the model to the complete data set we had collected (i.e., the 1-, 4-, 8-week labeling experiments and the prenatal labeling experiments together, Fig. 4B and 4C) revealed that mouse CD4$^+$ and CD8$^+$ effector/memory T cells have average turnover rates of 0.068 (95% CI: 0.065-0.088) and 0.050 (0.045-0.085) per day (Fig. 3E), corresponding to average life spans of 15 (11-15) days for CD4$^+$, and 20 (12-22) days for CD8$^+$ effector/memory T cells (Table 1).

The multi-exponential model reduces the difference between human T-cell life span estimates

We next applied the multi-exponential model to previously published human ^2H_2O labeling data[10] to obtain human T-cell life span estimates that are independent of the length of the labeling period. For each individual labeled with ^2H_2O for 9 weeks, the multi-exponential model (describing two kinetically different subpopulations; the addition of more subpopulations did not change the average turnover rate) fitted the memory CD4$^+$ and CD8$^+$ T-cell data significantly better (p-values<0.001), and in general yielded higher average turnover rates *p* (and therefore shorter average life spans) than the single-exponential model (Fig. 5A; Sup. Fig. 4). Hence, single-exponential models have overestimated the average life span of memory T cells in long-term labeling studies. According to the multi-exponential model, human memory CD4$^+$ and CD8$^+$ T cells have

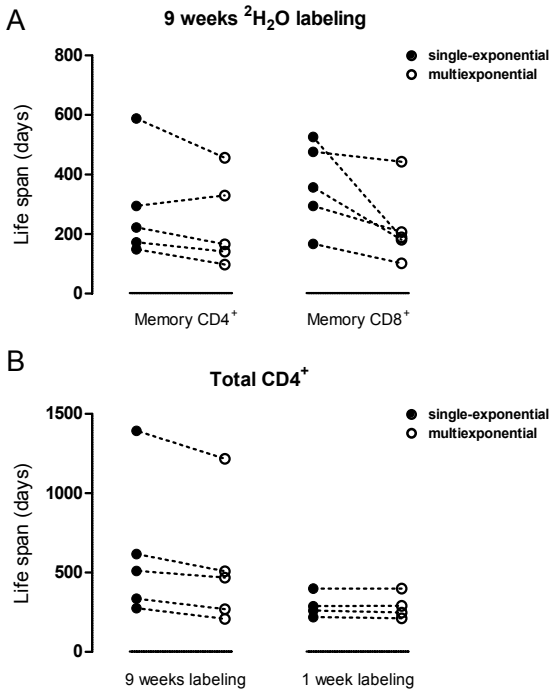

Figure 5. Average T-cell life spans re-estimated from published labeling experiments in humans. Data from two published experiments were used: 9-week heavy water labeling in five healthy individuals [10], and 1-week deuterated glucose labeling in four healthy individuals [13]. For each individual, the life span of the indicated cell population was estimated using a single-exponential (● closed circles) or a multi-exponential model (○ open circles, describing 2 kinetically different sub-populations; the addition of more sub-populations did not change the average turnover rate). Estimates obtained for one individual using the two models are connected by a dashed line (---). (A and B) For each individual in the 9-week heavy water labeling experiment, the average life span of $CD4^+$ and $CD8^+$ memory T cells was estimated using both models. Individual fits of the multi-exponential model to the memory T-cell data are shown in supplementary Figure 4. (B) The average life span of total $CD4^+$ T cells was re-estimated by fitting the single-exponential model (● closed circles) or the multi-exponential model (○ open circles) to the deuterium labeling data of individuals labeled with deuterated glucose for 1 week [13], or heavy water for 9 weeks [10]. For the 9-week labeling experiment, individual fits of the multi-exponential model are shown in supplemental Figure 5. For the 1 week glucose data, both models included a 1-day delay [22,17].

a median *p* of 0.0061 (range=0.0020-0.0141) and 0.0064 (range=0.0043-0.089) per day, corresponding to median life spans of 164 (range=71-500) days for $CD4^+$ and 157 (range=113-231) days for $CD8^+$ memory T cells.

Finally, we investigated whether the multi-exponential model could resolve the discrepancy between previously published human stable isotope-labeling studies. We confined our analysis to two data sets that clearly differed in the length of the labeling period, and had sufficient data points: a 1-week deuterated glucose labeling experiment[13] and a 9-week ^2H_2O labeling experiment[10]. Since the former experiment reported deuterium enrichment in total $CD4^+$ T cells, while the latter distinguished between naive and effector/memory T cells, we first recalculated the corresponding levels of deuterium enrichment in total $CD4^+$ T cells for the 9-week ^2H_2O labeling experiment (see Supplementary Information). When we fitted a single-exponential model to the data, the life spans estimated from the 9-week labeling experiment were longer than the ones based on the 1-week labeling experiment (Fig. 5B, individual fits in Sup. Fig. 5), in line with the positive correlation between estimated life spans and

the duration of label administration in the literature[2]. The multi-exponential model reduced the estimated life spans from the 9-week labeling experiment, and hence reduced the differences between the studies (Fig. 5B). Although the discrepancies between the two studies were not entirely resolved, largely because of one outlier in the ^2H_2O study whose memory turnover was much lower than in the other individuals (see Sup. Fig. 4D and reference[10]), correction of the length-of-labeling effect revealed that the current best estimate of the average life span of $CD4^+$ T cells in healthy human adults (based on the median values of both studies) lies between 270 and 469 days.

Discussion

The quantification of leukocyte life spans from stable isotope labeling data relies upon the use of mathematical models. The finite-term labeling experiments that we performed in mice show that single-exponential models fail to correctly describe the dynamics of kinetically heterogeneous cell populations, and thereby yield average life span estimates that depend on the duration of label administration. Longer labeling periods gave rise to longer estimated average life spans, confirming the correlation observed in the literature[2]. These analyses suggest that a considerable part of the discrepancy in published T-cell life spans is due to differences in the duration of label administration. We here show that the use of a multi-exponential model resolves the dependence on the length of the labeling period, and thereby yields reliable turnover parameters.

It has been proposed before that a multi-exponential model describing all subpopulations would be the ideal way to model kinetically heterogeneous cell populations, but that this would lead to models with too many parameters[6]. The mathematical model proposed by Asquith et al.[6] was a pragmatic solution that captured kinetic heterogeneity by allowing *p* to be different from *d**. However, the fact that single-exponential models fail to describe labeling curves that are identical during labeling but different after label cessation, stresses the need for a multi-exponential model to obtain reliable estimates of turnover rates, particularly when the labeling period is long.

Fitting multi-exponential models does not only reveal the average life span of a cell population, but also quantitative insights into the sizes α_i and turnover rates p_i of its subpopulations. The uncertainty on the latter parameters is, however, generally much larger than on the average turnover rate *p*, due to the strong correlation between the size of a subpopulation and its turnover rate (see Sup. Figure 6). The biological interpretation of the parameters describing the kinetically different subpopulations used in the model is therefore not straightforward. It is important to realize that the number of kinetically different subpopulations that is sufficient to describe the data may in fact be lower than their actual number, and that the subpopulations need not even

reflect phenotypically different subsets. Moreover, if the use of a multi-exponential model significantly improves the fit to the data, an alternative interpretation is that cells transiently have different turnover rates (i.e., that there is so-called temporal heterogeneity). For example, resting cells and cells that have recently been produced or activated may have different life expectancies, an illustrative example being activation-induced cell death[17,7].

Our analyses demonstrate that the use of single-exponential models may lead to overestimation of the average life span of kinetically heterogeneous cell populations, especially in long-term labeling studies. This problem can be overcome by implementing a multi-exponential model. Hence, both short-term and long-term labeling can be considered, and the decision should be based on the population of interest (slow or fast turnover) and on practical and/or ethical considerations. Although short-term labeling studies are less prone to underestimate cellular turnover rates, long-term labeling can also have advantages. First, longer labeling periods permit more frequent sampling during the labeling phase, which is the essential phase to estimate average turnover rates. It also allows better spreading of blood withdrawals over time, keeping the burden of blood sampling for patients relatively low. Second, prolonged exposure to label allows even cells with relatively slow turnover rates, such as naive T cells, to become sufficiently labeled to reliably estimate their turnover. Third, longer labeling gives recently produced, and hence labeled, cells ample time to appear in the blood, where most measurements are generally taken. Naturally, the shorter the labeling period, the less saturation of subpopulations is expected to occur, and the smaller the requirement for a multi-exponential model. However, even during short-term labeling saturation may already be present. Therefore it may be good to always use the multi-exponential model, both for short and long labeling periods. As long as label accrual reflects the average population turnover (before any signs of saturation), the multi-exponential model will behave like a single-exponential model and the fitting procedure will set the contribution of the extra exponential(s) to zero. It will hence yield the same average turnover rate.

Remarkably, two earlier studies have reported longer life span estimates for murine memory $CD8^+$ T cells than the 20-day average that we found. BrdU-labeling experiments in thymectomized mice revealed a $CD8^+$ effector/memory T-cell half-life of 63 days (corresponding to a life span of 91 days)[18], and later Choo et al.[19] showed that adoptively transferred LCMV-specific memory $CD8^+$ T cells but also bulk $CD44^{hi}$ T cells had an intermitotic time of ~50 days. A major advantage of stable-isotope labeling is that one can study cell turnover under physiological circumstances, without affecting immune homeostasis. This could be different for the (more manipulative) approaches employed by the earlier studies. Better in agreement with our results is a study by Younes et al.[20], who proposed that the $CD4^+$ memory pool is heterogeneous, comprising both slowly-dividing "authentic" antigen-experienced memory cells as well as rapidly-dividing "memory-phenotype" cells that arise by an antigen-independent mechanism. The level of BrdU incorporation they measured in $CD4^+$ ($CD44^{hi}$) memory-phenotype was calculated to correspond to a $CD4^+$ memory T-cell life span of 14 to 22 days[21]. This is very similar to our $CD4^+$ memory life span estimate of 15 days.

In humans, the current best estimates are that memory $CD4^+$ and $CD8^+$ T cells live 164 and 157 days, respectively. Again, these are considerably shorter than our previous estimates of 222 and 357 days for memory $CD4^+$ and $CD8^+$ T cells[10]. Discrepancies in the literature on human T-cell life span estimates[13,10] may thus to a large extent have been caused by the use of single-exponential models, which led to overestimation of T-cell life spans in long-term labeling studies. We cannot exclude that other, yet unidentified factors may cause differences in life span estimates, such as an intrinsic difference between ^2H_2O and deuterated glucose, which may underlie the remaining differences between the estimated life spans of the 1-week deuterated glucose experiment and the 9-weeks ^2H_2O experiment (Fig. 5B). The part of the variation that is due to the length of the labeling period has at least been resolved thanks to the use of a multi-exponential model.

Acknowledgments

We thank David Ho and Hiroshi Mohri for sharing their published data, and Linda McPhee for comments on the manuscript. This research was supported by the Landsteiner Foundation for Blood Transfusion Research (LSBR grant 0210), the Netherlands Organization for Scientific Research (NWO, grants 92750029, 917.96.350 and 016.096.350 and visitor's grant 040.11.128), by the VIRGO consortium (NGI, BB.000342.1), and by the Research Council for Earth and Life Sciences (ALW) with financial aid from the Netherlands Organisation for Scientific Research (NWO, grant 836.07.002).

Materials and Methods

Mice. C57BL/6 mice were maintained by in-house breeding at the Central Animal Facility at Utrecht University in accordance with institutional and national guidelines.

^2H_2O labeling. For finite-term labeling experiments, ~12-week old male mice were given a boost injection (i.p.) of 15 ml/kg ^2H_2O (99.8%, Cambridge Isotopes) in PBS and received 4% ^2H_2O for 1, 4 or 8 weeks. For prenatal labeling experiments, to obtain mice in which all cells were labeled to the same extent, females were given a boost injection of 15 ml/kg 99.8% ^2H_2O in PBS. They were placed together with males and drank 4% ^2H_2O until they gave birth. After weaning, male pups received 4% ^2H_2O until the age of 16 weeks. The 9-week labeling data in humans were previously published[10]

and the enrichment in total $CD4^+$ T cells was derived from naive and memory T cells as described in Supplementary Information.

Cell preparation and sorting. Spleens were isolated at different time points for further sorting. Thymocytes were isolated as rapid cell population to determine the maximum level of label enrichment. Blood was collected in EDTA vials and spun down to isolate plasma. Single-cell suspensions were obtained as previously described[10] Splenocytes were stained with CD62L-FITC, CD44-eFluor450 (eBioScience), CD4-APC-H7 and CD8-PerCP (BD PharMingen), in the presence of 2.4G2 blocking antibody. Within $CD4^+CD8^-$ and $CD4^-CD8^+$ splenocytes, naive T cells were defined as $CD62L^+CD44^-$ and effector/memory T cells as $CD44^+$. Cells were sorted using a FACSAria cell sorter and FACSdiva software (BD PharMingen). Genomic DNA was isolated according to the manufacturer's instructions (Nucleospin Blood QuickPure, Macherey-Nagel).

Measurement of deuterium enrichment in DNA and body water. Deuterium enrichment in DNA was measured according to the method described by Neese et al.[14] with minor modifications, as previously described[10]. Both natural enrichment and concentration-dependence (abundance sensitivity) were controlled for, using a naturally enriched background sample or standards of known isotopic enrichments. To determine deuterium enrichment in body water, plasma samples were measured using gas chromatography-mass spectrometry[15,16]. Mathematical modeling is described in Supplemental Materials.

Statistical analysis. ANOVA tests were performed to compare the different estimates using GraphPad Prism 5 (GraphPad Software, Inc.). Nested mathematical models were compared using an F-test. Differences with a p-value<0.05 were considered significant.

References

1. Asquith B., Borghans J.A., Ganusov V.V., Macallan D.C. Lymphocyte kinetics in health and disease. Trends Immunol. 30(4):182-189 (2009).
2. Borghans J.A., de Boer R.J. Quantification of T-cell dynamics: from telomeres to DNA labeling. Immunol. Rev. 216:35-47 (2007).
3. Hellerstein M.K., Hoh R.A., Hanley M.B., et al. Subpopulations of long-lived and short-lived T cells in advanced HIV-1 infection. J. Clin. Invest. 112(6):956-966 (2003).
4. van Gent R., Kater A.P., Otto S.A., et al. In vivo dynamics of stable chronic lymphocytic leukemia inversely correlate with somatic hypermutation levels and suggest no major leukemic turnover in bone marrow. Cancer Res. 68(24):10137-10144 (2008).
5. Busch R., Neese R.A., Awada M., Hayes G.M., Hellerstein M.K. Measurement of cell proliferation by heavy water labeling. Nat. Protoc. 2(12):3045-3057 (2007).
6. Asquith B., Debacq C., Macallan D.C., Willems L., Bangham C.R. Lymphocyte kinetics: the interpretation of labelling data. Trends Immunol. 23(12):596-601 (2002).
7. Macallan D.C., Asquith B., Irvine A.J., et al. Measurement and modeling of human T cell kinetics. Eur. J. Immunol. 33(8):2316-2326 (2003).
8. Macallan D.C., Wallace D., Zhang Y., et al. Rapid turnover of effector-memory CD4(+) T cells in healthy humans. J. Exp. Med. 200(2):255-260 (2004).
9. Wallace D.L., Zhang Y., Ghattas H., et al. Direct measurement of T cell subset kinetics in vivo in elderly men and women. J. Immunol. 173(3):1787-1794 (2004).
10. Vrisekoop N., den Braber I., de Boer A.B., et al. Sparse production but preferential incorporation of recently produced naive T cells in the human peripheral pool. Proc. Natl. Acad. Sci. U. S. A 105(16):6115-6120 (2008).
11. den Braber I., Mugwagwa T., Vrisekoop N., et al. Maintenance of peripheral naive T cells is sustained by thymus output in mice but not humans. Immunity 36(2):288-297 (2012).
12. Ganusov V.V., Borghans J.A., de Boer R.J. Explicit kinetic heterogeneity: mathematical models for interpretation of deuterium labeling of heterogeneous cell populations. PLoS Comput. Biol. 6(2):e1000666 (2010).
13. Mohri H., Perelson A.S., Tung K., et al. Increased turnover of T lymphocytes in HIV-1 infection and its reduction by antiretroviral therapy. J. Exp. Med. 194(9):1277-1287 (2001).
14. Neese R.A., Misell L.M., Turner S., et al. Measurement in vivo of proliferation rates of slow turnover cells by 2H2O labeling of the deoxyribose moiety of DNA. Proc. Natl. Acad. Sci. U. S. A 99(24):15345-15350 (2002).
15. van Kreel B.K., van der Vegt F., Meers M., Wagenmakers T., Westerterp K., Coward A. Determination of total body water by a simple and rapid mass spectrometric method. J. Mass Spectrom. 31(1):108-111 (1996).
16. Westera L., Zhang Y., Tesselaar K., Borghans J.A., Macallan D.C. Quantitating lymphocyte homeostasis in vivo in humans using stable isotope tracers. Methods Mol. Biol. 979:107-131 (2013).
17. de Boer R.J., Perelson A.S., Ribeiro R.M. Modelling deuterium labelling of lymphocytes with temporal and/or kinetic heterogeneity. J. R. Soc. Interface. 9(74):2191-2200 (2012).
18. Parretta E., Cassese G., Santoni A., Guardiola J., Vecchio A., Di Rosa F. Kinetics of in vivo proliferation and death of memory and naive CD8 T cells: parameter estimation based on 5-bromo-2'-deoxyuridine incorporation in spleen, lymph nodes, and bone marrow. J. Immunol. 180(11):7230-7239 (2008).
19. Choo D.K., Murali-Krishna K., Antia R., Ahmed R. Homeostatic turnover of virus-specific memory CD8 T cells occurs stochastically and is independent of CD4 T cell help. J. Immunol. 185(6):3436-3444 (2010).
20. Younes S.A., Punkosdy G., Caucheteux S., Chen T., Grossman Z., Paul W.E. Memory phenotype CD4 T cells undergoing rapid, nonburst-like, cytokine-driven proliferation can be distinguished from antigen-experienced memory cells. PLoS Biol. 9(10):e1001171 (2011).
21. de Boer R.J., Perelson A.S. Quantifying T lymphocyte turnover. J. Theor. Biol. 327:45-87 (2013).
22. Ribeiro R.M., Mohri H., Ho D.D., Perelson A.S. In vivo dynamics of T cell activation, proliferation, and death in HIV-1 infection: why are CD4+ but not CD8+ T cells depleted? Proc. Natl. Acad. Sci. U. S. A 99(24):15572-15577 (2002).

Supplementary Information

Calculation of enrichment in total CD4⁺ T cells. To be able to compare data from a previously published 9-week heavy water ^2H_2O labeling experiment, which distinguished naive ($CD27^+CD45RO^-$) from memory ($CD45RO^+$) T cells[1], and a 1-week deuterated glucose labeling experiment on total $CD4^+$ T cells[2] (data kindly provided by David Ho and Hiroshi Mohri), we calculated the corresponding enrichment level of total $CD4^+$ T cells from the heavy water ^2H_2O labeling experiment using the relative sizes and the enrichment levels of the naive and memory $CD4^+$ T-cell subsets[1]. This could be done for $CD4^+$ T cells because the fraction of $CD27^-CD45RO^-$ cells is negligible in the $CD4^+$ T-cell pool, but not for $CD8^+$ T cells. The enrichment levels of memory and total $CD4^+$ T cells were fitted with a single-exponential[3] and a multiexponential model describing two kinetically different subpopulations (the addition of more subpopulations did not change the average turnover rate).

Mathematical modeling of deuterium labeling data. Following Vrisekoop et al.[1], the availability of heavy water at any moment in time was calculated by fitting the following equations to the deuterium enrichment in the plasma:
For finite-term labeling experiments:

$$S(t) = f(1-e^{-\delta t}) + S_0 e^{-\delta t} \quad \text{during label intake } (t \le \tau), \qquad [1]$$

$$S(t) = \left[f(1-e^{-\delta\tau}) + S_0 e^{-\delta\tau} \right] e^{-\delta(t-\tau)} \quad \text{after label intake } (t > \tau). \qquad [2]$$

For prenatal labeling experiments: $S(t) = \beta e^{-\delta t}$. [3]

In these equations, $S(t)$ represents the fraction of ^2H_2O in plasma at time t (in days), f is the fraction of deuterium in the drinking water, labeling was stopped at $t = \tau$ days in finite-term labeling experiments, and at t=0 days in the prenatal labeling experiments, δ represents the turnover rate of body water per day, S_0 is the plasma enrichment level attained after the i.p. ^2H_2O boost at day 0 of finite-term labeling experiments, and β the plasma enrichment level at the start of the delabeling period in the prenatal labeling experiments. The best fits to the plasma data are shown in Sup. Fig. 1A and 2.

To model the label enrichment of adenosine in the DNA of cells, we used both single-exponential and multiexponential models. In the single-exponential model[3], cells have an average turnover rate p (meaning that a fraction p of cells is renewed per day; life spans are obtained by inverting p), and labeled cells are lost at a rate d^* per day. We previously extended this model to include the dependence on the actual enrichment of the body water (as described by $S(t)$)[1]. We also introduced a parameter c which accounts for the fact that the adenosine deoxyribose (dR) moiety contains multiple hydrogen atoms that can be replaced by deuterium. Basically one writes that each adenosine residue replicates at rate p per day and will incorporate a deuterium atom with probability $cS(t)$. The fraction of labeled DNA (L) at any given time is hence given by:

$$\frac{dL}{dt} = pcS(t) - d^*L \quad . \qquad [4]$$

To determine the maximum level of label incorporation that could possibly be attained in finite-term labeling experiments, we fitted this model to labeling data from mouse thymocytes (Sup. Fig. 1B), which are known to have a high rate of turnover[4, 5]. Turnover parameters for the different T-cell subsets were determined as described before[1]. Because we observed a lag in the appearance of labeled naive T cells in the spleen after start of (finite-term) labeling, suggesting that cells had divided in the thymus and then migrated to the spleen, we allowed for a time delay Δ with which labeled cells appear in the spleen. When fitting naive T-cell data, Δ was treated as a free parameter, while it was fixed to Δ=0 when fitting effector/memory T-cell data. The corresponding equations are:

if $t \le \Delta$: $L(t) = 0$, [5]

if $\Delta < t \le \tau + \Delta$:

$$L(t) = \frac{cpf}{\delta - d^*}\left[\frac{\delta}{d^*}(1-e^{(-d^*(t-\Delta))}) - (1-e^{-\delta(t-\Delta)}) + \frac{S_0}{f}(e^{-d^*(t-\Delta)} - e^{-\delta(t-\Delta)})\right], \qquad [6]$$

if $t > \tau + \Delta$:

$$L(t) = \frac{cpf}{\delta - d^*}\left[\frac{\delta}{d^*}(e^{-d^*(t-\Delta-\tau)} - e^{-d^*(t-\Delta)}) - (e^{-\delta(t-\Delta-\tau)} - e^{-\delta(t-\Delta)}) + \frac{S_0}{f}(e^{-d^*(t-\Delta)} - e^{-\delta(t-\Delta)})\right]. \qquad [7]$$

Alternatively, labeling data from the different T-cell subsets were fitted using a multiexponential model in which each subpopulation i contains a fraction α_i of cells with turnover rate p_i per day. Assuming a steady state for each kinetic subpopulation, the fraction of labeled deoxyribose residues of adenosine in the DNA of each subpopulation i was modeled by the following differential equation:

$$\frac{dL_i}{dt} = p_i cS(t) - p_i L_i \quad . \qquad [8]$$

For naive T cells, T-cell production may occur both in the thymus and in the periphery. The fraction of labeled DNA in the total T-cell population under investigation was subsequently derived from $L(t) = \sum_i \alpha_i L_i(t)$ and the average turnover rate p was calculated as $p = \sum_i \alpha_i p_i$.

For finite-term labeling experiments, the analytical solutions are:

if $t \le \Delta$: $L_i(t) = 0$,

if $\Delta < t \le \tau + \Delta$: $L_i(t) = \frac{c}{\delta - p_i}\left[p_i(S_0 e^{-p_i(t-\Delta)} - S(t-\Delta)) + f(1 - e^{-p_i(t-\Delta)}) \right]$, [9]

if $t > \tau + \Delta$: $L_i(t) = \frac{p_i c}{\delta - p_i}\left[S(\tau) e^{-p_i(t-\Delta-\tau)} - S(t-\Delta) \right] + L_i(\tau) e^{-p_i(t-\Delta-\tau)}$. [10]

Again, Δ was fixed to 0 when fitting effector/memory T-cell data, while Δ was a free parameter when fitting naive T-cell data.

For prenatal labeling experiments, the analytical solution is: $L_i(t) = \frac{\beta c}{\delta - p_i}\left[\delta e^{-p_i t} - p_i e^{-\delta t} \right]$.

Best fits were determined by minimizing the sum of squared residuals using the R function nlminb6. The 95% confidence intervals were determined using a bootstrap method where the residuals to the optimal fit were resampled 500 times.

The effect of the number of kinetically different subpopulations on the estimated average turnover rate. To estimate the average turnover rate using the multiexponential model, one has to consider a given number of kinetically different subpopulations. We investigated the effect of model specification by creating artificial data and fitting this data set using different models with increasing numbers of kinetically different subpopulations. We consider the following models during label intake:

$$\frac{dL_i}{dt} = p_i - p_i L_i \qquad (M_i) \text{ for i=1…6.}$$

And after label intake:

$$\frac{dL_i}{dt} = -p_i L_i \qquad (M_i) \text{ for i=1…6.}$$

Note that in the artificial data we consider perfect labeling, i.e., *cS(t)*=1 during label uptake and 0 after. Each subpopulation *i* contains a fraction α_i of cells with turnover rate pi per day. The fraction of labeled DNA in the total T-cell population is subsequently derived from $L(t) = \sum_i \alpha_i L_i(t)$ and the average turnover rate *p* is calculated as $p = \sum_i \alpha_i p_i$. For model M_1 we consider two variants (M_{1a} and M_{1b} in Sup. Fig. 3). In model M_{1a} we set α_1<1 to make it equivalent to the model proposed by Asquith et al 2, and model M_{1b} is a single-exponential model because we set α_1=1. The models M_2 to M_6 are multiexponential models including 2 to 6 kinetically different subpopulations (i.e., with 2 to 6 turnover rates).

Artificial data were generated using the model (M_2) (assuming two kinetically different subpopulations) and Gaussian white noise was added. The duration of label administration was assumed to be 90 days and the label enrichment was measured every 7 days until day 150. The data were fitted with the eight proposed models using Mathematica. The 95% confidence intervals were determined using a bootstrap method.

Sup. Fig. 3 presents the average turnover rates estimated by the different models from one generated data set. The models M_{1a} and M_{1b} clearly underestimate the average turnover rate, whereas adding more kinetically different subpopulations than really presented leads to accurate (and similar) estimates. In practice, if there are too many subpopulations, the algorithm chooses either to put in a very small fraction for a subpopulation, or to assign the same turnover rate to two or more subpopulations. Similar results were found for data generated from different sets of parameters. Note that this result is conditional to the sampling design as well as the noise level in the data, which were all set to mimic true experiments.

To determine the number of kinetically different subpopulations to include in the model we recommend a stepwise selection procedure, adding a new kinetically different subpopulation into the model and stopping when the average turnover rate no longer markedly changes provided sufficient data are available.

Finally, one may wonder whether a multiexponential model with 2 kinetically different subpopulations (model M_2) can describe labeling experiments from biological populations composed of several kinetically different subpopulations. We tested one example creating artificial data with model M_4, setting α_i=0.25 and p_i=1, 0.5, 0.25, 0.125 for *i*=1,2,3,4. In a similar setup as in supplemental Figure 3, model M_2 performed reasonably in estimating the average turnover rate: $p_{estimated}$= 0.40 (95%CI= 0.20;0.78) for the "true" turnover rate p_{true}= 0.46 (not shown).

Supplementary Table 1. Estimates for deuterium enrichment in plasma and thymocytes.

Parameter		Estimate (95% confidence interval)	
		Finite-term labeling	**Prenatal labeling**
Plasma	S_0	0.015 (0.012-0.018)	0.0248 (0.0238-0.0260)
	δ (per day)	0.261 (0.230-0.272)	0.2242 (0.2034-0.2439)
	f (per day)	0.024 (0.023-0.025)	n/a
Thymocytes	*p* (per day)	0.416 (0.377-0.468)	n/a
	c	3.093 (2.974-3.161)	3.755 (3.596-3.984)*

**c* is estimated directly from the level of enrichment of thymocytes at day 0 in prenatal labeling experiments. n/a: not applicable

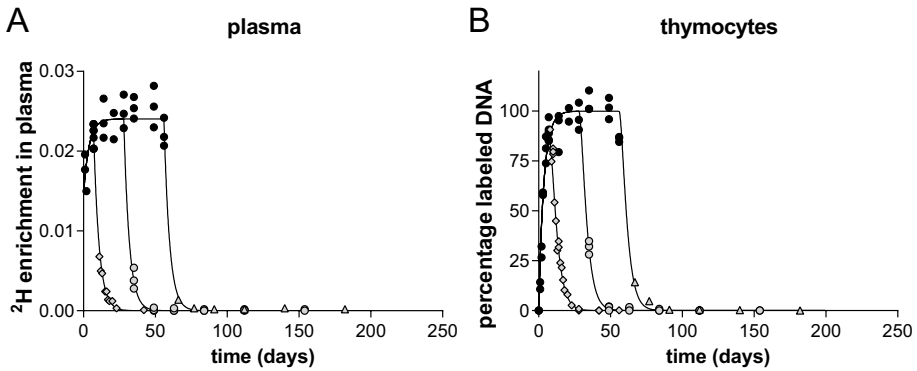

Supplementary Figure 1. Deuterium enrichment in plasma (A) and thymocytes (B) of mice labeled for 1, 4, or 8 weeks. Best fits are given by black lines. Thymocytes were used to determine the maximum percentage of labeled DNA that could possibly be attained (see Methods). Symbols represent measurements (i.e., individual mice) at different time points during uplabeling (● black circles) and different points post labeling, after 1 week (◈ gray diamonds), after 4 weeks (◎ gray circles), and after 8 weeks (◬ gray triangles) of labeling, respectively. Parameter estimates are given in Sup. Table 1.

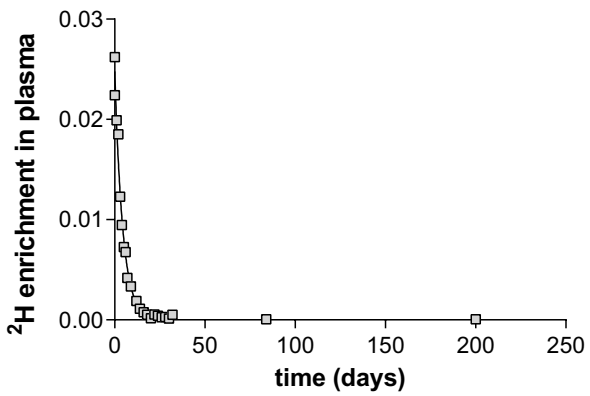

Supplementary Figure 2. Deuterium enrichment in plasma of prenatally labeled mice from the moment ^2H_2O was withdrawn from the drinking water (i.e., at 16 weeks of age). Gray squares (▫) represent plasma deuterium enrichment measurements (i.e., individual mice); the black curve represents the best fit of the model to the experimental data. The turnover rate of plasma (body water) in prenatal labeling experiments is somewhat slower than the turnover rate in finite-term labeling experiments (see Sup. Table 1), which is natural because deuterium is fully enriched in all available compartments in prenatally labeled mice.

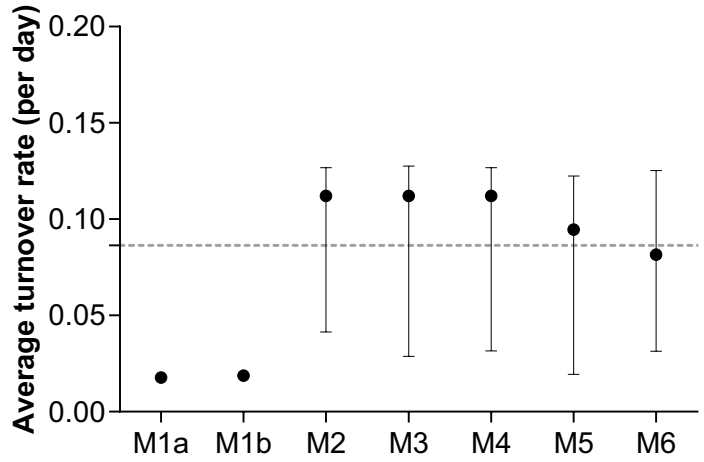

Supplementary Figure 3. Average turnover rates and 95% confidence intervals estimated with the 7 different models. Model M_{1a} is the one proposed by Asquith et al. [2] where only a fraction α of cells is turning over, while the rest of the cell population is kinetically inert. Model M_{1b} assumes that all cells have the same turnover rate (i.e., form a homogeneous population). Models M_2 to M_6 are kinetic-heterogeneity models including 2 to 6 kinetically different subpopulations (i.e., with 2 to 6 turnover rates). Artificial labeling data were generated with model M_2 for p_1= 0.720, p_2=0.016 and α_1=0.10, corresponding to an average turnover rate p=0.0864 (---- dashed gray horizontal line), and after adding a Gaussian white noise, these data were fitted with the 7 different models.

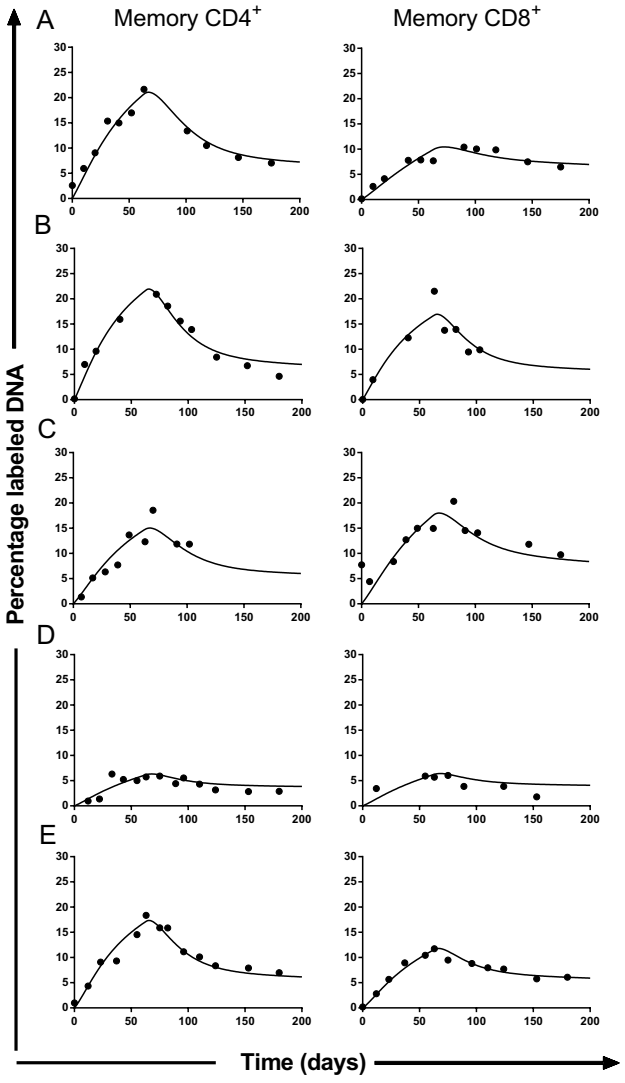

Supplementary Figure 4. Best fits of the multiexponential model to deuterium enrichment data in memory CD4⁺ and CD8⁺ T cells from five healthy individuals (A to E). During 9 weeks of $^{2}H_{2}O$ labeling, CD4⁺ (left) and CD8⁺ (right) memory T cells were isolated at different time points during and post-labeling, and deuterium enrichment of the DNA was determined and previously published [1]. The resulting labeling curves were fitted with a multiexponential model describing two kinetically different subpopulations (the addition of more subpopulations did not change the average turnover rate).

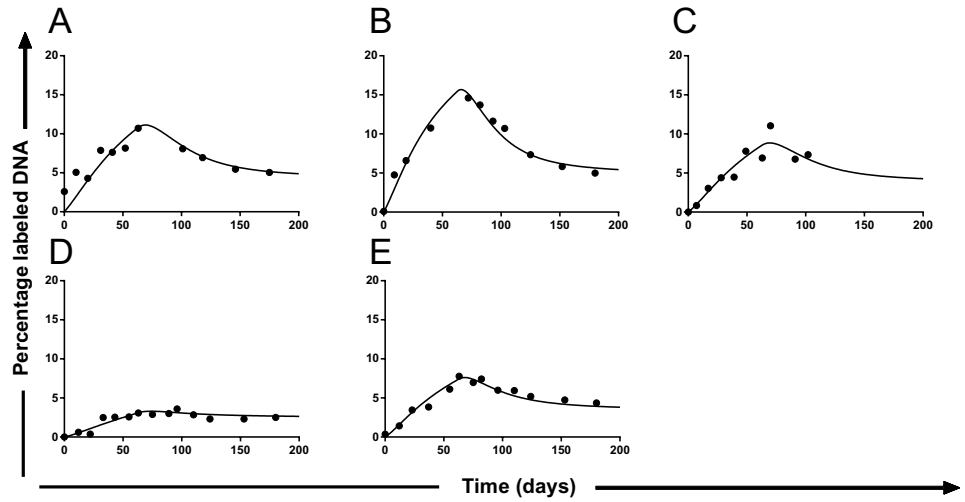

Supplementary Figure 5. Best fits of the multiexponential model to deuterium enrichment data in total CD4⁺ T cells from five healthy individuals (A to E). During 9 weeks of $^{2}H_{2}O$ labeling, CD4⁺ naive and memory T cells were isolated at different time points during and post-labeling, and deuterium enrichment was determined, and previously published [1]. From this the deuterium enrichment in total CD4⁺ T cells at every time point was recalculated, and the resulting labeling curves were fitted with a multiexponential model describing two kinetically different subpopulations (the addition of more subpopulations did not change the average turnover rate).

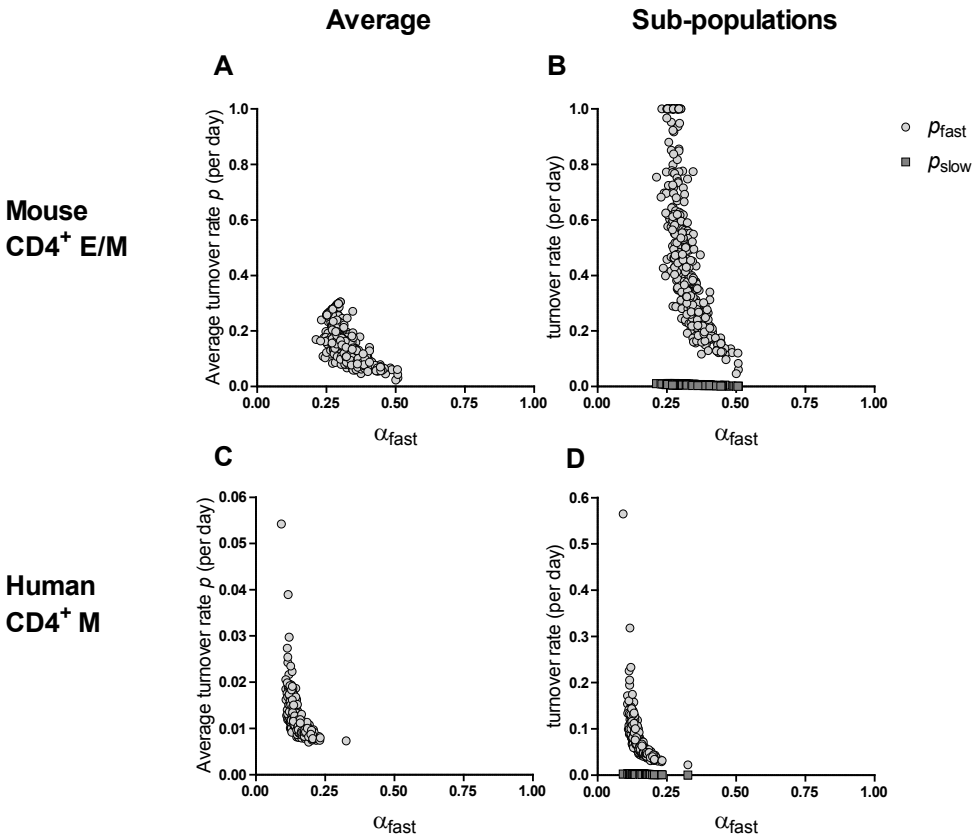

Supplementary Figure 6. Relationship between parameter estimates describing the individual subpopulations. As an illustration of the ranges of, and the relationship between, the sizes of the different subpopulations, the average turnover rate (panels A and C), and the individual turnover rates of the subpopulations (panels B and D), we selected two data sets: 8-week labeling of $CD4^+$ effector/memory (E/M) T cells in mice (panels A and B), and labeling of human $CD4^+$ memory T cells (individual A of Vrisekoop et al.[1], panels C and D, note the different scales!). For both data sets we plotted the 500 parameter sets obtained by the bootstrap analysis of Figure 2. We ordered the results of the bootstrap analysis such that the turnover rate of the fastest (p_{fast}) and the slowest (p_{slow}) subpopulations can be plotted as a function of the size of the fastest subpopulation (α_{fast}). The examples illustrate that there is quite a strong correlation between the size of a subpopulation and its rate of turnover (panels B and D). As a result, the confidence limits on the turnover rate of the fastest subpopulation (panels B and D) are much less restricted than on the average turnover rate *p* (panels A and C). Nevertheless, the data do provide some bounds on the sizes and turnover rates of the subpopulations. The mouse data show that the fastest subpopulation makes up between 24% and 51% of the $CD4^+$ E/M pool, while in humans it represents only 11-20% of the $CD4^+$ memory pool. In the mouse data set, the turnover rate of the fast subpopulation cannot be estimated as it varies from almost 0 to 1 (panel B), while the human labeling data reveal that the turnover rate of the fast subpopulation lies between 0.03 and 0.17 per day, and that of the slow subpopulation between 0.001 and 0.002 per day (panel D).

References Supplementary Information

1. Vrisekoop N., den Braber I., de Boer A.B., Ruiter A.F., Ackermans M.T., van der Crabben S.N., et al. Sparse production but preferential incorporation of recently produced naive T cells in the human peripheral pool. Proc. Natl. Acad. Sci. U. S. A 105(16):6115-6120 (2008).
2. Mohri H., Perelson A.S., Tung K., Ribeiro R.M., Ramratnam B., Markowitz M., et al. Increased turnover of T lymphocytes in HIV-1 infection and its reduction by antiretroviral therapy. J. Exp. Med. 194(9):1277-1287 (2001).
3. Asquith B., Debacq C., Macallan D.C., Willems L., Bangham C.R. Lymphocyte kinetics: the interpretation of labelling data. Trends Immunol. 23(12):596-601 (2002).
4. Hellerstein M., Hanley M.B., Cesar D., Siler S., Papageorgopoulos C., Wieder E., et al. Directly measured kinetics of circulating T lymphocytes in normal and HIV-1-infected humans. Nat. Med. 5(1):83-89 (1999).
5. Neese R.A., Misell L.M., Turner S., Chu A., Kim J., Cesar D., et al. Measurement in vivo of proliferation rates of slow turnover cells by 2H2O labeling of the deoxyribose moiety of DNA. Proc. Natl. Acad. Sci. U. S. A 99(24):15345-50 (2002).
6. R Development Core Team: A language and environment for statistical computing. (2010).

6

Similar Estimates of Cell Turnover from Stable Isotope-Labeling Experiments Using Deuterated Glucose or Water

Liset Westera[1]*, Raya Ahmed[2]*, Julia Drylewicz[1,3], Marjet Elemans[4], Yan Zhang[2], Kiki Tesselaar[1], Rob J de Boer[3], Derek C Macallan[2], José AM Borghans[1#], Becca Asquith[4#]

[1] Laboratory of Translational Immunology, University Medical Center Utrecht, Utrecht, The Netherlands; [2] Infection and Immunity Research Centre, St. George's, University of London, London, United Kingdom; [3] Theoretical Bilogy & Bioinformatics, Utrecht University, Utrecht, The Netherlands; [4] Department of Immunology, Imperial College, London, United Kingdom

*, [#] These authors contributed equally.

Stable-isotope labeling is considered the state of the art technique for in vivo quantification of lymphocyte turnover in humans, as in the doses used it is safe and does not interfere with physiological cell turnover. However, there is still a considerable discrepancy between lymphocyte turnover rates based on stable-isotope labeling studies, and this hampers our understanding of immune function in health and disease. In the literature, deuterated ($^2H_2$-)glucose-labeling studies consistently yield higher turnover estimates than deuterated water (^2H_2O)-labeling studies. Whether these discrepancies are caused by differences between biochemical properties of the two compounds or by methodological differences between these studies is not clear. We therefore performed 1-week labeling experiments in mice with $^2H_2$-glucose and ^2H_2O, and found very similar turnover rates when the data were interpreted using a multi-exponential model. Using the same model to reanalyze previously published human labeling studies, we reconcile 1-day $^2H_2$-glucose, 1-week glucose and 9-week ^2H_2O-labeling experiments. Taken together, our mouse and human data show that lymphocyte turnover estimates are influenced neither by biochemical differences between the $^2H_2$-labeled compounds, nor by methodological differences between the studies.

Introduction

Quantification of lymphocyte turnover is vital for our understanding of both normal immune homeostasis as well as clinical conditions that affect lymphocyte populations, such as rheumatoid arthritis, stem cell transplantation, and HIV infection. The recent development of stable isotope-labeling techniques, using either deuterium-labeled glucose ($^2H_2$-glucose) or deuterium-labeled water (^2H_2O), has made it feasible to safely quantify the turnover of lymphocytes in vivo, and has instigated widespread investigations in various clinical conditions, including aging, HIV infection, diabetes, and several B-cell malignancies[1-11] (and www.clinicaltrials.gov).

Despite this major breakthrough, estimates of T-cell turnover (and hence life span) were still found to differ up to 10-fold between stable isotope-labeling studies, with $^2H_2$-glucose-labeling studies consistently yielding higher turnover rates than ^2H_2O-labeling studies[12, 13]. We recently demonstrated that single-exponential models, which are typically used to interpret stable isotope-labeling data, yield estimates that are sensitive to the duration of label administration, with long labeling periods being prone to underestimation of turnover rates[14]. Using a multi-exponential modeling approach[14-16], we re-estimated the turnover rates from a 1-week $^2H_2$-glucose-labeling and a 9-week ^2H_2O-labeling experiments[1, 8]. This markedly reduced the difference between the two studies, probably because the turnover rate of the 9-week labeling experiment was no longer underestimated.

Despite the many similarities between $^2H_2$-glucose- and ^2H_2O-labeling experiments, they differ in several aspects, both in the exact experimental procedures as well as in the way the experimental data are translated into the biological parameters of interest. $^2H_2$-glucose is typically administered for short periods of time, i.e., hours to days, and is given intravenously or orally[17, 18]. The pool of blood glucose is small and has a high rate of turnover, so rapid up- and de-labelling can be achieved[19]. Because of the short labeling period, cell samples are typically collected during the de-labeling phase only. ^2H-enrichment in samples is measured in the ribose moiety of the DNA of the cell population of interest, and corrected for the level of $^2H_2$-glucose enrichment in the blood and a constant accounting for the intracellular dilution of labeled deoxyribonucleotides (0.65[20], 0.60[21-23], or 0.73 according to recent insights[18]).

^2H_2O is generally administered over a timescale of several weeks, and experiments typically start with an oral "ramp-up" bolus followed by a daily maintenance dose[18, 24]. Because of the long period of label administration, cell samples are usually collected both during up-labeling and post-labeling. The observed ^2H-enrichment in a cell population is normalized to the maximum level of enrichment that cells can possibly attain, which is determined in a population with rapid turnover, such as granulocytes, monocytes or thymocytes[1]. Because of the relatively slow turnover of body water, enrichment in the body fluids reaches its maximum and is washed-out from the body

more slowly than glucose. A correction for the actual level of ^2H_2O present in the body fluids at the time of cell division is therefore achieved by taking the enrichment of blood plasma or urine samples into account[1].

To study whether the use of different compounds could have contributed to the differences found in the literature, we performed stable isotope-labeling experiments in mice using either $^2H_2$-glucose or ^2H_2O, while keeping every other aspect (laboratory, mice, sampling, analysis, interpretation, …) of the study identical. We found that $^2H_2$-glucose and ^2H_2O experiments yielded very similar estimates of the average turnover rate of splenocytes and PBMC, suggesting that discrepancies in the literature are not caused by biochemical differences between the compounds. To further explore what might be causing these discrepancies, we reanalyzed previously published labeling studies in humans: 9-week ^2H_2O- [1, 11], 1-week $^2H_2$-glucose- [8], and 1-day $^2H_2$-glucose-labeling studies[4, 25]. Using the parameters resulting from the 9-week ^2H_2O labeling experiment[14], we were able to predict the labeling curves observed in the 1-week $^2H_2$-glucose-labeling experiment[8], reconfirming that discrepancies in the literature are not caused by biochemical differences between the $^2H_2$-labeled compounds. Although enrichment levels in a 1-day $^2H_2$-glucose study on T cells[4] appeared to be inconsistent with those in longer labeling studies, we reconciled 1-day $^2H_2$-glucose and 9-week ^2H_2O labeling studies on B cells[11, 25], suggesting that in principle labeling for 1 day or for several weeks yields similar turnover estimates.

Results and Discussion

Different normalization approaches do not affect turnover estimates

Because the approach that is used to normalize DNA enrichment is different in a typical $^2H_2$-glucose-labeling experiment (i.e., normalization to mean plasma enrichment*constant) and a typical ^2H_2O-labeling experiment (i.e., normalization to plateau enrichment of a fast population), we first investigated whether this difference could influence turnover rate estimates. In a previous $^2H_2$-glucose-labeling study of T cells in healthy and HIV-infected subjects, Mohri et al. measured both plasma enrichment and label incorporation in monocytes, a cell population with rapid turnover[8]. Their primary data show that maximum enrichment in monocytes of three individuals reaches between 52% and 61% of plasma enrichment (Sup. Fig. 1A-F), which is in reasonable agreement with the factor of 0.65 that is typically used for normalization[20]. Using the T-cell enrichment data, we re-estimated T-cell turnover rates by normalizing by the plateau enrichment of monocytes, instead of the mean plasma enrichment*0.65. This yielded $CD4^+$ and $CD8^+$ T-cell turnover rates that were very similar to the ones published by Mohri et al.[8] using the latter approach (Sup. Fig. 1G). Hence, the different normalization approaches that are typically used in ^2H_2O and $^2H_2$-glucose labeling studies do not seem to influence turnover rate estimates.

$^2H_2$-glucose- and ^2H_2O-labeling experiments in mice yield similar turnover rates

To compare $^2H_2$-glucose- and ^2H_2O-labeling experiments in mice, we chose a labeling period that was long enough to (1) obtain sufficient label incorporation by the cell populations under investigation; (2) permit sample collection during both up-labeling and de-labeling phases; and (3) sample a sufficient part of the labeling curve of thymocytes (as a population with rapid turnover to predict the maximum label enrichment that cells can possibly attain). We therefore chose to do a 7-day labeling study, with oral administration of both compounds to cause least inconvenience to mice: ^2H_2O via drinking water (8%), or $^2H_2$-glucose via liquid feed (30%), ad libitum and replacing regular feed. To keep circumstances identical, unlabeled liquid feed was given to ^2H_2O-labeled mice, and to all mice after administration of label. All mice consumed regular amounts of the liquid feed for the duration of the experiment and

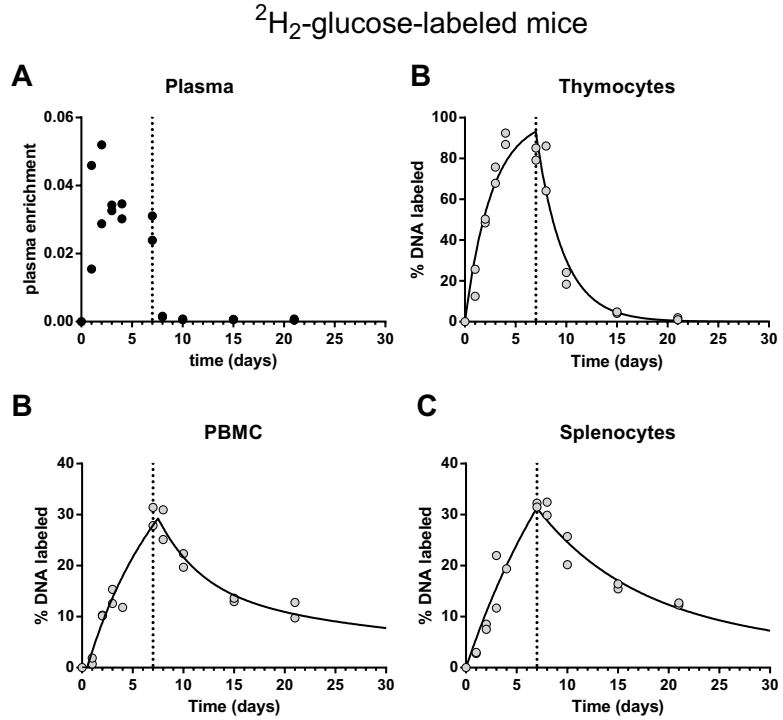

Figure 1. Enrichment curves of $^2H_2$-glucose-labeled mice. (A) Deuterium enrichment in plasma. (B-D) Best fits (black lines) to deuterium enrichment in DNA of thymocytes (B), PBMC (C), and splenocytes (D). Thymocytes were used to determine the maximum percentage of labeled DNA that cells could possibly attain (see Materials and Methods), and all measured enrichments were scaled to this maximum. Dots represent individual mice. The end of label administration at day 7 is marked by a dashed vertical line.

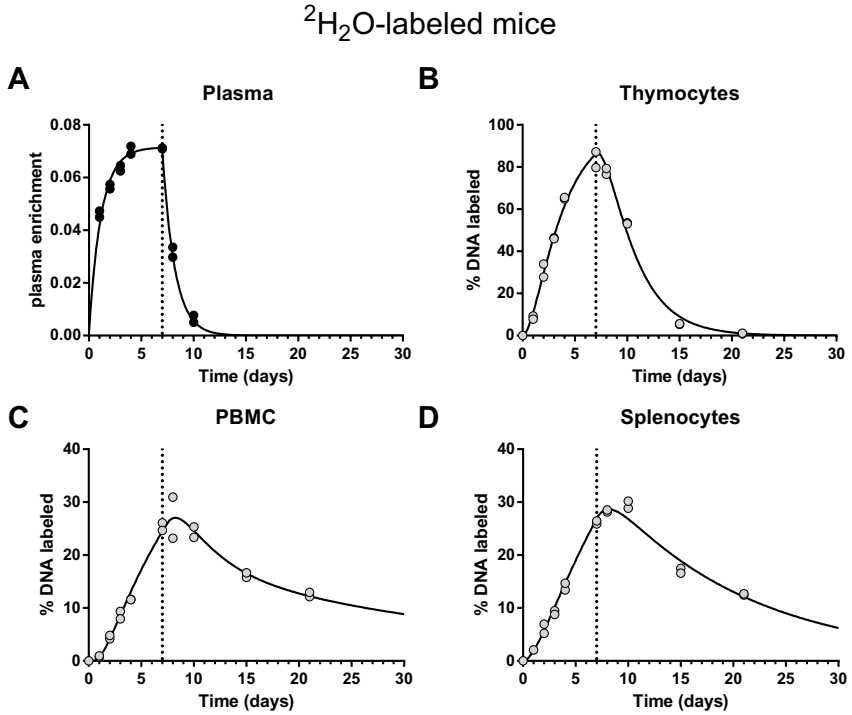

Figure 2. Enrichment curves of ^2H_2O-labeled mice. Best fits (black lines) to deuterium enrichment in plasma (A) and DNA of thymocytes (B), PBMC (C), and splenocytes (D). Thymocytes were used to determine the maximum percentage of labeled DNA that cells could possibly attain (see Materials and Methods), and all measured enrichments were scaled to this maximum. Dots represent individual mice. The end of label administration at day 7 is marked by a dashed vertical line.

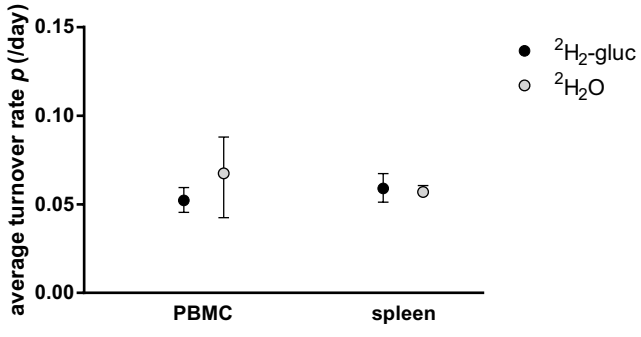

Figure 3. Comparing turnover estimates from a 1-week $^2H_2$-glucose-labeling experiment and a 1-week ^2H_2O-labeling experiment in mice. The average turnover rate p of PBMC and splenocytes, obtained by fitting the multi-exponential model to the data collected during 1 week of labeling with $^2H_2$-glucose (closed circles) or ^2H_2O (open circles). Error bars represent 95% confidence intervals.

slightly gained weight (data not shown). To check whether the $^2H_2$-glucose-labeled mice were consuming the labeled feed similarly on the 7 days of the up-labeling period, we measured plasma glucose enrichment daily at the same time of the day; plasma enrichment was indeed relatively stable during the labeling phase (Fig. 1A). However, $^2H_2$-glucose enrichment levels in the plasma at a given time of the day are probably not representative of the availability of $^2H_2$-glucose during 24 hours and hence during the whole up-labeling period. Since the normalization approach does not seem to influence turnover estimates, we therefore normalized the DNA enrichment in the different cell populations from both $^2H_2$-glucose and ^2H_2O-labeled mice to the estimated plateau enrichment of a cell population with rapid turnover, in this case thymocytes (see Materials and Methods), rather than to mean plasma enrichment. In our mouse ^2H_2O-labeling experiment, the best fit of the mathematical model to the observed ^2H_2O plasma enrichment levels was taken along (Fig. 2A), as previously described[1].

The labeling curves of thymocytes, PBMC, and splenocytes obtained in our 1-week $^2H_2$-glucose- and ^2H_2O-labeling experiments were fitted with a multi-exponential model to estimate the average turnover rate *p* of the cell population (Fig. 1B-D and Fig. 2, as previously described[14, 15]. Interpretation of the ^2H_2O- and the $^2H_2$-glucose-labeling experiments yielded similar daily turnover rates of 0.052 per day (95% CI= [0.045;0.059], $^2H_2$-glucose) and 0.067 per day (95% CI= [0.043;0.088], ^2H_2O) for PBMC, and 0.059 (95% CI= [0.051;0.067], $^2H_2$-glucose) and 0.057 (95% CI= [0.054;0.061], ^2H_2O) for splenocytes (Fig. 3). These findings suggest that biochemical differences between these deuterium-labeled compounds do not influence lymphocyte turnover estimates in mice.

Comparing $^2H_2$-glucose- and ^2H_2O-labeling experiments in humans

We next studied whether $^2H_2$-glucose and ^2H_2O labeling also yielded similar turnover estimates in humans. To this end, we reanalyzed five previously published labeling studies in healthy humans: two 1-day $^2H_2$-glucose-labeling studies[4, 25], a 1-week $^2H_2$-glucose-labeling study[8], and two 9-week ^2H_2O-labeling studies[1, 11]. To investigate whether these labeling studies of different duration were in agreement with each other, we predicted the labeling curves of the short-term labeling studies using the turnover parameters of a longer-term labeling experiment. Note that vice versa-- predicting the results of a long-term labeling study based on the parameters of a short-term labeling study-- may not at all work, because short-term labeling experiments may not be able to pick up information about the kinetic composition of a cell population which may be evident in longer-term labeling studies[14].

We first compared the 1-week $^2H_2$-glucose-labeling[8] and the 9-week ^2H_2O-labeling studies[1, 26]. Using the $CD4^+$ T-cell turnover parameters estimated in the 9-week

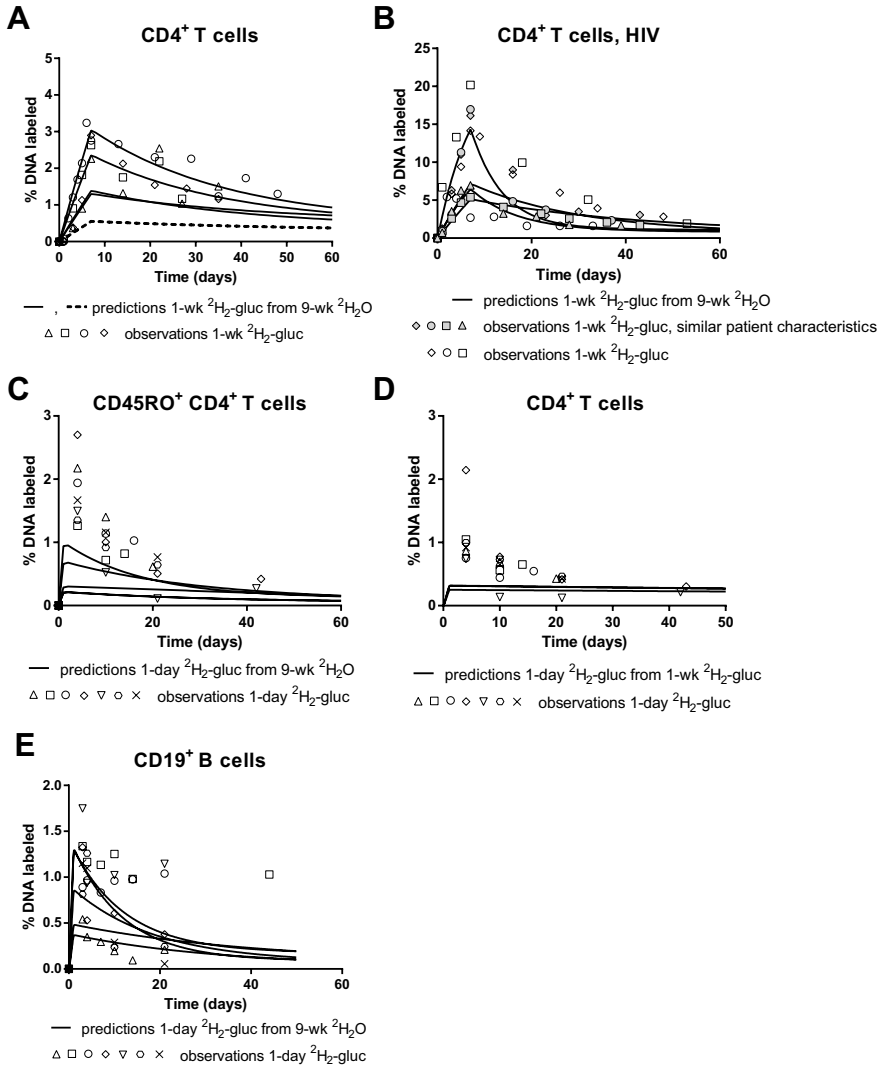

^2H_2O-labeling studies in healthy individuals and in HIV-1 patients (recalculated from naive and memory CD4$^+$ T-cell subsets), we predicted 1-week $^2H_2$-glucose labeling curves (Fig. 4A,B), and compared these curves to the observed CD4$^+$ T-cell enrichments in the real 1-week $^2H_2$-glucose-labeling experiment in healthy and HIV-1-infected individuals[8]. For healthy individuals, predicted labeling curves were in good agreement with the observed T-cell enrichment levels, except for one outlier (dashed line), which had an exceptionally low turnover rate compared to the other 4 subjects (Fig. 4A). Also the predicted 1-week T-cell labeling curves for HIV-1 patients were in agreement with observed enrichment levels in the 1-week $^2H_2$-glucose labeling study (Fig. 4B).

Figure 4. Prediction of $^2H_2$-glucose-labeling curves based on parameters from independent labeling experiments in humans. Lines indicate predictions for different individuals. Different symbols indicate observed enrichments in different individuals. (A) Prediction of 1-week $^2H_2$-glucose-labeling curves of CD4$^+$ T cells based on parameters from a 9-week ^2H_2O experiment[1]. Using the turnover parameters for total CD4$^+$ T cells estimated from the 9-week ^2H_2O experiment (which we previously calculated from the measured enrichments in naive and memory CD4$^+$ T cells and their relative sizes, as described in Westera et al.[14], we predicted the enrichment curves for a 1-week $^2H_2$-glucose experiment from the 9-week ^2H_2O experiment. We compared these predicted curves to the observed enrichments of CD4$^+$ T cells in the 1-week $^2H_2$-glucose experiment in healthy individuals[8]. The dashed lines indicates an outlier; this subject had an exceptionally low turnover rate. (B) Prediction of 1-week labeling curves of CD4$^+$ T cells based on parameters from a 9-week ^2H_2O experiment in untreated HIV-1 patients[26]. We first recalculated the enrichment in CD4$^+$ T cells based on the enrichment in naive and memory CD4$^+$ T cells and their relative sizes as determined in the 9-week ^2H_2O experiment[26]. From the enrichment in CD4$^+$ T cells we estimated the average turnover rates using the multi-exponential model (see fits in Sup. Figure 2). Based on these parameters we predicted 1-week $^2H_2$-glucose-labeling curves. We compared these predicted curves to the observed enrichments of CD4$^+$ T cells in the 1-week $^2H_2$-glucose experiment in untreated HIV-1 patients[8]; note that the gray symbols mark individuals that are similar to the patients in the 9-week ^2H_2O study regarding viral load and CD4 count; open symbols are the other 3 patients in the same study (C) Prediction of 1-day $^2H_2$-glucose-labeling curves of CD45RO$^+$ CD4$^+$ T cells based on parameters from a 9-week ^2H_2O-labeling experiment[1, 14]. Using the turnover parameters for CD45RO$^+$ CD4$^+$ T cells estimated in the 9-week ^2H_2O experiment, we predicted the enrichment curves for a 1-day $^2H_2$-glucose-labeling experiment. We compared these predicted curves to the observed enrichments of CD45RO$^+$ CD4$^+$ T cells in the 1-day $^2H_2$-glucose-labeling experiment[4]. (D) Prediction of 1-day $^2H_2$-glucose-labeling curves of CD4$^+$ T cells based on parameters from a 1-week $^2H_2$-glucose-labeling experiment[8]. Using the turnover parameters for total CD4$^+$ T cells estimated in the 1-week $^2H_2$-glucose experiment, we predicted the enrichment curves for a 1-day $^2H_2$-glucose-labeling experiment. We compared these predicted curves to the observed enrichments of CD4$^+$ T cells in the 1-day $^2H_2$-glucose-labeling experiment[4], which we calculated from the enrichments measured in CD45RA$^+$ and CD45RO$^+$ CD4$^+$ T cells (See Materials and Methods). (E) Prediction of 1-day $^2H_2$-glucose-labeling curves of total CD19$^+$ B cells based on parameters from a 9-week ^2H_2O-labeling experiment[11]. From previously published 9-week ^2H_2O-labeling data in CD19$^+$ B cells[11], we estimated B-cell turnover rates using the multi-exponential model (see fits in Sup. Figure 4). Using these turnover parameters we predicted the enrichment curves for a 1-day $^2H_2$-glucose-labeling experiment, and compared them to the observed enrichments of CD19$^+$ B cells in the 1-day $^2H_2$-glucose labeling experiment of total CD19$^+$ B cells[25].

Because the highest turnover rate estimates in the literature are based on the shortest labeling experiments[12], we next compared the 9-week ^2H_2O-labeling-[1] and the 1-week $^2H_2$-glucose-labeling studies[8] to the 1-day $^2H_2$-glucose-labeling studies[4]. To compare the 9-week and the 1-day labeling experiments, we looked at CD45RO$^+$ CD4$^+$ T cells, which were analyzed in both studies. To allow a fair comparison between the 1-week and the 1-day labeling experiments, which respectively analyzed total CD4$^+$ T cells, and CD45RA$^+$ and CD45RO$^-$ CD4$^+$ T cells, we calculated the deuterium enrichment in total CD4$^+$ T cells from the enrichment in CD45RA$^+$ and CD45RO$^+$ CD4$^+$ T cells in the 1-day labeling experiment (see Materials and Methods).

We predicted 1-day $^2H_2$-glucose labeling curves for CD45RO$^+$ CD4$^+$ T cells using the turnover parameters from the 9-week ^2H_2O experiment (Fig. 4C), and for total CD4$^+$

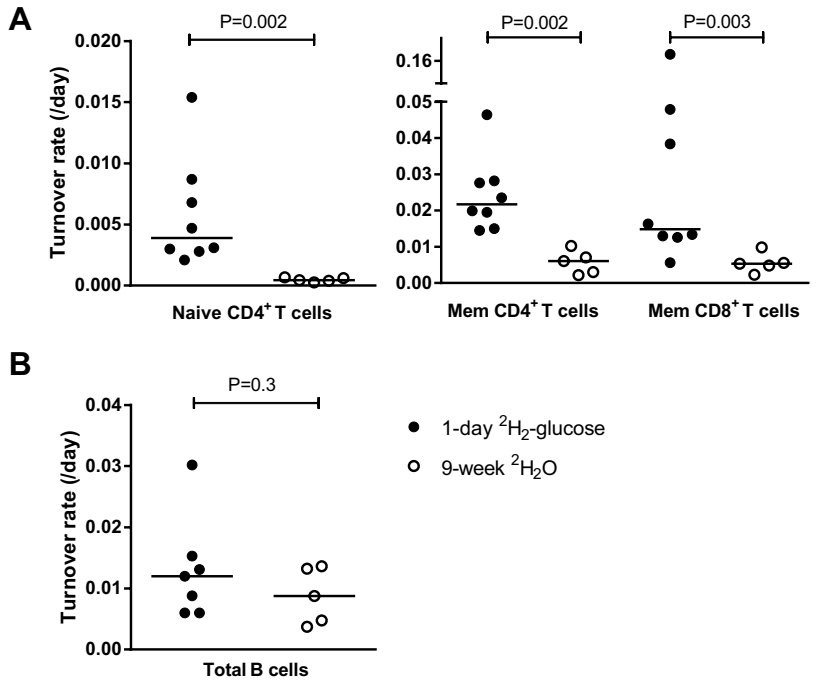

Figure 5. T-cell and B-cell turnover rates estimated from 1-day $^2H_2$-glucose- and a 9-week ^2H_2O-labeling studies in humans. Estimates of the average turnover rate of different individuals are indicated by circles. Groups were compared using a Mann-Whitney test. Closed circles are estimates from 1-day $^2H_2$-glucose labeling, open circles are estimates from 9-week ^{2}H2O labeling. (A) Naive CD4$^+$ and memory CD4$^+$ and CD8$^+$ T cells (naive CD8$^+$ T cells are not shown because the different phenotype definition in the labeling studies makes this subset incomparable); turnover rates are from Wallace et al.[4] ($^2H_2$-glucose) and Westera et al.[14] and chapter 6 (^2H_2O). (B) Total CD19$^+$ B cells; turnover rates are from Defoiche et al.[25] ($^2H_2$-glucose), and re-estimated from labeling data published in Van Gent et al.[11] (^2H_2O) (See Materials and Methods, See Sup. Fig. 3).

T cells using the turnover parameters from the 1-week $^2H_2$-glucose experiment (Fig. 4D). Remarkably, the observed enrichments levels in the 1-day labeling experiment appeared to be quite a bit higher than the predicted enrichment curves based on the parameters from the 9-week ^2H_2O- and the 1-week $^2H_2$-glucose-labeling experiments, with the observed peak enrichment level at day 4 in all 7 individuals being 2- to 7-fold higher than we predicted based on the parameters from the two longer labeling studies (Fig. 4C,D). Indeed, when comparing the observed total CD4$^+$ T-cell enrichment levels in the two $^2H_2$-glucose-labeling experiments, labeling for only 1 day appeared to have resulted in an enrichment level at day 4 similar to the enrichment level obtained after 4 days of labeling (Sup. Fig. 3). The difference in observed enrichment between the 1-day-labeling and the longer labeling experiments explains the differences in naive and memory T-cell turnover rates that have been estimated from these experiments (Fig. 5A).

Because the 1-day-labeling experiment seems to have yielded T-cell enrichment data that are higher than those in the longer labeling experiments of 1 and 9 weeks, we looked at another cell type that was analyzed both in a 1-day $^2H_2$-glucose labeling and in the 9-week labeling study: total CD19$^+$ B cells[11, 25]. Using the multi-exponential model, we first re-estimated the B-cell turnover rates of the 9-week ^2H_2O-labeling data[11] (Sup. Fig. 4), which yielded average turnover rates that were very similar to the ones reported in the 1-day $^2H_2$-glucose labeling study (Fig. 5B). Using the parameters based on the 9-week ^2H_2O-labeling study, we again predicted 1-day labeling curves (Fig. 4D). The observed enrichment levels in the 1-day labeling experiment[25] were in good agreement with the predicted enrichment curves based on the parameters of the 9-week labeling experiment (Fig. 4E). Taken together, these results suggest that also in humans, biochemical differences between the two compounds do not affect lymphocyte turnover estimates.

Conclusions

Discrepancies among published life span estimates have been attributed to (i) the length of the labeling period and (ii) methodological or biochemical differences between the deuterium-labeled compounds. We previously resolved part of the controversy by implementing a multi-exponential modeling approach[14]. In this work, we have obtained similar turnover estimates by $^2H_2$-glucose and ^2H_2O-labeling experiments in mice, and we have reconciled 1-day $^2H_2$-glucose, 1-week glucose and 9-week ^2H_2O-labeling studies, all together pointing out that neither biochemical differences between the compounds nor methodological differences between the approaches underlie differences in published lifespan estimates. Although the unexplained high enrichment levels measured shortly after label cessation in a 1-day T-cell labeling study[4] could not be reconciled with the enrichment levels measured in longer labeling studies, the consistency between B-cell labeling curves from 1-day $^2H_2$-glucose and 9-week ^2H_2O labeling studies strongly suggests that the length of the labeling period and the use of $^2H_2$-glucose or ^2H_2O should not affect the estimated turnover rates as long as data from longer-term labeling studies are interpreted using a multi-exponential model.

Acknowledgments

We thank David Ho and Hiroshi Mohri for sharing their published $^2H_2$-glucose-labeling data with us.

Materials and Methods

Mice. C57Bl/6J mice were housed in the animal facility of St George's University of London, agreement with institutional and Home Office guidelines.

Stable isotope labeling. C57Bl/6J males, aged ~12 wk, were labeled with either deuterated (6,6-$^2H_2$-) glucose or deuterated water (^2H_2O) for 7 days. For $^2H_2$-glucose labeling, mice ate a 30% deuterated glucose human liquid feed (company) ad libitum instead of their normal chow for the labeling period of 7 days; to keep feeding circumstances similar, mice also received normal drinking water. For ^2H_2O labeling, mice were given an i.p. boost of 15ml/kg ^2H_2O (Cambridge Isotope Laboratories) in PBS at t=0 and subsequently drank only 8% ^2H_2O; to keep circumstances similar, mice ate 8% ^2H_2O-labeled human liquid feed ad libitum instead of their normal chow for the labeling period of 7 days. For the duration of the experiment, weight of the mice, water consumption, and liquid feed consumption were monitored and recorded.

Sampling. Mice were sacrificed at the indicated time points (day 0, 1, 2, 3, 4, 7, 8, 10, 15, 21) and tissues were obtained by cardiac puncture (blood, collected in heparinized tubes) and dissection (thymus, spleen). Blood was spun down to isolate plasma. Organs were mechanically disrupted to obtain single-cell suspensions. Plasma was frozen and cells were cryopreserved in liquid nitrogen until further analysis. Prior to hydrolization for GC-MS analysis, samples with high cell numbers were processed using QiaGen DNA Mini Extraction kit to isolate DNA, and low-yield samples were boiled for an hour.

Measurement of deuterium enrichment in plasma and DNA. Deuterium enrichment in plasma and DNA from all sampling time points was analyzed by gas-chromatography/mass-spectrometry (GC/MS) using an Agilent 5973/6890 GC/MS system (Agilent Technologies). Plasma from $^2H_2$-glucose-labeled mice was derivatized to aldonitrile triacetate (ATA) as previously described[17]. The derivative was injected into the GC/MS equipped with a HP-225 column (Agilent technologies) and measured in SIM mode monitoring ions m/z 328 (M+0) and m/z 330 (M+2). Plasma from ^2H_2O-labeled mice was derivatized to acetylene (C_2H_2) as previously described[18]. The derivative was injected into the GC/MS equipped with a PoraPLOT Q 25x0.32 column (Varian), and measured in SIM mode monitoring ions *m/z* 26 (M+0) and *m/z* 27 (M+1). From the ratio of ions plasma deuterium enrichment was calculated by calibration against standard glucose or water samples of known enrichment. DNA obtained from thymocytes, PBMC, and splenocytes was hydrolyzed to deoxyribonucleotides and derivatized to penta-fluoro-triacetate (PFTA). The derivative was injected into the GC/MS equipped with a DB-17 column (Agilent Technologies) and measured in SIM mode monitoring ions *m/z* 435 (M+0), and *m/z* 436 (M+1; for ^2H_2O labeling) or *m/z* 437 (M+2; for ^2H-glucose labeling). From the ratio of ions plasma deuterium enrichment was calculated by calibration against deoxyadenosine (for ^2H_2O labeling) or deoxyribose (for $^2H_2$-glucose labeling) standards of known enrichment.

Recalculation of total CD4$^+$ T-cell enrichment curves. To compare CD4$^+$ T-cell enrichment curves of different labeling studies, we calculated the enrichment level of total CD4$^+$ T cells in the 1-day $^2H_2$-glucose-labeling experiment in healthy individuals[4] and in the 9-week ^2H_2O-labeling experiment in untreated HIV-1 patients[26], using the enrichment data of CD45RA$^+$ and CD45RO$^+$ CD4$^+$ T-cell subsets and their relative sizes within the total CD4$^+$ T-cell pool. Enrichment in CD4$^+$ T cells in the 9-week ^2H_2O-labeling experiment in healthy individuals was calculated previously[14] from enrichment in naive and memory CD4$^+$ T-cell subsets[1]. Recalculation of enrichment in total CD8$^+$ T cells in the 9-week labeling experiment could not be done because, due to the presence of a considerable fraction of CD27$^-$CD45RO$^-$ CD8$^+$ effector T cells, combining CD27$^+$CD45RO$^-$ and CD45RO$^+$ T cells is not equal to the total CD8$^+$ population.

Modeling of deuterium enrichment in plasma and cell populations. In the mouse ^2H_2O-labeling experiment, plasma enrichment was modeled by fitting a simple label enrichment/decay curve to the plasma enrichment data[1], yielding the fraction of ^2H_2O in the drinking water *f*. In both $^2H_2$-glucose and ^2H_2O mouse experiments, normalization of the enrichment in the DNA of cell populations was done against the maximum enrichment of a cell population with rapid turnover *f*c* (with *c* being a constant, in the case of ^2H_2O-labeling an amplification factor that needs to be introduced because the adenosine deoxyribose (dR) moiety contains seven hydrogen atoms that can be replaced by deuterium[1], and in the case of $^2H_2$-glucose labelling a factor to correct for intracellular dilution of label):

Normalized DNA enrichment = (measured DNA enrichment) / (*f*c*).

Both the $^2H_2$-glucose- and ^2H_2O-labeling experiment were analyzed by normalizing with thymocytes. Body water enrichment was modeled for the ^2H_2O-labeling experiment. We first fitted a simple label enrichment/decay curve to the cross-sectional plasma enrichment data of all mice from the ^2H_2O labeling group:

$$U(t) = f(1-e^{-\delta t}) + \beta e^{-\delta t}$$ during label intake ($t \le \tau$), and

$$U(t) = \left[f(1-e^{-\delta \tau}) + \beta e^{-\delta \tau} \right] e^{-\delta (t-\tau)}$$ after label intake ($t > \tau$)

as described previously[14], where $U(t)$ represents the fraction of labeled precursor (^2H_2O) in plasma at time *t* (in days), *f* is the fraction of labeled precursor in the drinking water, labeling was stopped at $t = \tau$ days, δ represents the turnover rate of body water per day, and (in the case of ^2H_2O labeling) β is the plasma enrichment attained after the boost of label by the end of day 0. We incorporated these best fits when analyzing the enrichment in different cell populations.

Up- and de-labeling data of total thymocytes of both $^2H_2$-glucose- and ^2H_2O-labeling experiments were analyzed as described previously for ^2H_2O labeling[14], to estimate the maximum level of label

intake that cells could possibly attain in the two labeling experiments. For the $^2H_2$-glucose- and ^2H_2O-labeling experiments, the label enrichment data of PBMC and splenocytes were subsequently scaled by the corresponding thymocyte asymptote[1]. Labeling data of PBMC and splenocytes were fitted with a multi-exponential model allowing for kinetic heterogeneity within the same population[14, 15]. Each kinetic sub-population *i* was modelled to contain a fraction α_i of cells with turnover rate p_i. Assuming a steady state for each kinetic sub-population, label enrichment of adenosine in the DNA of each sub-population *i* was modelled by the following differential equation:

For ^2H_2O:

$$\frac{dl_i}{dt} = p_i c U(t) \alpha_i A - p_i l_i$$

For $^2H_2$-glucose:

$$\frac{dl_i}{dt} = p_i \alpha_i A - p_i l_i$$

where l_i is the total amount of labeled adenosine in the DNA of sub-population *i* and *A* is the total amount of adenosine in the cell population under investigation, *c* is the amplification factor, and p_i is the average turnover rate of sub-population *i*. Scaling this equation by the total amount of adenosine in the DNA of sub-population *i*, i.e., defining $L_i = l_i/(\alpha_i A)$, yields

For ^2H_2O:

$$\frac{dL_i}{dt} = p_i c U(t) - p_i L_i$$

For $^2H_2$-glucose:

$$\frac{dL_i}{dt} = p_i - p_i L_i$$

throughout the up- and de-labeling period, where L_i represents the fraction of labeled adenosine dR moieties in the DNA of sub-population *i*.

The fraction of labeled DNA in the cell population under investigation was subsequently derived from

$$L(t) = \sum \alpha_i L_i(t)$$

and the average turnover rate *p* was calculated from

$$p = \sum \alpha_i p_i$$

Because all enrichment data were expressed as fractions, labeling data were arcsin(sqrt) transformed before the mathematical model was fitted. Best fits were determined by minimizing the sum of squared residuals using the R function nlminb[27]. The 95% confidence intervals were determined using a bootstrap method where the residuals to the optimal fit were resampled 500 times.

References

1. Vrisekoop, N. et al. Sparse production but preferential incorporation of recently produced naive T cells in the human peripheral pool. Proc. Natl. Acad. Sci. U. S. A 105, 6115-6120 (2008).
2. Macallan, D.C. et al. Rapid turnover of effector-memory CD4(+) T cells in healthy humans. J. Exp. Med. 200, 255-260 (2004).
3. Zhang, Y. et al. In vivo kinetics of human natural killer cells: the effects of ageing and acute and chronic viral infection. Immunology 121, 258-265 (2007).
4. Wallace, D.L. et al. Direct measurement of T cell subset kinetics in vivo in elderly men and women. J. Immunol. 173, 1787-1794 (2004).
5. Macallan, D.C. et al. B-cell kinetics in humans: rapid turnover of peripheral blood memory cells. Blood 105, 3633-3640 (2005).
6. Bollyky, J.B. et al. Evaluation of in vivo T cell kinetics: use of heavy isotope labelling in type 1 diabetes. Clin. Exp. Immunol. 172, 363-374 (2013).
7. Zhang, Y. et al. Accelerated in vivo proliferation of memory phenotype CD4+ T-cells in human HIV-1 infection irrespective of viral chemokine co-receptor tropism. PLoS. Pathog. 9, e1003310 (2013).
8. Mohri, H. et al. Increased turnover of T lymphocytes in HIV-1 infection and its reduction by antiretroviral therapy. J. Exp. Med. 194, 1277-1287 (2001).
9. Hellerstein, M. et al. Directly measured kinetics of circulating T lymphocytes in normal and HIV-1-infected humans. Nat. Med. 5, 83-89 (1999).
10. Hellerstein, M.K. et al. Subpopulations of long-lived and short-lived T cells in advanced HIV-1 infection. J. Clin. Invest 112, 956-966 (2003).
11. van Gent, R. et al. In vivo dynamics of stable chronic lymphocytic leukemia inversely correlate with somatic hypermutation levels and suggest no major leukemic turnover in bone marrow. Cancer Res. 68, 10137-10144 (2008).
12. Borghans, J.A. & de Boer,R.J. Quantification of T-cell dynamics: from telomeres to DNA labeling. Immunol. Rev. 216, 35-47 (2007).
13. de Boer, R.J. & Perelson,A.S. Quantifying T lymphocyte turnover. J. Theor. Biol. 327, 45-87 (2013).
14. Westera, L. et al. Closing the gap between T-cell life span estimates from stable isotope-labeling studies in mice and humans. Blood 122, 2205-2212 (2013).
15. Ganusov, V.V., Borghans,J.A., & de Boer,R.J. Explicit kinetic heterogeneity: mathematical models for interpretation of deuterium labeling of heterogeneous cell populations. PLoS. Comput. Biol. 6, e1000666 (2010).
16. de Boer, R.J., Perelson,A.S., & Ribeiro,R.M. Modelling deuterium labelling of lymphocytes with temporal and/or kinetic heterogeneity. J. R. Soc. Interface 9, 2191-2200 (2012).
17. Macallan, D.C. et al. Measurement of proliferation and disappearance of rapid turnover cell populations in human studies using deuterium-labeled glucose. Nat. Protoc. 4, 1313-1327 (2009).
18. Westera, L., Zhang, Y., Tesselaar, K., Borghans, J.A., & Macallan, D.C. Quantitating lymphocyte homeostasis in vivo in humans using stable isotope tracers. Methods Mol. Biol. 979, 107-131 (2013).
19. Asquith, B., Borghans, J.A., Ganusov, V.V., & Macallan, D.C. Lymphocyte kinetics in health and disease. Trends Immunol. 30, 182-189 (2009).
20. Macallan, D.C. et al. Measurement of cell proliferation by labeling of DNA with stable isotope-labeled glucose: studies in vitro, in animals, and in humans. Proc. Natl. Acad. Sci. U. S. A 95, 708-713 (1998).
21. Kovacs, J.A. et al. Induction of prolonged survival of CD4+ T lymphocytes by intermittent IL-2 therapy in HIV-infected patients. J. Clin. Invest 115, 2139-2148 (2005).
22. Read, S.W. et al. CD4 T cell survival after intermittent interleukin-2 therapy is predictive of an increase in the CD4 T cell count of HIV-infected patients. J. Infect. Dis. 198, 843-850 (2008).
23. Stevens, R.A. et al. General immunologic evaluation of patients with human immunodeficiency virus infection in Manual of molecular and clinical laboratory immunology (eds. Detrick,B., Hamilton,R.G. & Folds,J.D.) 2006).
24. Busch, R., Neese, R.A., Awada, M., Hayes, G.M., & Hellerstein, M.K. Measurement of cell proliferation by heavy water labeling. Nat. Protoc. 2, 3045-3057 (2007).
25. Defoiche, J. et al. Reduction of B cell turnover in chronic lymphocytic leukaemia. Br. J. Haematol. 143, 240-247 (2008).
26. Vrisekoop, N. et al. Quantification of naive and memory T-cell turnover during HIV-1 infection. to be submitted.
27. R Development Core Team: A language and environment for statistical computing. 2010.

Supplementary Information

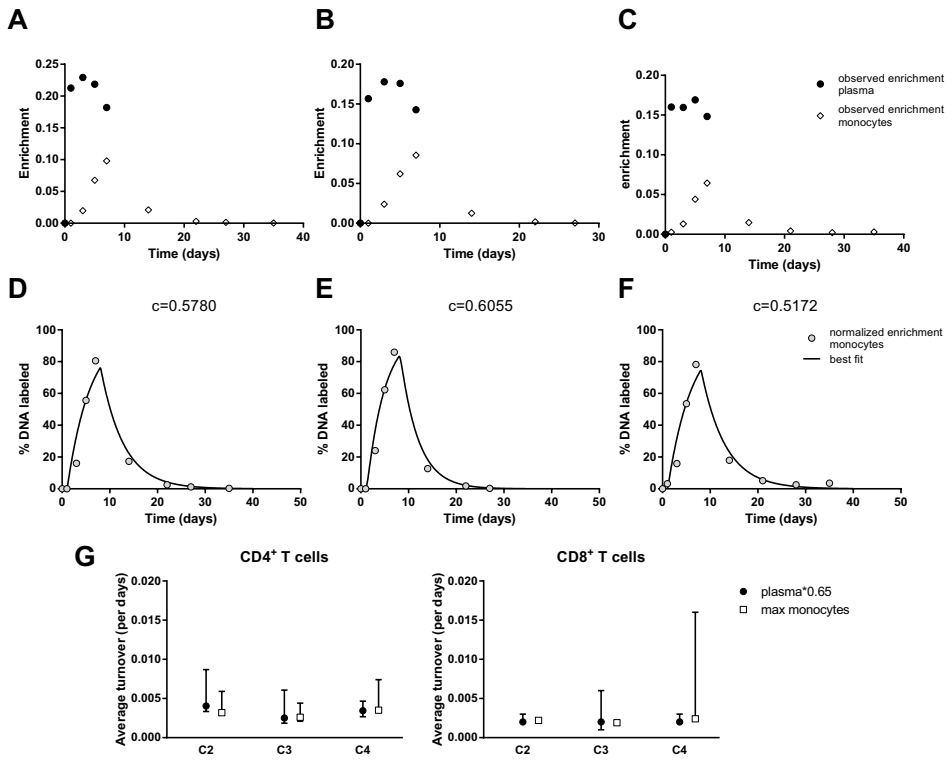

Supplementary Figure 1. Fitting monocyte curves to estimate the intracellular dilution factor in a previous 1-week $^2H_2$-glucose-labeling experiment in humans[8]. (A-C) Observed enrichment in plasma (closed circles) and monocytes (open diamonds) in 3 individuals of a 1-week $^2H_2$-glucose-labeling experiment[8]. Note that enrichment in monocytes reaches about half of the enrichment level in plasma. (D-F) Monocyte enrichment curves from the same 1-week $^2H_2$-glucose-labeling experiment[8] were fitted with our model (black lines indicate best fits) to estimate plateau enrichment, defined by $f*c$. The enrichment at all time points was normalized to this maximum. From plasma enrichment and monocyte enrichment, the constant c (for $^2H_2$-glucose labeling a dilution factor that should be close to 0.65) was calculated, as indicated above panels D-F. The obtained values for c for each of the 3 individuals are shown above the graphs. (G) From the primary enrichment data, the average turnover rates of $CD4^+$ (left) and $CD8^+$ (right) T cells were re-estimated for 3 individuals (C2-C4) with normalization to the estimated plateau enrichment in monocytes (closed circles), and these turnover rates were compared to the original turnover rates that were estimated by normalization to plasma*0.65 (open squares). Error bars are 95% confidence intervals.

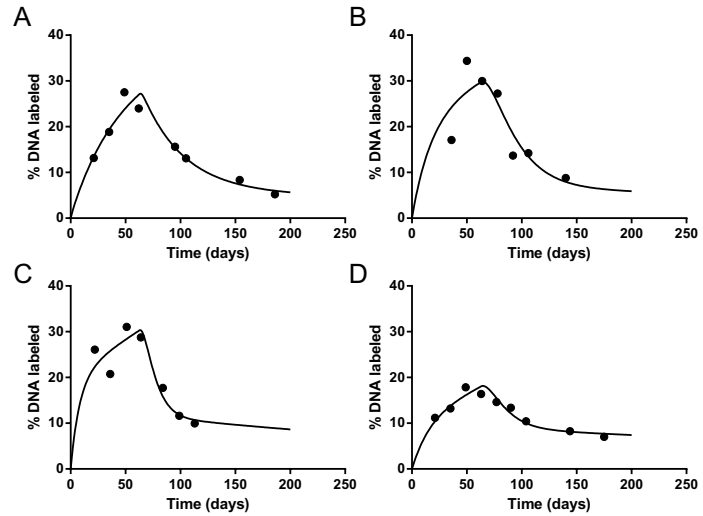

Supplementary Figure 2. Best fits of the multi-exponential model to enrichment in total $CD4^+$ T cells in a 9-week ^2H_2O-labeling study in untreated HIV-1 patients. Deuterium enrichment in the DNA of total $CD4^+$ T cells was calculated from the enrichments in naive and memory $CD4^+$ T cells and their relative sizes, as determined in 4 untreated HIV-1 patients (A-D) in a 9-week ^2H_2O-labeling study[26]. A multi-exponential model, describing two kinetically different sub-populations, was fitted to the data to estimate the average turnover rates. Label enrichment was scaled between 0 and 100% by normalizing for the percentage label obtained in granulocytes.

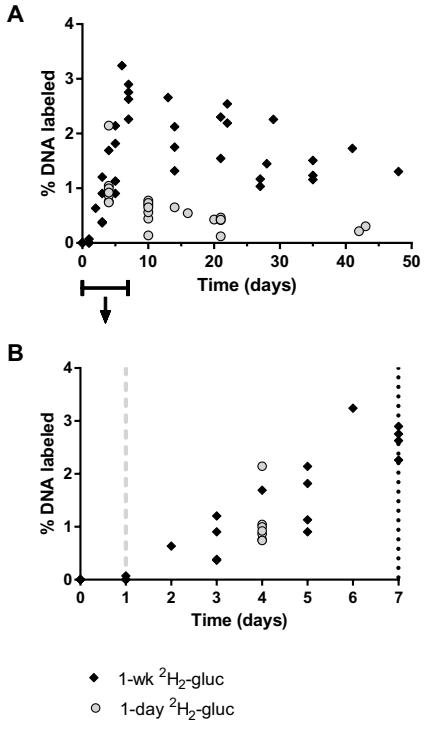

Supplementary Figure 3. Observed CD4⁺ T-cell enrichment in the 1-day and the 1-week $^2H_2$-glucose-labeling studies. The percentage of labeled DNA in CD4⁺ T cells as observed in the 1-week (closed diamonds) and 1-day (open circles) $^2H_2$-glucose labeling studies, (A) over the entire course of the experiment and (B) zoomed in at the first seven days. The end of the 1-day and the 1-week labeling period are marked by a dashed gray line and a dotted black line, respectively.

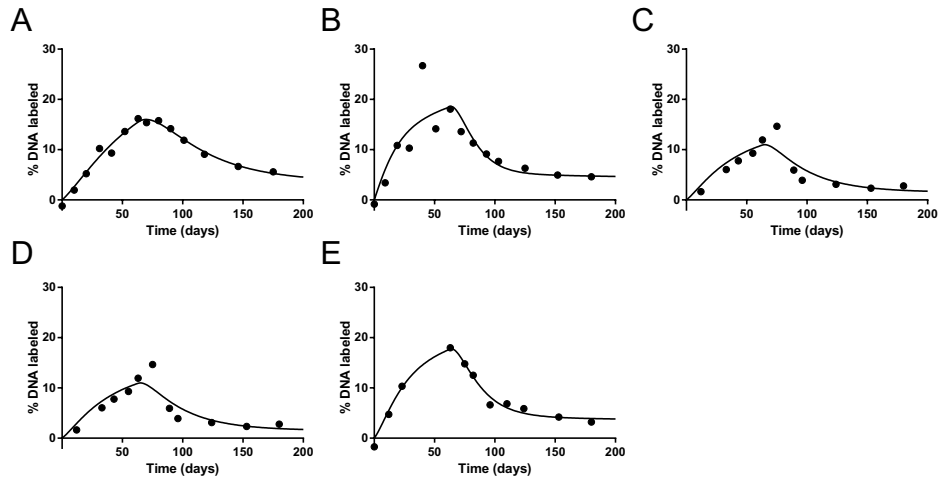

Supplementary Figure 4. Best fits of the multi-exponential model to enrichment in total B cells in a 9-week ^2H_2O-labeling study. Deuterium enrichment in the DNA of total CD19⁺ B cells was previously determined in 5 healthy young individuals (A-E) in a 9-week ^2H_2O-labeling study[11]. A multi-exponential model, describing two kinetically different sub-populations, was fitted to the data to estimate the average turnover rates. Label enrichment was scaled between 0 and 100% by normalizing for the percentage label obtained in granulocytes.

7

Lymphocyte Maintenance During Healthy Aging Requires No Substantial Alterations in Cell Dynamics

Liset Westera[1]*, Vera van Hoeven*, Julia Drylewicz[1,2], Gerrit Spierenburg[1], Jeroen F van Velzen[1], Rob J de Boer[2], Kiki Tesselaar[1#], José AM Borghans[1#]

[1] Laboratory of Translational Immunology, University Medical Center Utrecht, Utrecht, The Netherlands; [2] Theoretical Biology and Bioinformatics, Utrecht University, Utrecht, The Netherlands

*,# These authors contributed equally.

Submitted for publication

During healthy aging, T-cell and B-cell subsets are maintained at relatively stable numbers. It is generally thought that this is secured through increased lymphocyte proliferation or survival when lymphocyte numbers decline. Indeed, experiments in mice have shown that lymphopenia induces increased levels of peripheral T-cell division. Evidence for the existence and importance of such homeostatic mechanisms during healthy aging in humans is still lacking. Using in vivo $^{2}H_{2}O$ labeling, we here show that in humans there are no marked age-related differences in the pool sizes and turnover rates of most T-cell and B-cell subsets. In line with the detected tenfold decline in thymic output, naive T-cell numbers tended to be decreased in the elderly. Yet, we find no signs of homeostatic compensation during healthy aging.

Introduction

Advanced age is associated with greater susceptibility to infections, reduced vaccine efficacy, and a higher incidence of cancer and autoimmune disease[1, 2]. This is believed to be at least partly due to aging of the immune system. Immunological aging is a process characterized by several micro-environmental and cellular changes in the hematopoietic system that collectively affect both the production and functioning of the peripheral blood lineages. Particularly in the adaptive immune system profound age-associated changes have been reported for both the T-cell and B-cell pools.

In the human peripheral T-cell pool, immunological aging is reflected by a numerical decline of naive T cells and loss of T-cell receptor repertoire diversity, accompanied by an increase in the number and percentage of differentiated effector and memory T cells[2-7]. The general idea is that these changes are caused by a combination of life-long exposure to various pathogens and the gradual involution of the thymus, an irreversible process during which functional thymic tissue becomes progressively replaced by fat[8]. Thymic output is thought to decline considerably from adolescence to old age[8]. Several studies in rodents have suggested that the immune system has the intrinsic capacity to react to such changes by inducing a compensatory homeostatic response. Classical experiments that showed evidence for homeostasis-driven proliferation, also called lymphopenia-induced proliferation (LIP), involved transfer of T cells into lymphopenic hosts, resulting in robust T-cell expansion[9-13]. Such responses rely on the availability of, and hence cellular competition for, endogenous peptide/MHC complexes and cytokines, such as IL-7[14-18]. The occurrence of LIP in rodents has fueled the idea that compensatory mechanisms (e.g., increased T-cell division rates or cellular life spans) are also called into action during healthy aging, because thymic output declines[19].

Similar to αβ T cells, the number of circulating γδ T cells has been reported to decline with age, which is mainly due to a reduction in the most dominant Vδ2 subset[20, 21]. The composition of the γδ T-cell population is also skewed towards differentiated effector cells in the elderly[22]. In contrast to αβ T cells, the age-related decline of γδ T cells was found to be less dependent on thymic involution, as the absolute number of γδ T cells in thymectomized individuals was similar to that in age-matched controls[23].

Regarding the human peripheral B-cell pool, several studies have reported an age-related numerical decline of total B cells[24-27], unchanged or decreasing naive B-cell numbers[24, 25, 28-30], and decreasing absolute numbers of IgM^{+} natural effector B cells and IgM^{-} class-switched memory B cells[24, 25, 28-30]. To what extent these changes in B-cell numbers are related to lower bone marrow output or altered peripheral dynamics is unclear. A process of fatty degeneration similar to thymic involution was found to occur in the bone marrow environment of mice, with a suppressive influence of infiltrating adipocytes on hematopoiesis[31]. Other studies in mice reported a reduction in the

number of bone marrow progenitor B cells and a decline in bone marrow output with age[29, 32, 33], which was accompanied by an increase in the longevity of peripheral B cells[34]. In humans, there is no unambiguous evidence for declining bone marrow output with age, although an age-related reduction in B-cell progenitors has been reported by a few studies[35-37] and a pronounced loss of B-cell receptor repertoire diversity was observed in some elderly[38], which could reflect decreased bone marrow output.

Quantitative insights into leukocyte production and loss rates are scarce, but are crucial to understand how different leukocyte populations are maintained during healthy aging and why, for example, lymphocyte reconstitution occurs more slowly at older age[39]. We used in vivo labeling with deuterated water (^2H_2O) to quantify the average turnover rates of naive, memory, and natural effector B cells, naive and memory $CD4^+$ and $CD8^+$ T cells, and γδ T cells in healthy young and elderly individuals. By a combination of stable isotope labeling, TREC analysis, and mathematical modeling[40] we quantified to what extent thymic output declines during aging, and whether and how this decline is compensated for by peripheral homeostatic mechanisms. Our data show that the average turnover rates of almost all lymphocyte subsets remain fairly constant during aging. Only naive $CD8^+$ T cells had a significantly faster turnover in elderly individuals, which was related to a higher fraction of $CD95^+$ T cells in older individuals. Despite the observation that $CD4^+$ T-cell production by the thymus declines at least tenfold between the third and seventh decade of life, we find no signs of peripheral compensation for this loss of naive T-cell production.

Results

Individuals and follow-up

To quantify the dynamics of different leukocyte subsets in healthy aging, ten young individuals (five from Vrisekoop et al.[41]) and ten elderly individuals were enrolled in a heavy water (^2H_2O) labeling study (Table 1). During a 9-week labeling period, and a subsequent delabeling period of approximately 1 year, we frequently collected blood samples for measurement of deuterium enrichment in the DNA of granulocytes, B-cell subsets, total γδ T cells, and αβ T-cell subsets. The average turnover rate, i.e., the fraction of a cell population that is replaced by new cells per day, was estimated from the enrichment data using a multi-exponential model, which takes into account that populations can contain cells with different turnover rates[42-44]. The enrichment curves of all leukocyte subsets were normalized to the estimated maximum level of label incorporation in peripheral blood granulocytes, as this cell population is known to turn over rapidly. The dynamics of granulocytes were similar between young and elderly individuals (Sup. Fig. 1).

Table 1. Subject characteristics.

Age group	Subsets	Median age (range)	Gender
Young[41]	T cells	22 (20-25)	5 male
Young	B cells, γδ T cells	21 (20-24)	3 male, 2 female
Aged	T cells	68 (66-72)	5 male
Aged	B cells, γδ T cells	67 (66-75)	1 male, 4 female

Dynamics of naive, memory and natural effector B cells

To investigate whether aging is associated with alterations in peripheral B-cell dynamics we first determined the absolute number and distribution of the three main B-cell subsets present in the circulation, i.e., naive (IgM^+CD27^-), memory (IgM^-CD27^+), and natural effector (IgM^+CD27^+) B cells. For none of the subsets we found significant age-related differences in absolute B-cell counts, although the interindividual variation in naive B-cell numbers in the aged was relatively large (Fig. 1A, Table 2). As there are indications that B-cell production by the bone marrow declines with age[35-37], B-cell numbers may stay constant because of compensatory changes in peripheral B-cell dynamics. Fitting the multi-exponential model to the enrichment data of each individual (Sup. Fig. 2 and 3) revealed that the average turnover rates per day (*p*) of B cells in elderly individuals were not significantly different from those in young individuals (Fig. 2A, Table 2). The interindividual variation in memory B-cell turnover rates between young subjects was rather large; which was not related to the relative abundance of the different B-cell subsets in these individuals. In conclusion, variation in B-cell dynamics between individuals seemed to be related to factors other than aging.

Dynamics of γδ T cells and naive and memory $CD4^+$ and $CD8^+$ T cells

We compared absolute numbers of naive and memory $CD4^+$ and $CD8^+$ αβ T cells and γδ T cells in young and elderly individuals (Fig. 1B and C, Table 2). In agreement with previous studies[3, 5-7], naive T-cell numbers tended to be lower in elderly subjects; this difference was significant for $CD8^+$ (p-value=0.008; Fig. 1C) but not for $CD4^+$ (p-value=0.06) naive T cells. The number of memory $CD4^+$ T cells was significantly higher in elderly subjects (p-value=0.008), whereas the number of memory $CD8^+$ T cells was similar in young and aged individuals (Fig. 1D). The number of γδ T cells varied between individuals, and differences between the age groups were not significant (Fig. 1B). Within the γδ T-cell pool, the fraction of $V\delta2^+$ cells was similar in young and elderly subjects (median values were 40% for young, and 57% for elderly individuals).

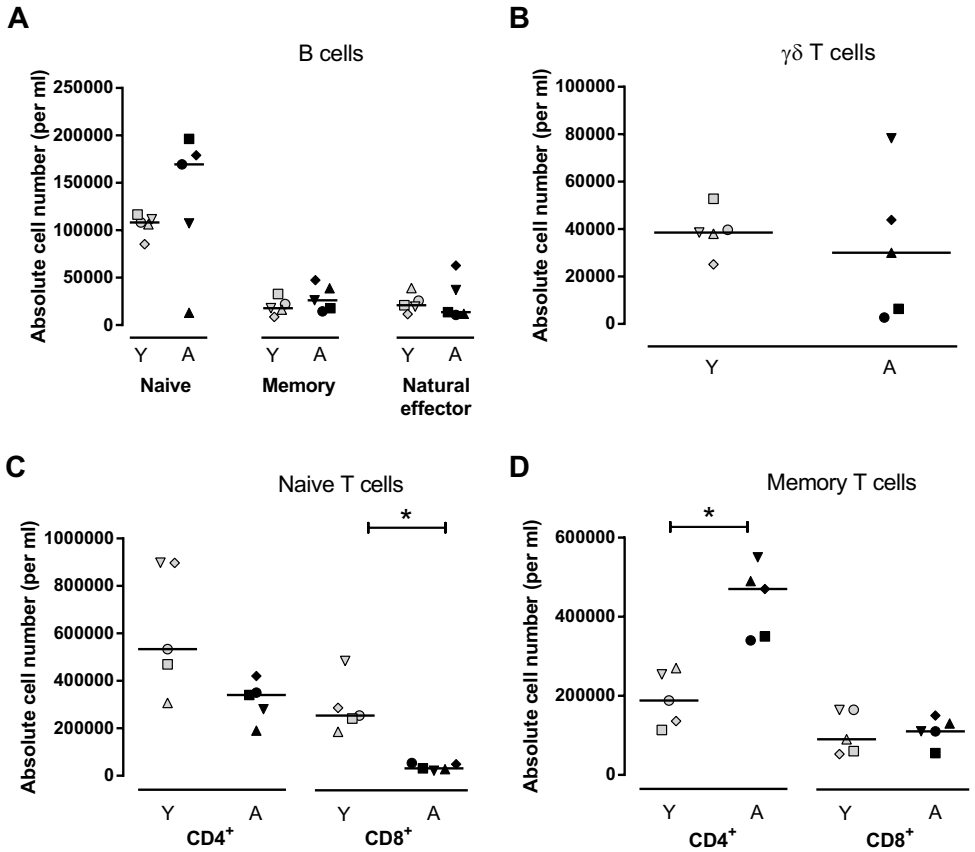

Figure 1. Absolute numbers of B cells and T cells in young and elderly individuals. Absolute numbers (per ml of blood) of (A) naive, memory, and natural effector B cells, (B) γδ T cells, (C) naive $CD4^+$ and $CD8^+$ T cells, and (D) memory $CD4^+$ and $CD8^+$ T cells, in young (gray symbols) and aged (black symbols) individuals. Horizontal lines represent median values. Asterisks mark the statistically significant difference (p-value<0.01) between young and aged individuals. Different symbols indicate different individuals within panels A+B and within panels C+D; note that different individuals were included for analysis of B-cell subsets and γδ T cells (A+B) and T-cell subsets (C+D).

As changes in the size of the T-cell subsets might be related to changes in their dynamics, we quantified their turnover rates. For γδ T cells, fitting the multi-exponential model to the deuterium-enrichment data (Sup. Fig. 2 and 3) yielded similar average turnover rates for young and aged individuals (Fig. 2B, Table 2). For memory T cells, the average turnover rates estimated from the enrichment data (Westera et al.[44] and Sup. Fig. 4) were also similar in young and elderly subjects (Fig. 2D, Table 2). Hence, the age-related increase in memory $CD4^+$ T-cell numbers was not associated with altered turnover rates.

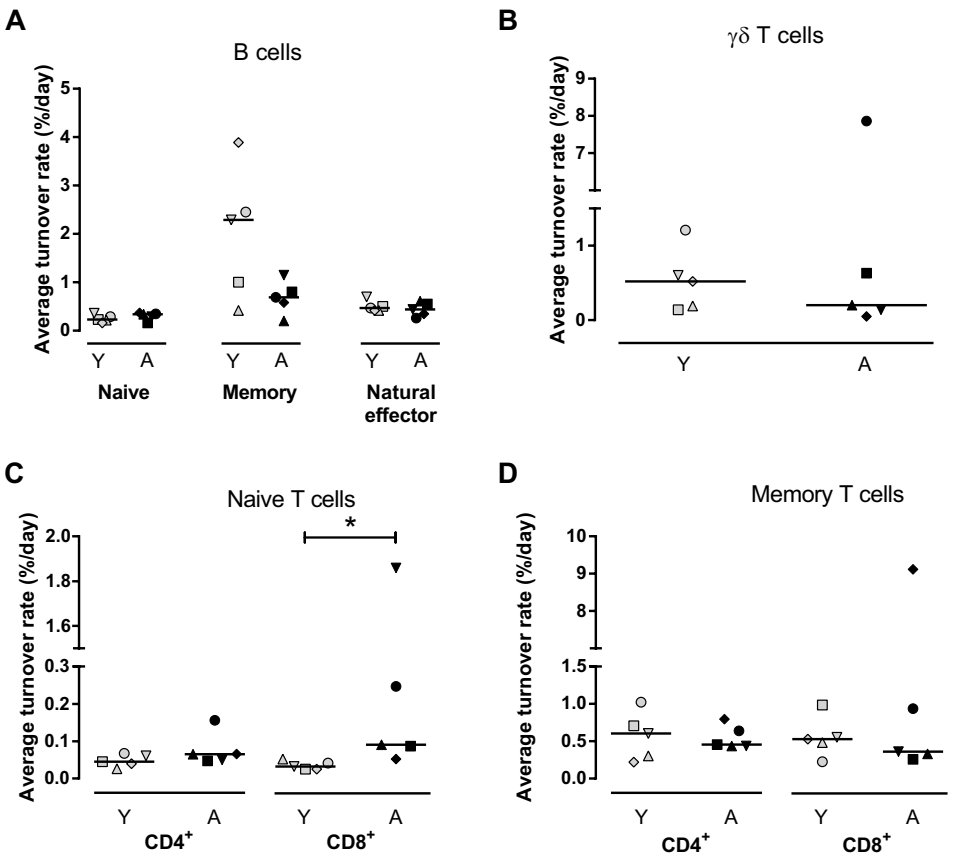

Figure 2. Summary of estimated average turnover rates in young and elderly individuals. Estimates of the average turnover rate of (A) naive, memory, and natural effector B cells, (B) γδ T cells, (C) naive $CD4^+$ and $CD8^+$ T cells, and (D) memory $CD4^+$ and $CD8^+$ T cells, in young (gray symbols) and aged (black symbols) individuals. All estimates were obtained by fitting the multi-exponential model to the individual data sets (see Materials and Methods). Horizontal lines represent median values. The asterisk marks the statistically significant difference (p-value<0.05) between young and aged individuals. Lymphocyte dynamics did not differ between males and females. Individual fits are shown in Sup. Fig. 1-3. Different symbols indicate different individuals within panels A+B and panels C+D.

Deuterium enrichment in naive T cells tended to be higher in elderly than in young individuals (Fig. 3A), especially in the case of naive $CD8^+$ T cells, suggesting a faster turnover for this subset in elderly individuals. Fitting the multi-exponential model to the enrichment data of each individual (Sup. Fig. 4) revealed that the average turnover rate of naive $CD4^+$ T cells was not significantly different between the age groups (median p_{young} = 0.04% and p_{aged} = 0.07% per day, p-value = 0.2), whereas the average turnover rate of naive $CD8^+$ T cells was significantly higher in elderly subjects (median p_{young} = 0.03% and p_{aged} = 0.09% per day, p-value = 0.02; Fig. 2C, Table 2).

Turnover-associated changes in the naive CD8⁺ T-cell pool in elderly subjects

To study whether the increased turnover of naive CD8⁺ T cells concurred with other alterations within this subset we analyzed the naive T-cell pools of the elderly subjects in more detail. Because samples of the young subjects who received ^2H_2O were no longer available, we also analyzed the composition of the naive CD8⁺ T-cell pool in healthy controls of different ages. In both young and elderly individuals, naive CD4⁺ and CD8⁺ T cells had a high expression of CCR7 and CD28 (median values for naive CD4⁺: 98% CCR7⁺ and 98% CD28⁺; for naive CD8⁺: 95% CCR7⁺ and 96% CD28⁺), confirming their naive phenotype. However, we found substantial age-related differences in the percentage of naive CD8⁺ T cells expressing CD95 (Fig. 3B). Whereas naive CD4⁺ T cells had a low expression of CD95 at any age (generally around 5% CD95⁺), the percentage of naive CD8⁺ T cells expressing CD95 increased over age, comprising between 18% and 36% in the elderly subjects (Fig. 3B), and appeared to be inversely correlated with the number of naive T cells (for CD4⁺: r=-0.37, p-value=0.01; for CD8⁺: r=-0.54, p-value<0.0001; Fig. 3C)**.** To investigate whether the relatively large CD95⁺ fraction of naive CD8⁺ T cells in elderly subjects could have contributed to the faster turnover rate of the aged naive CD8⁺ T-cell pool, we measured the expression of the cell-cycle marker Ki-67 in the CD95⁻ and CD95⁺ fractions of the naive CD4⁺ and CD8⁺ T-cell pools. Indeed, the percentage of Ki-67 expressing cells was significantly higher among CD95⁺ compared to CD95⁻ cells (p-value=0.03 for both CD4⁺ and CD8⁺) (Fig. 3D).

Lower thymic output without peripheral homeostatic compensation in the elderly

Because the thymus involutes with age[8], and deuterium is incorporated by new naive T cells that are produced in both the thymus and the periphery, the similar turnover rates of naive CD4⁺ T cells in our young and elderly individuals could be an indication for compensatory increases in peripheral T-cell division in the elderly. Therefore, we quantified the contribution of thymic T-cell production and peripheral T-cell division to the daily turnover of naive CD4⁺ T cells in young and elderly subjects. We previously demonstrated that daily thymic output can be deduced from the average turnover rate, the absolute cell number, and the TREC content of naive T cells[40]. Using this approach (Supplementary Information), we estimated that thymic output declined significantly from 16 million cells per day in young individuals to less than one million cells per day in elderly individuals (p-value=0.02; Fig. 4A), a change that is well in line

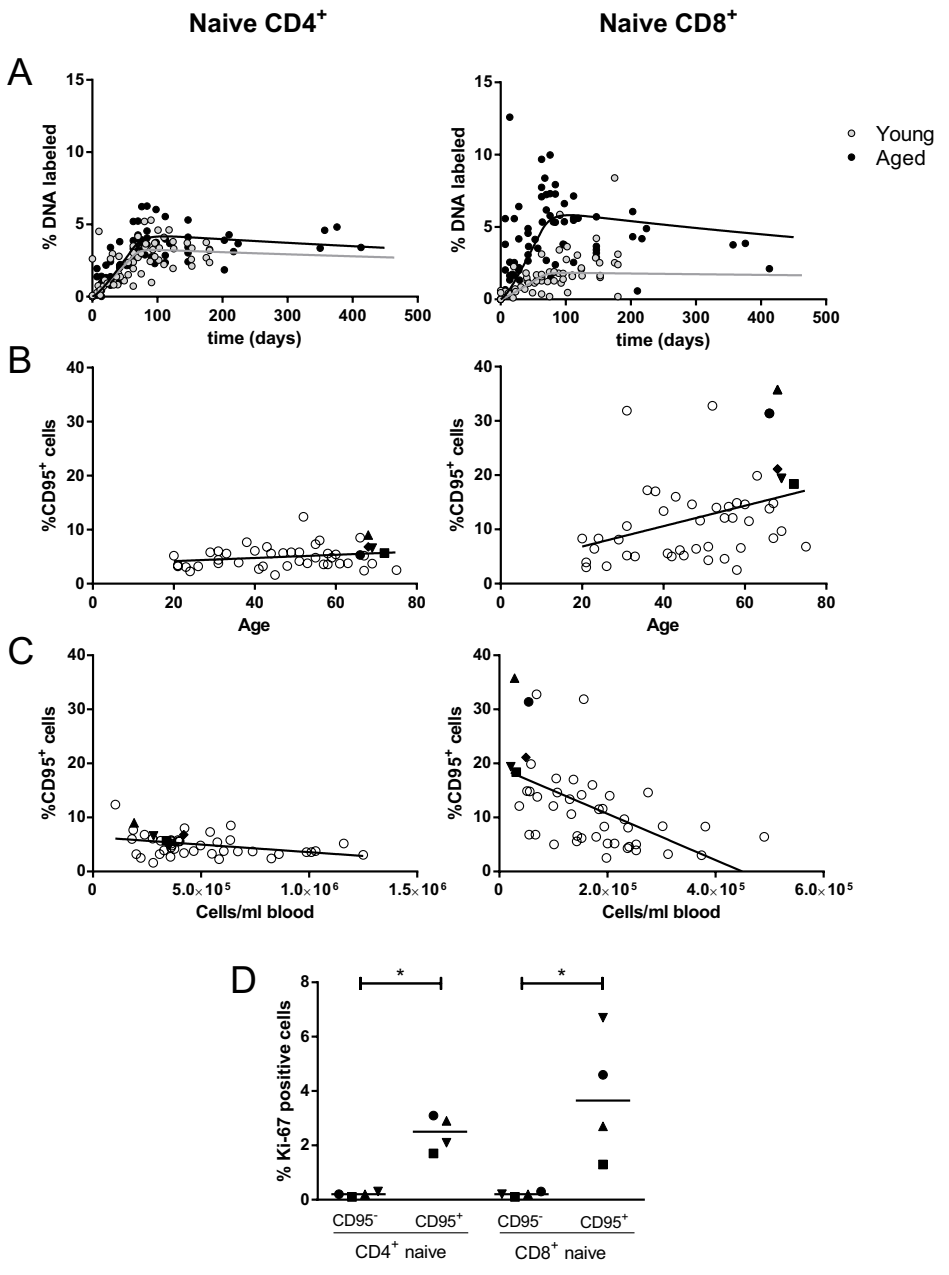

Figure 3. Analysis of CD95 expression within the naive T-cell pools. (A) Best fits of the mixed effect multi-exponential model (see Materials and Methods) to ^2H enrichment in the DNA of naive CD4⁺ and CD8⁺ T cells from young [41] (gray symbols and curve) and elderly individuals (black symbols and curve). Label enrichment was scaled between 0 and 100% by normalizing for the maximum enrichment in granulocytes (see Material and Methods). (B,C) The expression of CD95 on naive CD4⁺ (left) and CD8⁺ (right) T cells was determined in elderly males (black symbols) of the ^2H_2O labeling study and in other healthy donors of varying ages (open symbols, n=41). The percentage of CD95⁺ naive T cells was plotted against age (B) and against the number of naive CD4⁺ or CD8⁺ T cells per ml blood (C). The lines in panels C and D represent linear regression analyses. (D) Ki-67 expression was measured within the CD95⁻ and CD95⁺ fractions of naive CD4⁺ and CD8⁺ T cells in elderly males (n=4). The median is represented by a horizontal line. Different symbols indicate different individuals. Asterisks mark significant differences (p-value<0.05).

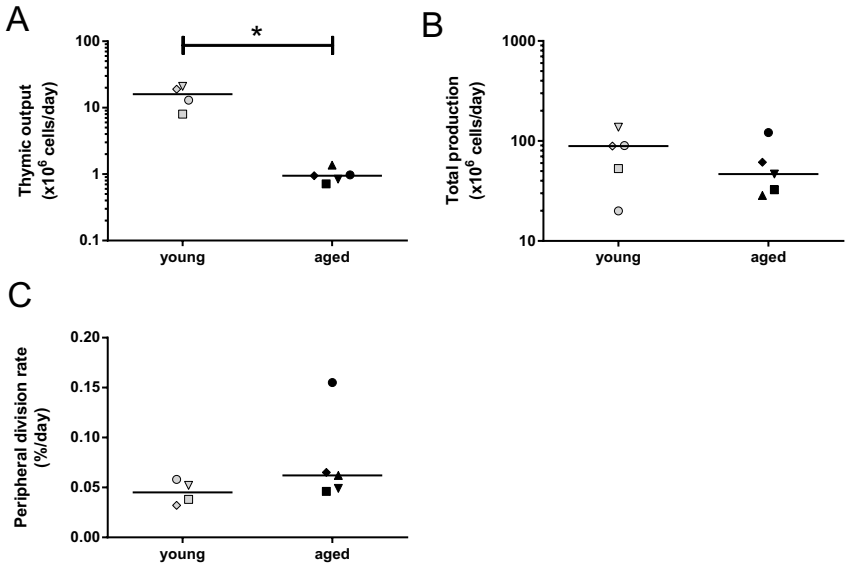

Fi… D4⁺ T-cell production. (A) Total production of naive CD4⁺ T cells per day in young [41] and aged individuals, calculated as (the average turnover rate p) x (the absolute number of naive CD4⁺ T cells per liter blood) x (5 liter blood) x 50, assuming that 2% of lymphocytes reside in the blood [57]. (B) Estimated daily thymic output (cells/day) in young [40] and aged individuals, calculated by multiplying the total daily naive CD4⁺ T-cell production by the normalized naive CD4⁺ T-cell TREC content, as described previously [40]. The asterisk marks a statistically significant (p-value<0.05) difference in daily thymic output between young and aged individuals. (C) Estimated daily peripheral division rate per cell, calculated by dividing the estimated total peripheral T-cell division (in Sup. Fig. 4B) by the total number of naive CD4⁺ T cells present in the periphery. The normalized TREC content of naive CD4⁺ T cells in young individuals was previously reported in [40]; as no TREC measurements were obtained for individual C, this individual was not included in the analysis. TREC contents are shown in Sup. Fig. 4A. Different symbols indicate different individuals.

with the previously estimated 10-fold decrease in thymic output during adulthood[8]. By subtracting this estimated daily thymic output from the total daily production of naive CD4⁺ T cells (Fig. 4A), we deduced the average naive CD4⁺ peripheral T-cell division rate in young and elderly subjects (Supplementary Information). Remarkably, despite the tenfold decrease in thymic output, peripheral naive CD4⁺ T-cell division rates were not significantly higher in the elderly (Fig. 4C), suggesting that peripheral homeostatic compensation for loss of thymic output did either not occur or was negligible.

Discussion

In the present work, using long-term in vivo ^2H_2O labeling in young and elderly individuals for a variety of B-cell and T-cell subsets, we found no major age-related differences in population dynamics or signs of compensatory mechanisms for

Table 2. Median (range) of average turnover rates, cell numbers, and total daily production of the different lymphocytes.

	Average turnover rate (%/day) median (range)		Cell number (per µl blood) median (range)		Total production (x10⁶ cells/day) median (range)	
	Young	*Aged*	*Young*	*Aged*	*Young*	*Aged*
Naive B cells	0.23 (0.16-0.36)	0.34 (0.16-0.37)	108 (85-117)	170 (13-196)	67 (33-101)	78 (11-167)
Mem B cells	2.29 (0.42-3.89)	0.69 (0.20-1.15)	18 (9-33)	26 (14-47)	85 (17-136)	36 (19-75)
Nat Eff B cells	0.47 (0.42-0.70)	0.44 (0.26-0.61)	21 (12-39)	14 (11-63)	31 (12-41)	19 (7-54)
γδ T cells	0.52 (0.14-1.21)	0.20 (0.05-7.86)	38 (25-53)	30 (3-78)	33 (18-120)	15 (5-53)
Naive CD4⁺ T cells	0.04 (0.03-0.07)	0.07 (0.05-0.16)	534 (307-898)	337 (192-417)	89 (20-137)	40 (31-138)
Naive CD8⁺ T cells	0.03 (0.03-0.05)	0.09 (0.05-1.86)	254 (185-484)	31 (21-54)	24 (15-39)	7 (6-98)
Mem CD4⁺ T cells	0.60 (0.22-1.02)	0.45 (0.44-0.80)	403 (221-448)	470 (339-546)	391 (221-911)	542 (393-936)
Mem CD8⁺ T cells	0.53 (0.23-0.98)	0.36 (0.26-9.12)	90 (53-165)	113 (55-153)	109 (70-227)	107 (35-3497)

population maintenance. Our data are consistent with a previous deuterated-glucose labeling study which reported no significant age-related difference in the turnover of total B cells[45], and extend these insights by showing that also within the different B-cell subsets as well as for γδ T cells, turnover rates do not change during healthy aging.

It is still debated whether in humans bone marrow output decreases with age[29, 36, 46, 47], but the exponential decline in de novo T-cell production by the thymus during aging is undisputed. The action of homeostatic mechanisms - if at all present

during healthy aging - would therefore be expected to be most evident in the aging naive T-cell pools. We indeed found an increased turnover rate of naive CD8$^+$ T cells in the aged, which was accompanied by the relative abundance of cycling CD95$^+$ T cells. As expression of CD95 has been shown to be upregulated in response to IL-7 in vitro[48], and IL-7 is known to play a key role in regulating proliferative responses in vivo[49], these CD95$^+$ cells could in theory reflect homeostatically dividing naive CD8$^+$ T cells. However, this idea is not supported by the observation that almost all CD95$^+$ cells expressed the IL-7R (> 90% CD127$^+$), which is typically downregulated upon IL-7 binding. Phenotype analyses suggested that the CD95$^+$ fraction contained both transitional memory T cells (31-50%, CCR7$^-$CD27$^+$)[50] and memory stem cells (50-69%, CCR7$^+$CD27$^+$)[51], two subsets that have a stronger proliferative capacity than truly naive T cells[50, 51].

Deuterium-labeling data of the naive CD4$^+$ T-cell pool gave more straightforward insights into the role of homeostatic compensation during healthy aging, as this population did not contain high levels of CD95$^+$ T cells at any age. In line with a previous deuterated-glucose labeling study[52] we found that the average turnover rate of naive CD4$^+$ T cells did not change during healthy aging. Thanks to the combination of deuterium-labeling data and TREC analyses we were able to dissect the contribution of thymic output and peripheral T-cell division to naive T-cell production during healthy aging. We found that thymic output declined from 16 million cells per day in young adults to less than one million cells per day in elderly individuals, in line with the previously estimated 10-fold decrease in thymic output based on histological studies[8]. Previously, Bains et al[53] also combined different techniques to estimate daily thymic output in young adults, by analyzing TREC contents and Ki-67 expression data. Remarkably, with roughly 350 million newly produced naive CD4$^+$ T cells per day, their estimate of thymic output was an order of magnitude higher than our estimated 16 million cells per day. Recent work suggests that Bains et al. have overestimated the fraction of dividing cells by measurement of Ki-67 expression, which appears to remain elevated for days after completion of cell division[54, 55] and have thereby indirectly overestimated daily thymic output. Despite this significant decline in thymic output that we observed during healthy aging, peripheral naive CD4$^+$ T-cell division rates were not increased. Loss of thymic output was also not compensated for by increased cell survival, as this should have been reflected by reduced naive T-cell turnover rates. Hence, our data show no signs of homeostatic compensation for reduced thymic output in the naive CD4$^+$ T-cell pool during healthy aging. The most likely explanation for our findings is that thymic output contributes so little to the total production of naive T cells even in young adults (Sup. Fig. 5C) that a compensatory response for the further decline in thymic output with age is simply not required or too small to be measured. Based on these data, we cannot exclude, however, that homeostatic mechanisms may become active in humans under more extreme lymphopenic circumstances.

The idea that homeostatic mechanisms are activated when cell numbers decline indeed originates from more extreme situations, e.g., involving T-cell transfer to lymphopenic rodents that resulted in massive proliferation of the injected cells[9-13]. Lymphopenia-induced proliferation was observed not only in the artificially empty pool of transgenic or otherwise manipulated mice, but was also shown to be induced in the more physiological lymphopenic environment of neonatal mice[56]. In the rhesus macaque model of immune senescence, levels of naive T-cell division (as measured by Ki-67 expression) were found to correlate positively with age and negatively with the percentage of naive cells in the CD4$^+$ and CD8$^+$ T-cell pools and TCR diversity[57]. Naive T-cell turnover rates increased exponentially when the percentage of naive T cells in the CD8$^+$ T-cell pool dropped below 4%[57], supporting the idea that a certain pool size threshold may exist below which compensatory mechanisms get activated.

Some previous studies have suggested that homeostatic compensation occurs in humans at very high age. A direct association was observed between decreased naive T-cell numbers and increased frequencies of Ki-67$^+$ naive T cells in healthy elderly individuals aged 76 and older[19]. Naylor et al. also reported an increase in CD4$^+$ T-cell division rates after the age of 70, but in line with our findings, before that age the frequency of Ki67$^+$ CD4$^+$ T cells remained remarkably constant[58]. Yet even among the oldest subjects, the percentages of Ki-67$^+$ T cells showed considerable overlap with those in younger subjects[19, 58]. Our data suggest that the increased T-cell turnover rates that have been observed at very old age are not due to a further decline in thymic output, since the contribution of thymic output to the maintenance of the naive T-cell pool is already very small in young adults. It is more likely that other factors related to immune status underlie the correlation between T-cell counts and proliferation rates at very high age. Because Ki-67 can be expressed by both homeostatically dividing cells and naive T cells that proliferate to become memory cells, the increased Ki-67 levels observed in some elderly might alternatively reflect increased immune activation, for example due to persistent infection with CMV which has a high prevalence in the elderly[59]. In this respect it is interesting to mention that 4 out of 5 of the elderly individuals included in our study were CMV negative. Although this may not be representative for the average human population, it provided us with the unique opportunity to study whether homeostatic mechanisms occur in human healthy aging in the absence of CMV as a possible confounder.

In summary, we have provided reliable estimates of the average turnover rates of various B-cell and T-cell subsets in healthy young and elderly individuals, and found no signs of homeostatic compensation during healthy aging, e.g., for reduced thymic output. Our insights will aid the interpretation of past, current, and future investigations in a variety of interventions and diseases, which may reveal whether in these situations compensatory mechanisms are evident in humans.

Acknowledgments

We thank Anouk B.C. Schuren for measuring TREC contents, Sigrid A. Otto for measuring CMV serology, the research nurses of the Julius Center Trial Unit for taking care of study participants, and Frank Miedema for critical reading of the manuscript. This research was supported by the Landsteiner Foundation for Blood Transfusion Research (LSBR grant 0812), the Netherlands Organization for Scientific Research (NWO, grant 917.96.350 and 836.07.002), and the VIRGO consortium (NGI, BB.000342.1).

Materials and methods

Subjects and in vivo ^2H_2O labeling. Five young and ten elderly healthy volunteers (Table 1) were enrolled in the study after having provided written informed consent. On day 1, volunteers received an oral ramp-up dose of 7.5ml of ^2H_2O (99.8% enriched, Cambridge Isotope Laboratories) per kg body water, in small portions throughout the day. Body water was estimated to be 60% (males) and 50% (females) of body weight. Blood was drawn before the first portion and urine was collected after the last portion. As maintenance dose, volunteers drank 1.25ml/kg body water at home daily for the duration of the labeling period (9 wk; for logistic reasons the labeling period was ~7.5 wk and ~10 wk for two subjects). Urine was collected an additional 15 times during the first ~100 days of the study. Blood was drawn 6 more times during labeling and 8 times during delabeling, with the last withdrawal ~1y after stop of ^2H_2O administration. All volunteers were healthy and did not take drugs (a questionnaire was taken to confirm that subjects were healthy and did not have serious illnesses (e.g., malaria; cancer) in the past; serological testing was performed to exclude infection with HIV, HBV, and HCV). Additional blood samples used to obtain reference values for the T-cell compartment were drawn from healthy volunteers not following the labeling protocol after having provided written informed consent. This study was approved by the medical ethical committee of the University Medical Center Utrecht and conducted in accordance with the Helsinki Declaration of 1975, revised in 2008.

Cell isolation, flow cytometry and sorting. Peripheral blood mononuclear cells (PBMC) were obtained by Ficoll-Paque (GE Healthcare) density gradient centrifugation from heparinized blood. Granulocytes were obtained by erythrocyte lysis of the granulocyte/erythrocyte layer. Total PBMC were frozen as a sample with baseline enrichment on the first study-day (t=0). Absolute cell numbers were determined using TruCOUNT tubes (BD), in which whole blood was stained using CD45-PerCP, CD3-FITC (BioLegend), CD8-V500 (BD), CD4-APC-eF780, and CD19-eFluor450 (eBioscience). After erythrocyte lysis with FACS Lysing Solution (BD) tubes were instantly analyzed. CD95 expression on $CD27^+CD45RO^-$ naive T cells was measured using CD3-eFluor450, CD27-APCeFluor780 (eBioscience), CD8-PerCP (BioLegend), CCR7-APC (R&D systems), CD45RO-PE-Cy7, CD95-APC, and CD28-FITC (BD). To analyze the expression of cell-cycle marker Ki-67,cells were stained with extracellular markers (CD3-eFluor450, CD4-APCeFluor780 (eBioscience), CD8-PerCP, CD27-PE (BioLegend), CD45RO-PE-Cy7, CD95-APC (BD)), fixed and permeabilized (Cytofix/Cytoperm, BD), and stained intracellularly with Ki-67-FITC (DAKO). Washing steps were done using Perm/Wash buffer (BD). Absolute numbers of cell subsets (e.g. $CD95^+$ naive) were calculated using the absolute number of $CD4^+$, $CD8^+$ T cells or $CD19^+$ B cells from TruCount analysis. All cells were analyzed on an LSR-II flow cytometer using FACSdiva software (BD). For sorting of T-cell subsets, cells were incubated with CD3-FITC, CD4-Pacific Blue, CD8-PerCP-Cy5.5, CD45RO-PE (BioLegend), and CD27-APC (eBioscience). For sorting of B-cell subsets and γδ T cells, cells were incubated with CD3-eFluor450, CD27-APC (eBioscience), CD19-PerCP (BioLegend), F(ab')2 IgM-FITC (Southern Biotech), and TCR-pan-γδ-PE (Beckman Coulter). Naive ($CD27^+CD45RO^-$) and memory ($CD45RO^+$) $CD4^+$ and $CD8^+$ T cells, or naive (IgM^+CD27^-), memory (IgM^-CD27^+), and natural effector (IgM^+CD27^+) $CD19^+$ B cells and $pan\gamma\delta^+$ T cells were sorted on a FACSAria II cell sorter (BD). Flow cytometric analysis and sorting were always done on freshly isolated cells.

DNA isolation. Genomic DNA was isolated from granulocytes, total PBMC (t=0) and sorted cells using the Blood QuickPure kit (Macherey-Nagel) or the Reliaprep Blood gDNA Miniprep System (Promega), and stored at -20°C before processing for gas chromatography/mass spectrometry (GC/MS).

TREC analysis. In sorted naive $CD4^+$ T-cell samples of elderly individuals, signal joint TREC numbers and DNA input were quantified with a ViiA™ 7 Real-Time PCR System (Applied Biosystems) and calculated as described previously[60].

Measurement of deuterium enrichment in body water and DNA. Deuterium enrichment in DNA from granulocytes and sorted T-cell fractions was measured according to the method described by Busch et al. with minor modifications[61]. Briefly, DNA was enzymatically hydrolyzed into deoxyribonucleotides and derivatized to penta-fluoro-triacetate (PFTA) before injection (DB-17MS column, Agilent Technologies) into the gas chromatograph (7890A GC System, Agilent Technologies). PFTA was analyzed by negative chemical ionization mass spectrometry (5975C inert XL EI/CI MSD with Triple-Axis Detector, Agilent Technologies) measuring ions m/z 435 and m/z 436. Deuterium enrichment in urine was analyzed on the same GC/MS system (using a PoraPLOT Q 25x0.32 column, Varian) by electron impact ionization as previously described[62]. For quantification of ^2H enrichment standards of known enrichment were used. To correct for abundance sensitivity of isotope ratios, we followed the approach proposed by Patterson et al.[63] on log10-transformed enrichment data.

Statistical analyses. Medians were compared between age groups using Mann-Whitney tests (GraphPad Software, Inc). Differences with a p-value<0.05 were considered significant. Correlations were analyzed using Pearson's correlation coefficient. Deuterium-enrichment data were fitted with R (functions nlme and nlm)[64]. The 95% confidence intervals were determined using a bootstrap method where the residuals to the optimal fit were resampled 500 times.

References

1. Goronzy, J.J. & Weyand, C.M. Understanding immunosenescence to improve responses to vaccines. Nat. Immunol. 14, 428-436 (2013).
2. Montecino-Rodriguez, E., Berent-Maoz, B., & Dorshkind, K. Causes, consequences, and reversal of immune system aging. J. Clin. Invest 123, 958-965 (2013).
3. Fagnoni, F.F. et al. Shortage of circulating naive CD8(+) T cells provides new insights on immunodeficiency in aging. Blood 95, 2860-2868 (2000).
4. Goronzy, J.J., Lee, W.W., & Weyand, C.M. Aging and T-cell diversity. Exp. Gerontol. 42, 400-406 (2007).
5. Lazuardi, L. et al. Age-related loss of naive T cells and dysregulation of T-cell/B-cell interactions in human lymph nodes. Immunology 114, 37-43 (2005).
6. Provinciali, M., Moresi, R., Donnini, A., & Lisa, R.M. Reference values for CD4+ and CD8+ T lymphocytes with naive or memory phenotype and their association with mortality in the elderly. Gerontology 55, 314-321 (2009).
7. Saule, P. et al. Accumulation of memory T cells from childhood to old age: central and effector memory cells in CD4(+) versus effector memory and terminally differentiated memory cells in CD8(+) compartment. Mech. Ageing Dev. 127, 274-281 (2006).
8. Steinmann, G.G., Klaus, B., & Muller-Hermelink, H.K. The involution of the ageing human thymic epithelium is independent of puberty. A morphometric study. Scand. J. Immunol. 22, 563-575 (1985).
9. Bell, E.B., Sparshott, S.M., Drayson, M.T., & Ford, W.L. The stable and permanent expansion of functional T lymphocytes in athymic nude rats after a single injection of mature T cells. J. Immunol. 139, 1379-1384 (1987).
10. Freitas, A.A., Agenes, F., & Coutinho, G.C. Cellular competition modulates survival and selection of CD8+ T cells. Eur. J. Immunol. 26, 2640-2649 (1996).
11. Freitas, A.A. & Rocha, B. Population biology of lymphocytes: the flight for survival. Annu. Rev. Immunol. 18, 83-111 (2000).
12. Miller, R.A. Age-associated decline in precursor frequency for different T cell-mediated reactions, with preservation of helper or cytotoxic effect per precursor cell. J. Immunol. 132, 63-68 (1984).
13. Rocha, B., Dautigny, N., & Pereira, P. Peripheral T lymphocytes: expansion potential and homeostatic regulation of pool sizes and CD4/CD8 ratios in vivo. Eur. J. Immunol. 19, 905-911 (1989).
14. Clarke, S.R. & Rudensky, A.Y. Survival and homeostatic proliferation of naive peripheral CD4+ T cells in the absence of self peptide:MHC complexes. J. Immunol. 165, 2458-2464 (2000).
15. Fry, T.J. & Mackall, C.L. Interleukin-7: master regulator of peripheral T-cell homeostasis? Trends Immunol. 22, 564-571 (2001).
16. Ge, Q., Rao, V.P., Cho, B.K., Eisen, H.N., & Chen, J. Dependence of lymphopenia-induced T cell proliferation on the abundance of peptide/ MHC epitopes and strength of their interaction with T cell receptors. Proc. Natl. Acad. Sci. U. S. A 98, 1728-1733 (2001).
17. Goldrath, A.W. & Bevan, M.J. Low-affinity ligands for the TCR drive proliferation of mature CD8+ T cells in lymphopenic hosts. Immunity. 11, 183-190 (1999).
18. Goldrath, A.W. & Bevan, M.J. Selecting and maintaining a diverse T-cell repertoire. Nature 402, 255-262 (1999).
19. Sauce, D. et al. Lymphopenia-driven homeostatic regulation of naive T cells in elderly and thymectomized young adults. J. Immunol. 189, 5541-5548 (2012).
20. Argentati, K. et al. Numerical and functional alterations of circulating gammadelta T lymphocytes in aged people and centenarians. J. Leukoc. Biol. 72, 65-71 (2002).
21. Michishita, Y. et al. Age-associated alteration of gammadelta T-cell repertoire and different profiles of activation-induced death of Vdelta1 and Vdelta2 T cells. Int. J. Hematol. 94, 230-240 (2011).
22. Re, F. et al. Skewed representation of functionally distinct populations of Vgamma9Vdelta2 T lymphocytes in aging. Exp. Gerontol. 40, 59-66 (2005).
23. Roux, A. et al. Differential impact of age and cytomegalovirus infection on the gammadelta T cell compartment. J. Immunol. 191, 1300-1306 (2013).
24. Chong, Y. et al. CD27(+) (memory) B cell decrease and apoptosis-resistant CD27(-) (naive) B cell increase in aged humans: implications for age-related peripheral B cell developmental disturbances. Int. Immunol. 17, 383-390 (2005).
25. Frasca, D., Diaz, A., Romero, M., Landin, A.M., & Blomberg, B.B. Age effects on B cells and humoral immunity in humans. Ageing Res. Rev. 10, 330-335 (2011).
26. Paganelli, R. et al. Changes in circulating B cells and immunoglobulin classes and subclasses in a healthy aged population. Clin. Exp. Immunol. 90, 351-354 (1992).
27. Wikby, A., Johansson, B., Ferguson, F., & Olsson, J. Age-related changes in immune parameters in a very old population of Swedish people: a longitudinal study. Exp. Gerontol. 29, 531-541 (1994).
28. Frasca, D. & Blomberg, B.B. Aging affects human B cell responses. J. Clin. Immunol. 31, 430-435 (2011).
29. Scholz, J.L., Diaz, A., Riley, R.L., Cancro, M.P., & Frasca, D. A comparative review of aging and B cell function in mice and humans. Curr. Opin. Immunol. 25, 504-510 (2013).
30. Shi, Y. et al. Regulation of aged humoral immune defense against pneumococcal bacteria by IgM memory B cell. J. Immunol. 175, 3262-3267 (2005).
31. Naveiras, O. et al. Bone-marrow adipocytes as negative regulators of the haematopoietic microenvironment. Nature 460, 259-263 (2009).
32. Miller, J.P. & Allman, D. The decline in B lymphopoiesis in aged mice reflects loss of very early B-lineage precursors. J. Immunol. 171, 2326-2330 (2003).
33. Shahaf, G., Johnson, K., & Mehr, R. B cell development in aging mice: lessons from mathematical modeling. Int. Immunol. 18, 31-39 (2006).
34. Kline, G.H., Hayden, T.A., & Klinman, N.R. B cell maintenance in aged mice reflects both increased B cell longevity and decreased B cell generation. J. Immunol. 162, 3342-3349 (1999).
35. Kuranda, K. et al. Age-related changes in human hematopoietic stem/progenitor cells. Aging Cell 10, 542-546 (2011).
36. McKenna, R.W., Washington, L.T., Aquino, D.B., Picker, L.J., & Kroft, S.H. Immunophenotypic analysis of hematogones (B-lymphocyte precursors) in 662 consecutive bone marrow specimens by 4-color flow cytometry. Blood 98, 2498-2507 (2001).
37. Ogawa, T., Kitagawa, M., & Hirokawa, K. Age-related changes of human bone marrow: a histometric estimation of proliferative cells, apoptotic cells, T cells, B cells and macrophages. Mech. Ageing Dev. 117, 57-68 (2000).
38. Dunn-Walters, D.K. & Ademokun, A.A. B cell repertoire and ageing. Curr. Opin. Immunol. 22, 514-520 (2010).
39. Savage, W.J. et al. Lymphocyte reconstitution following non-myeloablative hematopoietic

stem cell transplantation follows two patterns depending on age and donor/recipient chimerism. Bone Marrow Transplant. 28, 463-471 (2001).

40. den Braber, I. et al. Maintenance of peripheral naive T cells is sustained by thymus output in mice but not humans. Immunity. 36, 288-297 (2012).
41. Vrisekoop, N. et al. Sparse production but preferential incorporation of recently produced naive T cells in the human peripheral pool. Proc. Natl. Acad. Sci. U. S. A 105, 6115-6120 (2008).
42. de Boer, R.J., Perelson, A.S., & Ribeiro, R.M. Modelling deuterium labelling of lymphocytes with temporal and/or kinetic heterogeneity. J. R. Soc. Interface 9, 2191-2200 (2012).
43. Ganusov, V.V., Borghans, J.A., & de Boer, R.J. Explicit kinetic heterogeneity: mathematical models for interpretation of deuterium labeling of heterogeneous cell populations. PLoS. Comput. Biol. 6, e1000666 (2010).
44. Westera, L. et al. Closing the gap between T-cell life span estimates from stable isotope-labeling studies in mice and humans. Blood 122, 2205-2212 (2013).
45. Macallan, D.C. et al. B-cell kinetics in humans: rapid turnover of peripheral blood memory cells. Blood 105, 3633-3640 (2005).
46. Nunez, C. et al. B cells are generated throughout life in humans. J. Immunol. 156, 866-872 (1996).
47. Rossi, M.I. et al. B lymphopoiesis is active throughout human life, but there are developmental age-related changes. Blood 101, 576-584 (2003).
48. Cimbro, R. et al. IL-7 induces expression and activation of integrin alpha4beta7 promoting naive T-cell homing to the intestinal mucosa. Blood 120, 2610-2619 (2012).
49. Takada, K. & Jameson, S.C. Naive T cell homeostasis: from awareness of space to a sense of place. Nat. Rev. Immunol. 9, 823-832 (2009).
50. Chomont, N. et al. HIV reservoir size and persistence are driven by T cell survival and homeostatic proliferation. Nat. Med. 15, 893-900 (2009).
51. Gattinoni, L. et al. A human memory T cell subset with stem cell-like properties. Nat. Med. 17, 1290-1297 (2011).
52. Wallace, D.L. et al. Direct measurement of T cell subset kinetics in vivo in elderly men and women. J. Immunol. 173, 1787-1794 (2004).
53. Bains, I., Thiebaut, R., Yates, A.J., & Callard, R. Quantifying thymic export: combining models of naive T cell proliferation and TCR excision circle dynamics gives an explicit measure of thymic output. J. Immunol. 183, 4329-4336 (2009).
54. Hogan, T. et al. Clonally diverse T cell homeostasis is maintained by a common program of cell-cycle control. J. Immunol. 190, 3985-3993 (2013).
55. de Boer, R.J. & Perelson, A.S. Quantifying T lymphocyte turnover. J. Theor. Biol. 327, 45-87 (2013).
56. Min, B. et al. Neonates support lymphopenia-induced proliferation. Immunity. 18, 131-140 (2003).
57. Cicin-Sain, L. et al. Dramatic increase in naive T cell turnover is linked to loss of naive T cells from old primates. Proc. Natl. Acad. Sci. U. S. A 104, 19960-19965 (2007).
58. Naylor, K. et al. The influence of age on T cell generation and TCR diversity. J. Immunol. 174, 7446-7452 (2005).
59. Wikby, A. et al. Expansions of peripheral blood CD8 T-lymphocyte subpopulations and an association with cytomegalovirus seropositivity in the elderly: the Swedish NONA immune study. Exp. Gerontol. 37, 445-453 (2002).
60. Hazenberg, M.D. et al. Increased cell division but not thymic dysfunction rapidly affects the T-cell receptor excision circle content of the naive T cell population in HIV-1 infection. Nat. Med. 6, 1036-1042 (2000).
61. Busch, R., Neese, R.A., Awada, M., Hayes, G.M., & Hellerstein, M.K. Measurement of cell proliferation by heavy water labeling. Nat. Protoc. 2, 3045-3057 (2007).
62. Westera, L., Zhang, Y., Tesselaar, K., Borghans, J.A., & Macallan, D.C. Quantitating lymphocyte homeostasis in vivo in humans using stable isotope tracers. Methods Mol. Biol. 979, 107-131 (2013).
63. Patterson, B.W., Zhao, G., & Klein, S. Improved accuracy and precision of gas chromatography/mass spectrometry measurements for metabolic tracers. Metabolism 47, 706-712 (1998).
64. R Development Core Team: A language and environment for statistical computing. 2010.
65. Westermann, J. & Pabst, R. Lymphocyte subsets in the blood: a diagnostic window on the lymphoid system? Immunol. Today 11, 406-410 (1990).

Supplementary Information

Mathematical modeling of urine and DNA enrichment data. To control for changing levels of body water enrichment over the course of the experiment, urine enrichment curves were fitted with a simple label enrichment/decay curve as previously described[1, 2]. We incorporated the best fits of urine enrichment of each individual when analyzing the enrichment in the different cell populations. To estimate the maximum level of label incorporation that cells could possibly attain, ^{2}H enrichment in the granulocyte population of each individual was analyzed as described previously[1]. The enrichment data of all cell subsets were subsequently scaled by the granulocyte maximum enrichment asymptote of each individual[1]. Enrichment data of the different leukocyte subsets were fitted with a multi-exponential model which corrects for interindividual differences in the length of labeling, and allows populations to be kinetically heterogeneous (e.g., to consist of multiple subpopulations with distinct turnover rates)[2-4]. To determine the number of kinetically different subpopulations to include in the model we followed a stepwise selection procedure, adding a new kinetically different subpopulation into the model and stopping when the average turnover rate was no longer markedly changed[2]. The model was also used for populations that appeared to behave kinetically homogeneously; in these cases, the fitting procedure set the contribution of the extra exponential(s) in the model to zero. Average turnover rates ***p*** of different leukocyte populations were estimated by fitting the enrichment data for each individual. The enrichment data were also fitted using a mixed-effects model approach (Fig. 3*A*) to illustrate the difference in dynamics at the group level. The average turnover rates estimated using mixed effects models are not reported in the manuscript.

Calculation of daily thymic output. Daily thymic output was calculated as described previously[5]. Briefly, the total production of naive CD4$^+$ T cells per day was first calculated as (the average turnover rate ***p***) x (the absolute number of naive CD4$^+$ T cells per liter blood) x (5 liter blood) x 50, assuming that 2% of lymphocytes reside in the blood[6]. The total daily naive CD4$^+$ T-cell production was multiplied by the normalized naive CD4$^+$ T-cell TREC content to estimate the daily thymic output in cells/day. The peripheral T-cell division rate per day was obtained by subtracting daily thymic output from total daily production and dividing this value by the absolute number of naive CD4$^+$ T cells.

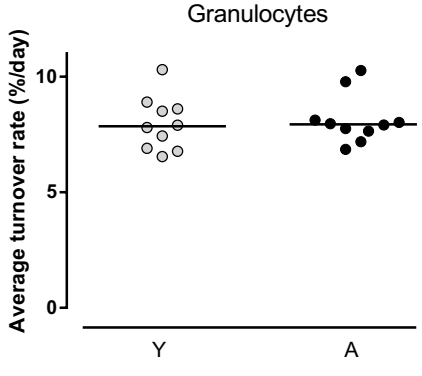

Supplementary Figure 1. Estimated average turnover rates of granulocytes in young and elderly individuals. Estimates of the average turnover rate of granulocytes in young (gray symbols) and aged (black symbols) individuals. Horizontal lines represent median values.

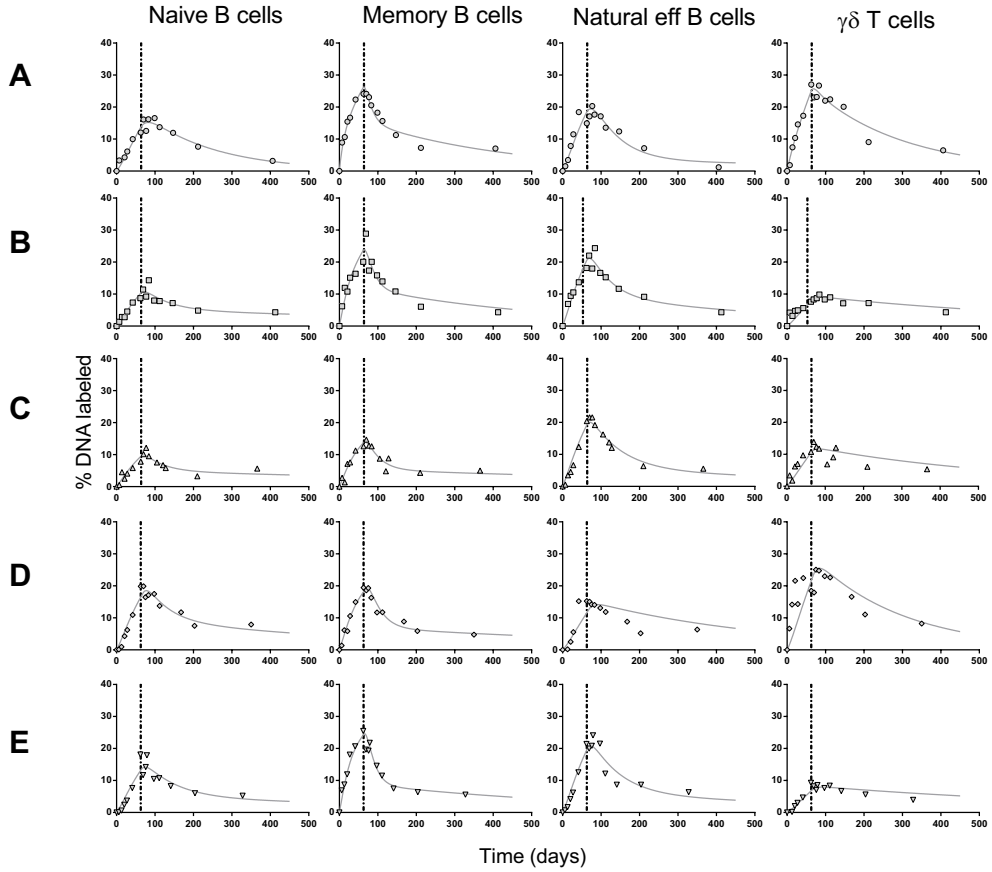

Supplementary Figure 2. Best fits of ^{2}H enrichment in B-cell subsets and in γδ T cells in young individuals. Best fits of the multi-exponential model to the enrichment in naive, memory, and natural effector (eff) B cells, and γδ T cells in the five young individuals (A-E). Label enrichment in the DNA was scaled between 0 and 100% by normalizing for the maximum enrichment in granulocytes (supplemental Methods). The end of ^2H_2O administration is marked by a dashed vertical line.

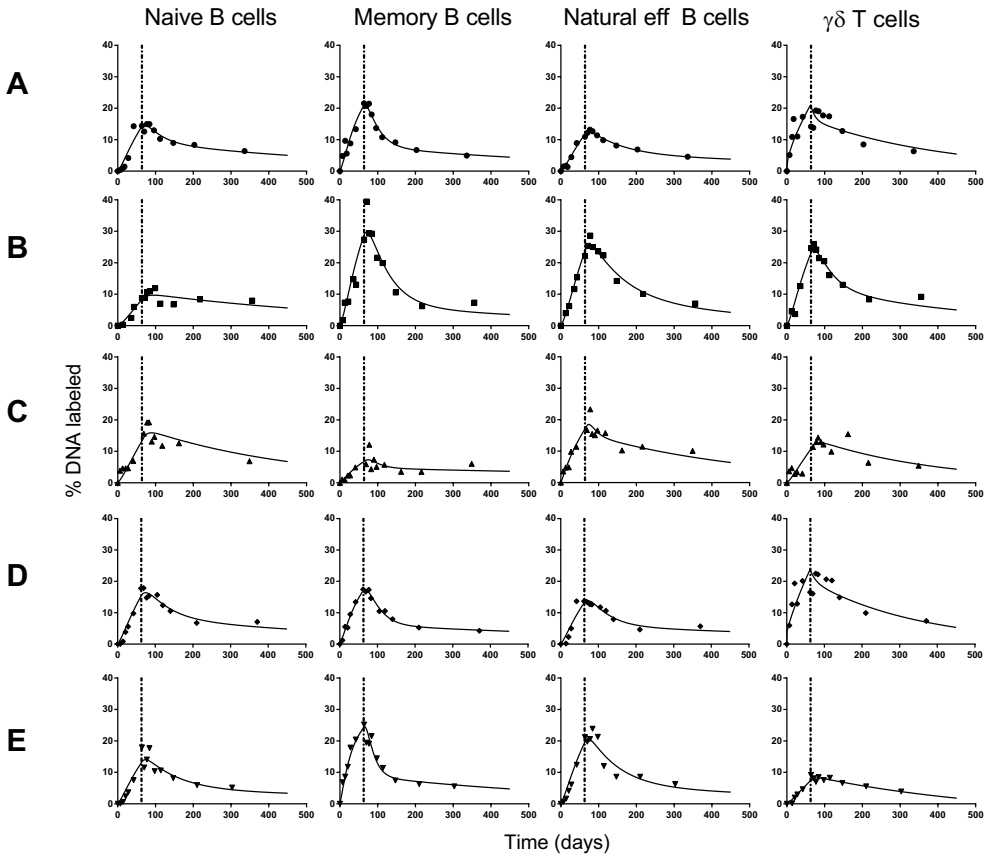

Supplementary Figure 3. Best fits of ^2H enrichment in B-cell subsets and in γδ T cells in elderly individuals. Best fits of the multi-exponential model to the enrichment in naive, memory, and natural effector (eff) B cells, and γδ T cells in the five aged individuals (A-E). Label enrichment in the DNA was scaled between 0 and 100% by normalizing for the maximum enrichment in granulocytes (Supporting Methods). The end of ^2H_2O administration is marked by a dashed vertical line.

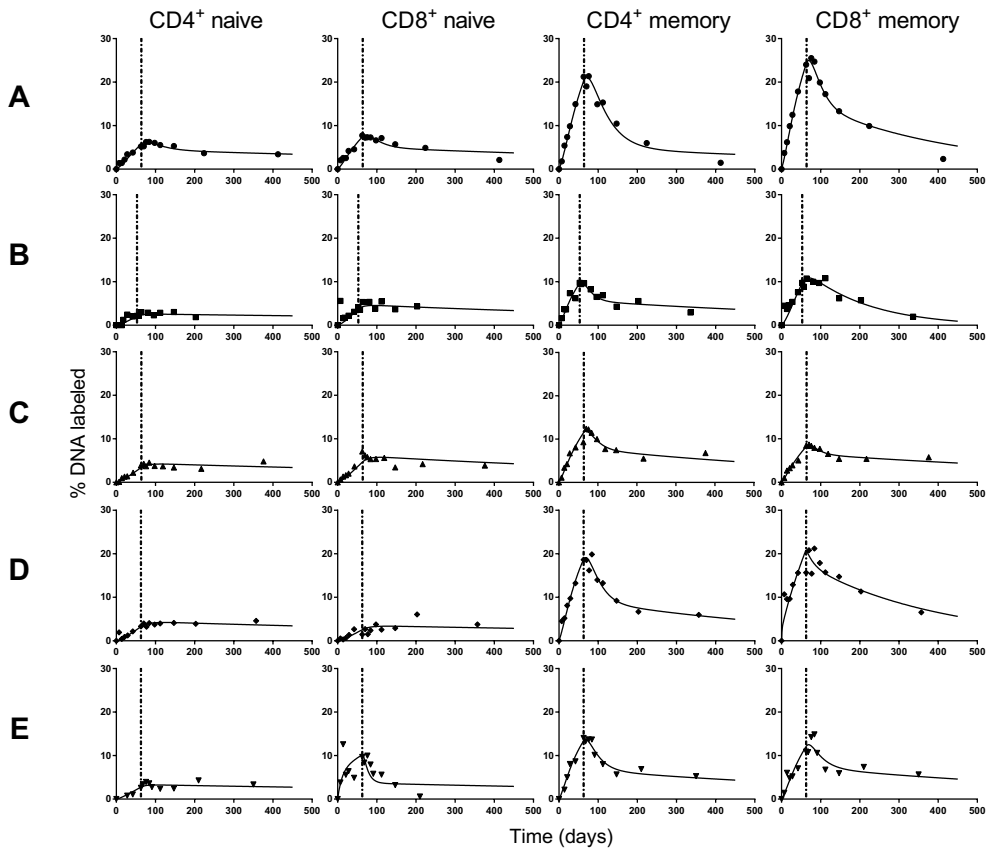

Supplementary Figure 4. Best fits of ^2H enrichment in T-cell subsets in elderly individuals. Best fits of the multi-exponential model to the enrichment in naive and memory $CD4^+$ and $CD8^+$ T cells in the five aged individuals. Label enrichment in the DNA was scaled between 0 and 100% by normalizing for the maximum enrichment in granulocytes (supplemental Methods). The end of ^2H_2O administration is marked by a dashed vertical line. Enrichment data of the corresponding subsets in young individuals were previously published [1, 2].

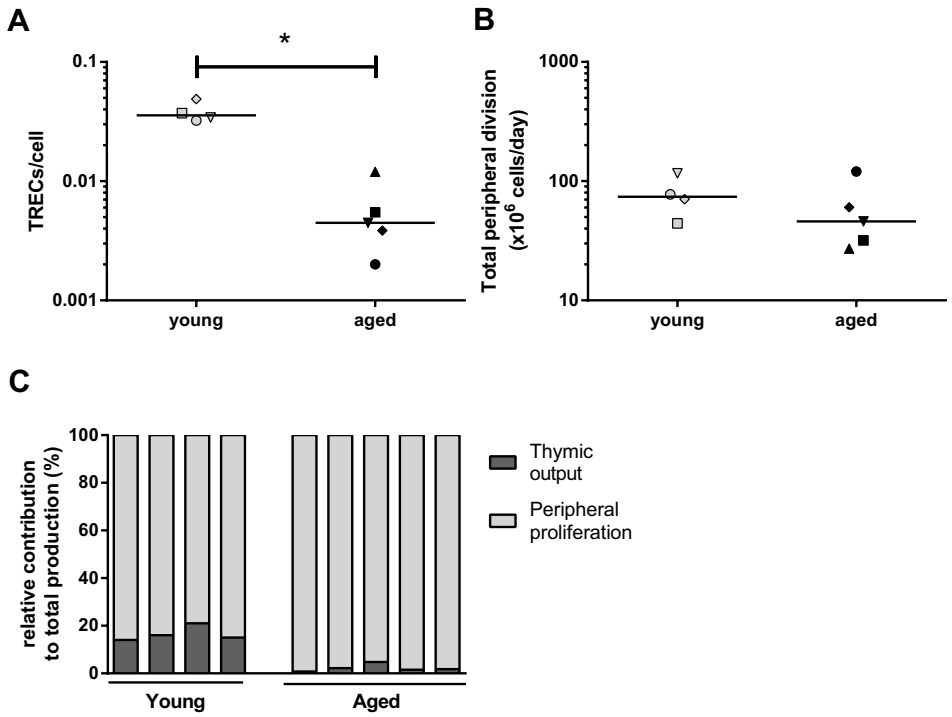

Supplementary Figure 4. TREC content and total peripheral division of naive CD4⁺ T cells in young and elderly individuals. (A) The number of TRECs/cell was determined in naive CD4⁺ cells of the five elderly individuals enrolled in this study for analysis of T cell subsets, and compared with the TREC content that was determined for four young individuals in the previous T-cell ^2H_2O study [3]. Due to limited material, TREC contents could not be measured for naive CD8⁺ T cells. The asterisk marks a statistically significant difference (p-value<0.05). (B) Estimated total peripheral division in cells per day, obtained by subtracting the estimated daily thymic output from the total naive CD4⁺ T-cell production. (C) Relative contributions of thymic output (dark gray bars) and peripheral T-cell division (light gray bars) to the total production of naive CD4⁺ T cells.

References Supplementary Information

1. Vrisekoop, N. et al. Sparse production but preferential incorporation of recently produced naive T cells in the human peripheral pool. Proc. Natl. Acad. Sci. U. S. A 105, 6115-6120 (2008).
2. Westera, L. et al. Closing the gap between T-cell life span estimates from stable isotope-labeling studies in mice and humans. Blood 122, 2205-2212 (2013).
3. de Boer, R.J., Perelson, A.S., & Ribeiro, R.M. Modelling deuterium labelling of lymphocytes with temporal and/or kinetic heterogeneity. J. R. Soc. Interface 9, 2191-2200 (2012).
4. Ganusov, V.V., Borghans, J.A., & de Boer, R.J. Explicit kinetic heterogeneity: mathematical models for interpretation of deuterium labeling of heterogeneous cell populations. PLoS. Comput. Biol. 6, e1000666 (2010).
5. den Braber, I. et al. Maintenance of peripheral naive T cells is sustained by thymus output in mice but not humans. Immunity. 36, 288-297 (2012).
6. Westermann, J. & Pabst, R. Lymphocyte subsets in the blood: a diagnostic window on the lymphoid system? Immunol. Today 11, 406-410 (1990).

8

General Discussion

"The lymphocyte presents a multiplicity of problems, and around these have accumulated a variety of facts which we are trying to fit together like the pieces of a jigsaw puzzle. In this puzzle there are unfortunately still a number of pieces which we cannot properly place."

J.M. Yoffey, The present status of the lymphocyte problem, 1962, The Lancet

The research presented in this thesis is focused on the quantification of human lymphocyte dynamics, primarily by stable isotope-labeling techniques and TREC analyses. It revealed two important biological insights. First, in humans the major source of new naive T cells is fundamentally different from that in mice, with a very limited role for thymic output throughout adulthood (chapter 3 and 7). Second, during healthy aging in humans there are no marked age-related differences in the pool sizes and turnover rates of most T-cell and B-cell subsets, and no signs of homeostatic compensation in response to declining thymic output and naive T-cell numbers (chapter 7).

The gain of combining techniques

As described in chapter 1, every technique that is used for quantification of lymphocyte dynamics has its own strengths and limitations. Combination of the unique pieces of information that are provided by the different techniques to quantify lymphocyte dynamics can be of considerable surplus value. Throughout this thesis we have reaped the rewards of the synergy between different tools, including stable-isotope labeling, TREC assessments, and mathematical modeling. A key example is our finding that naive T-cell maintenance in mice and humans is fundamentally different. We would not have been able to obtain this and other qualitative insights without a quantitative approach that combines multiple experimental techniques and mathematical modeling, as summarized below.

Since their first description as a tool to investigate thymic function, TRECs have made a valuable contribution to the research, diagnosis, and monitoring of clinical conditions involving T-cell immunity[1]. However, the interpretation of TRECs as a measure of thymic function is not as straightforward as was originally thought[2], because the average TREC content of a population of T cells is the result of a complex interplay between thymic output, peripheral T-cell division, and T-cell longevity[3]. For example, two individuals with the exact same daily thymic output may have totally different peripheral T-cell TREC contents, simply because they differ in the degree of peripheral T-cell division. Nevertheless, as we have shown in chapter 3, TREC contents can be used to deduce the *fraction* of cells originally produced by the thymus, i.e., the relative contribution of thymic output.

In mice, the combination of $^{2}H_{2}O$ labeling and thymectomy experiments revealed that the vast majority of newly produced naive T cells is produced by the thymus, and hence suggested a very limited role for peripheral naive T-cell division, throughout adulthood. This finding is supported by the observation that murine naive T-cell TREC contents hardly decline with age. In humans, the age-related naive T-cell TREC decline, starting at birth and continuing throughout adulthood[2, 4] (chapter 3), indicated that peripheral division of naive T cells rather than thymic output plays a

major role in maintenance of the human naive T-cell pool, being responsible for about 90% of all naive $CD4^+$ T-cell production in young adults. In line with this, mathematical analyses of thymus transplantation experiments in mice and ^2H_2O-labeling data in mice and humans suggest that in mice about half of naive $CD4^+$ and up to a quarter of naive $CD8^+$ T cells in the peripheral pool reside in the recent thymic emigrant (RTE) pool, while in humans this fraction of RTE is less than 2%[5]. By combining the information about the relative contribution of thymic output with quantitative information about the total daily production of naive T cells estimated by deuterium labeling, it is possible to estimate daily thymic output (in cells per day; chapter 3, 7). It is only because of this unique combination that we can now estimate that thymic output declines from an estimated 16 million cells per day in young individuals to less than 1 million cells per day in the elderly (chapter 7) – a statement that could not have been made based on TREC data or deuterium-labeling data only.

Bains et al. recently employed a different combination of techniques to quantify thymic output from birth to the age of 20 years[6]: they combined data on Ki-67 expression, as a measure of post-thymic naive T-cell production, with TREC dynamics in the naive $CD4^+$ T-cell pool. Mathematical analysis of these data revealed that, at the age of twenty, on average 3.6×10^8 naive $CD4^+$ T cells are produced by the thymus every day – which is an order of magnitude higher than our estimate of daily thymic output in young adults of 16×10^6 cells (chapter 3). The difference between these estimates may largely be due to overestimation of the fraction of dividing cells by measurement of Ki-67 expression in the study by Bains et al.[6]. Based on the relationship between the fraction of Ki-67^+ cells and turnover rates estimated by deuterium labeling[7], De Boer and Perelson have estimated that the daily T-cell turnover rate is roughly one fifth of the fraction of Ki-67^+ T cells, and hence that Ki-67 expression is likely to last longer than assumed in the study by Bains et al.[6, 8]. This notion is confirmed by a recent study by Hogan et al., who, by measuring Ki-67 expression levels and DNA content by DNA stain 7AAD, confirmed that Ki-67 expression is elevated long after completion of cell division[9]. A longer duration of Ki-67^+ expression would reduce the estimate of thymic output by Bains et al.[6] and would thereby bring the estimates closer together. Since stable-isotope labeling provides a more straightforward and accurate way to quantify cellular turnover rates, we think our lower estimate of daily thymic output at the age of 20 is more reliable. A common denominator of the two studies is the assumption that TRECs are very stable, and that declining TREC contents hence reflect cell division, an assumption that will be discussed next.

Long-term stability of TRECs

The conclusion that human naive T cells are produced predominantly through peripheral cell division is based on naive T-cell TREC contents, the interpretation of which relies on the assumption that TRECs are extremely stable and hence only decline by cell division. Although this assumption is supported by the observation that $TREC^+$ cells are still present in individuals who were thymectomized many decades ago, the interpretation of TREC dynamics after thymectomy is complicated by the possible regeneration of functional thymic tissue, which has been identified on magnetic resonance imaging scans in many thymectomized individuals[10]. In chapter 4 we therefore investigated the alternative scenario, namely that intracellular TREC decay, rather than cell division, causes the age-related decline in TREC contents. In this scenario, TREC contents would decline at a similar rate in the absence or presence of peripheral cell division. We show that patients treated for more than a decade with the immunosuppressive drug mycophenolate mofetil (MMF), which is known to inhibit lymphocyte proliferation[11,12], tend to have higher naive T-cell TREC contents than age-matched controls. These supranormal TREC contents in MMF-treated patients would not have been expected if the normal age-related TREC decline were solely due to intracellular TREC decay. These observations are therefore in favor of TREC dilution through peripheral naive T-cell division. However, as the findings presented in chapter 4 are still preliminary, and as we did not observe supranormal TREC contents in patients treated with the immunosuppressive drug azathioprine, further research is needed to confirm this. The assumption that TREC decay plays no significant role is also made for the interpretation of TREC contents in chapter 7, in which we estimate from TREC and ^2H_2O labeling data that between the third and the seventh decade of life the daily production of new naive $CD4^+$ T cells by the thymus declines by one order of magnitude. This is in agreement with biopsy studies which suggested a similar reduction in thymic output based on the tenfold decline of functional thymic tissue over age[13], a parallel that indirectly again supports our interpretation of naive T-cell TREC contents as a marker for the relative contributions of thymic output and peripheral naive T-cell division.

Resolving the controversy among published life span estimates

Although a major step forward in the quantification of lymphocyte dynamics was provided by the introduction of stable isotope-labeling techniques[14, 15], there was still some controversy because different laboratories estimated different lymphocyte turnover rates[16]. A meta-analysis of different T-cell life span estimates revealed a remarkable positive correlation between the duration of label administration and the estimated lymphocyte life span, with $^2H_2$-glucose-labeling studies consistently yielding shorter life span estimates than ^2H_2O-labeling studies[16]. Because the studies were based on different experimental protocols, a possible influence on life span estimates of (1) the duration of label administration and (2) the use of either $^2H_2$-glucose or ^2H_2O-labeling has been hard to investigate based on published data only. In this thesis we

have investigated these suspected sources of controversy, by a combination of new experiments and reanalysis of published data (chapter 5 and 6).

In chapter 5 we confirmed that indeed one source of controversy between short-term and long-term labeling studies is an influence of the length of the labeling period when using a commonly used single-exponential model for interpretation. In this approach, a possible influence of label saturation in subpopulations is not taken into account. By doing ^2H_2O-labeling experiments of different duration in mice, we have demonstrated that this problem can be solved by implementing a multi-exponential modeling approach, which takes into account that populations can in fact consist of multiple, kinetically different subpopulations with each their individual size and turnover rate[17, 18]. Application of this model demonstrated that ^2H_2O-labeling studies that were interpreted using the single-exponential model had in fact overestimated the average life span of cells from kinetically heterogeneous cell populations. Indeed, use of the multi-exponential model reduced the previous life span estimates of 222 and 357 days[19] for memory $CD4^+$ and $CD8^+$ T cells to life spans of only 164 and 157 days, respectively. We directly benefited from the multi-exponential modeling approach in chapter 7, in which we investigated the effect of healthy aging on the turnover characteristics of naive and memory $CD4^+$ and $CD8^+$ T cells, γδ T cells, and naive, memory, and natural effector B cells. Except for the naive T-cell pools in all but one individual, the majority of subsets were kinetically heterogeneous and required a multi-exponential model for reliable estimation of turnover rates.

In chapter 6 we show that the use of $^2H_2$-glucose or ^2H_2O in stable isotope-labeling studies is unlikely to be a source of life span discrepancies in the literature, as both deuterium-labeled compounds yielded similar life span estimates in mice experiments in which only the source of deuterium was varied. Indeed, we show that one can well predict the labeling curves of 1-day or 1-week $^2H_2$-glucose experiments[7,20] based on the turnover parameters from 9-week ^2H_2O labeling experiments[21, 22], with one unexplained exception[23]. Of note, predicting long-term labeling curves based on the parameters of a shorter labeling experiment need not be successful, because the shorter labeling period may be too short to pick up information about the kinetic composition of a kinetically heterogeneous cell population. Longer labeling experiments, at least when interpreted with a multi-exponential model, are more likely to pick up such information, and may thus reveal additional quantitative insights into the sizes and turnover rates of the subpopulations (chapter 5).

Taken together, we have shown that an influence of the duration of label administration in long-term labeling experiments can be corrected for by using a multi-exponential model (chapter 5), and that methodological or biochemical differences between $^2H_2$-glucose or ^2H_2O-labeling do not seem to influence the estimated life span (chapter 6). Stable-isotope labeling thus provides a means to reliably quantify cellular turnover, and thereby reaches beyond the possibilities of other measures of cell turnover that in fact only allow to *compare* dynamics within one study.

The role of the thymus

Humans differ fundamentally from mice in the dynamics underlying naive T-cell maintenance (chapter 3). While the murine naive T-cell pool is highly dynamic, with the naive $CD4^+$ and $CD8^+$ T-cell pools being fully replaced every 7 and 11 weeks, the turnover of the human naive T-cell pool is roughly 40 times slower. Moreover, while in mice new T cells are almost exclusively produced by the thymus throughout life, in humans peripheral division is the dominant mechanism of naive T-cell production; the human thymus produces as little as 10% of new T cells in young adults – and half a century later this contribution appears to have become a seemingly irrelevant percent (chapter 7). Hence, it seems that during the second half of our lives the thymus is doing nearly nothing. What does the virtual absence of a thymus mean? Its involution is associated with a decline in naive T-cell numbers, and there is no, or no sufficient, peripheral compensation for this decline (chapter 7). Moreover, peripheral naive T-cell division and de novo naive T-cell production, while both capable of generating naive T cells, are qualitatively different processes. The only source that can generate T cells with new specificities is the thymus. By contrast, peripheral division can only expand existing specificities, and can in the most ideal scenario and under completely random conditions only maintain diversity.

The relatively small contribution of thymic output, complemented with substantial peripheral naive T-cell division, is probably sufficient to maintain both a substantial naive T-cell pool size, sufficient TCR repertoire diversity, and a sufficient clonal size of each specificity throughout the largest part of human life. Yet at some point during healthy aging thymic output may become too low to fuel the repertoire, which may (1) not be perfectly maintained if peripheral naive T-cell division occurs non-randomly, and (2) contract further if naive T cells are non-randomly lost to the memory pool – in both cases differences in the strengths of TCR/peptide-MHC interactions may select for some and against other clones[24]. A collapse in $CD4^+$ T-cell diversity has indeed been reported to occur between the seventh and eighth decade of life, in association with increased naive T-cell proliferation[25]. Also in aging rhesus macaques naive T-cell pool size and diversity are reduced, concomitant with an age-related loss in vaccine responses[26]. One could argue that, in the long-term absence of significant thymic output, non-random peripheral division (either homeostatic division or conversion to the memory pool) may be the driver of repertoire contraction; and that further increases in cell division may accelerate this contraction process, becoming manifest between the seventh and the eighth decade of life[25].

Remarkably, despite thymic output still being the main source of new T cells in aged mice (chapter 3), TCR repertoire constriction is also observed in the murine naive T-cell pool[27, 28]. This could be because the absolute daily production of the thymus in aged mice, although the main source of new naive T cells, is also much lower than in young mice. Whether the residual repertoire is then peripherally expanded or not may not even matter that much; also a non-random survival of naive T cells, selecting for some and against other specificities, could lead to holes in the repertoire. In addition, both in humans and mice, there could be other factors involved than thymic involution, such as cell-intrinsic changes and persistent infections with for example cytomegalovirus. Johnson et al. recently claimed that the sudden collapse in TCR diversity around the age of 70, as opposed to a perhaps more expected gradual repertoire contraction, cannot be explained well by gradual thymic involution or declining pool size, and proposed an alternative model in which over time cells accumulate genetic or epigenetic cell-intrinsic changes that give certain clones a fitness advantage over others, e.g., an increased capacity to divide or survive[29]. In fact, whether non-random division or survival is effected by cell-intrinsic changes or by differences in TCR/peptide-MHC interactions, it is not difficult to imagine how selective division or survival in the absence of thymic output would lead to holes in the repertoire. Yet knowing the primary cause of selective (dis)advantages may be relevant for the development of therapeutic approaches to prevent or slow down repertoire contraction.

Hence, humans can maintain a normal immune system for decades in the absence of a substantial contribution of the thymus – in part due to the extreme longevity of naive T cells (chapter 7). However, too little thymic output for too long – probably several decades, at least substantially longer than the life span of naive T cells – is expected to have functional consequences on size, repertoire, and functioning of the peripheral naive T-cell pool. This implies that not only aging but also thymectomy would in the long run negatively affect the peripheral T-cell pool. Although within 20-25 years post-thymectomy the absence of a thymus has no evident adverse consequences, the immune systems of thymectomized individuals do indeed develop signs of premature immunological aging[30, 31] and the consequences on health status are likely to arise earlier than in healthy aging. Thymectomized individuals present an interesting model to study the essence of the thymus, but despite many documented alterations in several immune parameters, most available studies lack long-term follow-up to conclude whether these alterations ultimately have clinical consequences like an increased risk of infection or malignancy[32]. This is for a great part due to the fact that the cardiac neonatal surgical procedures involving thymectomy have only been regularly performed since the 1970s. The interpretation of research in thymectomized individuals is also complicated by incomplete documentation of whether partial or complete thymectomy was performed[32], and by the possible regrowth of thymic tissue[10]. Finally, having very little thymic output is disadvantageous in conditions that require regeneration of the T-cell compartment, for example immune reconstitution after cancer chemotherapy or stem cell transplantation (SCT). Evidently, our immune system did not evolve to receive stem cell grafts and establish a new immune system at older age; it may not have evolved to reach the age of 80-plus either. As in these "unnatural" situations increased thymic output would probably be most beneficial, strategies to improve immune function in the aged, or immune reconstitution in clinical conditions of lymphopenia, should be aimed at boosting the absolute daily de novo production of T cells (see last section, Clinical implications).

Homeostatic mechanisms in the human naive T-cell pool?

Homeostatic regulation of T-cell numbers in humans has been both an intriguing subject as well as a matter of large debate. Do compensatory increases in cell production or survival occur when the steady state of the naive T-cell pool is jeopardized (e.g., by thymic involution) or disturbed (e.g., by chemotherapy)? Or are constant low levels of naive T-cell turnover ("basal division") sufficient for the lifelong maintenance of the naive T-cell pool – and even sufficient to slowly but steadily repopulate an immune system after lymphocyte depletion? In chapter 7, we find no signs of homeostatic compensation for the age-related decline in thymic output and naive T-cell numbers. Our data suggest that the thymus is already contributing so little to naive T-cell production in young adults (~10%), that the loss of residual production during adulthood is not of a relevant order of magnitude to require compensation, which would be in line with the modestly reduced naive T-cell numbers in the elderly, or that this compensation can hardly be measured because it is very small. Although our findings in healthy aging reconfirm the very limited role of the thymus throughout adulthood (chapter 3), they do not give definite answers as to the existence and action of homeostatic mechanisms in the human naive T-cell pool; we may not see them, and hence cannot rule them out.

Many ideas on naive T-cell homeostasis come from animal models, but as we show in chapter 3, insights obtained in mice need not necessarily translate well to humans. Much less is clear about homeostatic responses to modest and severe lymphopenia in the human naive T-cell pool. Increased fractions of cycling cells after allogeneic SCT – although suggestive of a proliferative response to lymphopenia – turned out to be largely related to clinical events like graft-versus-host-disease and infections[33], introducing the possibility that, despite the evidence for homeostatic responses in mice, such processes may not occur in humans. In theory, and depending on the cause of lymphocyte depletion, homeostatic mechanisms in the peripheral pool could take the form of A) increased de novo production (e.g., thymic rebound), B) increased peripheral cell survival, and C) increased peripheral production by cell

division (e.g., lymphocyte-induced proliferation, LIP). Homeostatic mechanisms are generally thought to act in a cell density-dependent manner, based on cellular competition for space and signals within a certain niche.

Increased de novo production: thymic rebound

In the case of naive T cells, increased de novo production implies the existence of a feedback loop from the periphery to the thymus, which should in turn respond to signals from the empty pool by increasing thymopoiesis. It is known that the thymus can vary in size: in response to disease or physical stress it may transiently atrophy, after which it can revert to its original size, or even grow up to 50% larger[34]. Such "thymic rebound hyperplasia" is commonly observed in children but also occurs in adults, and is mainly seen after chemotherapy[34-37]. In children and young adults, thymic enlargement is found to be associated with a faster and more complete recovery of "naive" $CD4^+CD45RA^+$ T cells after chemotherapy[37, 38] – yet this association does not provide any quantitative information on thymic output. Supranormal TREC contents after SCT were originally taken as evidence for increased thymic output[39], but were later attributed to new, TREC-rich cells entering an empty pool[33]. Hence, despite radiographic evidence for thymic enlargement, to date there is no direct evidence that the daily thymic output of new naive T cells can increase in response to lower cell numbers. As the thymus contributes relatively little to the production of new naive T cells even in healthy young adults (chapter 3), a rebound of the thymus to increase its output by at most another 50% may quantitatively not have a major impact on the production of new naive T cells. Nevertheless, given the unique property of thymopoiesis to generate T cells with novel specificities, and considering that every thymus-derived cell may in turn produce progeny by peripheral division (*at least* a fixed number of daughter cells by basal level proliferation), any increase in production, however small, would be a relevant increase – in the elderly who are losing their peripheral T-cell repertoire, but even more so in lymphodepleted patients who have to rebuild a whole new T-cell pool – because both diversification of the repertoire as well as generation of a new T-cell pool depend on thymus-derived cells. In healthy aging, however, compensation mechanisms are naturally expected to act peripherally, not centrally, because thymic involution itself is likely to be the very cause of numerical declines in the naive T-cell pool.

Increased peripheral cell survival

Evidence for increased naive T-cell life spans at older age comes from experiments in mice[40, 41]. Following cotransfer of CFSE-labeled naive T cells from young and aged mice into young hosts, naive T cells from aged mice were found to persist longer (without extensive division)[40]. Rather than reflecting a direct competition-driven increase in life span based on the availability of survival factors like IL-7 or self-peptide/MHC, increased apoptosis resistance appeared to be an intrinsic property of aged cells, correlating with progressively lower levels of the pro-apoptotic molecule Bim[41]. Although the mechanism behind this is still unclear, it is thought to reflect a response to decreased thymic output. In humans, a similar age-related down-regulation of Bim was observed in old naive T cells[42], but whether this also resulted in a longer cellular life span has not been addressed. In our own mouse experiments, performed under physiological circumstances rather than involving adoptive transfers of CFSE-labeled cells, ^2H_2O labeling revealed no age-related change in naive $CD4^+$ T cell life span, and only a modest increase in naive $CD8^+$ T-cell life span, despite a considerable decline in thymic output (chapter 3). Also in elderly humans we did not find any evidence for increased average life spans of naive $CD4^+$ or $CD8^+$ T cells (chapter 7), which suggests that if there is either a density-dependent increase in life span, or a cell-intrinsic increase in apoptosis resistance during healthy aging, it must be very subtle. In another study, Bains et al. predicted, based on naive $CD4^+$ T-cell TREC contents between the ages of 0 and 20 years, that as the thymus involutes the survival time of naive T cells increases[43]. Given that the impact of thymic involution is quantitatively most profound during the first decades of life, possible changes in naive T-cell life span are expected to be more profound during this period, and to be much more subtle during adulthood. Nevertheless, since peripheral naive T-cell division plays an important role even in children[43-45], possible life span increases during childhood are probably still more subtle than in mice, in which peripheral division hardly occurs and the thymus is the primary source of new T cells at all times (chapter 3).

In fact, we did not detect life span increases in any of the lymphocyte subsets studied (chapter 7), which means that if compensation for decreased lymphopoiesis at the survival level is occurring in these subsets, the effect must be very small. A lack of substantial life span increase is perhaps not disadvantageous, as the extended survival of aged naive $CD4^+$ T cells in mice has been reported to facilitate the development of age-associated cellular defects that contribute to their functional impairment[40, 41].

Increased peripheral production by cell division

For naive T cells, the limiting resources for survival and those for expansion appear to be the same: IL-7 and self-peptide/MHC-derived signals[46-50]. The degree of cellular competition is thought to determine the balance between survival and proliferation in the naive T-cell pool: when the naive pool is of normal size, IL-7 and self-peptide/MHC ligands provide survival stimuli, but a drop in cell numbers may reduce the competition for IL-7 or even lead to elevated IL-7 levels (the result of reduced IL-7 consumption), causing self-peptide/MHC-derived signals to become mitogenic and to induce naive T-cell division[46, 47]. Considering this, it seems likely that in clinical conditions of

lymphopenia homeostatic compensation occurs by increased cell division, yet one may wonder whether the loss of thymic T-cell production during normal aging would provide enough empty space to tip this balance toward proliferation, or whether these naive T-cell pools are still of a "normal" size and, for their maintenance, rather depend on increased cell survival.

The most commonly held view is that compensation for low numbers occurs at the level of peripheral proliferation, which in the case of severe lymphopenia is thought to manifest as LIP, a phenomenon that has been widely observed in animal models[51-55] but for which no unambiguous evidence exists in humans. Upon transfer into lymphopenic mice, naive T cells undergo a proliferative response, with the majority of cells showing rapid expansion concomitant with the acquisition of a memory-like phenotype[56-59] ("spontaneous LIP"[60]), and a smaller fraction of cells displaying a slower, IL-7-dependent proliferation while retaining their phenotype ("homeostatic LIP")[60]. The latter type of proliferation is also found to occur in wildtype animals upon administration of IL-7[60], and it would provide a mechanism for naive T cells to maintain their own population (rather than just filling the total T-cell pool with memory-like cells), perhaps not only in severe lymphopenia but also in more lymphoreplete conditions like healthy aging. However, our labeling experiments in healthy mice revealed no age-related increases in the turnover of naive $CD4^+$ and $CD8^+$ T cells despite declining thymic output (chapter 3); $CD8^+$ naive T-cell life spans even increased modestly, as previously mentioned, suggesting that homeostatic compensation during aging may not be achieved through increases in cell division – because there may not be enough empty space to induce cell division.

Considering that naive T-cell division is uncommon in mice but a major mechanism of naive T-cell maintenance in humans (chapter 3), it would not be inconceivable that LIP manifests differently in the two species, with predominantly spontaneous LIP in mice, and perhaps a larger role for homeostatic LIP of naive T cells in humans – the latter could be more relevant to humans as the thymus is, throughout adulthood, less capable of reconstituting the naive T-cell pool (chapter 7). So what is the evidence for compensatory increases in cell division in humans under conditions of extreme or modest lymphopenia? T-cell recovery after chemotherapy or bone marrow transplantation has been reported to manifest as an initial expansion of peripheral $CD4^+$ T cells with a memory phenotype and a delayed appearance of naive $CD45RA^+$ $CD4^+$ T cells in the blood[61, 62]. While the latter observation presumably reflects naive T-cell repopulation by low, continuous thymic output, the rapid expansion of cells with a memory phenotype could indicate LIP of naive T cells acquiring a memory phenotype. When the long-term immune reconstitution after SCT for severe combined immune deficiency was studied, patients with poor long-term reconstitution showed increased percentages of proliferating ($Ki\text{-}67^+$) cells and reduced naive T-cell TREC contents[63]. Increased fractions of $Ki\text{-}67^+$ naive T cells were also observed in the first years after neonatal thymectomy[10] and during healthy aging[25, 64]. In all these studies, the elevated $Ki\text{-}67^+$ levels were interpreted to reflect a homeostatic increase in cell division rates in response to lower peripheral T-cell numbers. However, other studies are not in favor of homeostatic increases in naive T-cell division. Some studies revealed that increased fractions of cycling naive T cells in lymphopenia are explained by other factors: they turned out to be related to HIV-related immune activation or clinical events, rather than reflecting a homeostatic response[33, 65], casting doubt on the interpretation of the aforementioned studies that reported homeostatically increased division rates. From this perspective, the increased fractions of cycling cells observed in some but not all elderly subjects of the studies by Sauce et al.[64] and Naylor et al.[25] may alternatively reflect sustained recruitment of CMV-specific naive T cells into the memory pool, especially when considering the high prevalence of CMV among the elderly (up to 90% in the very old[66]). This idea is also compatible with the observation that in our own elderly subjects, who were all but one CMV-negative, there are no signs of peripheral increases in $CD4^+$ naive T-cell division despite a tenfold decline in thymic output and reduced naive T-cell numbers (chapter 7). Although one could argue that the difference between our study and the other two studies[25, 64] reflects an age-difference (their subjects were even older (70-96) than the ones in our study), it is unlikely that a homeostatic response is triggered by the further loss of thymic T-cell production that occurs *after* the seventh decade of life – a production that is expected to decline from extremely low to even lower.

Although homeostatic compensation by increased cell division may occur, it does not seem to present a profound mechanism during healthy aging, and even under more extreme conditions of lymphopenia the compensatory action of increased division is not undisputed. However, preliminary data from a current ^2H_2O labeling study after autologous SCT show that label incorporation by naive T cells is considerably higher in 3 out of 3 investigated patients than in healthy individuals (Van Hoeven et al., manuscript in preparation). This suggests that naive T-cell proliferation can be elevated even in the absence of graft-versus-host-disease or infections, and hence strongly argues for the occurrence of LIP in humans (although thymic rebound is not formally excluded).

Concluding remarks: homeostatic compensation during healthy aging?

We have proposed in chapter 7 that the naive T-cell pools of the healthy elderly individuals included in our study might not have been sufficiently depleted to trigger homeostatic mechanisms, and that a certain pool size threshold may exist below which these compensatory mechanisms are activated. However, as homeostasis is driven by competition for resources, it may just as well be a gradual phenomenon instead

of a threshold: the fewer cells, the less competition, and hence the more survival/division. Since homeostatic compensation seems to occur in humans after SCT (Van Hoeven et al., manuscript in preparation), homeostatic mechanisms may just as well be triggered during healthy aging. However, because the thymus already contributes so little to naive T-cell production in young adults, the further loss of thymic output only leads to a marginal reduction in cell-cell competition for limiting resources, and may therefore only lead to a very subtle increase in peripheral cell division or survival. In other words, even the slightest, undetectable increase in survival or division might already compensate for the loss in thymic output, an idea that is also fully compatible with our own findings (chapter 7). Based on our data, however, we cannot distinguish whether a homeostatic response is absent, or present but undetectable.

Nevertheless, if a homeostatic response is triggered, it seems to be insufficient to fully maintain naive pool sizes because both the naive $CD4^+$ and $CD8^+$ T-cell pools seem to be somewhat smaller than the naive T-cell pools in young adults. Notably, absolute cell numbers vary substantially between individuals, making it difficult to conclude whether and how much the naive T-cell pools in the elderly have decreased during their lives. But regardless of this uncertainty, a reduction in naive T-cell pool size at old age may in principle be explained by the absence of homeostatic compensation for thymic involution, because the loss of naive T cell production, however small it may be, will over time result in a net loss of new T cells *and* their progeny (generated through basal proliferation). Alternatively, and perhaps more likely from the perspective that compensatory mechanisms are active in healthy aging, the niche of the naive T-cell pool shrinks with age, for example because the production of IL-7 by lymphoid stromal cells or other tissue sites declines with age, as described for the aging thymus in mice[67], and as suggested by reduced serum levels of IL-7 in elderly humans[68]. Although in this scenario competition-driven survival or division may ensure that the pool size is maintained at its maximum, this simply is not the same maximum as half a century ago. A last possible explanation for decreased naive T-cell numbers is that, if T cells with different specificities occupy different niches, due to the loss of thymic output and hence loss of specificities some niches remain empty at higher age.

Immunological memory in short-lived cells?

In mice as well as humans, from young to old age, and in both the T-cell and B-cell arm, memory cells appear to have fairly short life spans. We found that in mice, memory T cells live for about 2 to 3 weeks (chapter 5), and in humans memory T and B cells live for roughly 50 to 300 days (chapter 7) – life spans that are only a tiny fraction of the duration of long-term immunity, which in humans can last for several decades in the absence of re-exposure to a pathogen[69]. The rapid turnover of memory cells reported by us and others[23, 70-72] implies that immunological memory is contained in a long-lived cell population in constant turnover, rather than in a long-lived, quiescent memory cell – a commonly held view, and probably also the most intuitive representation, of long-term immunity[73, 74].

Why would immunological memory be maintained in a long-lived population of short-lived cells rather than in long-lived cells? At first glance, maintenance of a population that is in constant turnover seems like a much more energy-consuming process than maintenance of a cell in quiescence. Nevertheless, there may be certain advantages to this continuous memory cell renewal. Specific ablation of dividing T cells in mice was found to abolish in vitro and in vivo memory responses, despite the presence of quiescent memory T cells, suggesting that T-cell division is an absolute requirement for maintenance of immunological memory[75]. Continuous cell division could be functionally beneficial because memory cells that are constantly cycling may be in a more activated state and can hence be recruited instantly into the immune response. Previous studies have described asymmetric division of T cells[76, 77] and B cells[78]. Asymmetric division of memory cells could also provide a mechanism to balance self-renewal (for maintenance of memory) and differentiation (for generation of immune responses), the two key aspects of immunological memory. A stem-like memory cell may asymmetrically divide, after which only one daughter cell may proliferate to generate a secondary effector pool, with the other daughter cell remaining the bona fide stem-like memory cell, the long-lasting source of long-term immunity. Such asymmetric division could occur in response to antigen re-exposure, but if the continuous presence of a cycling memory pool is required for robust memory responses, frequent, antigen-independent asymmetric divisions might perhaps provide a better mechanism as it would ensure that a pool of memory cells in a high state of alertness is present at all times – ready for action.

Although the continuous turnover in the memory pools is probably beneficial or even necessary for proper memory cell function, it may also come at a cost. Continuous replication may lead to extensive telomere erosion, which has been proposed to contribute to the cellular aging process[79]. Moreover, it may result in an accumulation of terminally differentiated cells, which are generally associated with reduced function and apoptosis-resistance[80]. The cellular milieu during cell division is one of increased cellular stress and free radicals, which can damage DNA and proteins and thereby affect a cell's vital functions. Cells may thus accumulate mutations that give rise to cell-intrinsic changes, such as a fitness (dis)advantage of certain clones over others[29]. The progressive loss of DNA methylation patterns with each division may lead to abnormal gene expression in cells that have extensively replicated, which is also a suspected cause of killer immunoglobulin-like receptor expression on $CD8^+$ T cells, particularly terminally differentiated ones, at older age[81]. Killer immunoglobulin-

like receptor expression on $CD8^+$ T cells is thought to contribute to the immune defect in the elderly. Although it has been argued that the expression of such inhibitory receptors could serve as a negative regulatory mechanism to prevent excessive inflammatory responses in the aged, it may also be no more than a trade-off for the necessary division-dependent maintenance of immunological memory.

Since the memory pools in mice and humans are kinetically heterogeneous populations that are likely to comprise many different cell types, we cannot rule out that also quiescent, long-lived memory cells may play a role. Interpretation of our memory T-cell labeling curves with a multi-exponential model revealed that the slowest detectable subpopulation has a roughly tenfold lower turnover rate than the fastest subpopulation, corresponding to a life expectancy of several years. We cannot rule out the additional presence of even longer-lived, quiescent memory cells that live for many decades: if this subpopulation comprises a minority of the memory pool, its kinetic information is less likely to be picked up in labeling experiments; moreover, such long-lived memory cells may reside at different tissue sites than the blood, for example in specialized bone marrow niches. Regardless of whether long-term immunity also requires long-lived cells or not, constant memory cell turnover is a striking feature of the memory pools in mice and humans, and probably presents an essential element of the maintenance of functional immunological memory.

Clinical implications

One of the most important biological findings of this work is that the human thymus only contributes very little to naive T-cell production, even in young adults. Nevertheless this contribution appears to be sufficient to stay healthy into *at least* the seventh decade of life (chapter 7). However, at even older age, or in adults thymectomized during childhood, as well as in clinical situations that demand regeneration of a whole new T-cell pool at adult age, e.g., SCT, the small contribution of thymic output can be disadvantageous. Regeneration of the naive T-cell pool as well as diversification – and in fact even maintenance – of the TCR repertoire strongly depends on thymus-derived cells. As the age of the average person in industrialized countries increases, clinical problems related to insufficient thymic output are likely to become more evident. A solution to this could be the development of therapies aimed at boosting thymic function. It is important to realize that, in contrast to patients with therapy-induced lymphopenia, elderly and thymectomized individuals are only mildly lymphopenic, yet they may still reach a stage at which partial naive T-cell pool regeneration, or rejuvenation, would be clinically relevant, perhaps mainly because their TCR repertoire might become insufficient. Boosting thymic function in the seventh decade of life may be sufficient to survive a few more decades in good health; considering the longevity of naive T cells, even a transient booster every few years might be beneficial. A slight increase in thymic output should already have a positive impact on T-cell maintenance or regeneration, because an increase in thymic output may be amplified by a basal level of peripheral expansion of every thymically derived cell – perhaps complemented with the natural action of peripheral homeostatic mechanisms, providing a more rapid and more complete regeneration of a diverse T-cell pool. Being able to delay the contraction of the TCR repertoire may also have important implications for vaccination in the elderly, as $CD4^+$ T-cell helper function would stay intact into older age. Research into the mechanisms that govern thymic regeneration after transient atrophy[34] or regrowth of functional thymic tissue in thymectomized individuals[10], should help identify factors that are key to the enhancement of thymic function. Several approaches for thymic rejuvenation are currently being explored at different stages in mice and humans, including pharmaceutical-mediated ablation of sex hormones, administration of the cytokines IL-7, IL-22, and keratinocyte growth factor, and the hormones ghrelin and growth hormone[82]. As thymic function in turn strongly depends on a source of bone marrow progenitors, this organ may require parallel boosting. Importantly, given the fundamental species difference regarding the contribution of the thymus, and with the ultimate goal being thymic rejuvenation in humans, it is evident that the emphasis of the research should be on humans, not mice. Nevertheless, mice may in fact prove to be a particularly useful model for basic thymic rejuvenation research, for the very reason that the thymus is so important in mice. Nevertheless, critical evaluation of the mouse as a model for humans is warranted.

In fact, the problem of immunological aging stretches far beyond thymic involution, with a variety of other changes suspected to affect immune function, including changes in other microenvironments than the thymus, a reduction in the quality of bone marrow progenitors, and changes in other arms of the immune system[83]. Although strategies that boost thymic function may help slow down the loss of diversity in the aged, it may be insufficient to fully prevent immune dysfunction in the elderly, for example because the boosted thymus may still be producing T cells of poor quality. As it may be difficult to revert such changes, a combination of preventive approaches should be developed aimed at not only boosting thymic function or preventing further thymic involution, but also at tackling other age-related changes like bone marrow niche aging. Importantly, also persistent infection with CMV is considered an important driving force in the aging of the immune system[66]. A study in young individuals thymectomized during early childhood, whose immune systems showed signs of premature aging, revealed that particularly the immune systems of CMV-positive individuals resembled that of a 75-year old healthy person, and the individuals that showed naive T-cell repertoire contraction were all CMV-seropositive[30]. Therefore, also vaccination to prevent primary CMV infection at a young age may prove effective in slowing down immunological aging. Promising results have been

achieved in a recent study by Eberhardt et al.: vaccination of rhesus macaques against a virus-encoded ortholog to interleukin-10, held responsible for the persistence of CMV, induced neutralizing antibodies that restricted viral infection[84]. Vaccination against CMV infection would come with other important clinical advantages as CMV reactivation is also a common problem after SCT and solid organ transplantation[85], and transmission of CMV to the fetus by pregnant women suffering primary infection or reactivation is associated with an increased risk of congenital defects[86]. Future research into the various aspects of immunological aging – both in healthy elderly as well as in elderly people with age-related immune dysfunction – should help identify the factors that favor and those that threaten the lifelong maintenance of a properly functioning immune system. These factors may in turn provide interesting targets for the development of interventions that combat the aging of the immune system.

References

1. Somech, R. T-cell receptor excision circles in primary immunodeficiencies and other T-cell immune disorders. Curr. Opin. Allergy Clin. Immunol. 11, 517-524 (2011).
2. Douek, D.C. et al. Changes in thymic function with age and during the treatment of HIV infection. Nature 396, 690-695 (1998).
3. Hazenberg, M.D., Borghans, J.A., de Boer, R.J., & Miedema, F. Thymic output: a bad TREC record. Nat. Immunol. 4, 97-99 (2003).
4. Jamieson, B.D. et al. Generation of functional thymocytes in the human adult. Immunity. 10, 569-575 (1999).
5. Van Hoeven, V. et al. Recent thymic emigrants form a substantial subpopulation of short-lived naive T cells in mice but not in humans. Manuscript in preparation.
6. Bains, I., Thiebaut, R., Yates, A.J., & Callard, R. Quantifying thymic export: combining models of naive T cell proliferation and TCR excision circle dynamics gives an explicit measure of thymic output. J. Immunol. 183, 4329-4336 (2009).
7. Mohri, H. et al. Increased turnover of T lymphocytes in HIV-1 infection and its reduction by antiretroviral therapy. J. Exp. Med. 194, 1277-1287 (2001).
8. de Boer, R.J. & Perelson, A.S. Quantifying T lymphocyte turnover. J. Theor. Biol. 327, 45-87 (2013).
9. Hogan, T. et al. Clonally diverse T cell homeostasis is maintained by a common program of cell-cycle control. J. Immunol. 190, 3985-3993 (2013).
10. van Gent, R. et al. Long-term restoration of the human T-cell compartment after thymectomy during infancy: a role for thymic regeneration? Blood 118, 627-634 (2011).
11. Allison, A.C. & Eugui, E.M. Mycophenolate mofetil and its mechanisms of action. Immunopharmacology 47, 85-118 (2000).
12. Khan, M.M. Immunosuppressive agents in Immunopharmacology 2008).
13. Steinmann, G.G., Klaus, B., & Muller-Hermelink, H.K. The involution of the ageing human thymic epithelium is independent of puberty. A morphometric study. Scand. J. Immunol. 22, 563-575 (1985).
14. Hellerstein, M.K. & Neese, R.A. Mass isotopomer distribution analysis: a technique for measuring biosynthesis and turnover of polymers. Am. J. Physiol 263, E988-1001 (1992).
15. Neese, R.A. et al. Measurement in vivo of proliferation rates of slow turnover cells by 2H2O labeling of the deoxyribose moiety of DNA. Proc. Natl. Acad. Sci. U. S. A 99, 15345-15350 (2002).
16. Borghans, J.A. & de Boer, R.J. Quantification of T-cell dynamics: from telomeres to DNA labeling. Immunol. Rev. 216, 35-47 (2007).
17. Ganusov, V.V., Borghans, J.A., & de Boer, R.J. Explicit kinetic heterogeneity: mathematical models for interpretation of deuterium labeling of heterogeneous cell populations. PLoS. Comput. Biol. 6, e1000666 (2010).
18. de Boer, R.J., Perelson, A.S., & Ribeiro, R.M. Modelling deuterium labelling of lymphocytes with temporal and/or kinetic heterogeneity. J. R. Soc. Interface 9, 2191-2200 (2012).
19. Vrisekoop, N. et al. Sparse production but preferential incorporation of recently produced naive T cells in the human peripheral pool. Proc. Natl. Acad. Sci. U. S. A 105, 6115-6120 (2008).
20. Defoiche, J. et al. Reduction of B cell turnover in chronic lymphocytic leukaemia. Br. J. Haematol. 143, 240-247 (2008).

21. van Gent, R. et al. In vivo dynamics of stable chronic lymphocytic leukemia inversely correlate with somatic hypermutation levels and suggest no major leukemic turnover in bone marrow. Cancer Res. 68, 10137-10144 (2008).
22. Vrisekoop, N. et al. Quantification of naive and memory T-cell turnover during HIV-1 infection. to be submitted.
23. Wallace, D.L. et al. Direct measurement of T cell subset kinetics in vivo in elderly men and women. J. Immunol. 173, 1787-1794 (2004).
24. Rudd, B.D. et al. Nonrandom attrition of the naive CD8+ T-cell pool with aging governed by T-cell receptor:pMHC interactions. Proc. Natl. Acad. Sci. U. S. A 108, 13694-13699 (2011).
25. Naylor, K. et al. The influence of age on T cell generation and TCR diversity. J. Immunol. 174, 7446-7452 (2005).
26. Cicin-Sain, L. et al. Loss of naive T cells and repertoire constriction predict poor response to vaccination in old primates. J. Immunol. 184, 6739-6745 (2010).
27. Yager, E.J. et al. Age-associated decline in T cell repertoire diversity leads to holes in the repertoire and impaired immunity to influenza virus. J. Exp. Med. 205, 711-723 (2008).
28. Ahmed, M. et al. Clonal expansions and loss of receptor diversity in the naive CD8 T cell repertoire of aged mice. J. Immunol. 182, 784-792 (2009).
29. Johnson, P.L., Yates, A.J., Goronzy, J.J., & Antia, R. Peripheral selection rather than thymic involution explains sudden contraction in naive CD4 T-cell diversity with age. Proc. Natl. Acad. Sci. U. S. A 109, 21432-21437 (2012).
30. Sauce, D. et al. Evidence of premature immune aging in patients thymectomized during early childhood. J. Clin. Invest 119, 3070-3078 (2009).
31. Haynes, B.F., Markert, M.L., Sempowski, G.D., Patel, D.D., & Hale, L.P. The role of the thymus in immune reconstitution in aging, bone marrow transplantation, and HIV-1 infection. Annu. Rev. Immunol. 18, 529-560 (2000).
32. Afifi, A., Raja, S.G., Pennington, D.J., & Tsang, V.T. For neonates undergoing cardiac surgery does thymectomy as opposed to thymic preservation have any adverse immunological consequences? Interact. Cardiovasc. Thorac. Surg. 11, 287-291 (2010).
33. Hazenberg, M.D. et al. T-cell receptor excision circle and T-cell dynamics after allogeneic stem cell transplantation are related to clinical events. Blood 99, 3449-3453 (2002).
34. Nasseri, F. & Eftekhari, F. Clinical and radiologic review of the normal and abnormal thymus: pearls and pitfalls. Radiographics 30, 413-428 (2010).
35. Kissin, C.M., Husband, J.E., Nicholas, D., & Eversman, W. Benign thymic enlargement in adults after chemotherapy: CT demonstration. Radiology 163, 67-70 (1987).
36. Yarom, N. et al. Rebound thymic enlargement on CT in adults. Int. J. Clin. Pract. 61, 562-568 (2007).
37. Mackall, C.L. et al. Age, thymopoiesis, and CD4+ T-lymphocyte regeneration after intensive chemotherapy. N. Engl. J. Med. 332, 143-149 (1995).
38. Sfikakis, P.P. et al. Age-related thymic activity in adults following chemotherapy-induced lymphopenia. Eur. J. Clin. Invest 35, 380-387 (2005).
39. Douek, D.C. et al. Assessment of thymic output in adults after haematopoietic stem-cell transplantation and prediction of T-cell reconstitution. Lancet 355, 1875-1881 (2000).
40. Tsukamoto, H. et al. Age-associated increase in lifespan of naive CD4 T cells contributes to T-cell homeostasis but facilitates development of functional defects. Proc. Natl. Acad. Sci. U. S. A 106, 18333-18338 (2009).
41. Tsukamoto, H., Huston, G.E., Dibble, J., Duso, D.K., & Swain, S.L. Bim dictates naive CD4 T cell lifespan and the development of age-associated functional defects. J. Immunol. 185, 4535-4544 (2010).
42. Haynes, L. & Swain, S.L. Aged-related shifts in T cell homeostasis lead to intrinsic T cell defects. Semin. Immunol. 24, 350-355 (2012).
43. Bains, I., Antia, R., Callard, R., & Yates, A.J. Quantifying the development of the peripheral naive CD4+ T-cell pool in humans. Blood 113, 5480-5487 (2009).
44. Hazenberg, M.D. et al. Establishment of the CD4+ T-cell pool in healthy children and untreated children infected with HIV-1. Blood 104, 3513-3519 (2004).
45. van Gent, R. et al. Refined characterization and reference values of the pediatric T- and B-cell compartments. Clin. Immunol. 133, 95-107 (2009).
46. Boyman, O., Letourneau, S., Krieg, C., & Sprent, J. Homeostatic proliferation and survival of naive and memory T cells. Eur. J. Immunol. 39, 2088-2094 (2009).
47. Jameson, S.C. Maintaining the norm: T-cell homeostasis. Nat. Rev. Immunol. 2, 547-556 (2002).
48. Sportes, C. et al. Administration of rhIL-7 in humans increases in vivo TCR repertoire diversity by preferential expansion of naive T cell subsets. J. Exp. Med. 205, 1701-1714 (2008).
49. Guimond, M., Fry, T.J., & Mackall, C.L. Cytokine signals in T-cell homeostasis. J. Immunother. 28, 289-294 (2005).
50. Fry, T.J. & Mackall, C.L. Interleukin-7: master regulator of peripheral T-cell homeostasis? Trends Immunol. 22, 564-571 (2001).
51. Bell, E.B., Sparshott, S.M., Drayson, M.T., & Ford, W.L. The stable and permanent expansion of functional T lymphocytes in athymic nude rats after a single injection of mature T cells. J. Immunol. 139, 1379-1384 (1987).
52. Freitas, A.A., Agenes, F., & Coutinho, G.C. Cellular competition modulates survival and selection of CD8+ T cells. Eur. J. Immunol. 26, 2640-2649 (1996).
53. Freitas, A.A. & Rocha, B. Population biology of lymphocytes: the flight for survival. Annu. Rev. Immunol. 18, 83-111 (2000).
54. Rocha, B., Dautigny, N., & Pereira, P. Peripheral T lymphocytes: expansion potential and homeostatic regulation of pool sizes and CD4/CD8 ratios in vivo. Eur. J. Immunol. 19, 905-911 (1989).
55. Miller, R.A. & Stutman, O. T cell repopulation from functionally restricted splenic progenitors: 10,000-fold expansion documented by using limiting dilution analyses. J. Immunol. 133, 2925-2932 (1984).
56. Cho, B.K., Rao, V.P., Ge, Q., Eisen, H.N., & Chen, J. Homeostasis-stimulated proliferation drives naive T cells to differentiate directly into memory T cells. J. Exp. Med. 192, 549-556 (2000).
57. Goldrath, A.W., Bogatzki, L.Y., & Bevan, M.J. Naive T cells transiently acquire a memory-like phenotype during homeostasis-driven proliferation. J. Exp. Med. 192, 557-564 (2000).
58. Gudmundsdottir, H. & Turka, L.A. A closer look at homeostatic proliferation of CD4+ T cells: costimulatory requirements and role in memory formation. J. Immunol. 167, 3699-3707 (2001).
59. Oehen, S. & Brduscha-Riem, K. Naive cytotoxic T lymphocytes spontaneously acquire effector function in lymphocytopenic recipients: A pitfall for T cell memory studies? Eur. J. Immunol. 29, 608-614 (1999).
60. Min, B., Yamane, H., Hu-Li, J., & Paul, W.E. Spontaneous and homeostatic proliferation of CD4 T cells are regulated by different mechanisms. J. Immunol. 174, 6039-6044 (2005).
61. Hakim, F.T. et al. Constraints on CD4 recovery postchemotherapy in adults: thymic insufficiency

and apoptotic decline of expanded peripheral CD4 cells. Blood 90, 3789-3798 (1997).

62. Dumont-Girard, F. et al. Reconstitution of the T-cell compartment after bone marrow transplantation: restoration of the repertoire by thymic emigrants. Blood 92, 4464-4471 (1998).

63. Borghans, J.A. et al. Early determinants of long-term T-cell reconstitution after hematopoietic stem cell transplantation for severe combined immunodeficiency. Blood 108, 763-769 (2006).

64. Sauce, D. et al. Lymphopenia-driven homeostatic regulation of naive T cells in elderly and thymectomized young adults. J. Immunol. 189, 5541-5548 (2012).

65. Hazenberg, M.D. et al. Increased cell division but not thymic dysfunction rapidly affects the T-cell receptor excision circle content of the naive T cell population in HIV-1 infection. Nat. Med. 6, 1036-1042 (2000).

66. Nikolich-Zugich, J. Ageing and life-long maintenance of T-cell subsets in the face of latent persistent infections. Nat. Rev. Immunol. 8, 512-522 (2008).

67. Andrew, D. & Aspinall, R. Age-associated thymic atrophy is linked to a decline in IL-7 production. Exp. Gerontol. 37, 455-463 (2002).

68. Kang, I. et al. Age-associated change in the frequency of memory CD4+ T cells impairs long term CD4+ T cell responses to influenza vaccine. J. Immunol. 173, 673-681 (2004).

69. Crotty, S. & Ahmed, R. Immunological memory in humans. Semin. Immunol. 16, 197-203 (2004).

70. Michie, C.A., McLean, A., Alcock, C., & Beverley, P.C. Lifespan of human lymphocyte subsets defined by CD45 isoforms. Nature 360, 264-265 (1992).

71. Parretta, E. et al. Kinetics of in vivo proliferation and death of memory and naive CD8 T cells: parameter estimation based on 5-bromo-2'-deoxyuridine incorporation in spleen, lymph nodes, and bone marrow. J. Immunol. 180, 7230-7239 (2008).

72. Tough, D.F. & Sprent, J. Turnover of naive- and memory-phenotype T cells. J. Exp. Med. 179, 1127-1135 (1994).

73. Janeway, C.A., Travers, P., Walport, M., & Shlomick, M.J. Adaptive immunity to infection in Immunobiology 2001).

74. Goldsby, R.A., Kindt, T.K., Soborn, B.A., & Kuby, J. Immunology (2003).

75. Bellier, B., Thomas-Vaslin, V., Saron, M.F., & Klatzmann, D. Turning immunological memory into amnesia by depletion of dividing T cells. Proc. Natl. Acad. Sci. U. S. A 100, 15017-15022 (2003).

76. Chang, J.T. et al. Asymmetric T lymphocyte division in the initiation of adaptive immune responses. Science 315, 1687-1691 (2007).

77. Ciocca, M.L., Barnett, B.E., Burkhardt, J.K., Chang, J.T., & Reiner, S.L. Cutting edge: Asymmetric memory T cell division in response to rechallenge. J. Immunol. 188, 4145-4148 (2012).

78. Barnett, B.E. et al. Asymmetric B cell division in the germinal center reaction. Science 335, 342-344 (2012).

79. Henriques, C.M. & Ferreira, M.G. Consequences of telomere shortening during lifespan. Curr. Opin. Cell Biol. 24, 804-808 (2012).

80. Effros, R.B., Dagarag, M., Spaulding, C., & Man, J. The role of CD8+ T-cell replicative senescence in human aging. Immunol. Rev. 205, 147-157 (2005).

81. Li, G., Yu, M., Weyand, C.M., & Goronzy, J.J. Epigenetic regulation of killer immunoglobulin-like receptor expression in T cells. Blood 114, 3422-3430 (2009).

82. Ventevogel, M.S. & Sempowski, G.D. Thymic rejuvenation and aging. Curr. Opin. Immunol. 25, 516-522 (2013).

83. Aw, D., Silva, A.B., & Palmer, D.B. Immunosenescence: emerging challenges for an ageing population. Immunology 120, 435-446 (2007).

84. Eberhardt, M.K. et al. Vaccination against a virus-encoded cytokine significantly restricts viral challenge. J. Virol. 87, 11323-11331 (2013).

85. Solana, R. et al. CMV and Immunosenescence: from basics to clinics. Immun. Ageing 9, 23 (2012).

86. Swanson, E.C. & Schleiss, M.R. Congenital cytomegalovirus infection: new prospects for prevention and therapy. Pediatr. Clin. North Am. 60, 335-349 (2013).

&

Nederlandse Samenvatting

Dankwoord

List of Publications

Curriculum Vitae

Nederlandse Samenvatting

De dynamiek die schuilgaat achter lymfocytenpopulaties

Het immuunsysteem gaat in gezonde mensen vele tientallen jaren mee, en biedt daarmee zo goed als levenslang bescherming tegen virussen, bacterien en parasieten. Wanneer een ziekteverwekker binnendringt, worden verschillende celtypen van het immuunsysteem geactiveerd om gezamenlijk de infectie de kop in te drukken. Maar ook in afwezigheid van acuut gevaar is het immuunsysteem voortdurend in beweging: nieuwe witte bloedcellen worden aangemaakt, bestaande witte bloedcellen maken delingen, veranderen van functie, en gaan weer verloren. Een goed evenwicht tussen aanmaak en verlies van witte bloedcellen is essentieel voor het behoud van het afweersysteem tot op hoge leeftijd. Dit proefschrift bestudeert, in gezonde muizen en mensen, de dynamiek die schuilgaat achter verschillende populaties van lymfocyten, een onmisbare klasse witte bloedcellen van het adaptieve immuunsysteem.

Aangeboren en adaptieve afweer

Alle gewervelden zijn uitgerust met zowel een aangeboren als een adaptief, of verworven, immuunsysteem, twee takken die in nauwe samenwerking weerstand bieden tegen indringers. Aangeboren afweer berust op de herkenning van evolutionair geconserveerde structuren die kenmerkend zijn voor ziekteverwekkers, zogeheten pathogeen-geassocieerde moleculaire patronen (PAMPs). De herkenning van dergelijke gevaarsignalen gebeurt door eiwitten die van nature aanwezig zijn op en in witte bloedcellen en waarvoor de informatie vastligt in het DNA. De cellen van het aangeboren immuunsysteem reageren zeer snel op gevaar. De reactie van het adaptieve immuunsysteem, gevormd door lymfocyten (een subklasse van witte bloedcellen), is veel trager, maar ook veel specifieker: elke lymfocyt beschikt over een unieke receptor waarmee een zeer specifiek onderdeel van een lichaamsvreemd eiwit herkend kan worden dat antigeen wordt genoemd. Het kan gaan om antigenen van ziekteverwekkers maar ook om lichaamsvreemde antigenen die aanwezig zijn op menselijke cellen van een andere HLA-bloedgroep dan de eigen, wat een groot probleem kan vormen bij orgaantransplantatie. De adaptieve immuunrespons wordt bovendien gekenmerkt door de ontwikkeling van immunologisch geheugen, waardoor de afweerreactie bij een tweede infectie met het zelfde pathogeen veel sneller op gang komt en veel krachtiger is – het principe waarop ook vaccinatie berust. Binnen de adaptieve tak van het immuunsysteem zijn T-lymfocyten, of T-cellen, verantwoordelijk voor celgemedieerde afweer: cytotoxische *killer* T-cellen kunnen een door virus geïnfecteerde cel benaderen en deze direct vernietigen. B-lymfocyten, of B-cellen, verzorgen de humorale afweerrespons: hierbij produceren B-cellen, geholpen door *helper* T-cellen, antistoffen die worden uitgescheiden en los van cellen een pathogeen onschadelijk kunnen maken, onder andere door het te neutraliseren.

Ontwikkeling van lymfocyten

Lymfocyten zijn er niet vanzelf; er gaat een complex ontwikkelingsproces aan vooraf, dat voor B-cellen grotendeels plaatsvindt in het beenmerg en voor T-cellen grotendeels in de thymus, of zwezerik. Hier worden B-cellen en T-cellen uitgerust met hun unieke antigeenreceptor, de B-celreceptor of T-celreceptor, die de cellen hun specificiteit geeft. Dankzij een enorme diversiteit aan antigeenreceptoren – binnen één individu kunnen alle lymfocyten samen vele miljoenen verschillende antigenen herkennen – biedt het adaptieve immuunsysteem bescherming tegen een breed scala aan pathogenen. Voor het genereren van deze enorme diversiteit aan receptoren vinden tijdens B-cel- en T-celontwikkeling op DNA-niveau complexe veranderingen plaats in de genen die de informatie bevatten voor de antigeenreceptor (verschuivingen, verwijderingen, toevoegingen). Slechts een fractie van deze reorganisaties verloopt succesvol en

leidt tot B-cellen of T-cellen die in staat zijn om lichaamsvreemde antigenen goed te herkennen, maar tegelijkertijd lichaamseigen antigenen te negeren – zulke *zelf-tolerantie* moet de kans op autoimmuniteit beperken. Alleen cellen die aan deze eisen voldoen worden geselecteerd en zullen verder uitrijpen om beenmerg en thymus te verlaten en verschillende afweerfuncties in bloed- en lymfestelsel (de *periferie*) te vervullen. Soms kunnen lymfocyten wel jarenlang door het lichaam circuleren zonder hun specifieke antigeen tegen te komen, en tot dat moment worden zij naïef genoemd. Zodra er echter contact plaatsvindt met antigeen zal dat leiden tot de activering van naïeve lymfocyten, waarbij deze zich vermeerderen en differentiëren tot effectorcel of geheugencel en zo de functies krijgen die nodig zijn voor de afweerrespons. Als het gevaar bestreden is zal het merendeel van de geactiveerde cellen sterven, maar een klein deel dat overblijft vormt het immunologisch geheugen voor de lange termijn.

Lymfocytenpopulaties in evenwicht

Elke verzameling cellen van een bepaald type vormt een populatie van een bepaalde grootte, d.w.z. bestaande uit een bepaald aantal cellen – een mens heeft bijvoorbeeld ongeveer een miljoen T-cellen per milliliter bloed. De grootte van verschillende lymfocytenpopulaties blijft redelijk stabiel tijdens veroudering. Hoe belangrijk dat is blijkt uit klinische situaties waarin het aantal lymfocyten sterk verminderd is (lymfopenie), zoals tijdens infectie met humaan immunodeficientievirus (HIV) of na chemotherapie of bestraling: deze patiënten hebben een sterk verzwakt immuunsysteem en lopen een verhoogd risico om ziek te worden of zelfs te overlijden aan infecties.

Achter een lymfocytenpopulatie van constante grootte gaat een dynamisch proces schuil waarbij aanmaak en verlies van cellen in balans zijn; cellen worden voortdurend vervangen door nieuwe cellen, m.a.w. de cellen zijn permanent in turnover. In dit proefschrift kwantificeren we deze dynamiek, en in het bijzonder die van naïeve T-cellen. In het geval van naïeve T-cellen is de grootte van de populatie het netto effect van de volgende processen: (1) de aanvoer van nieuw aangemaakte naïeve T-cellen uit de thymus (*thymusoutput*), (2) de aanmaak van cellen wanneer bestaande naïeve T-cellen in de periferie (lymfeklieren) zich door celdeling vermenigvuldigen, en (3) het verlies van naïeve T-cellen door celdood of doordat ze in aanraking komen met hun antigeen, differentiëren, en daardoor niet langer tot de naïeve T-celpopulatie behoren (Figuur 1).

Kwantitatief inzicht in de dynamiek van lymfocytenpopulaties is belangrijk om beter te kunnen begrijpen hoe het immuunsysteem werkt. Hoe wordt een functioneel en divers immuunsysteem in stand gehouden tot op hoge leeftijd? Welke mechanismen zijn verantwoordelijk voor het behoud van immunologisch geheugen na infectie of vaccinatie? Hoe reageert het immuunsysteem op veranderingen die het evenwicht van een lymfocytenpopulatie verstoren? En wat is de oorzaak van, of de drijvende kracht

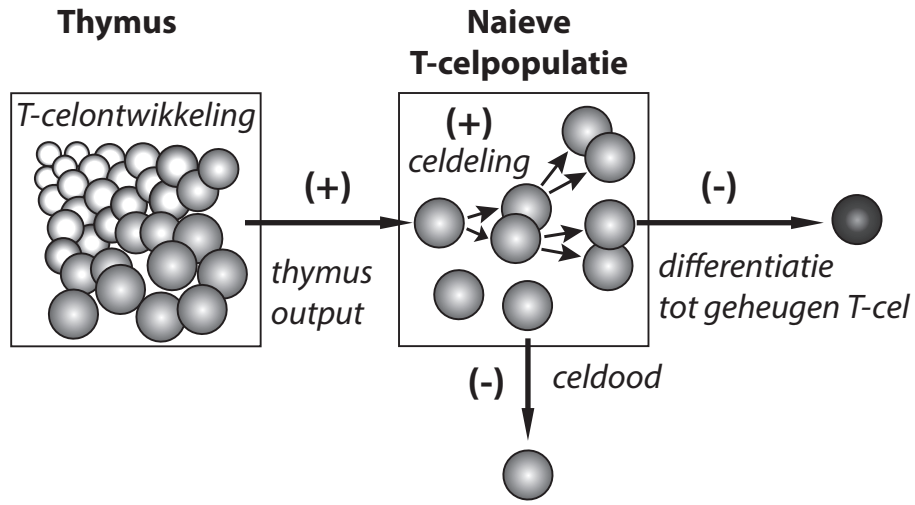

Figuur 1. De naïeve T-celpopulatie in dynamisch evenwicht. De naïeve T-celpopulatie is een evenwicht van productie (+) van nieuwe naïeve T-cellen door thymusoutput en door celdeling, en verlies (-) van bestaande naïeve T-cellen door celdood of door differentiatie van naïeve T-cellen tot geheugen T-cellen, waardoor zij niet langer naïef zijn.

achter ziekten waarin verstoorde aanmaak of sterfte van lymfocyten een rol speelt? Antwoorden op dit soort vragen vormen de basis voor ontwikkeling en verbetering van therapieën voor een breed scala aan ziekten. Opmerkelijk genoeg is er, ondanks een ware kennisexplosie op het gebied van immunologie, relatief weinig kwantitatieve kennis over lymfocytendynamiek beschikbaar, en daardoor is er onder andere nog veel onduidelijkheid over hoe lang lymfocyten leven, of hoeveel nieuwe T-cellen er dagelijks door de thymus worden geproduceerd. In dit proefschrift hebben we dankzij kwantitatief onderzoek van lymfocytendynamiek een aantal belangrijke kwalitatieve inzichten in het immuunsysteem verkregen.

Behoud van de naïeve T-celpopulatie: de muis is geen mens

Het wordt algemeen aangenomen dat de naïeve T-celpopulatie (Figuur 1) hoofdzakelijk in stand gehouden wordt door productie van nieuwe naïeve T-cellen door de thymus, en dat de aanmaak van naïeve T-cellen door celdeling in de periferie maar een beperkte rol speelt. In **hoofdstuk 3** hebben we in muizen en mensen onderzocht hoe de naïeve T-celpopulatie onderhouden wordt. Door een unieke combinatie van verschillende technieken en wiskundige modellen hebben we bevestigd dat in muizen de thymus inderdaad de hoofdrol speelt. In mensen blijkt het echter een totaal ander verhaal: niet productie door de thymus maar juist celdeling in de periferie is de belangrijkste bron van nieuwe naïeve T-cellen. Bovendien vonden we een groot verschil in de levensduur

van naïeve T-cellen: terwijl naïeve T-cellen in de muis een levensverwachting hebben van een aantal weken, leven ze in de mens gemiddeld maarliefst zes tot tien jaar. De dynamiek van de naïeve T-celpopulatie in de mens is daarmee maarliefst 40 keer zo traag als die in de muis. Deze resultaten laten een belangrijk kwalitatief verschil in T-celdynamiek zien tussen muis en mens, en geven daarmee een grote beperking aan in het gebruik van de muis als modelsysteem voor de mens in onderzoek naar ziektes waarbij de aanmaak van nieuwe T-cellen een rol speelt.

Minimale bijdrage van de thymus in volwassenen

In tegenstelling tot wat meestal gedacht wordt draagt de thymus van volwassen mensen dus maar weinig bij aan de totale productie van naïeve T-cellen (**hoofdstuk 3**.) In gezonde jongvolwassenen produceert de thymus, met ongeveer 16 miljoen naïeve T-cellen per dag, hooguit een tiende deel van de totale productie van naïeve T-cellen – de overige 90% ontstaat uit delingen van bestaande cellen in de periferie. In **hoofdstuk 7** laten we zien dat de dagelijkse thymusoutput tijdens veroudering terugloopt naar één miljoen cellen per dag. Hoewel dat nog steeds een groot aantal cellen lijkt draagt de thymus in een gezonde oudere daardoor nog maar voor 1% bij aan de totale productie van nieuwe naïeve T-cellen. Dit heeft functionele consequenties met betrekking tot de diversiteit aan antigeenreceptoren in de populatie: omdat alleen in de thymus T-cellen gevormd worden met een nieuwe, unieke antigeenreceptor, kan alleen thymusoutput de diversiteit van antigeenreceptoren in de periferie verhogen. Celdeling van bestaande cellen daarentegen leidt alleen tot een vermeerdering van het aantal cellen met dezelfde antigeenreceptor, maar zal de diversiteit nooit verhogen. Er zijn in de literatuur duidelijke aanwijzingen dat de diversiteit aan antigeenreceptoren op hoge leeftijd verminderd is, en dit zou een rol kunnen spelen bij verhoogde vatbaarheid voor infecties. Bijzonder relevant in deze context is onderzoek naar manieren om de ontwikkeling en productie van nieuwe T-cellen in de thymus te stimuleren, iets wat niet alleen in ouderen gunstig zou kunnen zijn, maar ook een enorme uitkomst zou bieden voor patienten die na een stamceltransplantatie een nieuw immuunsysteem moeten opbouwen.

Geen grote veranderingen in lymfocytendynamiek tijdens gezonde veroudering

Er wordt vaak gedacht dat wanneer het evenwicht van een lymfocytenpopulatie verstoord wordt door veranderingen in celaanmaak of -verlies, er *homeostatische* mechanismen actief worden waardoor dit evenwicht wordt hersteld. Zulke compensatiemechanismen berusten op competitie tussen lymfocyten voor bijvoorbeeld beperkte hoeveelheden overlevingsfactoren of groeifactoren. Wanneer er minder cellen zijn, zal deze competitie afnemen, waardoor de beschikbaarheid van dergelijke factoren *per cel* groter wordt: cellen gaan hierdoor mogelijk harder delen of langer leven, waardoor het aantal cellen weer toeneemt. Tijdens gezonde veroudering wordt de thymus kleiner, en we hebben in **hoofdstuk 3** gemeten dat de thymusoutput in ouderen ongeveer tien keer zo laag is als in jongvolwassenen. Het zou dus kunnen dat er tijdens veroudering compensatie optreedt voor het wegvallen van naïeve T-celproductie door de thymus. In **hoofdstuk 7** hebben we, ondanks de tienvoudig verlaagde thymusoutput in gezonde ouderen, geen aanwijzingen kunnen vinden voor een toename van naïeve T-celdelingen in de periferie, noch voor een verlengde levensverwachting van naïeve T-cellen. Dat een compensatiereactie niet lijkt op te treden zou verklaard kunnen worden door de beperkte rol die de thymus zelfs in jonge volwassenen al speelt: een verdere afname van deze toch al kleine thymusoutput zal niet leiden niet tot een groot verlies in de productie van naïeve T-cellen ná het 25e levensjaar – het merendeel van de cellen wordt in volwassenen, jong en oud, ten slotte geproduceerd door celdeling. Daarnaast hebben we bestudeerd of het in stand houden van diverse andere lymfocytenpopulaties tijdens gezonde veroudering gepaard gaat met veranderingen in de onderliggende dynamiek. We vonden dat de grootte van diverse T-cel- en B-celpopulaties inderdaad vrij constant blijft tijdens veroudering, maar dat dit niet hand in hand gaat met veranderd delings- en overlevingsgedrag van de meeste populaties. Ondanks het feit dat er geen duidelijke veranderingen in celdynamiek optreden tijdens gezonde veroudering zou het kunnen dat deze dynamiek onder andere omstandigheden wel verandert. We hebben indmiddels aanwijzingen dat compensatie door verhoogde celdeling duidelijk optreedt in mensen met zeer lage lymfocytenaantallen, zoals patienten die een stamceltransplantatie ontvangen en een zo goed als “leeg” immuunsysteem weer helemaal moeten opbouwen.

Immunologisch geheugen in kortlevende cellen

Een interessante waarneming in dit proefchrift is verder dat zowel geheugen T-cellen als geheugen B-cellen, zowel in muizen als mensen, en zowel op jonge als op oude leeftijd, relatief kort leven (**hoofdstuk 5, 7**). In muizen hebben geheugencellen een gemiddelde levensverwachting van 2 of 3 weken, en in mensen van grofweg 50 tot 300 dagen, afhankelijk van het celtype. Dat is vele malen korter dan de levensduur van naïeve B- en T-cellen en dan het tijdsbestek waarover immunologisch geheugen aanwezig blijft: het geheugen dat wordt opgebouwd na bijvoorbeeld vaccinatie biedt vaak vele decennia lang bescherming. Dit betekent dat immunologisch geheugen zich niet noodzakelijkerwijs bevindt in een langlevende cel. Onze resultaten laten zien dat het in ieder geval gehandhaafd lijkt te worden in een langlevende celpopulatie waarbinnen lymfocyten zichzelf voortdurend vernieuwen door deling – mogelijk is deze voortdurende turnover zelfs essentieel voor het goed functioneren van immunologisch geheugen.

Hoe hebben we dit gemeten?

Een belangrijk, meer technisch deel van dit proefschrift gaat over hoe we de dynamiek van lymfocytenpopulaties het beste kunnen meten, en hoe we deze metingen het beste kunnen interpreteren voor een betrouwbare schatting van bijvoorbeeld de levensduur van lymfocyten of van de dagelijkse productie van nieuwe T-cellen door de thymus. De gemiddelde levensduur van cellen hebben we gekwantificeerd met behulp van *deuteriumlabeling.* Door deze informatie te combineren met metingen van *T-celreceptor excisiecirkels (TRECs)* konden we ook de dagelijkse thymusoutput schatten.

Kwantificering van de levensduur van lymfocyten: deuteriumlabeling

Voor elke nieuwe cel die wordt aangemaakt wordt DNA gesynthetiseerd, en met elke verloren cel verdwijnt ook zijn DNA. Door nieuw aangemaakt DNA te voorzien van een label dat gemeten kan worden is het mogelijk om het lot van cellen in een populatie over de tijd te volgen. Dit is het principe waarop deuteriumlabelingstechnieken met zwaar water of zwaar glucose berusten, een manier om veilig *in vivo* (in het lichaam) de dynamiek van celpopulaties te bestuderen zonder dat deze wordt beïnvloed. In dit proefschrift maken we gebruik van deuterium-gelabeld of ook wel zwaar water. Een molecuul zwaar water, $^{2}H_2O$, bevat naast zuurstof een stabiele, niet-radioactieve isotoop van waterstof, deuterium (^{2}H), dat een grotere massa heeft dan normaal waterstof (^{1}H) doordat de atoomkern naast een proton ook een neutron bevat. Tijdens het drinken van zwaar water (naast gewoon water) zal er niet alleen normaal waterstof maar ook deuterium terechtkomen in de bouwstenen voor DNA. Nieuw aangemaakt DNA (in delende cellen) zal hierdoor zwaarder worden dan bestaand DNA: het wordt gelabeld met deuterium. Hoewel het hier om zeer kleine verzwaringen gaat is het mogelijk dergelijke verschillen in massa nauwkeurig te meten met behulp van gaschromatografie-massaspectrometrie. Hoe dynamischer een celpopulatie en dus hoe harder de aanmaak van nieuwe cellen, hoe sneller het DNA ten gevolge van deuteriuminbouw zal verzwaren tijdens de periode waarin zwaar water wordt gedronken; aangezien aanmaak en verlies in evenwicht zijn zal, na stoppen met de inname van zwaar water, de hoeveelheid deuterium in het DNA ook snel weer afnemen omdat de nieuw aangemaakte cellen, net als alle andere cellen, weer vlot verloren gaan (Figuur 2, links). Omgekeerd zal voor een celpopulatie met trage dynamiek nauwelijks deuteriuminbouw waarneembaar zijn (Figuur 2, rechts). Metingen van deuteriuminbouw in DNA tijdens het experiment kunnen met behulp van wiskundige modellen vertaald worden naar een *turnoversnelheid,* en daarmee ook naar een gemiddelde levensverwachting van cellen in een populatie. In **hoofdstuk 2** wordt de toepassing van labelingstechnieken met zwaar water en zwaar glucose beschreven, van studieopzet en uitvoer tot en met interpretatie.

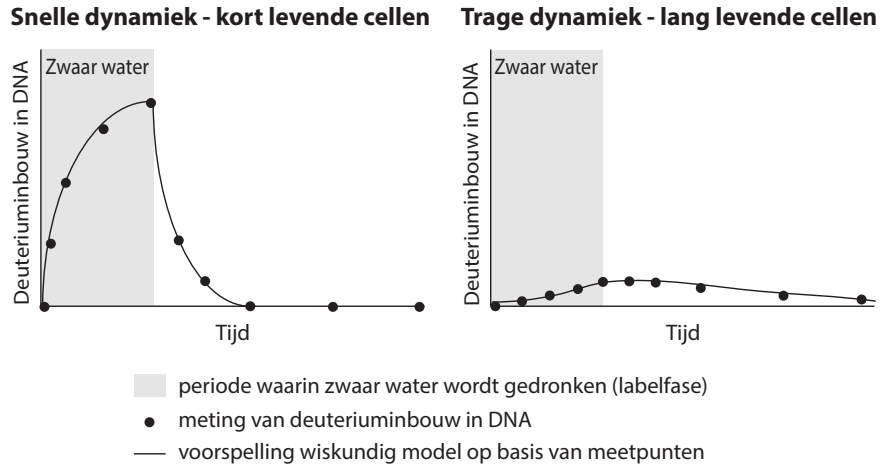

Figuur 2. Zwaar water labeling. Tijdens het drinken van zwaar water (grijs) zal het DNA van nieuw aangemaakte cellen gelabeld worden met deuterium. In een populatie met snelle dynamiek zal snel een hoge mate van deuteriuminbouw waarneembaar zijn, terwijl in een populatie met trage dynamiek deuteriuminbouw maar weinig toeneemt over de tijd. Zodra gestopt wordt met drinken van zwaar water neemt de hoeveelheid deuterium in het DNA van celpopulaties af wanneer cellen verloren gaan. Binnen een populatie met snelle dynamiek, waarin cellen automatisch een korte levensduur hebben, verdwijnt deuterium vrij snel, maar binnen een populatie met trage dynamiek kan deuterium nog geruime tijd in het DNA detecteerbaar zijn, omdat cellen hier veel langer in leven blijven.

Onenigheid over de levensduur van lymfocyten

Al decennia lang proberen onderzoekers de levensduur van lymfocyten te schatten. De technieken die in het verleden veel gebruikt werden, en die zonder meer belangrijke inzichten hebben opgeleverd, waren echter niet breed toepasbaar, onveilig, niet representatief voor een gezonde situatie, of moeilijk te vertalen naar een levensduur van cellen. De introductie van deuteriumlabelingstechnieken bracht daar verandering in, want hiermee kon de levensduur van cellen voor het eerst veilig en onder natuurlijke omstandigheden in mensen gekwantificeerd worden. Toch lopen de tot nu verkregen schattingen van de levensduur van lymfocyten in gezonde mensen uiteen. Het ontbreken van zulke basale kennis, die eigenlijk gewoon in tekstboeken thuishoort, vormt een groot obstakel voor verder onderzoek: als er al geen consensus is over hoe lang een lymfocyt leeft in een gezond individu, dan wordt het heel lastig om harde uitspraken te doen over hoe deze levensduur verandert tijdens ziekte. In dit proefschrift hebben we daarom ook onderzocht waar de verschillen in geschatte levensduur in de literatuur vandaan komen, omdat we voor elk type lymfocyt uiteindelijk toe willen naar één levensduur waar iedereen het over eens is. Wat opvalt aan de verschillen in de literatuur is dat er een patroon in zit: hoe langer de periode waarin zwaar water of zwaar glucose is toegediend, hoe langer de geschatte levensduur van cellen, en het

lijkt er daarbij op dat studies met zwaar glucose altijd kortere levensduren opleveren dan studies met zwaar water. In **hoofdstuk 5** hebben wij gevonden dat de duur van de labelingsperiode inderdaad invloed heeft gehad op de geschatte levensduur van cellen. Een alternatief wiskundig model bleek de oplossing voor dit probleem: in tegenstelling tot de normaal gebruikte modellen houdt dit model er rekening mee dat een celpopulatie geen homogene verzameling van cellen met dezelfde levensverwachting hoeft te zijn, maar ook *kinetisch heterogeen* kan zijn, en dus kan bestaan uit meerdere subtypen van cellen met elk hun eigen levensduur. Labeling met zwaar glucose of met zwaar water, vergeleken in **hoofdstuk 6**, bleek niet van invloed te zijn op de geschatte levensduur.

Informatie over thymusoutput: T-celreceptor excisiecirkels

Deuteriumlabeling kan geen onderscheid maken tussen cellen die in de thymus hebben gedeeld en daarna, gelabeld en wel, in de naïeve T-celpopulatie terecht zijn gekomen, en naïeve T-cellen die in de periferie hebben gedeeld. Om inzicht te krijgen in de bijdrage van de thymus hebben we daarom ook onderzoek gedaan naar T-celreceptor excisiecirkels (TRECs): kleine circulaire DNA fragmenten die ontstaan in de thymus als bijproduct van de reorganisaties die in het DNA van zich ontwikkelende T-cellen plaatsvinden. TRECs zijn zeer stabiel en blijven daardoor aanwezig in perifere T-cellen, maar ze worden niet meegekopiëerd wanneer een T-cel deelt. Het aantal TRECs in een celpopulatie zal dus verdunnen als er gedeeld wordt in de populatie. Het percentage naïeve T-cellen in de periferie dat een TREC draagt geeft aan wat de *relatieve* bijdrage van de thymus is aan de totale naïeve T-celproductie. Stel dat elke cel die de thymus verlaat 1 TREC heeft, en dat slechts één op de vier naïeve T-cellen in de perifere populatie een TREC heeft, dan is een kwart van alle naïeve T-cellen geproduceerd door de thymus, en de overige drie kwart is gevormd door celdeling (Figuur 3). Omdat er ook in de thymus al celdelingen plaatsvinden na het ontwikkelingsstadium waarin een TREC gevormd wordt, zullen in werkelijkheid lang niet alle cellen die de thymus verlaten een TREC hebben. Omdat we weten hoe groot in de thymus de fractie cellen met een TREC is, kunnen we hiervoor corrigeren. Door de relatieve bijdrage van de thymus te vermenigvuldigen met de totale productie van naïeve T-cellen, geschat met deuteriumlabeling, konden wij ook de *absolute* bijdrage van de thymus berekenen, m.a.w. hoeveel cellen de thymus per dag produceert.

We interpreteren de fractie naïeve T-cellen zonder TREC als het deel van de naïeve T-celpopulatie dat gevormd is door perifere celdeling. We nemen voor deze interpretatie aan dat TRECs zelf zeer stabiel zijn, en dat de fractie cellen met een TREC dus ook alleen maar omlaag kan gaan als gevolg van celdeling. Hoe stabiel TRECs werkelijk zijn is echter nooit onderzocht. Het is niet uitgesloten dat TRECs (langzaam) vanzelf vervallen, en in dat geval zouden er ook zonder celdeling naïeve T-cellen kunnen

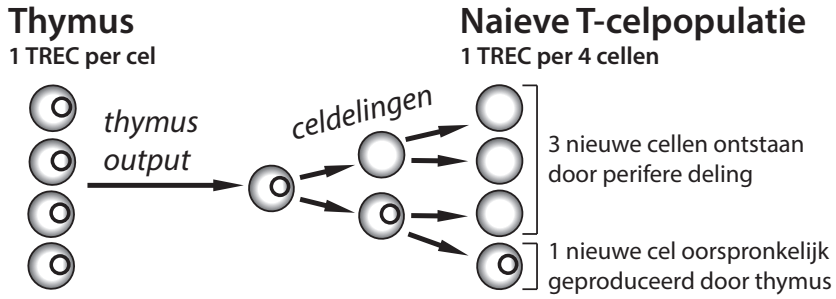

Figuur 3. TRECs. TRECs ontstaan tijdens T-celontwikkeling in de thymus en zijn ook aanwezig in perifere T-cellen. Omdat ze niet gekopieerd worden tijdens celdeling zullen er zo ook cellen zonder TREC gevormd worden. Als elke cel die de thymus verlaat een TREC heeft, en deze in de periferie 2 delingen maakt, zal uiteindelijk maar één op de vier naïeve T-cellen een TREC hebben. Dit bekenent dan ook dat één op de vier naïeve T-cellen oorspronkelijk door de thymus is geproduceerd, terwijl drie op de vier naïeve T-cellen gevormd zijn door perifere celdeling.

onstaan die geen TREC meer hebben. Dit scenario hebben we onderzocht in **hoofdstuk 4**, door TRECs te meten in nierpatienten die jarenlang afweeronderdrukkende medicijnen krijgen die ook de perifere deling van T-cellen onderdrukken. Hoewel deze studie nog niet is afgerond lijkt het erop dat naïeve T-celdeling wel degelijk een belangrijke rol speelt bij de verdunning van TRECs binnen de naïeve T-celpopulatie van gezonde volwassenen, en dat TRECs niet snel spontaan vervallen. Deze uitkomst ondersteunt de interpretatie van TRECs zoals die door ons en vele andere immunologen wordt gedaan.

Conclusie

In dit proefschrift hebben we, mede dankzij het optimaliseren van de gebruikte meet- en interpretatiemethodes, belangrijke biologische inzichten verkregen in hoe verschillende lymfocytenpopulaties een leven lang in stand gehouden worden. We vonden onder andere dat de dynamiek van de naïeve T-celpopulatie in muizen en mensen onvergelijkbaar is, met in mensen verrassenderwijs een zeer beperkte thymusoutput tegenover een veel grotere rol voor perifere celdeling in zowel jonge als oudere volwassenen. Ook vonden we dat er tijdens gezonde veroudering in mensen geen grote veranderingen plaatsvinden in de grootte en dynamiek van diverse T-cel- en B-celpopulaties, en dat er voor het verlies van thymusoutput met de leeftijd geen compensatie lijkt op te treden in de vorm van verhoogde celdeling of verlengde levensduur van naïeve T-cellen. De resultaten beschreven in dit proefschrift dragen bij aan de huidige kennis over het functioneren van het immuunsysteem in gezondheid, en vormen samen met de verkregen methodologische inzichten de basis voor verder onderzoek naar veroudering en naar ziekten waarbij de aanmaak of sterfte van lymfocyten verstoord is.

Curriculum Vitae

Liset Westera was born on 3 October 1985 in Vught, The Netherlands. In 2003 she graduated from Grotiuscollege in Heerlen (VWO-gymnasium), after which she started her bachelor education in Biomedical Sciences at Utrecht University. In 2006 she obtained her Bachelor of Science degree *cum laude.* In the same year, Liset enrolled in Biomedical Sciences master program Immunity and Infection at Utrecht University. She did her first 9-months research training in the group of prof. dr. Frank Miedema, dr. Kiki Tesselaar, and dr. José Borghans, at the department of Immunology of the University Medical Center Utrecht. Here she studied the dynamics of recent thymic emigrants. For her second research training Liset went to the United States to perform research at the department of microbiology at Mount Sinai School of Medicine in New York City. For 7 months she worked in the lab of prof. dr. Adolfo García-Sastre under supervision of dr. Eric Bortz, and studied how interactions between cellular proteins and the influenza virus polymerase influence the replication capacity of the virus. At the same institute she subsequently did an elective, short training in the lab of dr. Ana Fernandez-Sesma, where she investigated the inhibitory influence of the influenza non-structural 1 protein on human dendritic cell maturation. In 2008 Liset obtained her Master of Science degree *cum laude*.

In Januari 2009 Liset began her PhD at the department of immunology, now Laboratory of Translational Immunology, at the University Medical Center Utrecht, under supervision of copromotors dr. José Borghans and dr. Kiki Tesselaar, and promotors prof. dr. Frank Miedema and prof. dr. Rob de Boer. The results of her PhD research are reported in this thesis, entitled “Quantification of Lymphocyte Dynamics”.

List of Publications

Liset Westera*, Julia Drylewicz*, Ineke Den Braber*, Tendai Mugwagwa, Iris van der Maas, Lydia Kwast, Thomas Volman, Elise HR van de Weg-Schrijver, István Bartha, Gerrit Spierenburg, Koos Gaiser, Mariëtte T Ackermans, Becca Asquith, Rob J de Boer#, Kiki Tesselaar#, José AM Borghans#. Closing the gap between T-cell life span estimates from stable isotope-labeling studies in mice and men. *Blood.* 2013 Sep 26;122(13):2205-12

Liset Westera, Yan Zhang, Kiki Tesselaar, José AM Borghans, Derek C Macallan. Quantitating lymphocyte homeostasis in vivo in humans using stable isotope tracers. *Methods Mol Biol*. 2013;979:107-31

Irene Ramos, Elena Carnero, Dabeiba Bernal-Rubio, Christopher W Seibert, Liset Westera, Adolfo García-Sastre, Ana Fernandez-Sesma. Contribution of dsRNA and CPSF30 binding domains of influenza virus NS1 to the inhibition of type I IFN production and activation of human dendritic cells. *J Virol.* 2013 Mar;87(5):2430-4

Ineke den Braber*, Tendai Mugwagwa*, Nienke Vrisekoop*, Liset Westera, Ramona Mögling, Anne Bregje de Boer, Neeltje Willems, Elise HR Schrijver, Gerrit Spierenburg, Koos Gaiser, Erik Mul, Sigrid A Otto, An FC Ruiter, Mariëtte T Ackermans, Frank Miedema, José AM Borghans#, Rob J de Boer#, Kiki Tesselaar#. Maintenance of peripheral naive T cells is sustained by thymus output in mice but not humans. *Immunity,* 2012 Feb 24;36(2):288-97

Eric Bortz, Liset Westera, Jad Maamary, John Steel, Randy A. Albrecht, Balaji Manicassamy, Geoffrey Chase, Luís Martinez-Sobrido, Martin Schwemmle, Adolfo García-Sastre. Host- and strain-specific regulation of influenza virus polymerase activity by interacting cellular proteins. *mBio,* 2011 Aug 16;2(4)

Liset Westera*, Vera van Hoeven*, Julia Drylewicz, Gerrit Spierenburg, Jeroen F van Velzen, Rob J de Boer, Kiki Tesselaar#, José AM Borghans#. Lymphocyte maintenance during healthy aging requires no substantial alterations in cell dynamics. *Submitted for publication*

Ellen Veel*, Julia Drylewicz*, Steven van Lelyveld*, Liset Westera, Sigrid A Otto, Anita van Oort, Koos Gaiser, Gerrit Spierenburg, Inge de Kroon, Andy IM Hoepelman, José AM Borghans, Kiki Tesselaar. cART intensification with Maraviroc decreases T-cell turnover in HIV-1 immunological non responders. *Submitted for publication*

*,# these authors contributed equally